UNIVERSITÄT DUISBURG ESSEN

Offen im Denken

Functional characterisation of Survivin and the CPC in replication stress

Dissertation
zur Erlangung des Doktorgrades
Dr. rer. nat.

der Fakultät für Biologie
an der Universität Duisburg-Essen

vorgelegt von Katharina Falke
aus Essen

Dezember 2020

DOI: 10.17185/duepublico/74168
URN: urn:nbn:de:hbz:465-20250107-112319-7

Die der vorliegenden Arbeit zugrundeliegenden Experimente wurden am Zentrum für medizinische Biotechnologie (ZMB) in der Abteilung für Molekularbiologie II der Universität Duisburg-Essen durchgeführt.

1. Gutachter: Prof. Dr. Shirley Knauer
2. Gutachter: Prof. Dr. Christian Johannes

Vorsitzender des Prüfungsausschusses: Prof. Dr. George Iliakis

Tag der mündlichen Prüfung: 10.03.2021

Für meine Eltern,
die mir all dies ermöglicht haben.

Table of Contents

List of Abbreviations

%	Percent
(m)	derived from mouse
(r)	derived from rabbit
° C	degree Celsius
µ	Micro
53BP1	p53-binding protein
aa	amino acid
AF	Alexa Fluor
APC/C	Anaphase-promoting complex/cyclosome
APE	Apurinic/apyrimidine endonuclease
Aph	Aphidicolin
APLF	Aprataxin-and-PNK-like factor
APS	Ammonium peroxydisulfate
ATM	Ataxia telangiectasia mutated
ATP	Adenosine triphosphate
ATR	Ataxia telangiectasia and Rad3-related
ATRIP	ATR-interacting protein
BER	Base excision repair
BIR	Baculoviral IPA repeat
BIRC5	Baculoviral IPA repeat-containing 5
BLM	Bloom syndrome protein
BRCA1	Breast cancer type 1 susceptibility protein
BRCA2	Breast cancer type 2 susceptibility protein
BrdU	Bromodeoxyuridine
BSA	Bovine Serum Albumin
Bub1	Budding Uninhibited by Benzimidazoles 1
Bub3	Budding Uninhibited by Benzimidazoles 3
C- or N-term	C- or N-terminally
CAF1	Chromatin assembly factor 1
CAS	Cockayne syndrome WD repeat protein A
CD	Chromo domain
Cdc20	Cell division cycle 20

Cdc25	Cell division cycle 25
Cdc6	Cell division cycle 6
CDK	Cyclin-dependent kinase
Cdt10	Cdc10-dependent transcript 1
CENP-A	Centromere protein A
CFSs	Common fragile sites
Chk1, 2	Checkpoint kinase 1, 2
CK2	Casein kinase 2
CKI	Cyclin-dependent kinase inhibitor
CldU	Chlorodeoxyuridine
cm	Centimetre
CMG	Cdc45-MCM2-7-GINS
Co-IP	Co-immunoprecipitation
CPC	Chromosomal passenger complex
CPD	Cyclobutane pyrimidine dimer
CPT	Camptothecin
CREST	Scleroderma syndrome
CRL^{Lrr1}	Cullin RING Ligase 2 associated with Leucine Rich Repeats 1 [Lrr1]
CRM1	Chromosomal region maintenance 1
CSB	Cockayne syndrome group B
CSD	Chromo shadow domain
CSK	Cytoskeletal
CtIP	CtBP interacting protein
ddH_2O	Double-distilled water
DDI 1	DNA-damaged inducible 1 homolog 1
DDI 2	DNA-damaged inducible 1 homolog 2
DDK	Dbf4-dependent Cdc7 kinase
DDR	DNA damage response
DMEM	Dulbecco’s Modified Eagle’s Medium
DMSO	Dimethyl sulfoxide
DNA	Desoxyribonucleic acid
DNA-PKcs	Catalytic subunit of the DNA dependent
dNTP	Deoxyribonucleotides

DPBS	Dulbecco’s phosphate-buffered saline
dRP	Deoxyribose phosphate
DSB(s)	Double-strand break(s)
dsDNA	Double-stranded DNA
DTT	Dithiothreitol
ECL	Enhanced chemiluminescence
EDTA	Ethylenediaminetetraacetic acid
EdU	5-ethynyl-2’-deoxyuridine
EGTA	Ethylene glycol-bis(β-aminoethyl ether)
Exo1	Exonuclease 1
FCS	Fetal calf serum
FEN1	Flap structure-specific endonuclease
FLAG-tag	Sequence: DYKDDDDK
g	Gravitational constant
G1, G2, G0 phase	Gap or growth phase 1, 2, 0
GFP	Green fluorescent protein
GG-NER	Global genome NER
GINS	“Go-ichi-ni-san”, japanese for 5, 1, 2, 3
Gy	Gray; SI unit of absorbed dose, meaning to deposit 1 joule of energy in 1 kilogram of
H3K9me3	Histone H3 trimethylated on Lys9
H3S10p	Histone H3 phosphorylated on Ser10
HBS	HEPES buffered saline
HDAC	Histone deacetylase protein
HEPES	4-(2-hydroxyethyl)-1-piperazineethanesulfonic acid
HP1	Heterochromatin protein 1
HPXIP	Hepatitis B x-introducing protein
HR	Homologous recombination
HRP	Horseradish peroxidase
HU	Hydroxyurea
IAP	Inhibitor of apoptosis
IdU	Iododeoxyuridine
IF	Immunofluorescence
IGF-1	Insulin-like growth factor 1

INCENP	Inner centromere protein
IOD	Inter origin distance
IR	Ionizing radiation
KAP-1	KRAB-associated protein-1
kb	Kilobases
kDa	Kilo Dalton
KLD	Kinase, ligase, DpnI
LB medium	Luria-Bertani medium
M phase	Mitotic phase
M	Molar, mol/Litre
mA	Milliampere
Mad2	Mitotic arrest deficient 2
Mad3	Mitotic arrest deficient 3
MCC	Mitotic checkpoint complex
MCM2-7	Mini chromosome maintenance helicase
Mdc1	Mediator of DNA damage checkpoint 1
MES	2-(N-morpholino)ethanesulfonic acid
MiDAS	Mitotic DNA synthesis
Mklp2	Mitotic kinesin-like protein 2
ml	Millilitre
mm	Millimetre
MRN	MRE11-RAD50-NBS1
mut	Mutant
myc-tag	Sequence: N-EQKLISEEDL-C
NC	Nitrocellulose
NER	Nucleotide excision repair
NES	Nuclear export sequence
NF-κB	Nuclear factor 'kappa-light-chain-enhancer' of activated B-cells
ng	Nanogram
NHEJ	Non-homologous end-joining
nm	Nanometre
NP-40	Nonidet P40
ORC	Origin recognition complex

PALB2	Partner and localizer of BRCA2
PCNA	Proliferating cell nuclear antigen protein
PCR	Polymerase chain reaction
pH	Potentia Hydrogenii
PIKK	Phosphoinositide-3-kinase related kinase
PIP	PCNA-interacting protein
PKC	Protein kinase C
PLA	Proximity Ligation Assay
PLK1	Polo-like kinase
PMSF	Phenylmethylsulfonyl fluoride
PNKP	Bifunctional polynucleotide
POI	Protein of interest
Pol	Polymerase
pre-IC	Pre-initiation complex
pre-RC	Pre-replicative complex
PTM(s)	Post-translational modifications
RAP80	Receptor-associated protein 80
RAS	Rat sarcoma
Rb	Retinoblastoma-associated protein
RECQL4	ATP-dependent DNA helicase Q4
Rev1	Reversionless protein 1
RFC	Replication factor C
RIPA	Radioimmunoprecipitation assay buffer
RNA	Ribonucleic acid
RNAi	RNA interference
ROS	Reactive oxygen species
RPA	Replication protein A
RT	Room temperature
RTEL1	Regulator of telomere elongation helicase 1
RTF2	Replication termination factor 2
S phase	Synthesis phase
SAC	Spindle-assembly checkpoint
SD	Standard Deviation
SDS-PAGE	Sodium dodecyl sulfate polyacrylamide gel

siRNA	Small interfering RNA
SMARCAL1	SWI/SNF-related matrix-associated actin-dependent regulator of chromatin subfamily A-like protein 1
SMC1	Structural maintenance of chromosomes 1
SSB(s)	Single-strand break(s)
ssDNA	Single-stranded DNA
TAE	Tris-acetate-EDTA TBS
TBS	Tris buffered saline
TBST	Tris-buffered saline/Tween
TC-NER	Transcription coupled repair
TE	Tris-EDTA buffer
TEMED	N,N,N’,N’-Tetramethylethylenediamine
TFIIH	Transcription initiation factor II H
TLS	Translesion synthesis
TopBP1	Topoisomerase-binding protein-1
Tris	Tris (hydroxymethyl) aminomethane
Tris-HCl	Tris hydrochloride
Ufd1	Ubiquitin fusion degradation protein 1
UV	Ultraviolet light
V	Volt
v/v	Volume per volume
w/v	Weight per volume
WB	Western blotting
WHO	World Health Organisation
WRN	Werner syndrome ATP-dependent helicase
wt	Wild type
XLF	XRCC4-like factor
XPB	Xeroderma pigmentosum, complementation B
XPC	Xeroderma pigmentosum, complementation C
XPD	Xeroderma pigmentosum, complementation D
XPE	Xeroderma pigmentosum, complementation E
XPG	Xeroderma pigmentosum, complementation G
XRCC4	X-ray repair cross-complementing protein 4

List of Figures

List of Tables

Summary

Survivin, also known as BIRC5 (baculoviral IPA repeat-containing 5), is highly upregulated in most cancer entities and has been associated with a resistance against chemo- and radiotherapy. Besides its role as a member of the CPC (chromosomal passenger complex) and its role during mitosis, Survivin also belongs to the IAP (inhibitor of apoptosis) family, and as such fulfils a role as an inhibitor of apoptosis predominantly within the cytoplasm. During mitosis, the CPC is responsible for correction of chromosome-microtubule attachment errors, activation of the spindle assembly checkpoint as well as construction and regulation of the contractile apparatus that drives cytokinesis (Carmena et al. 2012b). However, Survivin's and the other CPC members' specific function in interphase still remains elusive.

Therefore, in this thesis localisation of the CPC in interphase was confirmed and co-immunoprecipitations and PLA could verify the interaction to the sliding clamp factor PCNA. PCNA is a key member of a replication fork by enhancing the processivity of the Polymerase δ. Thus, a direct interaction with the replication machinery was demonstrated. Next, DNA combing assays should reveal if CPC depletion leads to impact on ongoing replication machinery. Especially Aurora B depletion leads to an increase of asymmetric replication forks. Under normal circumstances, replication forks concur obstacles such as DNA lesions and stall at these sites of DNA damage. Through monoubiquitination of PCNA by Rad6 and Rad18, so-called transletion polymerases resumed the job as the active polymerase and replicate over these DNA lesions (Jones and Petermann 2012). Afterwards, the translesion polymerase leaves the DNA strand and the replicative polymerase is restored and DNA synthesis can proceed. Moreover, we could show an increased relocation of the CPC to the centromeres and an enhanced co-localisation to PCNA after irradiation. Since the translesion process is DNA-damaged induced, we supposed that the CPC was directly involved in the switching-process of polymerases at stalled replication forks. Therefore, we performed expression analysis of Polymerase η after CPC depletion in combination with co-immunoprecipitations. We could indeed demonstrate an Aurora B-dependent expression of Polymerase η and co-immunoprecipitations revealed a direct interaction of the CPC to Polymerase η. Detecting not only the overexpressed but also the endogenous proteins in polymerase η-immunoprecipitates corroborated our hypothesis.

Further experiments should confirm if depletion of CPC members provokes replication stress, which could not be counteracted by translesion synthesis. Metaphase spreads, 53BP1 nuclear bodies and mitotic DNA synthesis revealed an increase of under-replicated sites after S phase exit. Indeed, Survivin depletion induced an increase of gaps and breaks on metaphase chromosomes, representing under-replicated sites or damaged DNA which was not properly processed. Moreover, these under-replicated sites were visible in so-called 53BP1 nuclear bodies. 53BP1 protects damaged DNA by accumulated at damaged DNA sites. Our data revealed an increase of 53BP1 nuclear bodies, which is a hint for perturbed or interrupted replication in S phase. Furthermore, the suggestion that CPC depletion leads to an increase of damaged-induced replication stress, is confirmed by an increase of mitotic DNA synthesis. Normally, the doubling of DNA is finished before the exit of S phase. In our case, replication could not be completed properly and cells with under-replicated-sites entered mitosis.

In summary, we can conclude that the CPC, and especially Survivin, are necessary to mediate translesion synthesis in order to preclude replication fork collapses and thus DSB formation. Furthermore, our data suggests that Survivin revives its prominent role as a radio resistance factor with its newly detected function in translesion synthesis.

Zusammenfassung

Survivivn, auch bekannt als BIRC5 (baculoviral IPA repeat-containing 5), ist in den meisten Krebsentitäten vermehrt exprimiert, was mit einer erhöhten Resistenz gegen Radio und Chemotherapie einhergeht. Neben seiner Rolle als Mitglied des CPC‘s und seiner damit assoziierten Funktion in der Mitose, ist Survivin auch ein Teil der IAP Familie, und führt seine Rolle als Inhibitor der Apoptose dementsprechend vornehmlich im Zytoplasma aus. Während der Mitose ist der CPC hauptverantwortlich für die Korrektur von Anheftungsfehlern der Mikrotubuli an die Chromosomen, der Aktivierung des Kontrollpunkts der Spindelanordnung sowie der Bildung und Regulierung des kontraktilen Apparates, welcher schließlich die Zytokinese vorantreibt. Nichtsdestotrotz ist die biologische Funktion von Survivin und des CPC in der Interphase weiterhin nicht im Detail geklärt.

Daher wurde im Rahmen dieser Arbeit zunächst die Interaktion des CPC mit dem Ringklemmenprotein PCNA mittels Co-Immunopräzipitation und PLA-Assays zweifelsfrei bestätigt. PCNA ist als essentieller Teil der Replikationsgabel für eine verstärkte DNA-Bindung der Polymerase δ verantwortlich und gewährleistet so eine kontinuierliche Strangsynthese. Somit konnten wir eine direkte Verbindung des CPC an die Replikationsmaschinerie aufzeigen. Als nächstes sollten daher DNA combing Assays darüber Aufschluss geben, ob eine Depletion von CPC Mitgliedern die Replikationsmaschinerie beeinflusst. In der Tat führte insbesondere eine Depletion von Aurora B zur Ausbildung asymmetrischer Replikationsgabeln. Normalerweise führen Hindernisse wie beispielsweise DNA-Läsionen während der Replikation zu einem Anhalten der Maschinerie. Ausgelöst durch eine über Rad6 and Rad18 vermittelte Mono-Ubiquitinierung von PCNA übernimmt eine sogenannte Transläsions-Polymerase deren Aufgabe innerhalb der Replikationsgabel und repliziert ausschließlich diese DNA-Läsionen. Danach verlässt die Transläsions-Polymerase den DNA-Strang, und die replikative Polymerase setzt, zurück an ihrem Ursprungsort, die Synthese fort. Weiterhin konnten wir eine Verlagerung des CPC‘s in Richtung der Zentromere und zeitgleich einen Anstieg der CPC-PCNA Interaktion nach Bestrahlung demonstrieren. Da der Tranläsions-Prozess mit der Entstehung von DNA-Schäden assoziiert ist, ist anzunehmen, dass der CPC direkt am Wechselprozess der unterschiedlichen Polymerasen an blockierten Replikationsgabeln beteiligt ist. Um diese These zu untermauern, wurde die Expression der Polymerase η nach CPC-

Depletion und Bestrahlung genauer untersucht. In der Tat zeigte sich eine Aurora B-abhängige Expression der Polymerase η. Parallel durchgeführte Co-Immunopräzipitationen konnten zudem eine direkte Interaktion der Polymerase η nicht nur mit überexprimierten CPC Mitgliedern, sondern auch mit den endogenen CPC Proteinen aufzeigen.

So lag die Annahme nahe, dass die Depletion einzelner CPC-Mitglieder zu Replikationsstress führt, welcher mittels Transläsions-Synthese nicht reguliert und aufgelöst werden kann. Hierzu wurden Metaphasen-Präparationen angefertigt sowie 53BP1-Kernkörper und mitotische DNA-Synthese analysiert, und es zeigte sich in der Tat einen Anstieg von nicht-vollständig replizierten Genmaterial nach Beendigung der S-Phase. Dies war in Form von Lücken und Brüchen in Metaphase-Chromosomen nachweisbar, welche nicht-vollständig replizierte DNA repräsentieren. Diese DNA-Lücken sind zudem in der G1-Phase des Zellzyklus als 53BP1-Kernkörper zu erkennen. 53BP1 akkumuliert an Bereichen der DNA, die beschädigt sind oder nicht richtig repliziert wurden. Weiterhin verursachte die Depletion von Survivin einen Anstieg der mitotischen DNA-Synthese. Normalerweise wird die Replikation innerhalb der S-Phase abgeschlossen, sodass die Zelle mit einem vollständig verdoppelten Genomsatz in die Mitose gelangt. Die Depletion von Survivin führte nun dazu, dass die Zelle die Replikation in der Mitose beenden musste, da diese in der S-Phase gestört bzw. unterbrochen wurde.

Zusammenfassend kann man sagen, dass der CPC, und insbesondere Survivin, notwendig sind, um die Transläsions-Synthese zu ermöglichen und so Doppelstrangbrüche durch den Kollaps von Replikationsgabeln zu verhindern. Diese neu entdeckte Funktion innerhalb der Transläsions-Synthese unterstreicht ein weiteres Mal die Bedeutung von Survivin als Stahlenresistenz-Faktor in der Krebstherapie.

1 Introduction

1.1 Cancer

Cancer is based on genetic alterations, resulting in the uncontrolled growth of abnormal cells (Stratton et al. 2009; Hansemann 1890; Boveri 1914; Vogelstein and Kinzler 2004). Responsible for their abnormal growth are mutations in three types of genes, namely oncogenes (Huebner and Todaro 1969), tumour suppressor genes (Comings 1973) and genes involved in the maintenance of genetic integrity (Nowell 1976; Vogelstein and Kinzler 2004). In the course of cancer disease, cancer cells are able to migrate from their place of origin and form metastases at other locations within the human body, which can result in a poor clinical outcome (Alarcón and Tavazoie 2016). According to the World Health Organization (WHO), cancer is the second most cause of death globally behind heart diseases. Worldwide, approximately 18 million new cases of cancer occurred in 2018. The most common types of cancer are those of the lung (11.6 %), colorectum (10.2 %), stomach (5.7 %), liver (4.7 %) and the gender-related types breast (11.6 %) and prostate (7.1 %) (see Figure 1.1 A) and about 9.6 million cases led to death (see Figure 1.1 B). The situation in Germany is comparable with approximately 4.8 million new cases of cancer in 2018. The most commonly affected tissues are the lung (11.1 %), colorectum (11.5 %), bladder (4.8 %), melanoma of skin (3.6 %) and the gender-related types breast (12.3 %) and prostate (10.6 %) (see Figure 1.1 C) and about 2.1 million people died of cancer in Germany in 2018 (see Figure 1.1 D). With increasing quality of life, the burden of cancer will continue to rise. Estimates assume up to 20 % more cases in 2030 compared to 2008 (Bray et al. 2012). The reason for the increasing numbers is the constant pursuit of high levels of human development which includes population growth, aging and societal, economic and lifestyle changes (Fidler et al. 2016; World Cancer Report 2014 2014). Important characteristics for a high developed and industrialized society are smoking, alcohol use, overweight and obesity, physical inactivity and urban air pollution, which are also high-risk factors that influence the development of cancer. However, the extent of technologies to detect cancer at an early stage has been improved in the last decades to counteract increasing cancer rates, but dependent on the health system of each country, these treatment interventions are used more or less (Danaei et al. 2005).

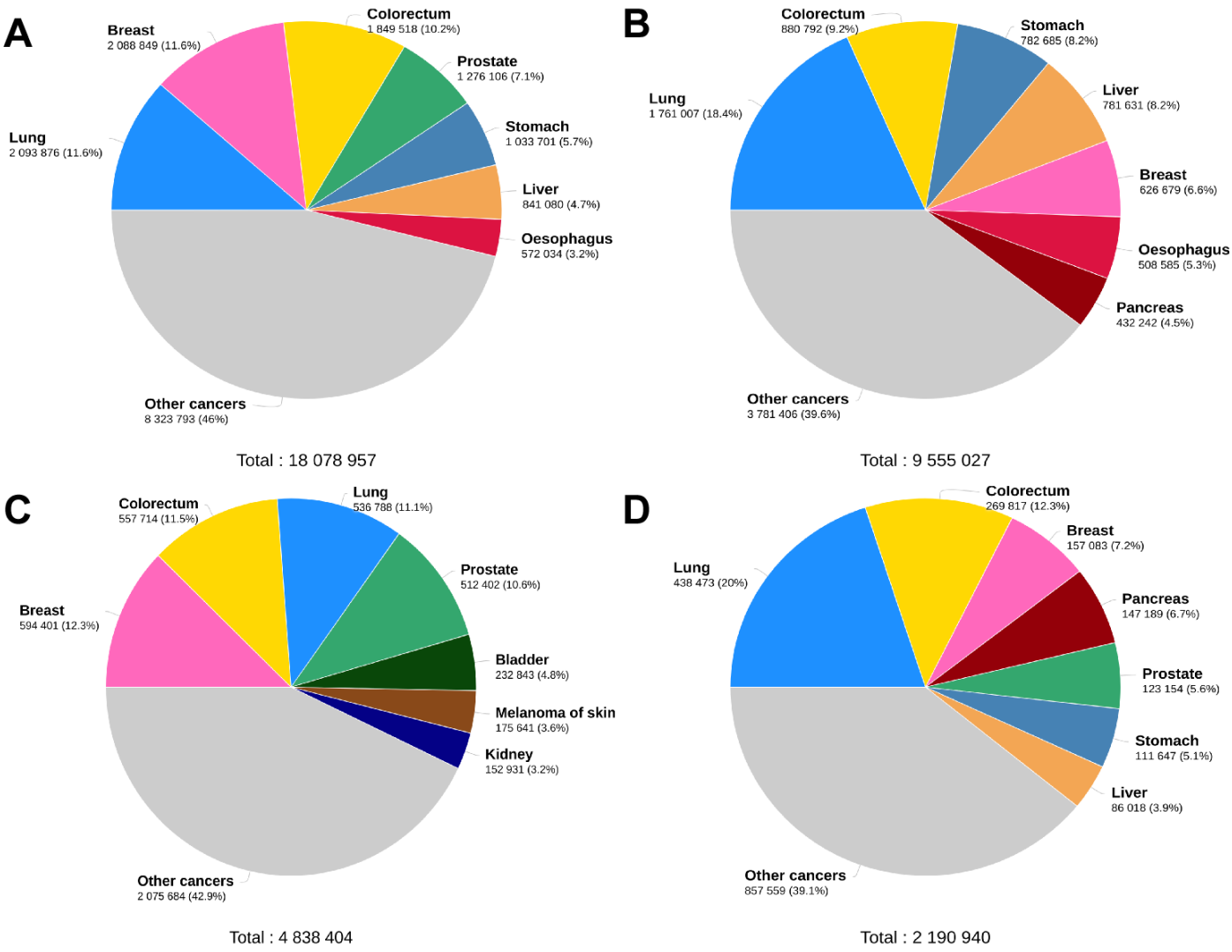

Figure 1.1: Estimated cancer incidences and death worldwide and in Germany in 2018

A) Estimated incidences worldwide in 2018 including all cancers, both sexes and all ages. **B)** Estimated deaths worldwide in 2018 including all cancers, both sexes and all ages. **C)** Estimated incidences in Germany in 2018 including all cancers, both sexes and all ages. **D)** Estimated deaths in Germany in 2018 including all cancers, both sexes and all ages. Adapted from The Global Cancer Observatory, 2018 (Cancer today 2020).

1.1.1 Carcinogenesis

Somatic cells in healthy tissues are permanently subjected to alterations within their genome (Martincorena et al. 2017). These alterations or mutations can be categorized into three groups. First, neutral mutations, which have no effect on the phenotype. Second, mutations, which have such a disadvantageous effect on the cell that the programmed cell death (apoptosis or senescence) is initiated as a consequence (Martincorena et al. 2017; Chaffer and Weinberg 2015). Last, mutations that confer

advantageous phenotypes to cells. These mutations increase proliferation and survival of the cell clone and are therefore called driver mutations (Martincorena and Campbell 2015; Martincorena et al. 2017). This process follows the principle of Darwinian evolution (Chaffer and Weinberg 2015) with a selective growth advantage for the respective cell (Nowell 1976). However, it is still unknown how many mutations are needed to develop cancer (Martincorena and Campbell 2015). Mostly occurring in tumour cells are point mutations, gene modifications or chromosomal translocations (Croce 2008).

The transformation to cancer cells can be enhanced if driver mutations occur in certain genes, such as oncogenes or tumour suppressor genes (Anderson et al. 1992; Weinberg 1991). For oncogenes, a mutation can imply a gain-of-function, meaning that the proteins, which are encoded by an oncogene are either highly expressed, or have a novel or enhanced activity in cancer cells. An increased expression of these proteins promotes cell survival because of their involvement in cell growth, differentiation and apoptosis (Anderson et al. 1992; Croce 2008). Prominent examples are MYC and RAS. MYC is an important junction of many receptor signal transduction pathways, which regulate transcription of genes involved in cell growth and proliferation (Armelin et al. 1984; Dang 2012; Kelly et al. 1983). RAS transduces signals to cell surface receptors which, in turn activate intracellular effector pathways (Pylayeva-Gupta et al. 2011). It is constantly overexpressed in 30 % of all cancers (Schubbert et al. 2007). Tumour suppressor genes are usually inactivated (loss-of-function mutation) in cancer cells and thus promote cell survival (Martincorena and Campbell 2015; Weinberg 1991; Knudson 1971). pRB and p53 are well-known examples. pRB is responsible to check if the cell is ready to proceed in the cell cycle and leave G1 phase. In cancer cells this checkpoint is not existent and cell proliferation can continue (Hahn and Weinberg 2002). p53 arrests cells with DNA damage until their damage is repaired. Is this checkpoint missing can cells with DNA damage proceed through the cell cycle (Hahn and Weinberg 2002). The main reasons for malignant transformation are genomic alterations, which promote the cells' capabilities to survive. In 2000 Hanahan & Weinberg published these capabilities as their "hallmarks of cancer" including self-sufficiency in growth signals, insensitivity to anti-growth signals, tissue invasion & metastasis, limitless replicative potential, sustained angiogenesis and evasion of apoptosis (Hanahan and Weinberg 2000). In 2011 Hanahan & Weinberg expanded their "hallmarks of cancer" capabilities, by adding tumour inflammation, genomic

instability, the evasion of immune destruction and the deregulation of cellular energetics (see Figure 1.2) (Hanahan and Weinberg 2011).

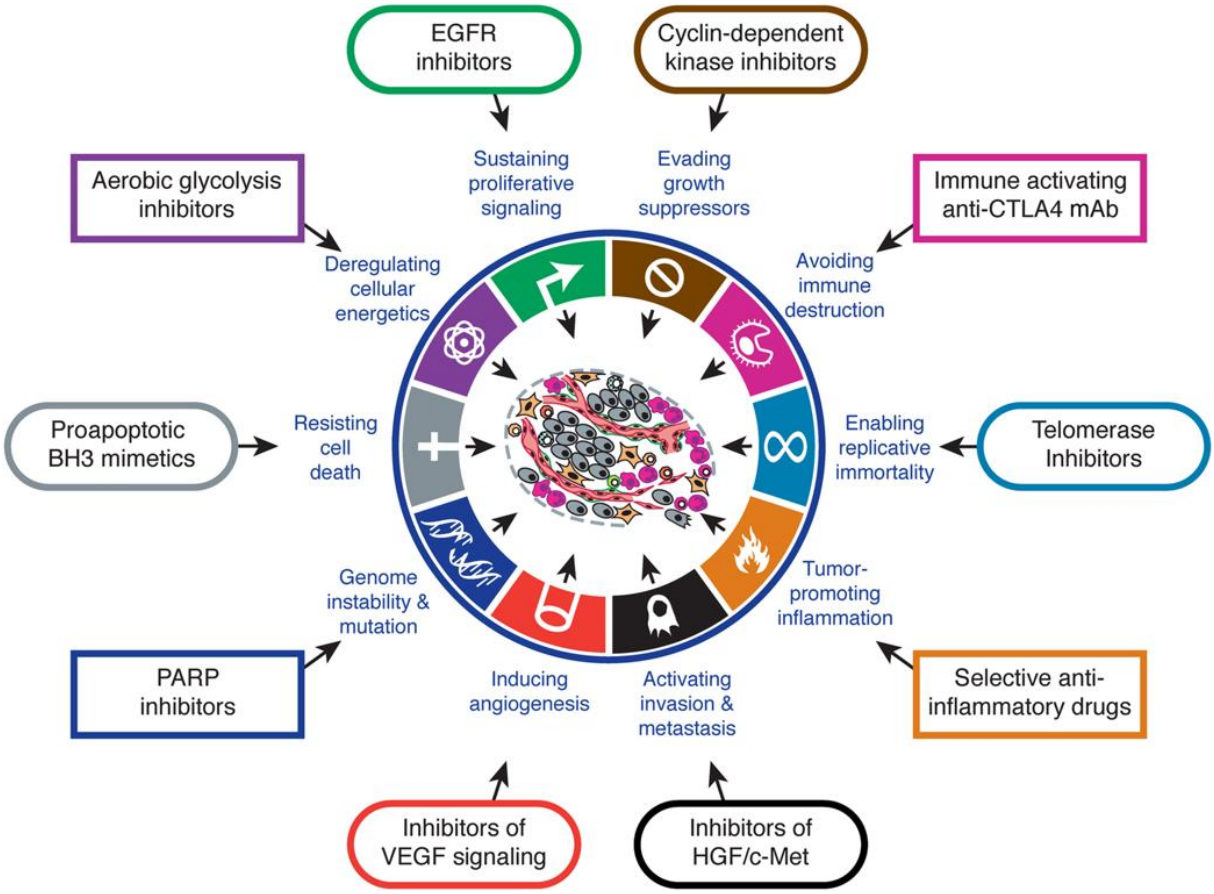

Figure 1.2: Hallmarks of cancer and their therapeutic targeting

The graphic illustrates the “hallmarks of cancer” proposed b Hanahan & Weinberg in 2011 including possible treatment approaches for each individual aspect (Hanahan and Weinberg 2011).

1.1.2 Cancer treatment

The principal task when treating cancer is to remove cancerous tissue, while maintaining healthy cells. The most prominent treatment approaches are surgery, radiotherapy and chemotherapy (Huang et al. 2017). But also immunotherapy, targeted therapy, hormone therapy and stem cell transplants are efficient approaches to conquer cancer (Types of Cancer Treatment - National Cancer Institute 2020). In most instances, these therapies are used in combination with each other. Surgery is applied in about 80 % of all cancer cases and is therefore the primary therapy. It is used as a diagnostic, preventive, curative, supportive, palliative and reconstructive instrument (Sullivan et al. 2015).

Radiotherapy shrinks the tumour, but in many cases x-rays alone are limited by tumour radio resistance in form of systemic tumour progression or metastases (Huang et al. 2017; Lavine et al. 1999; Shinoura et al. 2002). However, in two-third of cancer cases radiotherapy is applied. Mostly based on the fact that in the last years radiotherapy was highly improved by increasing the overall survival rate from 30 % to 80 % (Chen and Kuo 2017; Baumann et al. 2016). Essentially, radiotherapy acts in two ways.

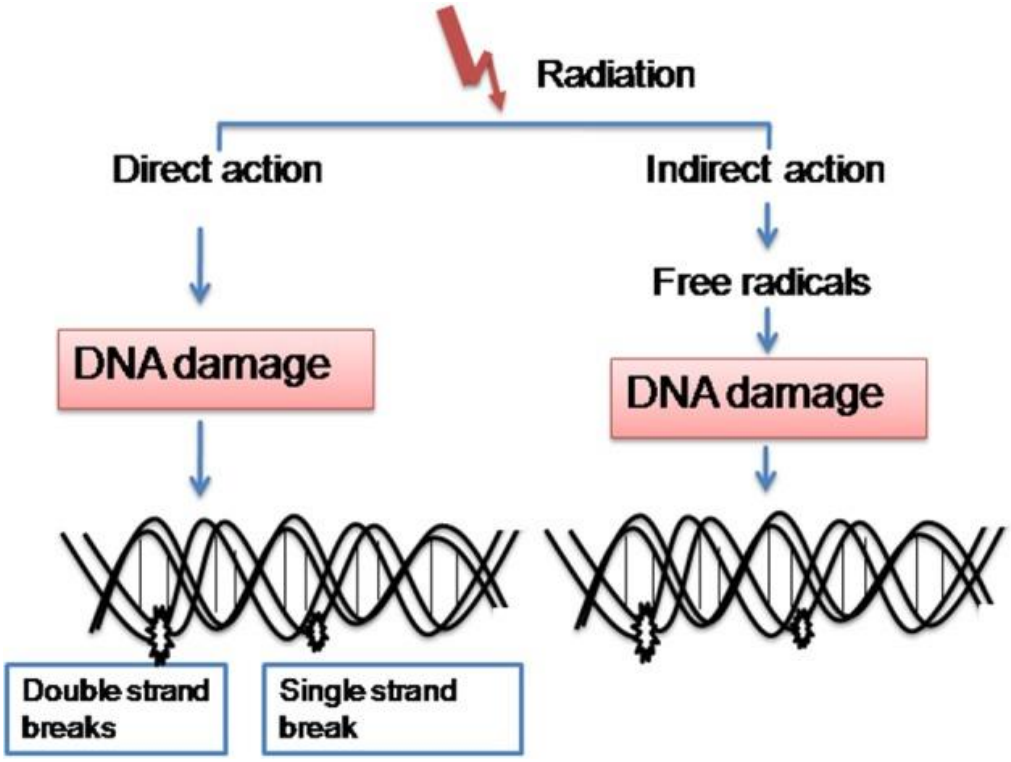

Figure 1.3: Radiation acts in two ways

Radiation either induces DSBs and/or SSBs within the DNA or indices free radicals derived from the water component of the cell, which causes damage (Baskar et al. 2014).

First, in a direct way, where x-rays cause DNA double strand breaks (DSBs) and/or single strand breaks (SSBs), respectively (see Figure 1.3). The indirect way induces free radicals that arise from the water component of the cell (see Figure 1.3) (Baskar et al. 2014). By definition, chemotherapy means the application of drugs or chemicals to attack cancer cells. Up to now there are six groups of chemicals used that are classified as follows: a) alkylating agents that induce DNA damage, b) anti-metabolites that replace the physiological nucleotides of RNA and DNA, c) antibiotics that target the enzymes of the DNA replication machinery, d) topoisomerase inhibitors that interfere with DNA unwinding enzymes essential for replication and transcription,

e) mitotic inhibitors that halt cell division and, f) corticosteroids approved for cancer treatment or to palliate side effects induced by other drugs (Huang et al. 2017). The biggest disadvantage is that this form of therapy is systemic. This means that also healthy cells are assaulted by the chemical drugs (Huang et al. 2017).

1.2 DNA damage

A continual effort to maintain genomic stability is essential for cell survival and accurate genome propagation (Aguilera and Gómez-González 2008). Therefore, cells have developed certain capabilities to ensure genomic integrity including cell cycle checkpoints and several DNA damage response (DDR) pathways, which immediately initiate DNA repair (Aguilera and García-Muse 2013; Lord and Ashworth 2012; Ciccia and Elledge 2010). If damaged cells are still able to divide because of an inactive repair system, the chance of an accumulation of mutations across generations is highly increased (Bouwman and Jonkers 2012). Typically, cancers have deregulated DNA repair pathways (Ciccia and Elledge 2010) and DNA damage is prone to induce genetic mutations (Lord and Ashworth 2012; Jackson and Bartek 2009; Ghosal and Chen 2013).

1.2.1 Sources of DNA damage and types of DNA lesions

There are two major categories of DNA damage: endogenous and exogenous damage (see Figure 1.4). The main reason for endogenous DNA damage is the DNA's involvement in hydrolytic and oxidative reactions with surrounding water and reactive oxygen species (ROS). This characteristic provokes the development of sporadic cancers (Chatterjee and Walker 2017; Visconti and Grieco 2009; Reuter et al. 2010; Perrone et al. 2016). However, replication errors, DNA mismatches and topoisomerase-DNA complexes also contribute to endogenous DNA damage (Chatterjee and Walker 2017). Base substitutions and base insertions or deletions, respectively, occur daily with a frequency of 10^{-6} to 10^{-8} per cell (Chatterjee and Walker 2017; Kunkel 2004; Kunkel 2009). Examples for replication errors are insertions or deletions of nucleotides, which can alter the reading frame (Viguera et al. 2001; Nimrat Chatterjee et al. 2013), and polymerases integrating uracil or a compromised

nucleotide because of altered concentrations of dNTPs in the cell's surrounding environment (Chatterjee and Walker 2017; Andersen et al. 2005b; Vértessy and Tóth 2009; Kumar et al. 2011; Clausen et al. 2013; Buckland et al. 2014; Potenski and Klein 2014). Topoisomerase I is responsible for uncoiling the DNA helix during replication or

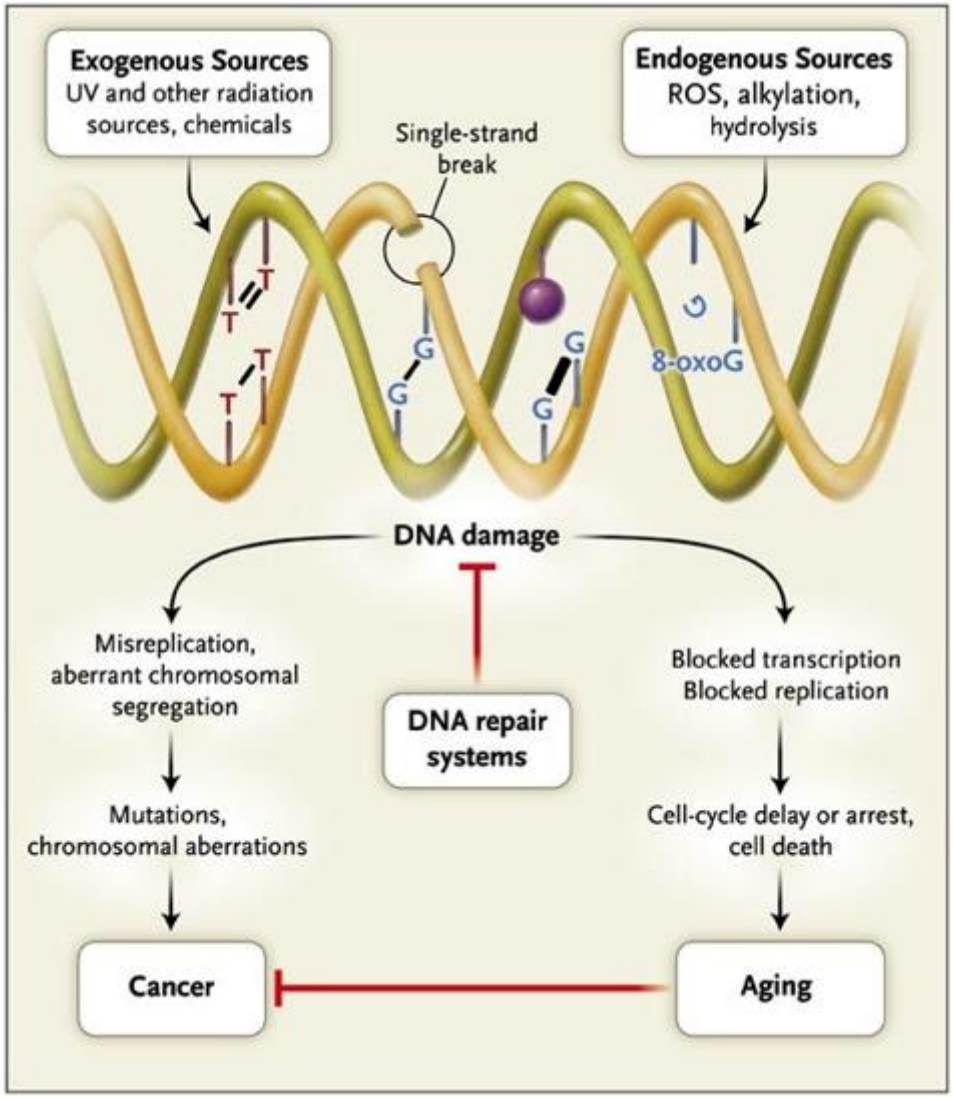

Figure 1.4: Sources and consequences of DNA damage

DNA damage can be of endogenous or exogenous origin. Reactive oxygen species (ROS) or hydrolysis within the cell are responsible for endogenous damage. This damage can lead to oxidative stress or abasic sites. Exogenous damage is induced by IR, UV-light or cigarette smoke and causes photoproducts or DSBs and SSBs, respectively. Both pathways can result in incorporated mutations which can lead either to misreplication and mutations across generations followed by the development of cancer, or to blocked transcription or replication, which can lead to damage-induced cell death (Hoeijmakers 2009).

transcription. For this, topoisomerase I has to cut the DNA strand. After replication or transcription, respectively, the DNA strand has to reassemble again. This is conducted by topoisomerase I, which ligates the 5'-OH group of the DNA to the tyrosine-DNA phosphodiester bond (Chatterjee and Walker 2017; Carey et al. 2003; Stewart et al. 1998). Occurrences of misalignments in this step can lead to DNA lesions (Pommier and Cherfils 2005; Pommier and Marchand 2005). Another major reason for spontaneous mutagenesis is base deamination, which can change one nucleotide into another (Sinha and Häder 2002).

Exogenous DNA damage is caused by environmental and/or genotoxic chemicals like ionizing radiation (IR) (wavelength 10^{-3}-10 nm), UV light (wavelength 10-400 nm) or cigarette smoke (Hoeijmakers 2001). As above-mentioned (see section 1.1.2), IR or radio therapy, respectively, damage the DNA directly by inducing DSBs and SSBs or indirectly by inducing free radicals, which attack the DNA (Baskar et al. 2014). While the principal consequences of UV radiation are cyclobutene pyrimidine dimers (CPD) and 6-4 photoproducts (Sinha and Häder 2002). Agents, such as cigarette smoke (1,000 DNA lesions per cell), industrial chemicals, mustard gases and several drugs used in chemotherapy (see section 1.1.2) also induce DNA damage (Lord and Ashworth 2012).

1.2.2 DNA damage response

To maintain genetic integrity, cells have developed a specific mechanism – the DNA damage response (see Figure 1.5) – to recognize DNA lesions and promote their repair (Jackson and Bartek 2009; Li et al. 2016a). Cell cycle checkpoints become activated to arrest cells and allow time for DNA damage repair (Harper and Elledge 2007). The predominant roles are adopted by the DNA-dependent protein kinase (DNA-PK), ataxia-telangiectasia-mutated (ATM) and ATM and Rad3-related (ATR) (Li et al. 2016a), which are all members of the phosphoinositide 3-kinase-related kinase (PIKK) family. The DDR includes processes like base excision repair (BER), nucleotide excision repair (NER), homologous recombination (HR) and non-homologous end-joining (NHEJ) (Lombard et al. 2005; Shimizu et al. 2014). DNA-PK and ATM are common mediators in DSB response and ATR acts as a downstream factor of replication protein A (RPA) mediating together with its partner ATR interacting protein (ATRIP) the SSB response (Li et al. 2016a; Zou and Elledge 2003). First step in the

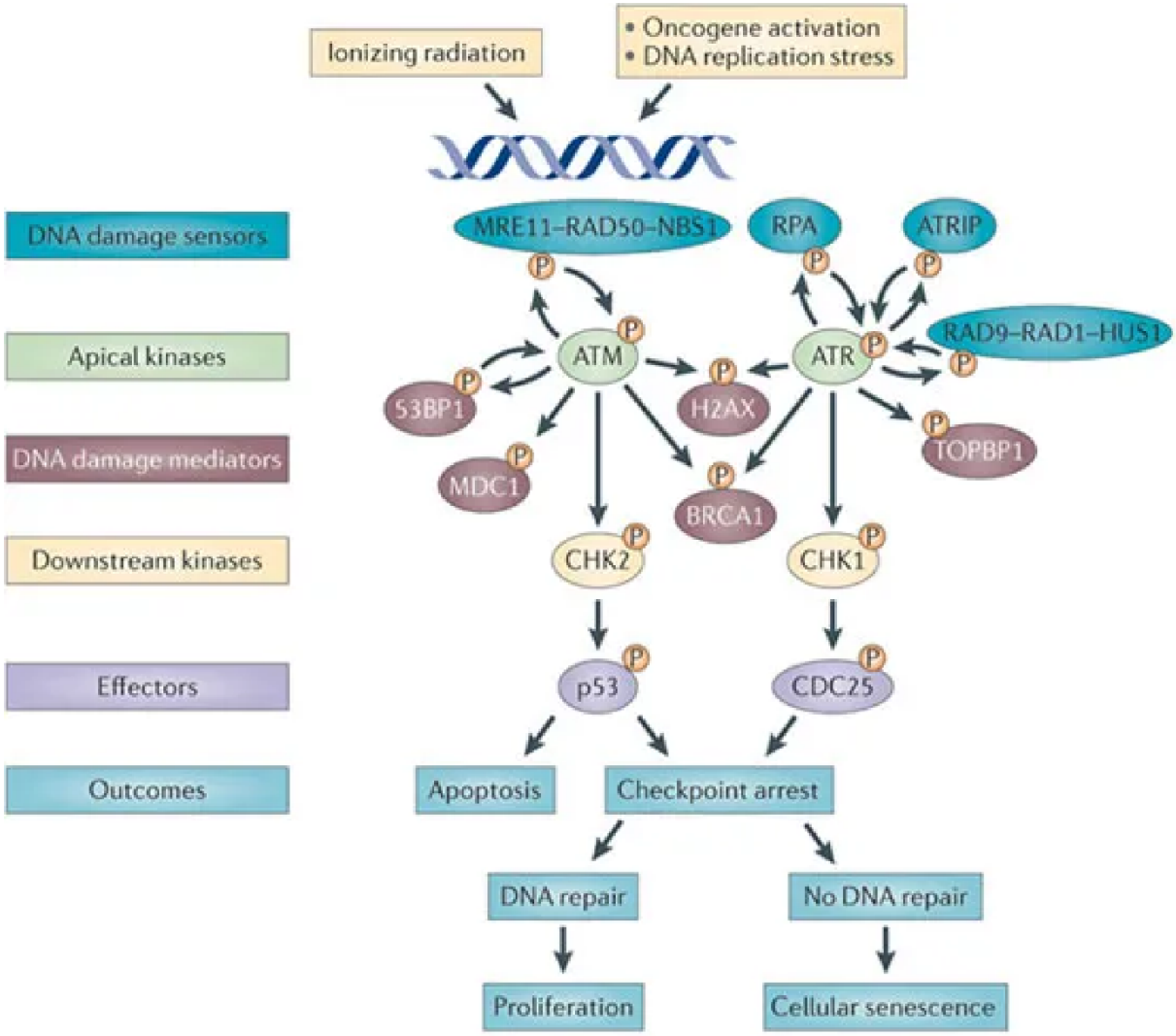

Figure 1.5: The DNA Damage Response (DDR)

At the beginning, there are two essential sensors: the Mre11-Rad50-Nbs1 (MRN) complex for detecting DSB and RPA and Rad9-Rad1-Hus1 (9-1-1) complex for detecting SSB. These two activate by phosphorylation either ATM and ATR in interaction with ATRIP. On the one hand, both phosphorylate H2AX at Ser139 which is able to recruit Mdc1 for further activation of other DNA damage mediators like 53BP1 and BRCA1, or on the other hand they recruit Chk1 and 2 for checkpoint activation and cell cycle arrest (Sulli et al. 2012).

DDR is the recognition of DNA damage. Depending on which DNA damage occurs several proteins can detect the DNA lesions. DSBs are recognized by the Mre11-Rad50-Nbs1 (MRN) mediator complex, which activates ATM and guides it to the place of damage (Harper and Elledge 2007). SSBs are immediately coated by RPA that is then recognized by the ATR-ATRIP complex, which binds to the DNA and mediates the DNA repair (Zou and Elledge 2003). At the site of DNA lesion H2AX is phosphorylated on Ser139 (γH2AX) by ATM, ATR and DNA-PK (Rogakou et al. 1998), leading to the recruitment of mediator of DNA damage checkpoint 1 (Mdc1) (Harper

and Elledge 2007; Stucki and Jackson 2006). Mdc1 together with γH2AX is responsible for recruitment of further repair proteins, for example RAP80, 53BP1, KAP-1 and BRCA1 (Jackson and Bartek 2009; Paull et al. 2000; Vignard et al. 2013; Thompson 2012; Stewart et al. 2003). Further downstream, checkpoint kinases Chk2 and Chk1 are phosphorylated by ATM and ATR, respectively. They in turn phosphorylate p53 and the cell division cycle 25 (Cdc25) phosphatases. These two effectors are responsible for checkpoint activation and cell cycle arrest (Vignard et al. 2013). After recognition of damage, certain repair pathways take action to repair the DNA depending on the type of (see section 1.3).

1.3 DNA repair pathways

As above-mentioned (see section 1.2.1), many types of DNA lesions exist. Typically, SSBs undergo either base excision repair or nucleotide excision repair, while DSBs are repaired by either homologous recombination or non-homologous end-joining (Lombard et al. 2005).

1.3.1 Base excision repair (BER)

BER mainly repairs damage that include oxidative damage, deamination, alkylation and abasic single base alterations (see Figure 1.6) (Chatterjee and Walker 2017; Friedberg 2003). Two ways of BER exist, the short patch repair way and the long patch repair way. In short patch repair, first, the DNA glycosylase distinguishes DNA lesions (Odell et al. 2013; Chatterjee and Walker 2017) and excises the damaged base. Afterwards, an apurinic/apyrimidinic endonuclease (APE) induces a nick within the phosphodiester bond and simultaneously creates a hydroxyl residue (Caldecott 2008). The remaining deoxyribose phosphate (dRP) is recognized by the DNA polymerase β (Pol β) that reconstructs the dRP residue with its lyase domain (Caldecott 2008; Chatterjee and Walker 2017; Fu et al. 2012; Almeida and Sobol 2007). At the same time the polymerase fills the gap with the corresponding nucleotide (Fu et al. 2012; Chatterjee and Walker 2017). Finally, a ligase finishes the repair by creating the final phosphodiester bond (Caldecott 2008). During long patch repair a longer DNA

fragment is exchanged instead of one single base, but the mechanisms are comparable (Fu et al. 2012).

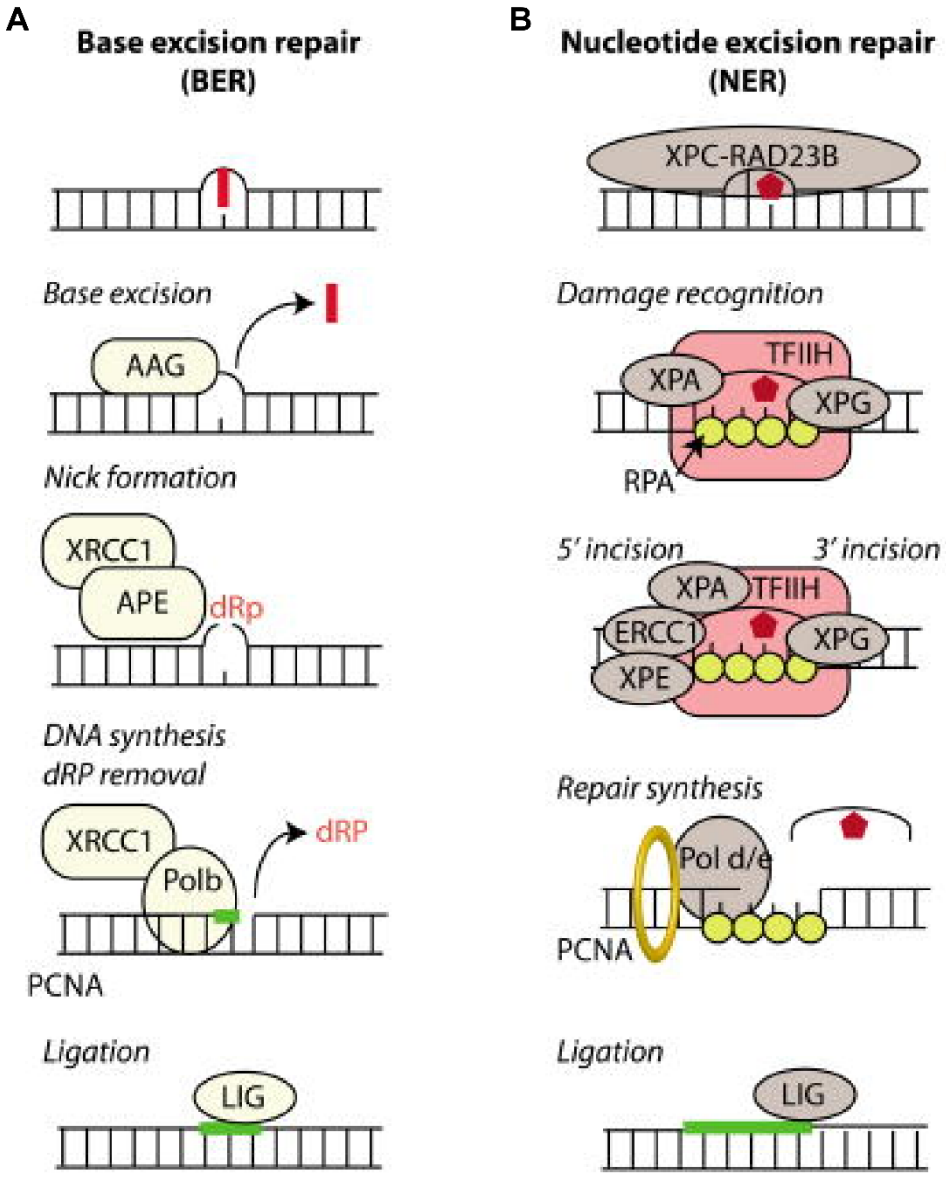

Figure 1.6: Excision repair pathways

A) BER is responsible for repair of alkyl or oxidative base lesions. Therefore, a DNA glycosylase removes the damaged base. Afterwards, an AP-endonuclease detect the dRP residue and cuts the sugar backbone. Pol β fills the gap with a corresponding nucleotide and finally the ligase assembles the phosphodiester bond. **B)** NER removes bulky lesions within the DNA. The lesions are recognized by a XPC complex and the TFIIH complex unwinds the DNA. Activated XPG and XPF proteins cut the DNA upstream and downstream of the lesion and release an oligonucleotide of 27–29 bases. The gap is filled with nucleotides by Pol ε or Pol δ followed by a ligation step (Fu et al. 2012).

1.3.2 Nucleotide excision repair (NER)

In contrast to BER, NER (see Figure 1.6) repairs bulk lesions like CPDs or (6-4) photoproducts induced by UV-light or genotoxic chemicals (Chatterjee and Walker 2017). The NER pathway can be distinguished into two sub pathways, global genome NER (GG-NER) and transcription-coupled NER (TC-NER). They differ with respect to the lesion they repair and the participating proteins (Lombard et al. 2005; Mitchell et al. 2003). During GG-NER the main sensor proteins for detecting lesions are XPC (Xeroderma pigmentosum, complementation group C) and XPE (Masutani et al. 1994; Nishi et al. 2005; Nouspikel 2009). The detecting proteins during TC-NER are CAS (cockayne syndrome WD repeat protein A) and CSB, which remove the RNA polymerase II from the DNA. In both pathways a common NER factor is activated to uncoil the DNA at the place of damage, namely TFIIH (transcription initiation factor II H), with its two subunits XPB and XPD (Lombard et al. 2005; Chatterjee and Walker 2017). The unwound DNA is protected by RPA. Activated endonucleases XPG und ERCC1-XPF cleave the DNA upstream and downstream of the lesion and remove an oligonucleotide of 27-29 nucleotides (Fu et al. 2012). After excision, the DNA is filled template-dependent by Pol ε or Pol δ with corresponding nucleotides and is re-ligated (Yang 2011).

1.3.3 Homologous recombination (HR)

HR (see Figure 1.7) is predominantly employed in late S phase or G2 phase as it uses template-directed DNA repair (Jackson and Bartek 2009; Li and Heyer 2008). As mentioned in section 1.2.2 the MRN complex recognizes DSBs and recruit ATM (Stracker and Petrini 2011). ATM then phosphorylates H2AX (γH2AX), which then recruits Mdc1 (Bhatti et al. 2011). Both γH2AX and Mdc1 monitor the activation of 53BP1 and BRCA1 (Scully et al. 2004), which in turn ubiquitinate downstream target CtIP (CtBP interacting protein) (Chapman et al. 2012; Yu et al. 2006). To resect the DNA lesion, CtIP and the endonuclease activity of the MRN complex cut the DNA (Sartori et al. 2007) and EXO1 or BLM together with DNA2 (Chen et al. 2008a; Nimonkar et al. 2011) remove a long-range DNA fragment. The result is a 3’ single stranded tail, which is immediately coated by RPA (Chatterjee and Walker 2017). Later,

Rad51 replaces RPA and forms a nucleoprotein filament with the help of BRCA2 and PALB2 (Chatterjee and Walker 2017; Jackson and Bartek 2009; Lord and Ashworth 2012). The ssDNA invades the undamaged DNA template (Khanna and Jackson 2001)

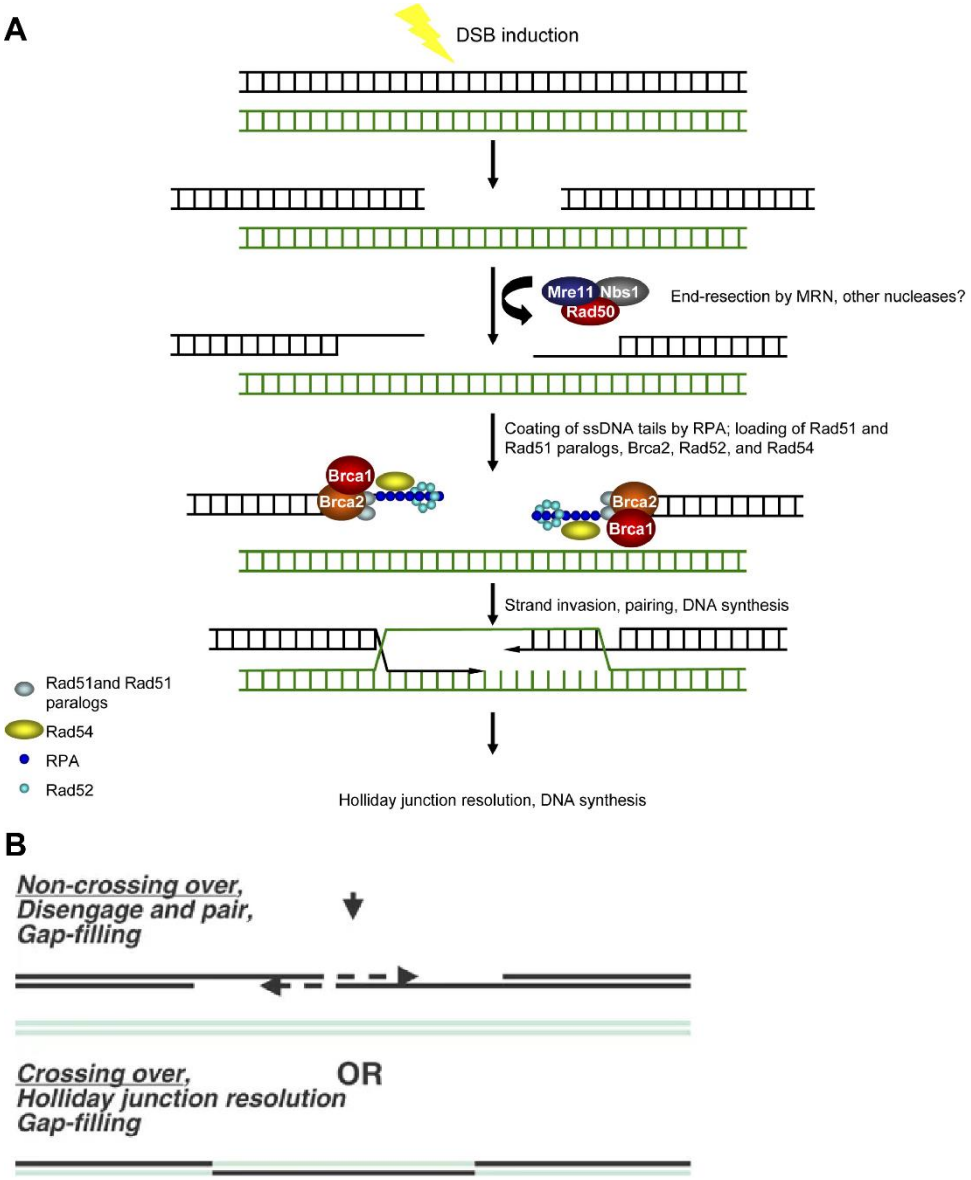

Figure 1.7: Homologous recombination at DSBs

A) At an early stage, the MRN complex recognizes the DNA lesion and activates ATM, which in turn phosphorylates H2AX. γH2AX recruits Mdc1 and both activate monitor proteins 53BP1 and BRCA1. They have downstream targets such as CtIP, which cuts with the help of the MRN complex the DNA. The resulting 3' single stranded tails are coated by RPA and later Rad51. With the help of BRAC2 and PALB2 they form nucleoprotein filaments, which invade the unbroken DNA sister chromatid (D-loop). Gaps are filled up with DNA polymerase activity (Lombard et al. 2005). **B)** Two different ways can conclude HR, non-crossing over while the new DNA strand is ligated to the original DNA strand and crossing over, while the Holliday junctions are crossed over and the new DNA strand is ligated to the sister chromatids DNA (Valerie and Povirk 2003).

and forms a so-called displacement loop (D-loop) (Chatterjee and Walker 2017; Holloman 2011; Zhang et al. 2009) that is extended by DNA polymerase, which takes its information from the template (Khanna and Jackson 2001). After invasion so called Holliday junctions are formed (Khanna and Jackson 2001). There are two ways to end HR. Firstly, the Holliday junctions can be displaced and the newly synthesized strand is re-ligated with its original DNA strand, while the gaps are filled up and sealed by ligase (see Figure 1.7 A) (Valerie and Povirk 2003). Here, the D-loop is dissolved by the RTEL1 enzyme (Barber et al. 2008). Secondly, the Holliday junctions can cross-over and the gaps then are filled up and sealed by ligase (see Figure 1.7 B) (Valerie and Povirk 2003). In mammalian cells the non-crossing over event is favoured during HR (Johnson and Jasin 2000).

1.3.4 Non-homologous end-joining (NHEJ)

In contrast to HR, NHEJ (see Figure 1.8) is less accurate, because the broken DNA ends are directly ligated without a DNA template, which can lead to loss of nucleotides and ultimately to a loss of genetic integrity (Weterings and Chen 2008). Because a DNA template is not needed, NHEJ can occur at all times during the cell cycle (Weterings and Chen 2008). The first step is initiated by the Ku heterodimer (Ku70 and Ku80) recognizing DSBs and coating both ends of the lesion (Weterings and Chen 2008; Mari et al. 2006; Soutoglou et al. 2007; Pang et al. 1997). The heterodimer prevents end resection and forms a scaffold for other repair factors such as DNA-PK$_{cs}$, XRCC4/DNA ligase 4 (X4LIG4) complex (Wu et al. 2009), XRCC4-like factor (XLF) and Aprataxin-and-PNK-like factor (APLF) (Chatterjee and Walker 2017; Gottlieb and Jackson 1993; Nick McElhinny et al. 2000; Costantini et al. 2007; Yano et al. 2008; Grundy et al. 2013). Among them is DNA-PK$_{cs}$ one of the first members, which is recruited to the site of damage. It phosphorylates other scaffold members in its vicinity and it, furthermore, auto phosphorylates itself (Gottlieb and Jackson 1993; Weterings and Chen 2008; Yoo and Dynan 1999). At the same time stabilizes XRCC4 the scaffold in association with Ku70/80 (Hammel et al. 2011; Malivert et al. 2010; Andres et al. 2012). The whole complex of Ku70/80, DNA-PKcs and XRCC4 brings both DNA ends together (Weterings and Chen 2008). Further components of the complex Artemis, PNKP, APLF, WRN, Aprataxin and Ku process the DNA ends to obtain suitable termini

(Ma et al. 2002; Bernstein et al. 2005; Ahel et al. 2006; Perry et al. 2006; Roberts et al. 2010; Li et al. 2011), however, during this step nucleotides get lost (Weterings and Chen 2008). After processing, the XRCC4/ligase 4 complex induces ligation of the DNA ends, enhanced by XLF (Cottarel et al. 2013; Gu et al. 2007; Tsai et al. 2007).

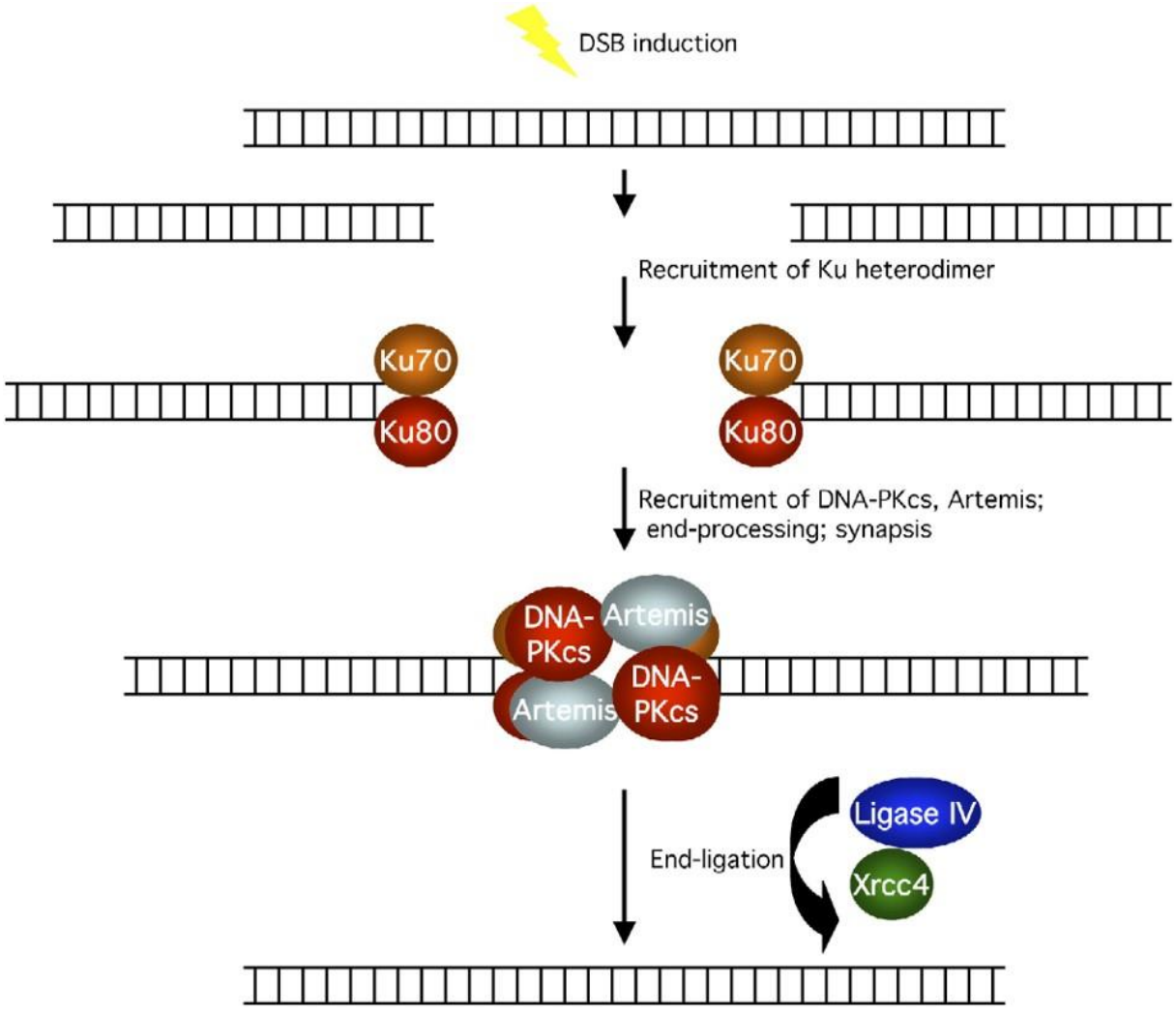

Figure 1.8: Non-homologous end-joining at DSBs

The first component, which recognizes a DSB is the Ku70/80 heterodimer. It builds a scaffold for other repair proteins. The first member recruited by Ku70/80 is DNA-PK$_{cs}$. By phosphorylation and autophosphorylation of DNA-PK$_{cs}$ both DNA ends are brought together. Processing the DNA ends provides suitable ends, which can be ligated. During this step nucleotides can get lost. The XRCC4 complex ligates the gaps to complete NHEJ (Lombard et al. 2005).

1.4 Chromatin

Eukaryotic cells contain thousands of genes that all need to be accommodated within the nucleus, therefore the DNA is highly packed. For this the DNA associates with a number of different proteins and RNAs, which is called chromatin (Misteli 2007). The chromatin is involved in all essential nuclear processes, including DNA transcription, DNA replication and DNA repair (Fyodorov et al. 2018; Richmond and Davey 2003).

1.4.1 Chromatin architecture and modification

The first level of compaction is the formation of nucleosomes (see Figure 1.9) (Kornberg 1977). Here, about 145-147 base pairs are wrapped around an octamer consisting of two copies of each histone protein H2A, H2B, H3 and H4 (Luger et al. 1997). All histone proteins are positively charged to enable bounding of the negatively charged backbone of the DNA (Fyodorov et al. 2018). Nucleosomes recur every 200 base pairs (McGhee and Felsenfeld 1980), forming a 10 nm “beads-on-a-string” fibre (Tonna et al. 2010). The next higher-order structure consists of the nucleosome with the bound linker histone H1 or H5, called chromatosome (Fyodorov et al. 2018; Luger et al. 1997). The chromatosome core particle is packed into short-range internucleosomal interactions to build a 30 nm chromatin fibre (Bonev and Cavalli 2016). Further condensation is reached during mitosis and meiosis, where the chromatin fibre is packed in a metaphase chromosome to protect the DNA and to provide physical strength for segregation (Saha et al. 2006).

Due to the high level of compaction of the genetic material, the nucleosome also acts as a repressor for DNA-binding transcription factors and RNA polymerases (Bonev and Cavalli 2016; Weber and Henikoff 2014). To maintain faithful gene expression several mechanisms have developed, such as post-translational modifications of histones, chromatin remodelling or replacement of individual histones for certain histone variants (Weber and Henikoff 2014; Cremer et al. 2006). The most common epigenetic modifications are acetylation, methylation, phosphorylation, ubiquitination and sumoylation (Kouzarides 2007). They are responsible for loosening chromatin by

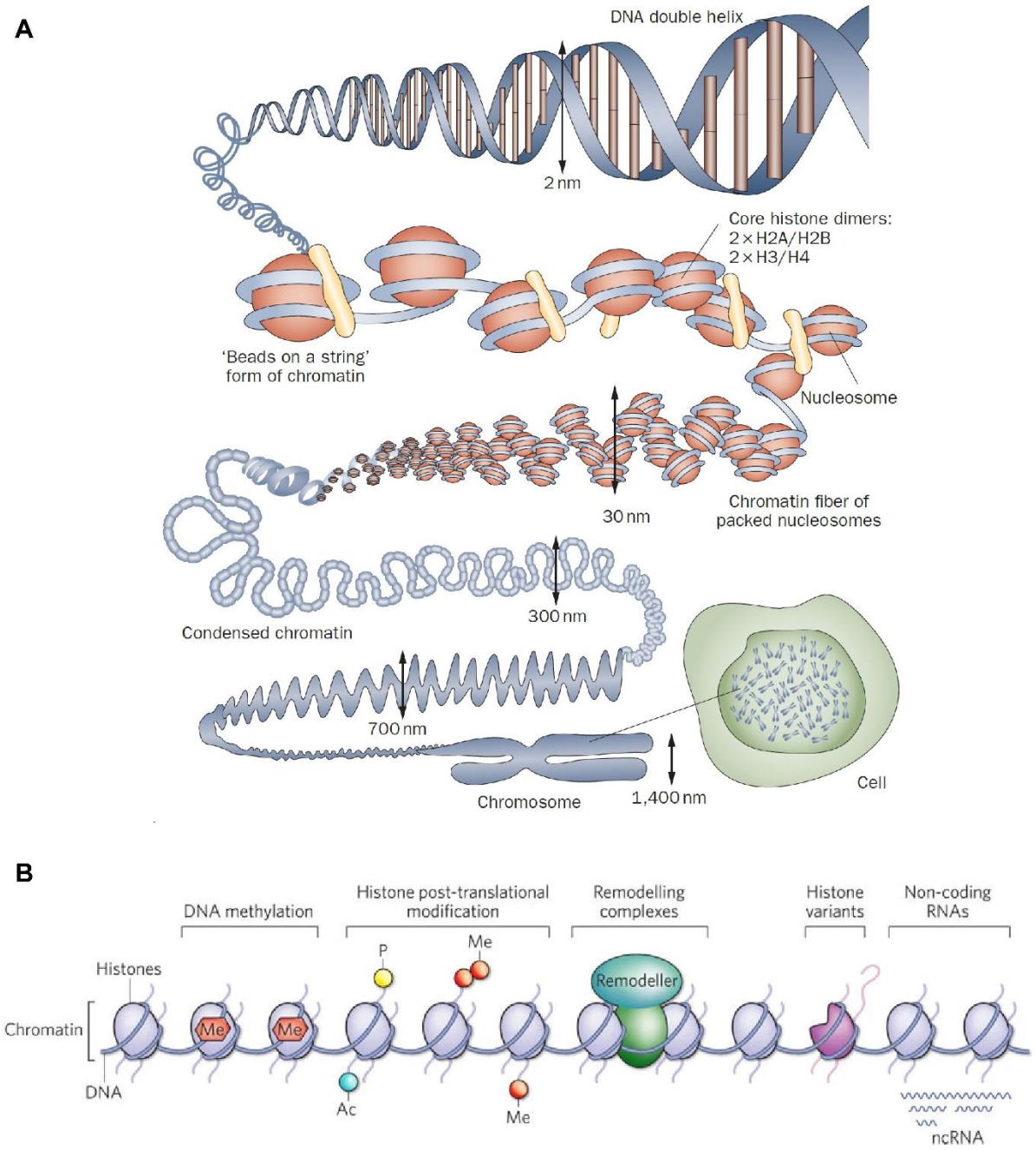

Figure 1.9: Composition and modifications of chromatin

A) 145-147 base pairs are wrapped around an octamer consisting of two copies of each histone protein H2A, H2B, H3 and H4, building a nucleosome. Several nucleosomes form a "bead-on-a-string" formation linked with linker DNA. Further packing is achieved by a linker histone H1 or H5, which links nucleosomes to form a chromatin fibre. A metaphase chromosome is obtained during mitosis and meiosis, respectively, by further compaction of the genetic material (Tonna et al. 2010). **B)** Although the DNA can be highly condensed it can still be regulated by post-translational modifications like methylation (Me), acetylation (Ac), phosphorylation (P), remodelling complexes or histone variants (Dulac 2010).

interfering with the contact between two nucleosomes and/or for the recruitment of non-histone proteins (Kouzarides 2007). Acetylation for example opens the DNA by neutralizing the charge of a lysine causing a reduced binding to the negatively charged

DNA backbone (Kouzarides 2007). In contrast, methylation of histones causes a more tightened DNA, which restricts regulatory factors' access to genes, thereby silencing the expression of genes (Jenuwein and Allis 2001; Rothbart and Strahl 2014). Replacement of histone proteins H2A, H2B, H3 or H4 by their variants not only influences the physical properties of nucleosomes but also their dynamic (Weber and Henikoff 2014). Histone variants are for example CENP-A (also called cenH3), which replaces H3 in centromeric nucleosomes to indicate the centromere (Schalch and Steiner 2017; Earnshaw and Rothfield 1985; Earnshaw et al. 2013; Talbert et al. 2012; Talbert and Henikoff 2013; Palmer et al. 1987), and H2A.Z, which stimulates chromatin remodelling activity (Weber and Henikoff 2014; Volle and Dalal 2014).

Chromatin can be distinguished into two domains (Bickmore and van Steensel 2013). On the one hand, euchromatin with its more relaxed chromatin status to allow transcription factors access, and on the other hand heterochromatin, which is highly condensed and not accessible (Grewal and Jia 2007; Huisinga et al. 2006; Dillon 2004). Heterochromatin formation comprises several information such as chromosomal location, nuclear localization and repetitive DNA elements (Grewal and Jia 2007; Craig 2005; Weiler and Wakimoto 1995; Birchler et al. 2000; Steitz 2004). It can be divided into two sub categories: constitutive heterochromatin remains highly packed throughout an organisms lifespan and contains elements such as centromeres and telomeres, and facultative heterochromatin is established to permanently silence genes such as the inactive X chromosome or promotors for genes silenced during development (Craig 2005; Brockdorff 2002; Orlando 2003; Rand and Cedar 2003).

1.4.2 Chromatin-binding protein HP1

As mentioned (see section 1.4.1), heterochromatin can be divided into facultative and constitutive heterochromatin, with centromeres and telomeres belonging to the latter. A major factor playing a part in the repression of gene expression within constitutive heterochromatin is the heterochromatin-associated protein 1 (HP1) (Saunders et al. 1993). HP1 predominantly binds to K9-trimethylated H3 (H3K9me3), which is mainly present in constitutive heterochromatin (Machida et al. 2018; Bannister et al. 2001a; Lachner et al. 2001; Nakayama et al. 2001; Jacobs and Khorasanizadeh 2002; Nielsen et al. 2002; Nishibuchi et al. 2014). There are three different isoforms of HP1, HP1α, HP1β and HP1γ (Canzio et al. 2014). While HP1α and HP1β are located at the

constitutive chromatin, is HP1γ evenly spread throughout the nucleus (Minc et al. 1999; Nielsen et al. 2001). The binding of HP1 to H3K9me3 histone is mediated by its N-terminal chromodomain (CD) (Nishibuchi et al. 2014; Canzio et al. 2014; Lachner et al. 2001; Nakayama et al. 2001; Bannister et al. 2001b; Rea et al. 2000; Yi et al. 2018), while its C-terminal chromoshadow domain (CSD) represents a binding stage for other effector proteins (Brasher et al. 2000; Cowieson et al. 2000; Maison and Almouzni 2004). Because of this, HP1 is directly involved in the repression of gene expression (Bannister et al. 2001a; Jacobs and Khorasanizadeh 2002; Lachner et al. 2001).
Beyond that, HP1 is involved in processes like DNA repair, mitosis and DNA replication (Kwon and Workman 2011). The protein that links HP1 to replication is the chromatin assembly factor (CAF1), which is responsible for dispersing histone H3 and H4 on newly synthesized DNA during replication (Kaufman et al. 1995; Gaillard et al. 1996). Together with the proliferating cell nuclear antigen (PCNA), CAF1 ensures the proper distribution of parental and newly synthesized histones to the two daughter strands and helps to assemble the nucleosomes ahead of the replication fork (Moggs et al. 2000; Shibahara and Stillman 1999). However, transition of the replication fork leads to a loss of HP1 binding to the chromatin, an instance CAF1 is likely to compensate for. Therefore, HP1 is able to recruit proteins that generate post-translational modification (PTM's) on the nucleosomes (Kwon and Workman 2011). Moreover, the CAF1-HP1 complex has been shown to be recruited to DNA damage sites and assume responsibility in DNA damage signalling and repair (Baldeyron et al. 2011; Ayoub et al. 2009; Luijsterburg et al. 2009; Zarebski et al. 2009). In mitosis, HP1 mediates the dissociation of the inner centromere protein (INCENP) from the chromosomes to allow for it to be relocated to the spindle apparatus (Ainsztein et al. 1998). After Aurora B-mediated phosphorylation of H3 (H3S10p), HP1 dissociates from the heterochromatin to promote mitosis progression (Hirota et al. 2005).

1.5 Cell cycle

The cell cycle (see Figure 1.10) assumes the responsibility to control the doubling of the genetic material and other cell components and afterwards the separation of the cell into two daughter cells (Barnum and O'Connell 2014). The doubling of DNA takes

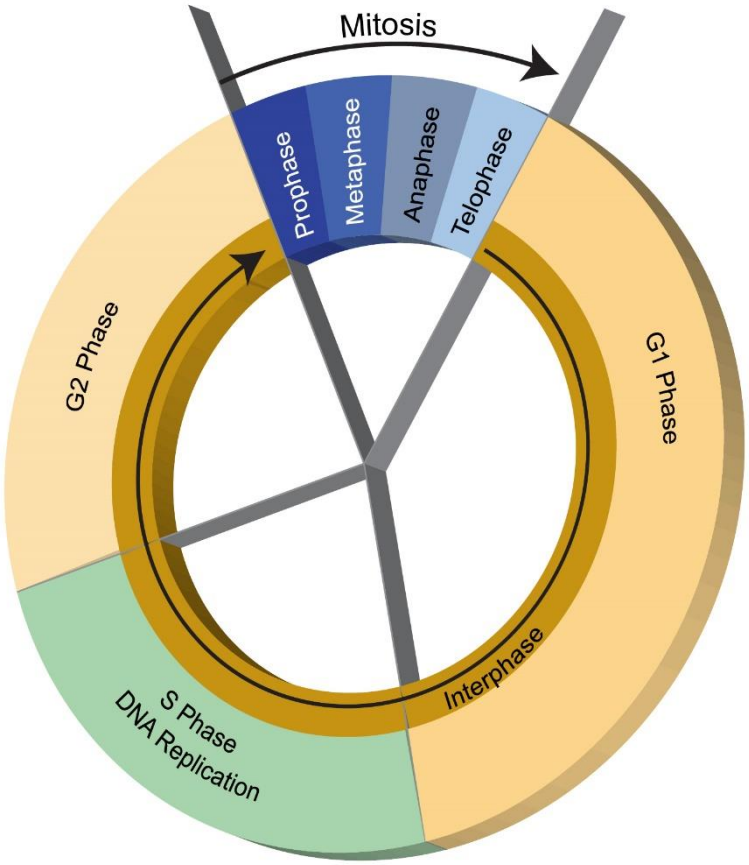

Figure 1.10: The cell cycle

The cell cycles responsibility is to double the genetic material and various cell components and to distribute those onto two daughter cells. Two main phases exist, interphase and mitosis. The interphase consists of G1 phase, S phase and G2 phase. During S phase is the DNA content doubled and during G1 and G2 is phase the cell prepared for either DNA replication or segregation, respectively. During mitosis, the condensed chromosomes are separated into two daughter cells within five phases, prophase, metaphase, anaphase, telophase and the cytokinesis (Adapted from the National Human Genome Research Institute, 2020).

place in the so-called S phase (synthesis phase) during replication, whereas the doubled DNA is parcelled into two separate cells during M phase, the mitosis. Both phases are separated by two gap phases, G1- and G2 phase. These gap phases are not informed by inactivity, on the contrary the cell rather undergoes several control mechanisms to monitor entry into S or M phase, respectively. Cells grow in size,

organize replication of the genome and prepare for chromosome segregation (Barnum and O'Connell 2014; Norbury and Nurse 1992; Vermeulen et al. 2003). G1, S and G2 phase together are referred to as interphase and account for up to 90 % of the cell cycles' duration, whereas mitosis only makes up a short period of time. Mitosis can be subdivided into prophase, metaphase, anaphase, telophase and cytokinesis (Barnum and O'Connell 2014). Cells, which have experienced a certain amount of DNA damage or certain numbers of cell cycles, are forced to leave the cell cycle during G1 phase and enter the G0 phase. In this phase, the cells are quiescent or senescent, while remaining viable, however they will not enter the cell cycle again (Zhang 2007).

1.5.1 Cell cycle regulation

The main drivers for cell cycle progression are the cyclin-dependent kinases (CDKs). They phosphorylate downstream targets to provoke entry into S or M phase, respectively (Barnum and O'Connell 2014; Morgan 1995). CDKs are activated by their corresponding cyclin subunits (see Figure 1.11). The expression of certain cyclins varies throughout the cell cycle, whereas the concentration of CDKs remains stable. This leads to a periodical activation of CDKs at certain time points (Morgan 1995; Barnum and O'Connell 2014; Lim and Kaldis 2013; Vermeulen et al. 2003).

Starting in G1 phase, growth factors stimulate cyclin D expression, which then binds to CDK4 and CDK6. This association leads to phosphorylation of pRB (retinoblastoma tumour suppressor gene), which dissociates from its binding partner histone deacetylase protein (HDAC). Disruption of this complex causes a release of transcription factors E2F-1 and DP-1 that regulate expression of genes required for progression to S phase like cyclin A, cyclin E and DNA polymerase (Vermeulen et al. 2003; Buchkovich et al. 1989; Brehm et al. 1998; Kato et al. 1993). As a result, the complex of cyclin E with CDK2 mainly occurs at G2/S phase transition (Ohtsubo et al. 1995) and is responsible for phosphorylation of histone H1 (see section 1.4.2), which plays a pivotal role for chromosome condensation (Bradbury et al. 1974; Vermeulen et al. 2003). Especially the expression of cyclin E decreases over the time the cell needs to progress to S phase (Vermeulen et al. 2003). Throughout this process is cyclin E replaced by cyclin A as a binding partner of CDK2. This complex is then responsible for the onset of replication by phosphorylating DNA polymerase α-primase (Voitenleitner et al. 1997; Walker and Maller 1991). After initiation of replication,

cyclin A forms a complex with CDK1 to reinforce entering into mitosis. The process of mitosis itself, however, is mediated by the cyclin B-CDK1 complex, which coordinates the breakdown of the nuclear envelope and initiates prophase (Sánchez and Dynlacht 2005). To stop the cell cycle progression under unfavourable conditions,

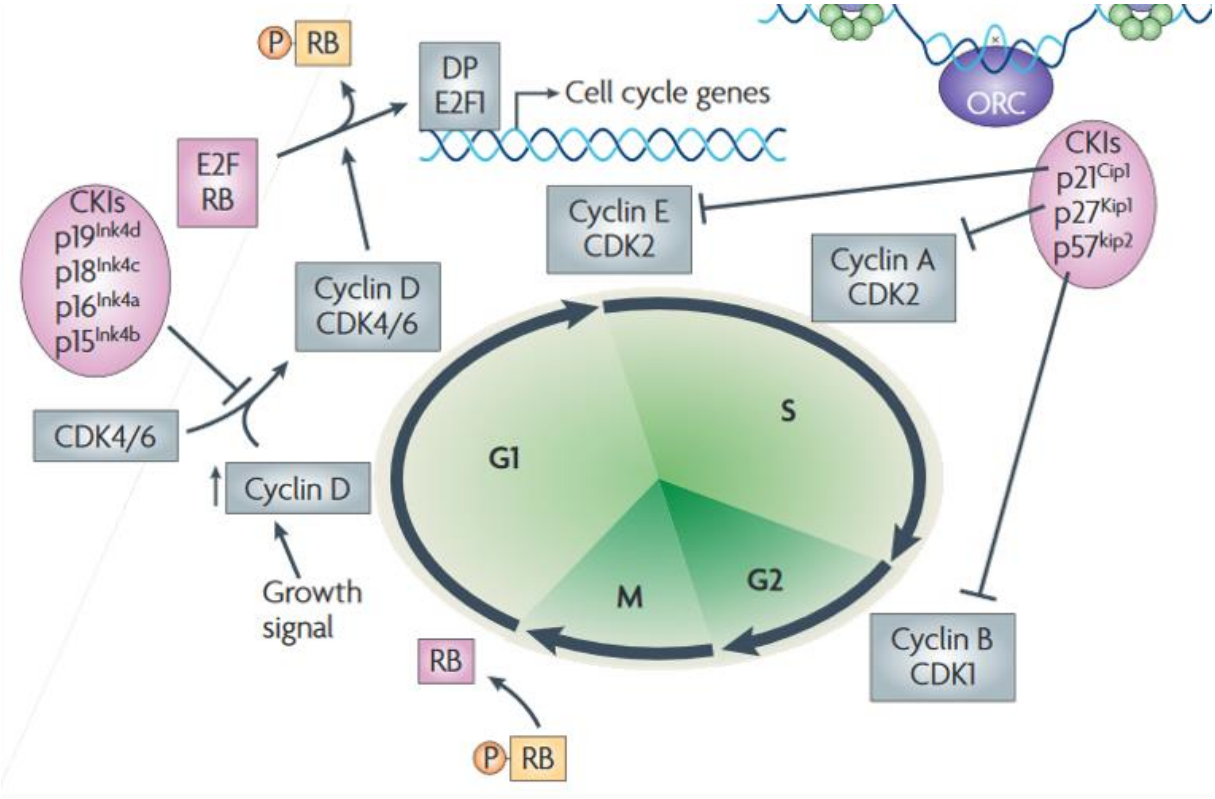

Figure 1.11: Composition of CDKs and cyclins during the cell cycle

The main drivers of cell cycle progression are CDKs, which are activated by interacting with corresponding cyclins. CKIs are also involved in the regulation of cell cycle, mostly by hindering its progression (RB: retinoblastoma protein, CDK: cyclin-dependant kinase, CKI: cyclin-dependant kinase inhibitor, ESF1 and DP1: transcription factors). Modified after (Herrup and Yang 2007).

the cyclin-CDK complex can be negatively regulated by so-called cyclin-dependent kinase inhibitors (CKIs) (see Figure 1.11), which block phosphorylation of downstream targets (Barnum and O'Connell 2014; Lim and Kaldis 2013; Morgan 1995; Vermeulen et al. 2003). Two families of CKIs exist, the INK4 family, which includes p15, p16, p18 and p19, and the Cip/Kip family including p21, p27 and p57 (Sherr and Roberts 1995). INK4 inhibitors mainly inactivate CDK4 and CDK6 during G1 phase by binding as competitive binding partners to the CDK (Carnero and Hannon 1998). The Cip/Kip family members inactivate mainly CDK2 in complex with cyclin E and A, as well as the cyclin B-CDK1 complex (Herrup and Yang 2007; Polyak et al. 1994; Lee et al. 1995; Hengst and Reed 1998).

1.5.2 Cell cycle checkpoints

Throughout the cell cycle checkpoints are implemented to ensure that a certain processes has been completed before the cell enters the next phase of the cell cycle (Wenzel and Singh 2018). If errors or DNA damage occur, checkpoints delay the cell cycle progression and provide enough time for damage repair or the elimination of errors, respectively (Nyberg et al. 2002). First, there is the G1/S phase checkpoint (see Figure 1.12 A), which is mainly p53-dependent (Schafer 1998; Vermeulen et al. 2003). p53 is a downstream target of ATM and ATR (see section 1.2.2) and becomes highly increased after detection of DNA damage (Vermeulen et al. 2003; Levine 1997). This overexpression leads to the transcription of p21 (Shaltiel et al. 2015; Agarwal et al. 1998), a CDK inhibitor, which blocks cyclin E-CDK2 complex formation and prevents progression to S phase (Kastan et al. 1992; Huang et al. 1996; Bartek and Lukas 2001). At the same time another downstream target of ATM and ATR, Chk2, is responsible for the phosphorylation-mediated degradation of the phosphatase Cdc25A. This phosphatase normally mediates the activation of CDK2, however, when it is absent, CDK2 remains in an inactive state and cannot build a complex with cyclin E to stimulate progression to S phase (Bartek and Lukas 2001; Mailand et al. 2000; Costanzo et al. 2000; Löbrich and Jeggo 2007 Nov). Second, to prevent progression from G2 to M phase while there is under-replicated or misreplicated DNA, cells are halted at the G2/M phase checkpoint (see Figure 1.12 C). This checkpoint acts similarly as the G1/S checkpoint. During G2 phase, Cdc25 is phosphorylated and loses its ability to dephosphorylate CDK1. Formation of the cyclin B-CDK1 complex is blocked and, accordingly, mitosis entry is prevented (Vermeulen et al. 2003; Sanchez et al. 1997; Zeng et al. 1998; Iliakis et al. 2003). There are also additional checkpoints, which control the correct execution of certain processes. Most prominent during mitosis is the spindle-assembly checkpoint (SAC). This checkpoint identifies improper attachments of the chromosomes to the spindle (Musacchio and Salmon 2007) and is able to stop the cell cycle during metaphase (Vermeulen et al. 2003). Responsible for the stop of progression are mitotic arrest deficient (Mad) and budding uninhibited by benomyl (Bub), which inhibit the subunit Cdc20 of the anaphase-promoting complex (APC) (Vermeulen et al. 2003; Fang et al. 1998; Amon 1999). The most important challenge during the cell cycle is to protect the genetic integrity. During S phase myriad types of errors can occur, thus making S phase, or more precisely replication the most susceptible process. Consequently, there are three S phase checkpoints, the

replication checkpoint (see Figure 1.12 B), the intra-S phase checkpoint and the S-M checkpoint (Bartek and Lukas 2001). The replication checkpoint is activated in response to stalled replication forks, which respond to stresses such as

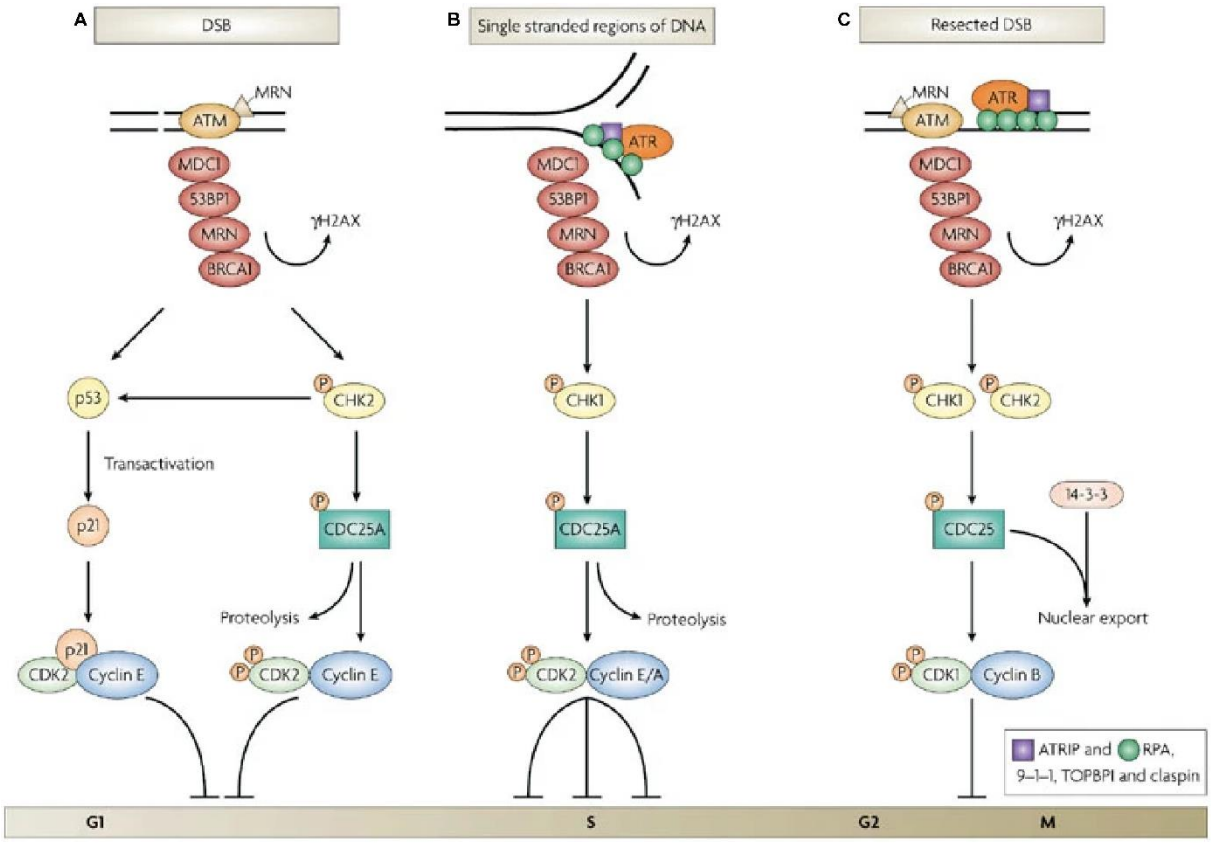

Figure 1.12: Damage-induced cell cycle checkpoint pathways

DNA damage repair is initiated by ATM or ATR-ATRIP complex, respectively. Downstream targets of these two are mainly Chk1 and Chk2. **A)** The G1 checkpoint is mediated by Chk2, which phosphorylates the phosphatase Cdc25A. This leads to its degradation and inactivity. Thus, CDK2 remains inactive and cannot initiate S phase progression. Simultaneously, the downstream target of ATM, p53, initiates transcription of p21, which is a CDK inhibitor. p21 blocks the formation of cyclin 3-CDK2 complexes and S phase entry. **B)** Here, only the replication checkpoint is depicted. Stalled replication forks initiate ATR activation, followed by a Chk1 phosphorylation and degradation of Cdc25A. CDK2 remains inactive and firing of further replication origins is inhibited. **C)** G2/M transition is inhibited by the degradation of Cdc25C, thereby inactivating cyclin B-CDK1 complex, which is required for progression. ATM, ataxia telangiectasia mutated; ATR, ataxia telangiectasia and RAD3-related; MRN, NBS1-MRE11-RAD50; ATRIP, ATR-interacting protein; 9-1-1, RAD9-RAD1-HUS1; Chk1 and Chk2, checkpoint kinases 1 and 2; CDK, cyclin-dependent kinase (Löbrich and Jeggo 2007 Nov).

depletion of dNTPs, inhibition of DNA polymerases or stumbling across DNA lesions (Bartek and Lukas 2001; Petermann and Caldecott 2006). Mainly responsible for the initiation of this checkpoint are RPA, the ATR-ATRIP complex, RAD17 and the 9-1-1-complex that work together to inhibit firing of further replication origins and to protect stalled replication forks (Zou and Elledge 2003; Bartek et al. 2004; Nyberg et al. 2002; Dimitrova and Gilbert 2000; Lopes et al. 2001; Tercero and Diffley 2001; Shimada et

al. 2002). The inhibition of origin firing is in particular inhibited by CDK2 inactivity, which leads to the degradation of Cdc25A. This phosphatase is responsible for recruitment of DNA polymerase α to the DNA (Bartek et al. 2004). The S-M checkpoint makes sure that cells only continue to cell division if they have completely and faithfully duplicated their genome, otherwise onset of under-replicated cells to mitosis can lead to fatal consequences. Here, the main player is the cyclin B-CDK1 complex (Zachos et al. 2005). In contrast to the other two checkpoints is the intra-S phase checkpoint replication-independent and it is initiated when DSBs occur throughout the genome outside of active replicons (Bartek et al. 2004). Ongoing replication forks are unaltered by the initiation of this checkpoint (Bartek et al. 2004; Painter and Young 1980; Merrick et al. 2004), rather late replication origin firing is inhibited (Grallert and Boye 2008). Here, the key player is SMC1 (structural maintenance of chromosome-1), which is phosphorylated by the Mdc1-MRN complex. This leads to a stop of DNA replication in response to DNA damage (Bartek et al. 2004; Kim et al. 2002; Kitagawa et al. 2004; Yazdi et al. 2002).

1.6 Replication

Once per cell cycle, the cell has to ensure a faithful and correct duplication of more than three billion base pairs to maintain the inheritance of genetic information (Prioleau and MacAlpine 2016). Replication forks firing more than once from a single origin lead to so-called re-replication, which is responsible for creating multiple copies of a genomic region and consequently gene amplification (Siddiqui et al. 2013; Green et al. 2010). This in turn leads to genomic instability, resulting finally in cancer (Siddiqui et al. 2013; Lengauer et al. 1998). In addition, replication has to be coordinated with other cellular processes like cell cycle progression, transcription and DNA repair (Bell and Dutta 2002). Replication can be roughly divided into three phases: a) initiation, in which the DNA is unwound, b) elongation, in which the DNA is duplicated and c) termination, in which converging of replication forks ends DNA synthesis (Dewar and Walter 2017).

1.6.1 Mechanisms and regulation

The first step of initiating replication takes place already during late M or G1 phase, respectively (see Figure 1.13) (Siddiqui et al. 2013). Here, the origin recognition complex (ORC) binds to replication origins, which are defined DNA sequences, and mediates the recruitment of Cdc6 and Cdt1 (Cdc10-dependent transcript 1) (Siddiqui et al. 2013; Machida et al. 2005; Fragkos et al. 2015). These two in turn recruit the mini chromosome maintenance (MCM) complex to the DNA, which is needed to unwind the DNA with its helicase activity (Evrin et al. 2009; Remus et al. 2009; Bell and Kaguni 2013; Fragkos et al. 2015; Prioleau and MacAlpine 2016). The MCM complex consists of the six subunits Mcm2-7 and completes the assembly of the pre-replicative complex (pre-RC). The pre-RCs “license” the origin for further activation in S phase (Prioleau and MacAlpine 2016; Siddiqui et al. 2013). To activate licensed origins the MCM helicase complex needs to be phosphorylated multiple times, mainly by Dbf4-dependent kinases (DDKs) or by CDKs (Fragkos et al. 2015). This recruits Cdc45 and GINS (go-ichi-ni-san) to the origin to form the Cdc45/Mcm2-7/GINS (CMG) helicase complex that starts DNA unwinding (Prioleau and MacAlpine 2016; Moyer et al. 2006; Aparicio et al. 2009). However, further factors like RECQL4, Mcm10, Treslin, TopBP1 (Kumagai et al. 2010, 2011; Boos et al. 2011; Thu and Bielinsky 2013; Im et al. 2009) and polymerases ε and δ for either leading or lagging strand (Kunkel and Burgers 2008) are necessary to active the CMG helicase complex (Tanaka et al. 2011; Zou and Stillman 2000; Heller et al. 2011; Deegan et al. 2016; Miyazawa-Onami et al. 2017; Yeeles et al. 2015; Ilves et al. 2010; Douglas et al. 2018). After forming an active pre-initiation complex (pre-IC), helicase activation leads to the recruitment of the replication factor C (RFC), proliferating cell nuclear antigen and RPA, generating the replisome, to build a functional replication fork (Kunkel and Burgers 2008; Pacek et al. 2006; Yao and O'Donnell 2009). Simultaneously, the helicase activation leads to the separation of the Mcm2-7 double hexamer into two hexamers with their own replisomes that diverge in opposite directions starting from the origin (Fragkos et al. 2015).

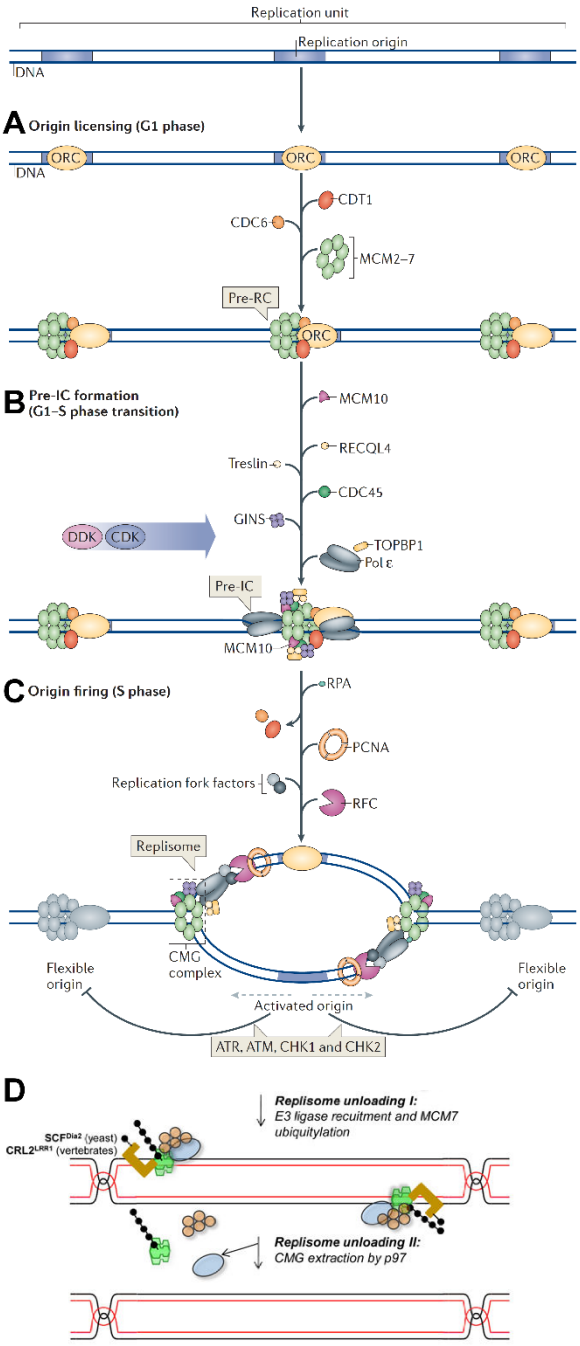

Figure 1.13: Mechanisms and regulation of replication

A) First, the ORC binds to defined genome regions called origins and recruits Cdc6 and Cdt1. Both of these are responsible for the recruitment of Mcm2-7 in order to form the pre-IC. These steps take already place during G1 phase. **B)** During G1/S phase transition, licensed pre-ICs are activated by phosphorylation of Mcm2-7 by DDKs and CDKs. This also recruits Cdc45 and GINS to form the so-called CMG helicase complex. **C)** Recruitment of further proteins such as RFC, RPA, PCNA and polymerases leads to the building of a functional replisome and firing of the activated pre-IC. The CMG helicase starts to unwind the DNA. **D)** After elongation, converging replication forks meet and the CMG helicase is ubiquitinylated by the ligase CRLLrr1 and subsequently uncoupled by p97. A-C modified after (Prioleau and MacAlpine 2016) and D modified after (Dewar and Walter 2017).

The process of replication proceeds differently at the two branches of a replication fork. DNA synthesis occurs continuously on the leading strand, while it is carried out discontinuously on the lagging strand creating Okazaki fragments, which need to be ligated in the next step by FEN1 (Ogawa and Okazaki 1980; Zheng et al. 2011). Regions of ssDNA between two Okazaki fragments are protected by RPA to prevent degradation or formation of secondary structures (Wold 1997). After elongation of DNA, converging replication forks meet and the CMG helicase needs to be removed from the DNA. This happens through polyubiquitination of Mcm7 by E3 ubiquitin ligase CRL^{Lrr1} (Cullin RING Ligase 2 associated with Leucine Rich Repeats 1 [Lrr1]) (Maric et al. 2014; Moreno et al. 2014; Dewar et al. 2017; Sonneville et al. 2017). This ubiquitination leads to the extraction of the helicase by the ATPase p97 (Moreno et al. 2014; Maric et al. 2014; Franz et al. 2011).

1.6.2 Replication in the context of DNA damage

It is quite possible that during DNA synthesis a replication fork faces several obstacles. These can be DNA repeat sequences, DNA fragile sites, replication termination sites, replication slow zones (Postow et al. 2001; Mirkin and Mirkin 2007; Barlow et al. 2013; Durkin and Glover 2007; Casper et al. 2002), transcription factors, absence of dNTPs and DNA lesions (Wyatt and Pittman 2006), which are collectively referred to as replication stress (Yates and Maréchal 2018). When encountering an obstacle, the replication fork stalls, which leads to unreplicated ssDNA regions. These ssDNA regions are coated with RPA, which subsequently induces the S phase checkpoint (see section 1.5.2) (Zou and Elledge 2003; Byun et al. 2005). For both, lagging and leading strand, differs how they encounter these obstacles (Marians 2018). On the one hand, replication fork stalling on the lagging strand does not disturb replication progression as the fork is forced to leave the DNA anyway while generating Okazaki fragments. Thus, re-initiation of replication can occur (Yeeles et al. 2013). On the other hand, DNA damage on the leading strand is more complicated. Here, several bypass pathways can be applied. First, in some cases a replication fork downstream of the stalled fork can replicate up to the inactive one. However, if downstream forks are also unable to replicate, back-up origins between the two inactive forks can stand in to prevent un-replicated regions (Yekezare et al. 2013). They are called dormant origins and are activated only under conditions of replication stress (Ge and Blow 2010). In

addition, a so-called translesion synthesis (TLS) can resume work to bypass a DNA lesion. Here, polymerases like Pol η, Pol ζ and REV1 are recruited to the stalled replication fork, through a monoubiquitination of PCNA by Rad6 and Rad18 (Stelter and Ulrich 2003; Kannouche et al. 2004; Yeeles et al. 2013). Afterwards, TLS polymerases incorporate bases within the gap and are then displaced by a replicative polymerase, which continues DNA synthesis (Johnson et al. 2000; Woodgate 2001; Shachar et al. 2009; Moldovan et al. 2007). Post-replicative TLS can also occur, where replicative polymerases re-prime downstream of the lesion leaving ssDNA regions behind, which are repaired by TLS polymerases afterwards (Yeeles et al. 2013). However, TLS polymerases are quite error-prone, because they do not use a template while incorporating bases (Hoeijmakers 2001). In contrast to TLS, there is a potential error-free bypass pathway called template switch. To initiate template switch, PCNA is polyubiquitinated, which inhibits TLS (Zhang and Lawrence 2005; Pfander et al. 2005; Papouli et al. 2005; Haracska et al. 2004; Branzei et al. 2004). The replicative polymerase remains at the damaged site and the resulting gap is filled by using the sister chromatid as a template. Here, several factors are involved, which also play a major role during HRR (Hoeijmakers 2001). In general, replication stress can be visible as gaps or breaks in metaphase chromosomes or as persisting 53BP1 foci in G1 phase. These incidents usually occur at loci called “common fragile sites” (CFS’s). They are an indicator for replication stress and are associated with genome instability in cancer cells (Durkin and Glover 2007).

If stalled replication forks remain unprotected the chance for replisome dissociation and collapse of the fork is highly increased (Petermann and Helleday 2010). Therefore, the cell has established some protective mechanisms. As mentioned above, ssDNA is a characteristic for stalled replication forks, that is why RPA is one of the first responders (Binz et al. 2004; Fan and Pavletich 2012; Fanning et al. 2006). RPA’s main responsibility is to recruit the remodelling protein SMARCAL1 (SWI/SNF-related matrix-associated actin-dependent regulator of chromatin subfamily A-like protein 1) to prevent fork collapse (Ciccia et al. 2009; Bétous et al. 2012). In addition, increasing ssDNA-RPA levels lead to the activation of the ATR-Chk1 replication checkpoint, which prevents further origin firing (see section 1.5.2). Further proteins, such as DDI1/2 and RTF2 prevent the accumulation of ssDNA regions. Here, DDI1/2 removes RTF2 from stalled replication forks and limits ssDNA generation (Liao et al. 2018). However, RPA’s role is only transient and it is replaced during further processes by Rad51

(Sugiyama and Kowalczykowski 2002), which mediates replication fork reversal (Liao et al. 2018). Replication fork reversal allows forks to reverse their direction to continue DNA synthesis without chromosomal breakage (Neelsen and Lopes 2015). Here, the two newly synthesized strands are annealed to form a four-way junction structure that is able to restart reversed forks. Also, this structure allows the lesion to be removed (Quinet et al. 2017b).

1.7 The chromosomal passenger complex

As mentioned, a faithful and complete chromosome separation during mitosis is of high importance to prevent mis-segregation leading to genetic defects and subsequently oftentimes to cancer. A pivotal role during mitosis plays the chromosomal passenger complex (CPC) (Ruchaud et al. 2007). The CPC conducts important processes including chromosome condensation, spindle assembly, kinetochore-microtubule attachments, cell cycle progression and finally cytokinesis (Carmena et al. 2012a).

1.7.1 Structural organization

The CPC consists of four subunits. On the one hand, as an enzymatic component the kinase Aurora B and on the other hand, three regulatory subunits including INCENP (inner centromere protein), Survivin and Borealin (Carmena et al. 2012b; Honda et al. 2003). The regulatory part is responsible for the proper localization, stability and activity of the CPC. In contrast, Aurora B guarantees proper kinetochore-microtubule attachments and phosphorylates other centromere-associated proteins (Carmena et al. 2012b; Liu and Lampson 2009; Lampson and Cheeseman 2011). Both, Survivin and Borealin are needed for the recruitment of the complex to the mitotic spindle (Carmena et al. 2012b). Borealin is phosphorylated by the Cyclin B-CDK1 complex and mediates centromeric localization (Tsukahara et al. 2010), while Survivin recognizes the PTM H3T3p at the chromatin (Kelly et al. 2010; Wang et al. 2010; Trivedi et al. 2019). Together with INCENP, these three form a three-helix bundle at the N-terminus of INCENP (Jeyaprakash et al. 2007; Carmena et al. 2012b; Klein et al. 2006; Ruchaud et al. 2007; Jeyaprakash et al. 2011). Indeed, INCENP acts as a linker between the regulatory subunit and the enzymatic subunit. At INCENP's C-

terminus, also called IN-box, is the kinase Aurora B bound and thereby simultaneously activated by INCENP and Borealin (Gassmann et al. 2004; Adams et al. 2001a). RNAi knockdown studies of each CPC member demonstrate disruption of mitotic progression and destabilization of the other complex members (Ruchaud et al. 2007; Honda et al. 2003; Gassmann et al. 2004; Adams et al. 2001b; Carvalho et al. 2003; Lens et al. 2003; Vader et al. 2006).

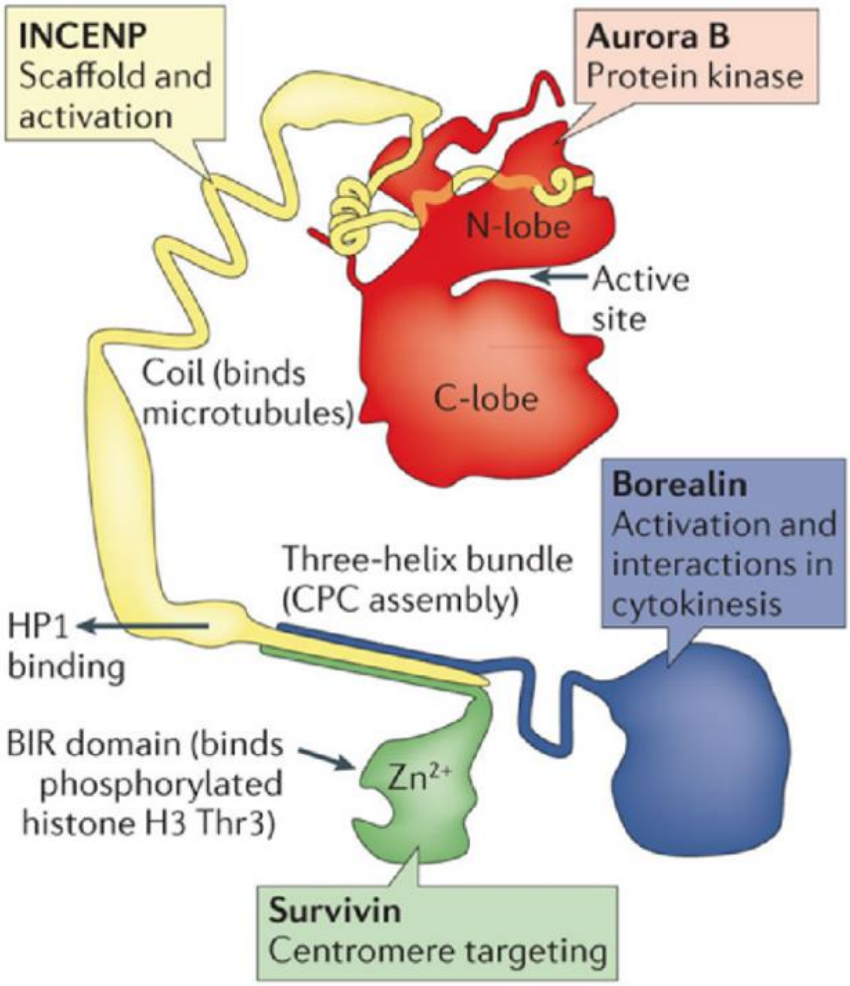

Figure 1.14: Architecture of the CPC

The CPC consists of two subunits. First, the enzymatic subunit, which is the kinase Aurora B and second, the regulatory subunit, including INCENP, Survivin and Borealin. Here, INCENP acts as linker between these two subunits but is also responsible for the activation of the kinase. Both, Survivin and Borealin are responsible for the proper recruitment to the mitotic spindle and also activate together with INCENP the kinase. The regulatory subunit is interconnected via a three-helix bundle at the N-terminus of INCENP. The kinase is bound to INCENP's C-terminus. Modified after (Carmena and Wheelock et al. 2012).

1.7.2 Localisation and function during mitosis

The CPC's localization is highly dynamic throughout mitosis. Starting in prophase (see Figure 1.15 A, a+b), the CPC is located at the chromosome arms. This binding is mediated by the interaction of INCENP and Borealin with HP1 (Ainsztein et al. 1998; Nozawa et al. 2010; Liu et al. 2009; Kang et al. 2011) via their PxVxL/I motif (Brasher et al. 2000; Smothers and Henikoff 2000; Nozawa et al. 2010). During its localisation at the chromosome arms, histone H3 is phosphorylated by Aurora B on Ser10 and Ser28, which leads to the release of HP1 (Hirota et al. 2005): Consequently, the CPC

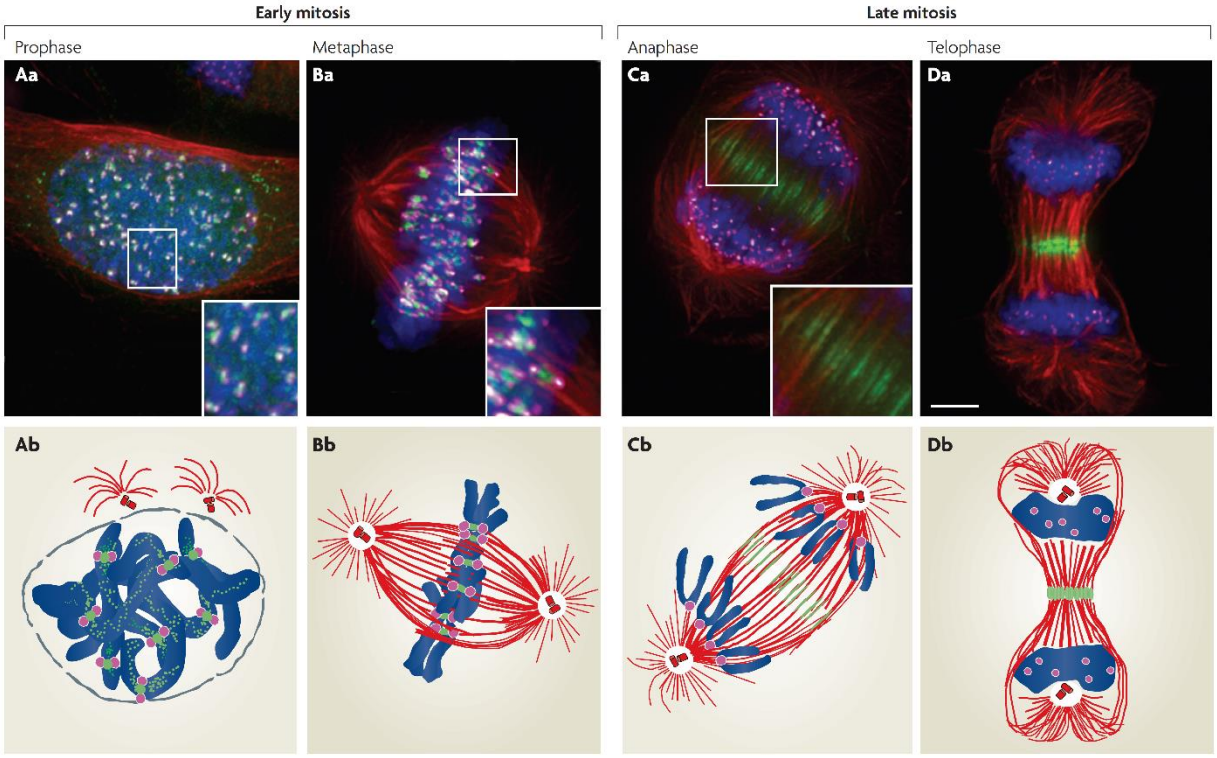

Figure 1.15: Localisation of the CPC during mitosis

Panels Aa-Da show immunofluorescence of HeLa cells during mitosis and panels Ab-Db show schematic diagrams, with Aurora B in green, kinetochores in pink, α-tubulin in red and DNA in blue. Starting in prophase Aurora B is located at chromosome arms and partly at centromeres (A, a+b). During prometa- and metaphase the chromosomes are assembled at the spindle equator. Aurora B is mainly located at the centromere during this phase (B, a+b). In a further step, Aurora B relocates to the spindle midzone (C, a+b). Finally, during telophase Aurora B is located at the midbody (D, a+b). Scale bar: 5 µm. (Ruchaud et al. 2007).

do not have a binding partner anymore and dissociates from the chromosome arms (Vader et al. 2006). The release of HP1 triggers chromosome condensation and progression of mitosis (Hirota et al. 2005). During prometa- and metaphase, the CPC is located at the centromeres (see Figure 1.15 B, a+b). This is mainly mediated by the

interaction of Survivin with Haspin-mediated histone mark H3T3p (Kelly et al. 2010; Wang et al. 2010; Wheatley 2011). Thus, Aurora B can in association with the mitotic checkpoint complex (MCC), consisting of Mad2, Bubr1/Mad3, Bub3 and Cdc20 (Sudakin et al. 2001) contribute to the spindle-assembly checkpoint (SAC) and ensure proper kinetochore-microtubule attachments and correct chromosome alignment at the spindle equator (Ruchaud et al. 2007; DeLuca and Musacchio 2012). In general, the SAC is responsible to prevent overhasty separation of the sister chromatids by controlling the anaphase-promoting complex or cyclosome (APC/C) (Sudakin et al. 2001; Musacchio 2011). During transition to anaphase (see Figure 1.15 C, a+b), the CPC changes its localization to the spindle midzone and mediates together with the mitotic kinesin-like protein 2 (Mklp2) the formation of the central spindle (Hümmer and Mayer 2009). Finally, during telophase (see Figure 1.15 D, a+b) the CPC relocates to the midbody. Here, Aurora B phosphorylates the intermediate filament protein vimentin contributing to its disassembly and the separation of the two daughter cells (Goto et al. 2003).

1.7.3 Localisation during interphase

There is less knowledge regarding CPC's function during interphase. Transient inhibition of Aurora B during interphase shows that chromosome mis-segregation occurs (Hayashi-Takanaka et al. 2009), leading to the assumption that H3Ser10 phosphorylation already takes place before entering mitosis (see section 1.7.2) (Hirota et al. 2005; Nozawa et al. 2010). Consequently, if phosphorylation of H3 occurs before mitosis, the CPC also has to interact with the chromatin before cells progress to mitosis. Several studies showed that the CPC co-localizes with pericentric heterochromatin in late S phase via the INCENP-HP1 interaction (Ainsztein et al. 1998; Beardmore et al. 2004; Kang et al. 2011). In addition, several phosphorylation targets of Aurora B during interphase are known (Koch et al. 2011), such as p53, which is negatively regulated by Aurora B phosphorylation (Gully et al. 2012; Wu et al. 2011) and p21, which is inhibited by Aurora B phosphorylation, subsequently leading to an activation of CDK1 (see section 1.5.1) (Trakala et al. 2013).

It was also is shown that INCENP and Borealin are both present during interphase. Death-receptor induced apoptosis results in a Caspase-7-mediated degradation of INCENP leading to the loss of centromere-CPC interaction (Faragher et al. 2007).

Borealin, which is mainly located in the nucleus during interphase, co-localises and interacts with the nucleoli-residing SUMO isopeptidase SENP3 (Klein et al. 2009; Andersen et al. 2005a; Gassmann et al. 2004; Rodriguez et al. 2006).
Finally, Survivin, with its dual role as a CPC member and a member of the IAP family, is also involved in several cellular processes (see section 1.8) (Li 2005).

1.8 Survivin

Survivin is a multifunctional protein and performs a dual role in important cellular processes. It is a member of the CPC and mediates proper centromere targeting during mitosis and as member the IAP family it prevents apoptosis pre-dominantly in the cytoplasm (Li et al. 1998). Besides the wild type form of Survivin, ten further splicing variants haven been identified, which have different functions, namely 2B, 3B, ΔEx3, 2α, 3α, ΔptEx2/3, ΔptEx1/2, ΔptEx1/2G/T, 2206cptEx2 and Survivin image (Sah and Seniya 2015).

1.8.1 Structure and functions

Survivin, also called baculoviral inhibitor of apoptosis repeat-containing 5 or BIRC5 has a molecular weight of 16.5 kDa and consists of 142 amino acids (aa). It includes several different domains, with the N-terminal baculoviral IAP repeat (BIR) domain (15-88 aa) being a common feature in all members of the IAP family. The BIR domain is responsible for Survivin's anti-apoptotic function by interacting with HPXIP (hepatitis B x-interacting protein) to bind to pro-caspase 9 (Deveraux and Reed 1999; Marusawa et al. 2003), and the C-terminal domain (98-142 aa) forming an α-helix that interacts with INCENP (1-49 aa) and Borealin (15-79 aa) building a three-helix bundle within the CPC (Jeyaprakash et al. 2007). The binding site for histone H3 resides within the BIR domain and it is crucial for binding to phosphorylated H3 (H3T3p) during mitosis (Jeyaprakash et al. 2011; Kelly et al. 2010). Survivin's nucleo-cytoplasmic shuttling is mediated by chromosomal-maintenance 1 (CRM1), which binds to Survivin's nuclear export signal (NES, 89-98 aa, VKKQFEELTL). In addition, CRM1 also mediates the

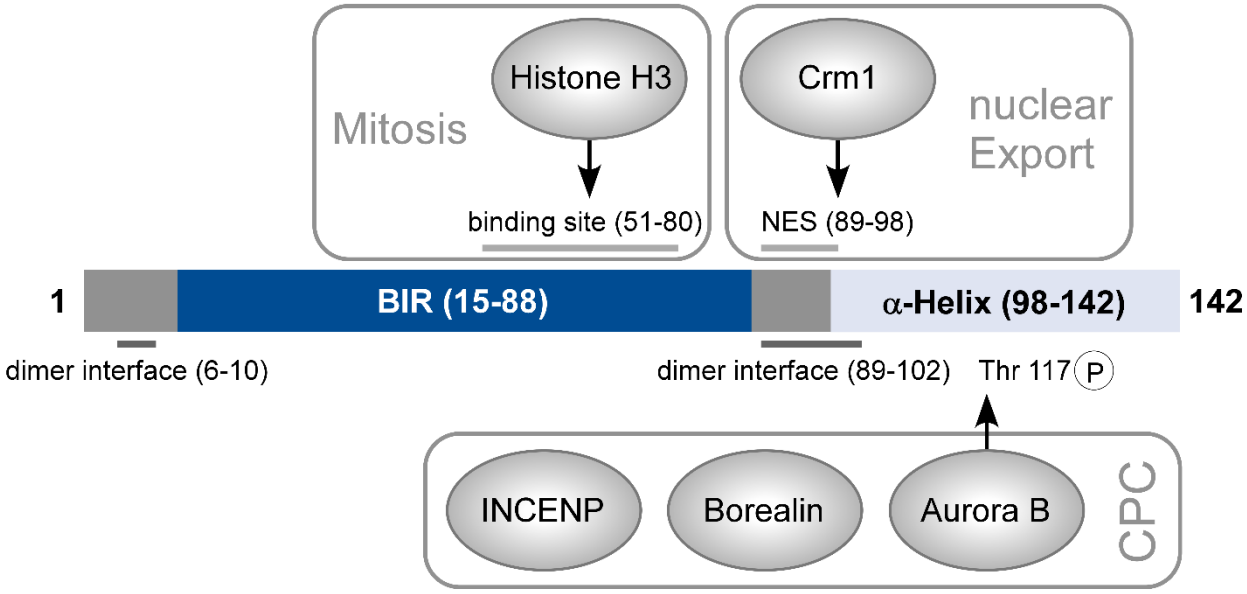

Figure 1.16: Domain organization of Survivin

Survivin possesses a N-terminal BIR domain including a histone H3 binding site, and a C-terminal α-helix, that interacts with CPC members INCENP and Borealin via a three-helix bundle. The helix also contains a NES, which is bound by export receptor CRM1 for nucleo-cytoplasmic shuttlingas well as a dimer interface for homodimerization. Thr117 is phosphorylated by Aurora B due to improper kinetochore attachments in order to dissociate the CPC from the centromere. Modified after (Altieri 2008).

proper centromere targeting of the CPC during mitosis (Knauer et al. 2007b; Knauer et al. 2006; Knauer et al. 2007a). Partly overlapping the NES sequence is the dimer interface (6-10 aa and 89-102 aa), which mediates Survivin's homodimerization in solution (Chantalat et al. 2000; Muchmore et al. 2000). Survivin possesses several phosphorylation sites, including Ser20, Thr117, Thr48 and Thr34. Ser20 is phosphorylated by polo-like kinase 1 (Plk1) to completely activate Aurora B during mitosis (Chu et al. 2011; Colnaghi and Wheatley 2010). Thr117 is phosphorylated by Aurora B during mitosis due to improper kinetochore attachments, inhibiting Survivin's interaction with INCENP and resulting in the release of the CPC from the centromeres (Delacour-Larose et al. 2007; Wheatley et al. 2007; Wheatley et al. 2004). Furthermore, phosphorylation of Thr48 by casein kinase 2 (CK2) mediates Survivin's interaction with Borealin (Barrett et al. 2011) and Thr34 phosphorylation by CDK1 promotes Survivin's anti-apoptotic function (O'Connor et al. 2000). Ubiquitination of Survivin plays also a crucial role. Ubiquitination of Lys63 by Ufd1 (ubiquitin fusion degradation protein 1) mediates Survivin's localisation to the centromeres, whereas de-ubiquitination by hFAM leads to its dissociation (Vong et al. 2005).

1.8.2 Deregulation in cancer and Survivin as a therapeutical target

Usually, Survivin is upregulated during embryonic development. Mice with a Survivin knock-out exhibit embryonic lethality (Uren et al. 2000), deficiency of self-renewing bone marrow progenitor cells and bone marrow ablation (Fukuda et al. 2015). Survivin expression decreases during further development and is absent in adult tissues (Adida et al. 1998). However, it was shown, that in nearly all human cancer types high levels of Survivin are present due to downregulation of transcriptional factors such as Rb and p53, promotor mutations, gene amplification, IGF-1-mediated mRNA stabilisation and NF-κB-induced transcription (Vaira et al. 2007; Xu et al. 2004; Tracey et al. 2005; Jiang et al. 2004; Hoffman et al. 2002). A strong accumulation of Survivin correlates with chemo- and radiotherapy resistance, increases tumour recurrence and shortens patient survival (Adida et al. 1998; Chen et al. 2014; Capalbo et al. 2007; Engels et al. 2007; Xu et al. 2014). Because of this, Survivin is used as a biological marker for cancer entities and is also a promising target for anti-cancer therapies (Altieri 2001, 2013; Coumar et al. 2013; Rödel et al. 2012). Different strategies have been considered to target Survivin: a) small molecule inhibitors, b) immunotherapeutic approaches, c) nucleic acid based approaches and d) gene depletion of Survivin (Garg et al. 2016). Here, development of small molecule inhibitors takes less time and is more cost-efficient than for example immunotherapies (Garg et al. 2016). Most promising small molecules are YM155 (Cheng et al. 2012; Na et al. 2012; Nakahara et al. 2011) and FL118 (Li 2014). Both suppress promotor activity by directly binding to Survivin's promotor (Nakahara et al. 2011; Ling et al. 2012; Coumar et al. 2013). Besides, playing a role in mitosis Survivin is also a member of the inhibitor of apoptosis (IAP) family and has anti-apoptotic characteristics, which mainly occur in the cytosol (Li et al. 1999; Li et al. 1998; Li et al. 2016b). Here, interaction with the export receptor CRM1 is essential, which is responsible for Survivin's predominant localisation in the cytosol. Hence, two small nuclear export inhibitors targeting CRM1's interaction to Survivin were identified, called C3 and C5, to encounter Survivin's anti-apoptotic function (Fetz et al. 2009; Stauber et al. 2010).

1.9 Aim of the thesis

Survivin is overexpressed during embryonic development and absent in adult tissues. However, in cancer Survivin expression is highly upregulated and associated with tumour resistance against chemo- and radiotherapy and a poor clinical outcome. Therefore, Survivin might be one of the most cancer-specific proteins and thus a promising target for cancer therapies.

While its role during mitosis as part of the CPC is well documented, the role of the CPC and especially Survivin in other cellular processes is still elusive. Moreover, Survivin fulfils a dual role during cell cycle. Beyond being a part of the CPC during mitosis, Surivivn is a member of the IAP family and its predominantly cytoplasmic localisation is associated with cytoprotective activity against treatment-induced apoptosis.

Previous work of our group suggested an additional cellular function for Survivin during interphase, where increasing foci formation was detected after irradiation, also including the other CPC members. Interestingly, we could reveal a relocation of the CPC not only to centromeric regions but also towards the vicinity of the sliding clamp protein PCNA. In addition, Aurora B and Survivin knockdown lead to decreased velocities of the replication fork (Schröder 2014; Mosel 2018).

This now prompted us to elucidate Survivin's functions during replication processes, and with this to gain further insights into its manifold cellular roles.

Therefore, irradiation-induced localisation changes of all CPC members were analysed in detail. In this context, a putative targeting of Survivin to replication sites should be investigated via immunofluorescence and co-immunoprecipitation. Furthermore, if a connection with replication sites could be identified, potential interaction partners of the CPC members within the replisome should be investigated and analysed via co-immunoprecipitation and western blotting.

Moreover, RNAi-mediated knockdown should allow to elucidate a functional involvement of the CPC and Survivin in replication. Here, especially so-called "common-fragile sites" (CFS) should be distinguished after replication stress as chromosome breaks and gaps via metaphase spreads and immunofluorescence. Furthermore, 53BP1 nuclear bodies arise during G1 phase after cells suffer replication stress during the preceding S phase and should be illustrated by immunofluorescence. Regarding the knockdown-induced altered replication fork speed, a possible interplay

with translation polymerases, which are responsible for replication of damaged DNA regions, should be analysed via co-immunoprecipitation and immunofluorescence.

2 Material and Methods

2.1 Material

2.1.1 Instruments

Instruments and devices used in this work are listed in Table 2.1.

Table 2.1: Instruments and devices.

instrument	manufacturer
Agarose gel electrophoresis chamber	Peqlab Biotechnologie GmbH, Erlangen
Allegra™ X-22R Centrifuge	Beckman Coulter GmbH, Krefeld
Analytical balance CP124S-ACE	Sartorius Lab Instruments GmbH & Co. KG, Göttingen
BioPhotometer Plus	Eppendorf AG, Hamburg
Centrifuge 5417 C/R	Eppendorf AG, Hamburg
Centrifuge ROTINA 380 R	Andreas Hettich GmbH & Co. KG, Tuttlingen
Centrifuge Heraeus Fresco 21	Thermo Fisher Scientific, Waltham, USA
Centrifuge Heraeus Pico 17	Thermo Fisher Scientific, Waltham, USA
ChemiDoc™ MP Imaging System	Bio-Rad Laboratories GmbH, München
CO_2 incubator	Binder GmbH, Tuttlingen
CO_2 incubator INC153	Memmert GmbH & Co. KG, Schwabach
Confocal laser scanning microscope TCS SP8	Leica Microsystems GmbH, Mannheim
Confocal laser scanning microscope TCS SP8X	Leica Microsystems GmbH, Mannheim
FiberComb® (Molecular Combing System)	Genomic Vision, Bagneux, FR
FiberVision®	Genomic Vision, Bagneux, FR
Five Easy Plus pH meter FP20	Mettler Toledo, Gießen
Freezer (-20 °C) Liebherr BioFresh	Liebherr GmbH, Biberach
Freezer (-80 °C) Forma 900S-RIFS	Thermo Fisher Scientific, Waltham, USA

instrument	manufacturer
Gel caster	Bio-Rad Laboratories GmbH, München
Gel documentation system E-Box VX2	Vilber Lourmat GmbH, Eberhardzell
Grant Bio orbital shaking platform POS-300	Grant Instruments Ltd, Camebridge, UK
Heating plate	Medax GmbH & Co. KG, Rendsburg
Incubation trays (multiple sizes)	Advansta Inc., San Jose, USA
Incubator IN30	Memmert GmbH & Co. KG, Schwabach
Inverted research microscope TCM 400	Labo America Inc, Fremont, USA
Magnetic stirrer HI 180	Hanna Instruments Deutschland GmbH, Kehl
Magnetic stirrer MMS-300	Grant Instruments Ltd, Camebridge, UK
Magnetic stirrer MR Hei-Mix L	Heidolph Instruments GmbH & CO. KG, Schwabach
Microscope Primo Vert	Carl Zeiss, Oberkochen
Mini Microcentrifuge C1301-B	Labnet International Inc., Edison, USA
Mini Microcentrifuge Spectrafuge	Labnet International Inc., Edison, USA
Mini Trans-Blot® Electrophoretic Transfer Cell	Bio-Rad Laboratories GmbH, München
Mr. Frosty™ storage container	Thermo Fisher Scientific, Waltham, USA
Olympus CKX41	Olympus Europa SE & CO. KG, Hamburg
Orbital benchtop shaker MaxQTM 4000	Thermo Fisher Scientific, Waltham, USA
Orbital shaker standard 3500	VWR International GmbH, Darmstadt
Orbital tabletop shaker Forma 420 Series	Thermo Fisher Scientific, Waltham, USA
PAGE chamber Mini-PROTEAN® Tetra Cell	Bio-Rad Laboratories GmbH, München
PIPETBOY acu 2	Integra Bioscience, Zizers, CH
PIPETMAN ® P/Neo	Gilson International B.V., Limburg-Offheim
Pipettes Research Plus	Eppendorf AG, Hamburg
Power Supply peqPOWER 300	Peqlab Biotechnologie GmbH, Erlangen
Power Supply peqPOWER 250	Peqlab Biotechnologie GmbH, Erlangen

instrument	manufacturer
Power supply PowerPac Basic	Bio-Rad Laboratories GmbH, München
Precision balance 440-21A	Kern & Sohn GmbH, Balingen
Precision balance 440-47N	Kern & Sohn GmbH, Balingen
ProBlot™ Rocker 25	Labnet International Inc., Edison, USA
Refrigerator Liebherr BioFresh	Liebherr GmbH, Biberach
Refrigerator Liebherr Comfort	Liebherr GmbH, Biberach
Refrigerator Liebherr Medline	Liebherr GmbH, Biberach
Reservoir Bench Holder	Genomic Vision, Bagneux, FR
Rocking shaker E-1113	NeoLab Migge Laborbedarf-Vertriebs GmbH, Heidelberg
Rocky® 3D shaker	Labortechnik Fröbel GmbH, Lindau
Safety cabinet NuAire NU-437-400E	Integra Biosciences GmbH, Fernwald
Safety cabinets HERAsafe	Thermo Fisher Scientific, Waltham, USA
Sonopuls mini20	BANDELIN electronic GmbH & Co. KG, Berlin
Spectrophotometer NanoDrop™ 2000c	Thermo Fisher Scientific, Waltham, USA
Tank electro blotter PerfectBlue™	Peqlab Biotechnologie GmbH, Erlangen
Thermal mixer MHR 11	HLC BioTech, Bovenden
Thermal mixer ThermoMixer® C	Eppendorf AG, Hamburg
Thermal printer DPU-414	Seiko Instruments GmbH, Neu-Isenburg
Thermal printer P95D	Mitsubishi Chemical Europe GmbH, Düsseldorf
Thermocycler TProfessional gradient 96	Biometra GmbH, Göttingen
Tube roller RS-TR 5	Phoenix Instrument GmbH, Garbsen
Ultrasonic homogenizer mini20	Bandelin electronic GmbH & Co. KG, Berlin
UV sterilizing PCR workstation	Peqlab Biotechnologie GmbH, Erlangen
Vacuum removal system AZ 02	HLC BioTech, Bovenden
Vortexer	Heathrow Scientific® LLC, Vernon Hills, USA
Vortexer PV-1	Grant Instruments Ltd, Camebridge, UK
Vortexer Vortex-Genie 2	Scientific Industries, Bohemia, USA
Wash-N-Dry™ coverslip rack	Sigma-Aldrich Chemie GmbH, München

instrument	manufacturer
Water bath 1002-1013	Gesellschaft für Labortechnik mbH, Burgwedel
Water purification system Milli-Q®	Merck KGaA. Darmstadt
X-ray cabinet CIX2	Xstrahl Deutschland, Ratingen
X-ray cabinet RX-650	Faxitron Bioptics, LLC, Tucson, USA

2.1.2 Consumables

Consumables used in this thesis are listed in Table 2.2.

Table 2.2: Consumables

item	supplier
Agar plates	Sarstedt AG & Co., Nümbrecht
Bottle top vacuum filter (0.45 µm)	Sarstedt AG & Co., Nümbrecht
Cell culture dish (6/10 cm)	Sarstedt AG & Co., Nümbrecht
Cell culture flask (T-25, T-75)	Sarstedt AG & Co., Nümbrecht
Cell scraper	Sarstedt AG & Co., Nümbrecht
Counting chamber	Kova International, Inc., Garden Grove, USA
Cover slips	Carl Roth GmbH & Co. KG, Karlsruhe
Cryogenic tubes	Sarstedt AG & Co., Nümbrecht
Disposable pasteur pipettes graduated	Carl Roth GmbH & Co. KG, Karlsruhe
Disposable Reservoirs	Genomic Vision, Bagneux, FR
Engraved Combicoverslips	Genomic Vision, Bagneux, FR
FiberVision® Sample Holders	Genomic Vision, Bagneux, FR
Film wiper	Kaiser Fototechnik GmbH & Co.KG, Buchen
Glass bottom dishes (35 mm)	MaTek Corporation, Ashland
PCR tubes	Bio-Rad Laboratories GmbH, München
Pipette tips (10/20/200/1000/1250)	Sarstedt AG & Co., Nümbrecht
Pipette filter tips (10/20/200/1250)	Sarstedt AG & Co., Nümbrecht

item	supplier
Reaction falcons (15/50 ml)	Sarstedt AG & Co., Nümbrecht
Reaction tubes (1.5/2 ml)	Sarstedt AG & Co., Nümbrecht
Rotilabor®-Blotting papers	Carl Roth GmbH & Co. KG, Karlsruhe
Serological pipettes (2/5/10/25 ml)	Sarstedt AG & Co., Nümbrecht
Sterile serological pipettes (2/5/10/25 ml)	Sarstedt AG & Co., Nümbrecht
THERMO specimen slides Superfrost	Carl Roth GmbH & Co. KG, Karlsruhe
UV cuvettes	Sarstedt AG & Co., Nümbrecht

2.1.3 Chemicals

Chemicals and reagents used in this thesis are listed in Table 2.3.

Table 2.3: Chemicals and reagents

chemical/reagent	supplier
2-(N-morpholino)ethanesulfonic (MES) acid	Applichem GmbH, Darmstadt
5-Chloro-2'-deoxyuridine	Sigma-Aldrich Chemie GmbH, München
5-Iodo-2'-deoxyuridine	Sigma-Aldrich Chemie GmbH, München
Acetic acid	Applichem GmbH, Darmstadt
Acrylamide solution (30 %)	Applichem GmbH, Darmstadt
Agarose	Applichem GmbH, Darmstadt
Ammonium persulfate (APS)	Applichem GmbH, Darmstadt
Antibotic-Antimycotic	Life Technologies GmbH, Darmstadt
Aphidicolin	Santa Cruz Biotechnology Inc., Santa Cruz, USA
Bambanker serum-free cell freezing medium	NIPPON Genetics Europe GmbH, Dueren
β-Agarase	New England BioLabs GmbH, Frankfurt a.M
β-Mercaptoethanol	Applichem GmbH, Darmstadt

chemical/reagent	supplier
Bio-Rad Protein Assay Dye Reagent (5x)	Bio-Rad Laboratories GmbH, München
Block AID solution	Thermo Fisher Scientific, Waltham, USA
Bovine serum albumin (BSA)	Carl Roth GmbH & Co. KG, Karlsruhe
Bromphenol blue sodium salt	Applichem GmbH, Darmstadt
Calcium chloride dihydrate	Applichem GmbH, Darmstadt
Camptothecin	Santa Cruz Biotechnology Inc., Santa Cruz, USA
Carbenicillin (Carb) disodium salt	Applichem GmbH, Darmstadt
Colcemid	Sigma-Aldrich Chemie GmbH, München
Deoxynucleotide triphosphate (dNTP) solution mix	New England BioLabs GmbH, Frankfurt a.M.
Dithiothreitol (DTT)	Applichem GmbH, Darmstadt
Dulbecco's Modified Eagle Medium (DMEM)	Life Technologies GmbH, Darmstadt
Dulbecco's Phosphate-Buffered Saline (DBPS)	Life Technologies GmbH, Darmstadt
Ethanol	VWR International GmbH, Darmstadt
Ethanol technical grade	Applichem GmbH, Darmstadt
Ethidium bromide	Applichem GmbH, Darmstadt
Ethylenediaminetetraacetic acid (EDTA) disodium salt dihydrate	Applichem GmbH, Darmstadt
Fetal calf serum (FCS)	Life technologies GmbH, Darmstadt
Giemsa stain	Applichem GmbH, Darmstadt
Glycerol 87 %	Applichem GmbH, Darmstadt
Glycine	Applichem GmbH, Darmstadt
HCS CellMask™ Deep Red Stain	Life Technologies GmbH, Darmstadt
HEPES	Applichem GmbH, Darmstadt
Hoechst 33342	Applichem GmbH, Darmstadt
Hydrochloric acid 1 M	Applichem GmbH, Darmstadt
Hydroxyurea	Sigma-Aldrich Chemie GmbH, München
Isopropanol	Applichem GmbH, Darmstadt
Isopropanol technical grade	Applichem GmbH, Darmstadt

chemical/reagent	supplier
Kanamycin (Kan) sulfate	Applichem GmbH, Darmstadt
LB agar powder	Applichem GmbH, Darmstadt
LB medium powder	Applichem GmbH, Darmstadt
Lipofectamine 2000	Life Technologies GmbH, Darmstadt
Lipofectamine RNAiMAX Transfection Reagent	Thermo Fisher Scientific, Waltham, USA
Magnesium chloride hexahydrate	Applichem GmbH, Darmstadt
McCoy's 5A (Modified) Medium	Life Technologies GmbH, Darmstadt
Methanol	Applichem GmbH, Darmstadt
Methanol technical grade	Applichem GmbH, Darmstadt
Milk powder	Applichem GmbH, Darmstadt
N,N,N',N'-Tetramethylethylenediamine (TEMED)	Applichem GmbH, Darmstadt
N-Lauroylsarcosine sodium salt	Applichem GmbH, Darmstadt
Nonidet P-40 (NP-40)	Applichem GmbH, Darmstadt
Normal Goat Serum	Dako Deutschland GmbH, Hamburg
Optimized Minimum Essential Medium (Opti-MEM)	Life Technologies GmbH, Darmstadt
Phenylmethanesulfonylfluoride (PMSF)	Applichem GmbH, Darmstadt
Potassium chloride	Applichem GmbH, Darmstadt
Potassium dihydrogen phosphate	Applichem GmbH, Darmstadt
Protease inhibitor cocktail tablets Complete	Roche, Mannheim
RO-3306 inhibitor	Sigma-Aldrich Chemie GmbH, München
Roti-Histofix 4 %	Carl Roth GmbH & Co. KG, Karlsruhe
Sodium azide	Applichem GmbH, Darmstadt
Sodium chloride	Carl Roth GmbH & Co. KG, Karlsruhe
Sodium deoxycholate	Applichem GmbH, Darmstadt
Sodium dodecyl sulfate (SDS)	Applichem GmbH, Darmstadt
Sodium hydrogen phosphate	Applichem GmbH, Darmstadt
Sodium hydroxide pellets	Applichem GmbH, Darmstadt
Tris hydrochloride (Tris-HCl)	Applichem GmbH, Darmstadt

chemical/reagent	supplier
Tris(hydroxymethyl)aminomethane (Tris)	Applichem GmbH, Darmstadt
Trisodium citrate	Applichem GmbH, Darmstadt
Triton X-100	Applichem GmbH, Darmstadt
TrypLE Express	Life Technologies GmbH, Darmstadt
Tween 20	Applichem GmbH, Darmstadt

2.1.4 Buffers, solutions and media

Buffers, solutions and media used in this thesis are listed in Table 2.4. Unless stated otherwise, ingredients were dissolved in ultra.pure Milli-Q H_2O.

Table 2.4: Buffers, solutions and media

buffer/solution/media	ingredients	final concentration
APS		10 % (w/v)
Calcium chloride		2 M
Carbenicillin		100 mg/ml
CSK buffer	Sodium chloride Magnesium chloride hexahydrate HEPES Sucrose Triton X-100 PMSF Protease inhibitor	100 mM 3 mM 10 mM HEPES, pH 7.4 300 mM 0.3 % (v/v) 1 mM one tablet
DMEM -+	FCS	10 % (v/v) in DMEM
DMEM ++	Antibiotic-antimycotic FCS	1 % (v/v) 10 % (v/v) in DMEM

buffer/solution/media	ingredients	final concentration
DNA loading dye (10x)	Bromophenol blue	0.25 % (w/v)
	EDTA	100 mM
	Glycerol	20 % (w/v)
	Xylene cyanole	0.25 % (w/v)
DTT		1 M
EDTA buffer	EDTA	0.5 M
		pH 8.0
2x HBS buffer	sodium chloride	280 mM
	disodium phosphate	1.5 mM
	HEPES	50 mM
		pH adjusted to 7.13 with sodium hydroxide
HEPES buffer	HEPES	1 M
Hoechst solution	Ethanol	25 % (v/v)
	Hoechst 33342	1 mg/ml
		in PBS
IF antibody dilution buffer	BSA	1 % (w/v)
	Triton X-100	0.3 % (v/v)
		in PBS
IF blocking buffer	Normal goat serum	5 % (v/v)
	Triton X-100	0.3 % (v/v)
		in PBS
Giemsa staining solution	Giemsa solution	5 % (v/v)
	Phosphate buffer	20 % (v/v)
IP lysis buffer	Tris (pH 8)	50 mM
	NaCl	150 mM
	EDTA	5 mM
	NP-40	0.5 % (v/v)
	DTT	1 mM
	PMSF	1 mM
	Protease inhibitor	one tablet
Kanamycin		50 mg/ml

buffer/solution/media	ingredients	final concentration
LB agar	LB agar powder	40 g/L pH 7.5
LB medium MES buffer	LB medium powder MES	25 g/L pH 7.5 0.5 M pH 5.5
Phosphate-buffered saline (PBS)	Disodium hydrogen phosphate Potassium chloride Potassium dihydrogen phosphate Sodium chloride	10 mM 2.7 mM 2 mM 137 mM pH 7.4
Phosphate buffer for Giemsa staining	Sodium hydrogen phosphate Potassium dihydrogen phosphate	25 mM 25 mM
PMSF		0.2 M in ethanol
Radioimmunoprecipitation assay (RIPA) buffer	Tris-HCl NaCl EDTA NP-40 Sodium deoxycholate DTT PMSF Protease inhibitor	50 mM 150 mM 5 mM 1 % (v/v) 1 % (w/v) 1 mM 1 mM one tablet
Sarcosyl	N-Lauroylsarcosine sodium salt	10 % (w/v) in 0.5 M EDTA, pH 8.0
SDS-Page running buffer	Glycine SDS Tris	192 mM 0.1 % (w/v) 25 mM

buffer/solution/media	ingredients	final concentration
SDS sample buffer (5x)	Bromophenol blue EDTA Glycerol β-Mercaptoethanol SDS Tris-HCl	0.1 % (w/v) 5 mM 30 % (v/v) 7.5 % (v/v) 15 % (w/v) 60 mM, pH 6.8
Separation gel buffer (4x)	SDS Tris	0.8 % (w/v) 1.5 M, pH 8.8
Sodium azide		0.1 % (w/v) in PBS
Stacking gel buffer (4x)	SDS Tris-HCl	0.8 % (w/v) 0.5 M, pH 6.8
TAE buffer	Tris Acetic acid EDTA	40 mM 20 mM 1 mM pH adjusted to 8.8 with acetic acid
TE buffer	Tris buffer EDTA buffer	1 % (v/v) 0.2 % (v/v)
Transfer buffer	Glycine Methanol SDS Tris	192 mM 20 % (v/v) 0.01 % (w/v) 25 mM pH 8.3
Tris Base buffer	Tris	1 M
Tris buffer 1 M	Tris-HCl buffer 1 M	25 % (v/v) adjusted to 8.0 with Tris Base 1 M
Tris-HCl buffer	Tris-HCl	1 M
Tris-buffered saline (TBS) buffer	Sodium chloride Tris-HCl	150 mM 50 mM

buffer/solution/media	ingredients	final concentration
Tris-buffered saline and Tween-20 (TBST)	Sodium chloride Tris-HCl Tween-20	150 mM 50 mM 0.1 % (v/v)
Trisodium citrate buffer	Trisodium citrate	1 % (w/v)
Western blotting (WB) blocking buffer	Milk powder	5 % (w/v) in TBST

2.1.5 Antibodies

The listed specific primary (Table 2.5) and secondary antibodies (Table 2.6) were used for protein detection in western blotting (WB, see section 2.2.3.6) and in immunofluorescence (IF, see section 2.2.2.7).

Table 2.5: Primary antibodies

antigen	origin	dilution		supplier
		WB	IF	
53BP1	rabbit		1:2000	Novus Biologicals (NB100-304)
Aurora B	rabbit		1:2000	Sigma-Aldrich (A5102)
Borealin	mouse		1:200	MBL/Biozol (M147-3)
BrdU	mouse		1:6.25	BD Pharmingen (347580)
BrdU	rat		1:12.5	AbD Serotec (MCA2060GA)
CREST	human serum		1:300	Antibodies Incorporated (15-234)
Cyclin A2	mouse		1:100	Santa Cruz (sc-271682)
DNA Ligase I	mouse		1:100	MBL/Biozol (K0190-3)
FLAG-tag	mouse	1:2000		Sigma Aldrich (F3165)
GFP	rabbit	1:2000		Santa Cruz (sc-8334)
HA-tag	mouse	1:1000		Biolegend (905001)
histone H3	mouse	1:1000		abcam (ab195277)

antigen	origin	dilution		supplier
		WB	IF	
INCENP	mouse		1:150	Invitrogen (39-2800)
INCENP	rabbit		1:400	NEB Cell Signaling (2807)
mAID-tag	mouse	1:500		MLB/Biozol (M214-3)
myc-tag	mouse	1:1000		NEB Cell Signaling (2276)
myc-tag	rabbit	1:1000 (BSA/TBST)		NEB Cell Signaling (2272)
PCNA	mouse		1:3200	NEB Cell Signaling (2586)
PCNA (PC10)	mouse	1:200		Santa Cruz (sc-56)
PCNA	rabbit		1:200	abcam (ab92552)
Polymerase η	rabbit	1:1000		Novus Biologicals (NB100-60424)
ssDNA	mouse		1:6.25	Developmental Studies Hybridoma Bank
Survivin	rabbit		1:300	Novus Biologicals (NB500-201)
αTubulin	mouse	1:8000		Sigma Aldrich (T6074)
yH2AX	mouse	1:5000		Biolegend 613402

Table 2.6: Secondary Antibodies

antigen	origin	dilution		supplier
		WB	IF	
IgG anti-human AF 568	goat		1:1000	Invitrogen (A21090)
IgG anti-mouse AF 568	goat		1:1000	Invitrogen (A11004)
IgG anti-mouse AF 633	goat		1:1000	Invitrogen (A21052)
IgG anti-rabbit AF 488	goat		1:1000	Invitrogen (A11008)

antigen	origin	dilution		supplier
		WB	IF	
IgG anti-mouse BV480	goat		1:12.5	Jackson Immuno Research (155-685-166)
IgG anti-mouse HRP	sheep		1:10000	GE Healthcare (NXA931)
IgG anti-rabbit HRP	donkey		1:10000	GE Healthcare (NA934)

2.1.6 Oligonucleotides

2.1.6.1 DNA Oligonucleotides

Synthetically generated DNA oligonucleotides used for PCR were purchased from Eurofins Genomics, Ebersberg. DNA oligonucleotides for sequencing were provided by LGC Genomics, Berlin.

2.1.6.2 siRNAs

Synthetically generated siRNAs (Table 2.7) used for RNA interference (RNAi, section 2.2.2.6) were purchased in 20 or 40 nmol scale, resuspended in RNAse-free water and stored as 20 or 40 µM stocks solution at -20 °C.

Table 2.7: siRNAs for RNA interference

name	target/sense strand (5’ – 3’)	reference/supplier
siAurora B	human Aurora B (CDS)/ GGUGAUGGAGAAUAGCAGUTT	(Hauf et al. 2003)/ Microsynth AG, Balgach, CH
siCtrl	Non mammalian homology (Luciferase)/ UUCUCCGAACGUGUCACGUTT	(Dobrynin et al. 2011)/ Microsynth AG, Balgach, CH
siSurvivin (B02)	human Survivin (3’-UTR)/ AAGAAGAGCACAGUUGAAACAUCA	Invitrogen, Karlsruhe
siSurvivin (F02)	human Survivin/ GAAUGUGUCUGGACCUCAUGUUGUU	Invitrogen, Karlsruhe

name	target/sense strand (5' – 3')	reference/supplier
siSurvivin (BIRC5.5)	human Survivin/ GCAUUCGUCCGGUUGCGCUTT	Qiagen, Hilden

2.1.7 Plasmids

The plasmids used in this work are listed in Table 2.8.

Table 2.8: Eukaryotic expression plasmids

plasmid	feature	reference
pC3-Aurora B-myc	Aurora B fused C-terminal with myc	Knauer group
pC3-Borealin-myc	Borealin fused with C-terminal myc	Knauer group
pC3-myc-INCENP	INCENP fused with N-terminal myc	courtesy of Prof. H. Meyer (University of Duisburg-Essen
pC3-myc-INCENP-PIPmut	INCENP with aa exchange of Gln853, Ile856, Thr859 and Thr860 to Ala fused N-terminal with myc	Knauer group
pC3-Survivin-FLAG	Survivin fused with C-terminal FLAG	Knauer group
pC3-Survivin-mAID	Survivin fused with C-terminal mAID	this thesis
pC3-Survivin-myc	Survivin fused with C-terminal myc	Knauer group
pENeGFP-PCNA	PCNA fused N-terminal with GFP	courtesy of Prof. C. Cardoso (TU Darmstadt)
pEN-HA-PCNA	PCNA fused with N-terminal HA	this thesis
pIRES-FLAG-POLH	Polymerase Eta fused with N-terminal FLAG	courtesy of Prof. Masutani (Nagoya University)

2.1.8 Eukaryotic cell lines

The eukaryotic cell lines used in this thesis are listed in Table 2.9.

Table 2.9: Eukaryotic cell lines

cell line	characteristics	ATCC number/reference
HEK 293T	*Homo sapiens*, embryonic kidney	CRL-11268
HeLa Kyoto	*Homo sapiens*, cervical adenocarcinoma	CCL-2

2.1.9 Bacterial strains

All bacterial strains used in this work are listed in Table 2.10.

Table 2.10: Bacterial strains

bacterial strain	genotype	supplier
NEB® 5-alpha *E. coli*	fhuA2 Δ(argF-lacZ)U169 phoA glnV44 Φ80 Δ(lacZ)M15 gyrA96 recA1 relA1 endA1 thi-1 hsdR17	New England BioLabs, Frankfurt a. M.
NEB® 10-beta *E. coli*	Δ(ara-leu) 7697 araD139 fhuA ΔlacX74 galK16 galE15 e14- ϕ80dlacZΔM15 recA1 relA1 endA1 nupG rpsL (StrR) rph spoT1 Δ(mrr-hsdRMS-mcrBC)	New England BioLabs, Frankfurt a. M.

2.1.10 DNA and protein standards

All DNA and protein standards used in this work are listed in Table 2.11.

Table 2.11: DNA and protein standards

name	supplier
GeneRuler 1 kb DNA ladder	Thermo Fisher Scientific, Waltham, USA
GeneRuler 1 kb Plus DNA ladder	Thermo Fisher Scientific, Waltham, USA
Spectra Multicolour Broad Range Protein ladder	Thermo Fisher Scientific, Waltham, USA

2.1.11 Kits

All kits that were used in this work are listed in Table 2.12.

Table 2.12: Kits

kit	supplier
Chromatin Extraction kit	Abcam, Camebridge, UK
CRISPR/Cas9 KO plasmid and HDR plasmid transfection kit	Santa Cruz Biotechnology Inc., Santa Cruz, USA
Click-iT™ EdU Alexa Fluor™ 488 Imaging kit	Thermo Fisher Scientific, Waltham, USA
Duolink® In Situ Detection Reagents Orange	Sigma-Aldrich Chemie GmbH, München
Duolink® In Situ PLA® Probes mouse/rabbit	Sigma-Aldrich Chemie GmbH, München
FiberPrep® (DNA Extraction kit)	Genomic Vision, Bagneux, FR
NucleoBond Xtra Midi kit	Macherey-Nagel GmbH & Co. KG, Düren
NucleoSpin Plasmid (NoLid) Mini kit	Macherey-Nagel GmbH & Co. KG, Düren
NucleoSpin Gel and PCR Clean-Up kit	Macherey-Nagel GmbH & Co. KG, Düren
µMACS® Isolation kit for tagged proteins	Miltenyi Biotec B.V. & Co. KG, Bergisch-Gladbach

kit	supplier
Pierce™ ECL Plus Western Blotting Substrate	Pierce Biotechnology, Inc., Rockford, USA
Q5® Site-directed mutagenesis	New England BioLabs, Frankfurt a. M.
Subcellular Protein Fractionation kit for cultured cells	Thermo Fisher Scientific, Waltham, USA
SuperSignal™ West Femto Maximum Sensitivity Substrate	Pierce Biotechnology, Inc., Rockford, USA
TaKaRa DNA Ligation kit	Takara Bio Inc., Saint-Germain-en-Laye, FR

2.1.12 Software

The software used in this thesis is listed in Table 2.13.

Table 2.13: Software

software	manufacturer
Adobe Photoshop CS4	Adobe Systems GmbH, München
A plasmid Editor (ApE)	Wayne Davis (University of Utah), Salt Lake City, USA
Canvas 11	ACD Systems International Inc., Seattle, USA
CellProfiler 3.1.9	Carpenter Lab (Broad Institute of Harvard and MIT), Camebridge, USA
Citavi 5	Swiss Academic Software GmbH, Wädenswill, CH
Clustal Omega	EMBL-EBI, Camebridge, UK
FiberStudio 2.0.2	Genomic Vision, Bagneux, FR
GraphPad Prism 5	GraphPad Software, Inc., La Jolla, USA
ImageJ	U.S. National Institutes of Health, Bethesda, USA
Leica Application Suite X (LASX)	Leica Microsystems GmbH, Mannheim
Microsoft Office	Microsoft Corporation, Redmond, USA
SnapGene Viewer 3.3.4	GSL Biotech, Chicago, USA

2.2 Methods

2.2.1 Molecular Biology

2.2.1.1 Polymerase Chain Reaction (PCR)

For the amplification of selected DNA fragments was the polymerase chain reaction (Mullis and Faloona 1987) applied, which is based on cyclic repetitions of denaturation, annealing and elongation steps. In order to obtain single base mutations or mutations of longer plasmid sequences by PCR, the Q5® Site-directed mutagenesis kit from New England BioLabs was used according to the manufacturer's instructions. The composition of a typical PCR reaction mix can be found in Table 2.14.

Table 2.14: Composition of a PCR reaction mix.

reagent	volume	final concentration
Q5 Hot Start High-Fidelity 2x Master Mix	12.5 µl	1x
10 µM forward primer	1.25 µl	0.5 µM
10 µM reverse primer	1.25 µl	0.5 µM
template DNA (1–25 ng/µl)	1 µl	1–25 ng
nuclease-free water	9 µl	

The reaction mixes were placed in a thermocycler, where they were subjected to specific cycling conditions according to the primers' annealing temperature, the length of the desired PCR product and the processivity of the polymerase.

Table 2.15: Cycling conditions of a PCR.

step		temperature	time
initial denaturation		98 °C	30 seconds
25 cycles	denaturation	98 °C	10 seconds
	annealing	50–72 °C	30 seconds
	elongation	72 °C	30 seconds/kb
final extension		72 °C	2 minutes
hold		10 °C	∞

2.2.1.2 KLD treatment

The amplified PCR reaction mix (see section 2.2.1.1) was then subjected to a KLD treatment according to the manufacturer's instructions. The KLD enzyme mix consists of kinases, ligases and DpnI enzymes, which allow phosphorylation, intramolecular circularization and template removal. The composition of the KLD reaction mix can be found in Table 2.16. The KLD reaction mix was incubated for at least 5 minutes at room temperature (RT).

Table 2.16: Composition of a KLD reaction mix.

reagent	volume	final concentration
PCR product	1 µl	
2x KLD reaction buffer	5 µl	1x
10x KLD enzyme mix	1 µl	1x
nuclease-free water	3 µl	

2.2.1.3 Transformation of competent bacteria

Afterwards, 5 µl of the KLD reaction mix (see section 2.2.1.2) was added to 50 µl of chemically competent NEB® 5-alpha or NEB® 10-beta bacterial cells, respectively. The bacteria were incubated for 30 minutes on ice, heat shocked by 42 °C and then again incubated on ice for another 5 minutes. Then, 950 µl SOC medium was added and the bacteria were gently shook and incubated at 37 °C for 1 hour. 100 µl of the dilution was plated on an antibiotic-containing LB agar plate and incubated over night at 37 °C.

2.2.1.4 Agarose gel electrophoresis

Horizontal agarose gel electrophoresis was used to separate nucleic acids according to their size. Here, negatively charged DNA moves through the agarose gel that is placed in an electric field. Small DNA fragments move faster through the gel than larger ones achieving size separation. Agarose gels were made by solving 1–2 % agarose in 1x TAE buffer, boiling the mixture and adding DNA intercalating agents such as ethidium bromide before casting the gel. After polymerization, the gel was inserted into

a gel chamber filled with 1x TAE buffer. The DNA samples were mixed with 10x loading dye and loaded on the gel with an appropriate DNA ladder. Electrophoresis was performed with a constant voltage of 100 V for 45–90 minutes. Afterwards, the DNA was visualized with UV light (E-Box VX2, Vilber Lourmat).

2.2.1.5 Extraction of DNA fragments from agarose gels and PCR samples

The NucleoSpin Gel and PCR Clean-Up kit from Macherey-Nagel was used according to the manufacturer's instructions to extract DNA fragments from agarose gel slices (see section 2.2.1.4) and to purify PCR samples (see section 2.2.1.1). The DNA was eluted in 30 µl elution buffer.

2.2.1.6 DNA restriction and ligation

Restriction enzymes were used for the restriction of plasmids and PCR fragments to verify successful cloning or to obtain specific DNA fragments. The enzymes cut dsDNA by catalysing the hydrolysis of phosphodiester bonds of the DNA backbone recognized through palindromic recognition site.
For analytical digests 200 ng DNA were incubated with the adequate buffer and 4 units of the respective restriction enzymes at 37 °C for 1 hour. For preparative digests 5–10 µg DNA were digested in the adequate buffer with 40 units of restriction enzymes at 37 °C for 4 hours. Afterwards, DNA fragments were separated by agarose gel electrophoresis (see section 2.2.1.4) and subsequently purified (see section 2.2.1.5).
Ligation of digested DNA fragments was performed by using the TaKaRa DNA ligation kit from TaKaRa Bio Inc.. The ligation reaction mix contains 2 µl insert, 0.5 µl vector and 2.5 µl solution I of the kit and was incubated at RT for 30 minutes. Afterwards, the ligated plasmid was transformed in competent NEB® 5-alpha or NEB® 10-beta bacterial cells, respectively (see section 2.2.1.3).

2.2.1.7 Preparation of plasmids from bacteria

Depending on the required amount of DNA either the NucleoBond Xtra Midi or the NucleoSpin Plasmid (NoLid) Mini kit from Macherey-Nagel GmbH was used for the preparation of plasmids from bacterial cells. Either 200 ml LB medium for midi preparation or 8 ml LB medium for mini preparation, containing the respective

antibiotics, was inoculated with a single bacterial colony from a LB agar plate (see section 2.2.1.3) or a sample from a bacterial glycerol stock (see section 2.2.1.8). The inoculated culture was grown at 37 °C over night while shaking at 120 rpm in an orbital shaker. The plasmids were prepared according to the manufacturer's instructions and either eluted in ddH_2O or elution buffer. The concentration and purity of the plasmid was determined via UV spectroscopy (see section 2.2.1.9).

2.2.1.8 Preparation of bacterial glycerol stocks

For long-term storage of bacterial cells containing plasmid DNA, bacterial glycerol stocks were obtained by mixing 800 µl of overnight bacterial culture with 200 µl 87 % glycerol. The bacterial glycerol stock was stored at -80 °C.

2.2.1.9 Quantification of DNA concentrations

Concentration and purity of plasmids was determined by NanoDrop2000c (Thermo Fisher Scientific). DNA concentrations were determined by measuring the absorbance at 260 nm, which is the absorbance maximum for nucleic acids. Here, an absorption of 1 equates a DNA concentration of 50 ng/µl. DNA purity was determined by measuring the absorbance at 230 nm and 280 nm to obtain A260/230 and A260/280 ratios. The A260/230 ratio indicates contamination with salts or organic components and should ideally be 1.8. The A260/280 ratio indicates contamination with proteins and RNA and should also ideally be 1.8.

2.2.1.10 DNA sequence analysis

DNA sequencing was performed by LGC Genomics using a chain-terminating method or rather Sanger sequencing (Sanger et al. 1977). The DNA concentration was adjusted to 100 ng/µl in 20–40 µl. Sequencing primers were provided by the company and the sequencing results were analysed with Clustal Omega (EMBL-EBI) and SnapGene Viewer.

2.2.2 Cell Biology

2.2.2.1 Culture of cell lines

All cell lines were cultured under sterile conditions and an atmosphere of 37 °C, 5 % CO_2 and approximately 90 % relative humidity. They were maintained in T-75 cell culture flasks with 10 ml of the respective medium supplemented with 10 % fetal calf serum (FCS) and 1 % antibiotic-antimycotic. When reaching a confluency of 70–90 % cells were passaged by aspirating the medium, washing the cell layer with 5 ml DPBS and adding 2 ml TrypLE Express solution to detach the cells from the cell culture flask. 8 ml of cell culture medium was added to stop the enzymatic detachment and the cells were diluted depending on their growth rate in a ratio of 1:5 to 1:20 into a new cell culture flask. For subsequent experiments cells were cultured in cell culture medium supplemented only with 10 % FCS.

2.2.2.2 Freezing and thawing of cell lines

For cryoconservation, cells were trypsinised and resuspended in 10 ml cell culture medium. Afterwards, the cell suspension was transferred to a 15 ml reaction tube and centrifuged for 5 minutes at 300 x g. The cell pellet was resuspended in an appropriate volume of Bambanker medium. Aliquots of 1 ml cell suspension per cryo tube were placed in a Mr. Frosty™ freezing container and stored over night at -80 °C to sustain a cooling of -1 °C/min. For long-term storage, the cells were transferred to a liquid nitrogen tank and stored at -160 °C.
Cryoconserved cells were thawed by heating the cryo tube in a water bath at 37 °C and adding the cells to a 15 ml reaction tube with 9 ml of appropriate cell culture medium. The cells were centrifuged for 5 minutes at 300 x g. The cell pellet was resuspended in 10 ml appropriate cell culture medium and the cell solution was transferred into a T-75 cell culture flask. After 24 hours, the cell culture medium was replaced and the cells were further incubated as described in section 2.2.2.1.

2.2.2.3 Inhibitor treatment

To inhibit the kinase Aurora B the inhibitor Hesperadin was used in a final concentration of 100 nm (stock solution 1 mM in DMSO). Hesperadin interacts with the

ATP binding pocket as well as with the adjacent hydrophobic binding pocket of Aurora B (Hauf et al. 2003; Sessa et al. 2005). A selective ATP-competitive inhibitor of CDK1, RO-3306, was used in a final concentration of 9 µM to arrest cells in G2/M phase (Vassilev et al. 2006). To induce replication stress several inhibitors were used. Camptothecin (CPT) is used to target topoisomerase I, hindering the re-ligation of SSB that are generated by topoisomerase I during replication or transcription to reduce torsional stress in der DNA. Ongoing replication then generates DSBs (Pommier 2006). CPT was used in a final concentration of 1 µM (stock solution 25 mM in DMSO). Hydroxyurea (HU) inhibits the ribonucleotide reductase, which is responsible to build deoxyribonucleotides, an important component of DNA. A loss of deoxyribonucleotides results in stalled forks and, subsequently, an inhibition of DNA synthesis (Jossen and Bermejo 2013). HU was used in a final concentration of 0.5 mM (stock solution 1.5 M in H_2O). Aphidicolin (Aph) inhibits polymerases α, β and ε by binding to their active site, thereby blocking the incorporation of nucleotides into the DNA, which leads to stalled replication forks. Low concentrations can lead to SSBs or DSBs, respectively (Sheaff et al. 1991). Aph was used in a final concentration of 0.1 µM (stock solution 2.954 µM in DMSO). Colcemid inhibits the formation of the spindle apparatus by binding to the microtubules. Colcemid was used in a final concentration of 0.08 µg/ml to arrest the cell cycle during metaphase.

2.2.2.4 X-ray irradiation

To analyse the effects of irradiation, cells were exposed to 10 Gy of X-ray. Irradiation was carried out with the X-ray cabinet CIX2. Cells were returned to the incubator after the irradiation and incubated for appropriate time points.

2.2.2.5 Transient transfection of eukaryotic cells

Transient transfection of eukaryotic cells with plasmid DNA was achieved either with calcium phosphate for 293T cells or with the liposomal transfection reagent Lipofectamine 2000 for all other cell lines. Calcium phosphate binds to the negatively charged DNA and supports cellular uptake via endocytosis, while Lipofectamine 2000 forms a liposomal embracement around the DNA that fuses with the cell membrane. For transfection with calcium phosphate, cells were seeded in 10 cm dishes 24 hours prior to transfection. 495 µl of 10 mM Tris/HCl pH 7.6 was mixed with 55 µl $CaCl_2$.

Approximately 14 µg DNA was added to the Tris/HCl/$CaCl_2$ mix, the amount of DNA was adjusted if more than one plasmid was used. Afterwards, 550 µl of 2x HBS was added to the mixture while pulling the pipet from the bottom to the top of the reaction tube. The mixture was incubated for approximately 10 minutes and 1000 µl of it was then added dropwise to the cells. The cells were assayed 24 hours after transfection.
For transfection with Lipofectamine 2000, cells were seeded in 6-well plate 24 hours prior to transfection. Two transfection solutions were prepared. In solution 1 3 µl of Lipofectamine 2000 was mixed with 100 µl Opti-MEM medium. In solution 2 approximately 1 µg DNA was diluted in 100 µl Opti-MEM. Both solutions were mixed gently by vortexing and then combined. The reaction mix was again mixed gently and incubated for 5 minutes at RT before it was added dropwise to the cells. The cells were incubated at standard growth conditions and assayed 24 hours after transfection.
If other than the described cell culture dishes were used, the noted volumes were adjusted accordingly.

2.2.2.6 RNA interference (RNAi)

For RNAi experiments, small interfering RNA (siRNA) was used to inhibit the expression of specific proteins to study their biological function. siRNA binds complementary to the corresponding mRNA and prevents translation of the protein. The cells were transfected with the Lipofectamine RNAiMAX transfection reagent by following the manufacturer's instructions. Cells were seeded in a 6-well plate 24 hours prior transfection. Two transfection solutions were prepared. In solution 1 9 µl of RNAiMAX transfection reagent were diluted in 150 µl Opti-MEM medium. In solution 2 30 pmol DNA were diluted in 150 µl Opti-MEM medium. Both solutions were mixed gently by vortexing and then combined. The reaction mix was again mixed gently and incubated for 5 minutes at RT before it was added dropwise to the cells. The cells were incubated at standard growth conditions and assayed 48 hours after transfection.
If other than the described cell culture dishes were used, the noted volumes were adjusted accordingly.

2.2.2.7 Immunofluorescence

Indirect Immunofluorescence (IF) was applied to visualize proteins in cells by using a specific primary antibody, recognizing the appropriate antigen, and a secondary

antibody, conjugated with a fluorophore. Cells were seeded in 3 cm microscopic glass bottom dishes (MatTek Corporation) and treated or transfected, respectively. At appropriate time points, cells were fixed with Roti®-Histofix 4 % for 20 minutes at RT. After three washing steps with DPBS, the cells were permeabilised and unspecific binding sites were blocked for 30 minutes at RT with NEB blocking buffer containing 5 % normal goat serum in 0.3 % TritonX-100/DPBS for 10 minutes at RT. The cells were washed again three times with DPBS before they were incubated with the appropriate primary antibody (Table 2.5) diluted in NEB antibody dilution buffer (10 % (w/v) BSA/DPBS) overnight at 4 °C. After washing three times with DPBS, the fluorophore-conjugated secondary antibody (Table 2.6) diluted again in NEB antibody dilution buffer was added to the cells for 1 hour at RT in the dark. Here, the antibody solution also contained 10 µg/ml Hoechst33342 dye to stain the DNA. Following three final washing steps with DPSB, the samples were stored at 4 °C in 0.1 % (w/v) sodium azide/DPBS before they were microscopically analysed. Images were acquired with a Leica TCS SP8X laser scanning microscope.

2.2.2.8 Proximity ligation assay

The proximity ligation assay (PLA) is an antibody-based method to analyse protein-protein interactions in cells on an endogenous level. Two primary antibodies (Table 2.5) bind to the proteins of interest (POI). These antibodies are then recognized by secondary antibodies that are conjugated with single-stranded oligonucleotides (PLA probes). If the POIs are in close proximity (< 40 nm), the PLA probes will hybridize with the connector oligos, which then get ligated to form a complete DNA circle. A DNA polymerase amplifies this circular structure through rolling-circle amplification with fluorescent nucleotides that can be detected as a PLA signal via fluorescence microscopy.

PLA staining was performed with Duolink® In Situ PLA® Probes mouse/rabbit together with the Duolink® In Situ Detection Reagents Orange from Sigma-Aldrich and by following the manufacturer's instructions. Cells were seeded in 3 cm microscopic glass bottom dishes (MatTek Corporation) and treated or transfected, respectively. At appropriate time points, cells were fixed with Roti®-Histofix 4 % for 20 minutes at RT. After three washing steps with DPBS, the cells were permeabilized and unspecific binding sites were blocked for 30 minutes at RT with NEB blocking buffer containing

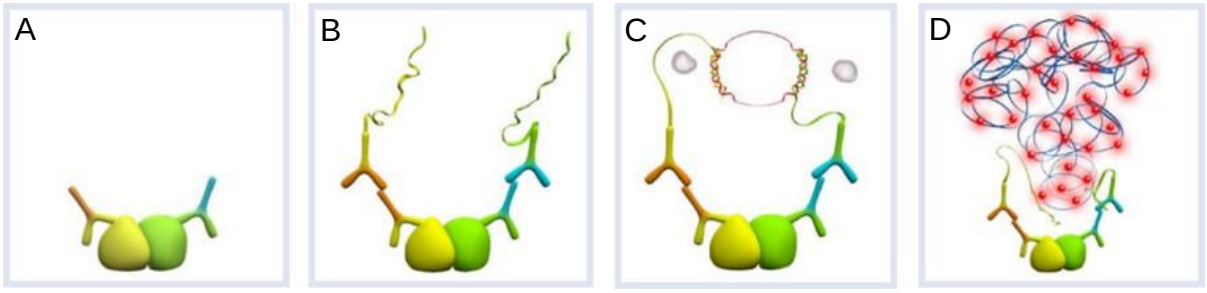

Figure 2.1: Principle of the Proximity Ligation Assay

A) Two primary antibodies bind to the proteins of interest (POI). **B)** These antibodies are then recognized by secondary antibodies that are conjugated with single-stranded oligonucleotides (PLA probes). **C)** If the POIs are in close proximity (< 40 nm), the PLA probes will hybridize with the connector oligos, which then get ligated to form a complete DNA circle. **D)** A DNA polymerase amplifies this circular structure through rolling-circle amplification with fluorescent nucleotides. (modified after (How Proximity Ligation Assay (PLA) Works | Sigma-Aldrich [updated 2020])

5 % normal goat serum in 0.3 % TritonX-100/DPBS for 10 minutes at RT. The cells were washed again three times with DPBS before they were incubated with the appropriate primary antibody (Table 2.5) diluted in NEB antibody dilution buffer (10 % (w/v) BSA/DPBS) overnight at 4 °C. Here, the two POIs were targeted with antibodies derived from mouse and rabbit, respectively. Following three washing steps with DPBS, the cells were incubated with Duolink® In Situ PLA probes anti-rabbit PLUS and anti-mouse MINUS for 1 hour at 37 °C in a humidified chamber. Again, the cells were washed three times with DPBS, the ligation solution was added and the cells were incubated for 30 minutes at 37 °C in a humidified chamber. After another three washing steps, the amplification solution was added and incubated for 100 minutes at 37 °C in a humidified chamber. Afterwards, the cells were stained with 10 µg/ml Hoechst33342 and HCS CellMask™ Deep Red Stain (dilution: 1:5000) in DPBS for 20 minutes at RT in the dark before they were stored at 4 °C in 0.1 % (w/v) sodium azide/DPSB until they were microscopically analysed. Images were acquired with a Leica TCS SP8X confocal laser scanning microscope. CellProfiler was used to analyse maximum projection images of z-stacks. The nuclei were defined based on the Hoechst33342 staining as primary objects and the entire cells was defined based on the CellMask staining as secondary objects. PLA signals within the cells were detected, counted and assigned to the respective parental cell.

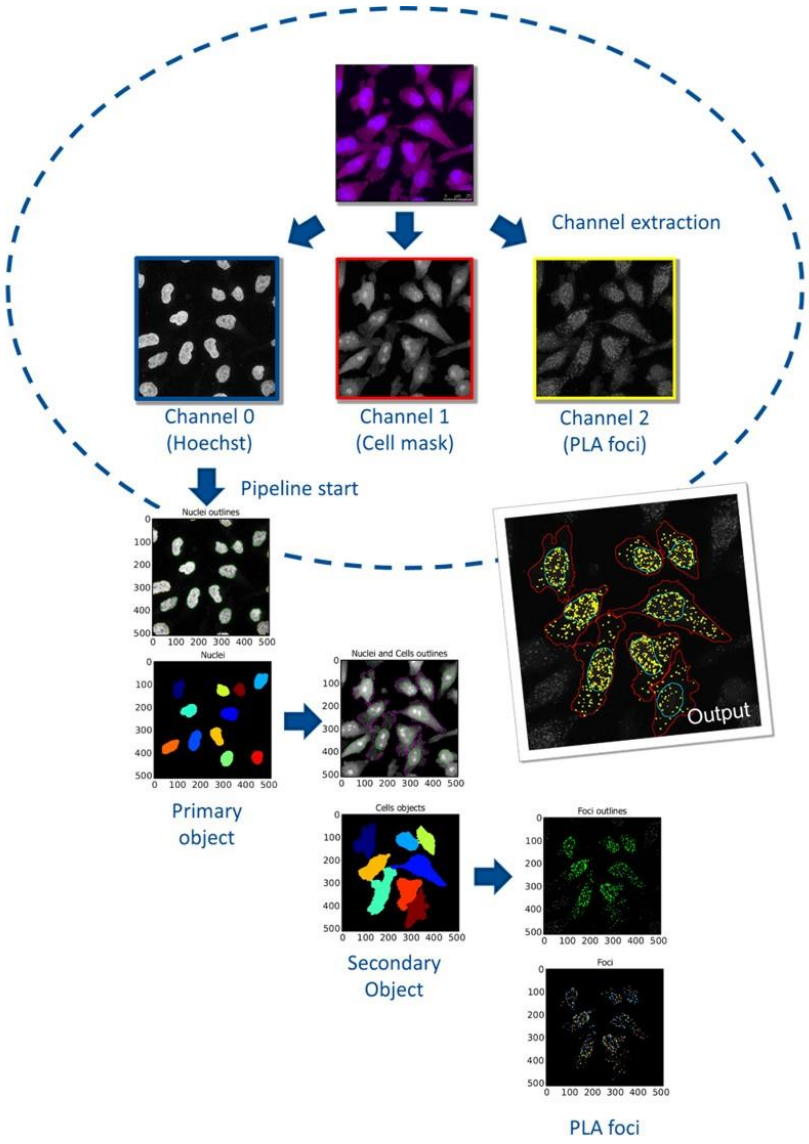

Figure 2.2: PLA analysis conducted with CellProfiler

Nuclei were defined as primary objects based on the Hoechst33342 staining (blue) and the entire cells were defined as secondary objects based on the CellMask staining (red). For quantification, PLA foci (yellow) within the cell were counted and assigned to the respective parental cell. Cells which were cropped out of the field of view were not included into the analysis (modified after (David Dannheisig 2016)). The source code for analysis was generated by Dr. Nina Schulze from the ICCE.

2.2.2.9 EdU incorporation and staining

The Click-iT™ EdU Alexa Fluor™ Imaging kit from Thermo Fisher Scientific was used to identify cells that were actively involved in DNA replication by incorporating the thymidine analogue EdU into newly synthesized DNA and labelling it with an Alexa Fluor fluorescent dye via click chemistry. The kit was used according to the manufacturer's instructions. The cells were incubated with 9 µM RO-3306 for 16 hours

to arrest the cells at G2/M transition. Afterwards, the cells were released in fresh medium containing 10 µM EdU for 20 minutes before fixation and permeabilization (see section 2.2.2.7). Following three washing steps with DPBS, the Click-iT reaction cocktail was prepared according to the manufacturer's instructions, added to the cells and incubated for 30 minutes at RT in the dark. After three more washing steps with DPBS, the cells were incubated with primary antibodies for fluorescent co-staining as described in section 2.2.2.7. Images were acquired with a Leica TCS SP8 confocal laser scanning microscope.

2.2.2.10 DNA combing assay

The DNA combing assay is used to visualize the progression of replication forks during replication and gives information about various aspects of DNA synthesis, such as replication fork speed, fork stalling or collapsing, initiation and termination events and interorigin distances (IOD). For this, the DNA is sequentially labelled by two consecutive pulses with halogenated thymidine analogues, such as chlorodeoxyuridine (CldU) and iododeoxyuridine (IdU). The assay was performed with the FiberPrep® (DNA Extraction kit) from Genomic Vision according to the manufacturer's instructions.

Exponentially growing cells in a 6-well plate were transfected or treated and at appropriate time points pulse-labelled with the thymidine analogues by first adding CldU in a final concentration of 20 µM for 20 minutes under normal growth conditions. After 20 minutes, IdU was added in a final concentration of 200 µM (excess of IdU makes removal of CldU needless) for a further 20 minutes under normal growth conditions. The cells were then washed, trypsinised and collected in DPBS. After that, the cells were counted and diluted to a final concentration of 1 x 10^5–1.5 x 10^5 cells in 45 µl DPBS. Afterwards, 45 µl cell suspension was mixed with 45 µl low-melting agarose at 50 °C and the solution was homogenized by pipetting up and down. The solution was immediately dispensed into a DNA plug mould. The mould was kept at 4 °C for 30 minutes to let the agarose solidify. The solidified plug was then ejected in a proteinase K buffer and incubated for 2 hours at 50 °C. Afterwards the proteinase K buffer was changed for a fresh one to incubate the plug overnight at 50 °C. The following day, the plug was transferred into a 15 ml reaction tube and washed with TE buffer for 1 hour on a test tube rollator. The washing steps were repeated in total three times. Afterwards, the plug was transferred into a 2 ml reaction tube and 1 ml of MES

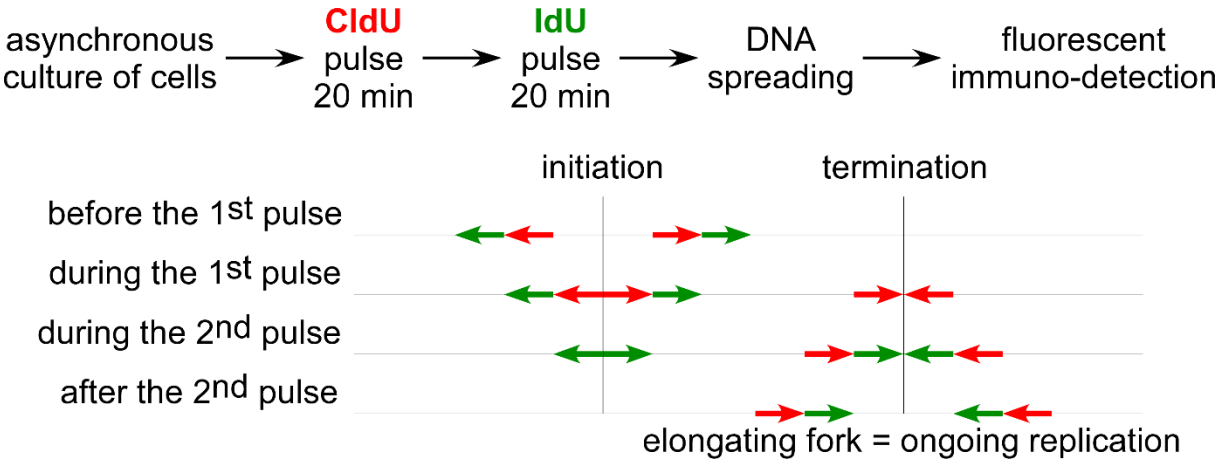

Figure 2.3: DNA combing assay

Cells were sequentially double pulse labelled with CldU and IdU. This allows analysis of ongoing forks, and initiation and termination events. The red and green arrows represent neo-synthesized DNA labelled with CldU and IdU, respectively. The labelling pattern differs depending on when the considered event occurs. For example, before the first pulse, during the first pulse, during the second pulse or after the second pulse. Six different patterns of initiations and terminations can occur (1–6). Modified after (Técher et al. 2013).

buffer was added. The plug was incubated for 20 minutes at 68 °C before it was immediately transferred to a heating block at 42 °C. Here, it was important to avoid any cooling of the plug. At 42 °C the plug was incubated for 10 minutes before adding 5 µl beta-agarase and further incubating over night at 42 °C. The next day, DNA reservoirs were prepared with 1200 µl MES buffer and the DNA solution was gently poured into them. After cooling down, the DNA solution can be combed on a silanized coverslip with the FiberComb® Molecular Combing System. Afterwards, the coverslips were baked for 2 hours at 70 °C before they were immunostained or stored at -20 °C. If the coverslips had been kept at -20 °C, they were dehydrated with 70 %, 90 % and 100 % ethanol for 1 minute each before proceeding to immunostaining.

For immunostaining, the dsDNA was denatured by covering the coverslips with 0.5 M NaOH + 1 M NaCl solution for 8 minutes at RT. Afterwards, the coverslips were washed three times with DPBS for 10 seconds each on an orbital shaker. The coverslips were then dehydrated with 70 %, 90 % and 100 % ethanol for 1 minute each before saturated with 25 µl Block Aid solution for 30 minutes at 37 °C in a humidity chamber. Afterwards, the coverslips were incubated with the first antibodies against CldU and IdU, respectively, diluted in Block Aid for 1 hour at 37 °C in a humidity chamber. Next, the coverslips were washed with DPBS containing 0.05 % Tween three times for 3 minutes each on an orbital shaker. Hereupon, the coverslips were incubated with 25 µl secondary antibody solution for 45 minutes at 37 °C in a humidity chamber.

Subsequently, the coverslips were washed again three times for 3 minutes with DPBS/0.5 % Tween. Following an incubation step for the third antibody solution containing an antibody against ssDNA diluted in Block Aid. The antibody solution was incubated for 2 hours at 37 °C in a humidity chamber. Again, the coverslips were washed three times for 3 minutes each with DPBS/0.5 % Tween on an orbital shaker. Then, the coverslips were incubated for 45 minutes at 37 °C in a humidity chamber for the second secondary antibody solution. After that, the coverslips were again washed three times for 3 minutes with DPBS/0.5 % Tween on an orbital shaker before dehydrating the coverslips with 70 %, 90 % and 100 % ethanol for 1 minute each. The coverslips were stored at 4 °C in a 50 ml reaction tube until image acquisition. Images can be acquired with a fluorescence microscope or the EasyScan service by Genomic Vision. For analysis, the FiberStudio® Analysis Software was used.

2.2.2.11 Metaphase chromosome spreading

Metaphase chromosome spreading was used to visualize gaps and breaks on metaphase chromosomes after replication stress. For this, the cells were cultivated and treated accordingly. Afterwards, the cells were incubated for 2 hours with 0.08 µg/ml colcemid to arrest the cells in metaphase. Metaphase cells are normally detached from the cell culture flask bottom and can be washed away and collected in a 15 ml reaction tube. The cells were centrifuged for 7 minutes at 130 x g and then incubated with 5 ml preheated (37 °C) sodium citrate for 10 minutes. Afterwards, the cells were centrifuged and the pellet was fixed with 5 ml dropwise fixation solution (150 ml methanol + 50 ml acetic acid) while using a vortexer at the same time. The cells were washed in total three times with 5 ml fixation solution. After the last washing step, just a bit of the fixation solution is removed to get a solution with a high concentration of cells. The spreads were performed by dropping the cell solution onto a microscope slide from a distance of about 50 cm. The slides were dried over night at RT. The next day, the slides were stained by incubating them with Giemsa staining solution (10 ml Giemsa and 40 ml phosphate buffer). Brightfield images were acquired with an Olympus CKX41 microscope. Images were randomized with ImageJ to prevent biased evaluation.

2.2.2.12 Confocal fluorescence microscopy

A fluorescence microscope uses laser light of certain wavelengths to excite fluorophores. As a result, these fluorophores emit light of longer wavelengths that can be detected by a fluorescence microscope. Confocal microscopy is a special form of fluorescence microscopy, where a focused laser beam is used to excite the specimen and out-of-focus light is eliminated by a pinhole in front of the detector increasing contrast and lateral resolution of the images.
Confocal fluorescence images were acquired with two different microscopes. First, a Leica TCS SP8 confocal laser scanning microscope, equipped with four lasers (Argon: 458/476/488/469/514 nm; DPSS: 561 nm; Helium Neon: 633 nm; UV diode: 405 nm), two PMT confocal imaging detectors and one sensitive imaging hybrid detector (HyD). The samples were imaged with a HC PL APO 63x/1.2 W CORR UVIS CS2 water objective. The microscope was operated with the Leica Application Suite X (LASX) software. Second, a Leica TCS SP8X confocal laser scanning microscope, equipped with four lasers (Argon: 458/476/488/469/514 nm; WLL E laser: 470 nm to 670 nm; UGA-42 Caliburn 355/42: 355 nm; UV diode: 405 nm), two PMT confocal imaging detectors, one sensitive imaging hybrid detector and two HyD SMD detectors. The samples were imaged with HC PL APO 63x/1.2 W motCORR CS2 objective. The microscope was operated with the Leica Application Suite X software.

2.2.3 Biochemistry

2.2.3.1 Whole-cell extract preparation

Whole cell extracts were prepared by chemically lysing cells with a RIPA buffer containing NP-40 and sodium deoxycholate. Cells seeded in a 6-well plate were washed with 1 ml DPBS and afterwards 100–150 µl RIPA buffer was added to the cells. The cells were incubated for 30 minutes on ice on an orbital shaker. Then, the cell suspension was transferred into a 1.5 ml reaction tube and sonicated with a Sonopuls mini20 ultrasonic homogenizer at an amplitude of 95 % for 20 seconds. After centrifugation at 20,000 x g for 20 minutes at 4 °C, supernatant was transferred into a new 1.5 ml reaction tube. The protein concentration was determined as described in section 2.2.3.3. Lysates were mixed with 5x Laemmli sample buffer, denatured for

5 minutes at 95 °C and stored at -20 °C before they were used in SDS-PAGE (see section 2.2.3.5) and western blotting (see section 2.2.3.6).

2.2.3.2 Subcellular fractionation

For subcellular fractionation, the Subcellular Protein Fractionation kit from Thermo Fisher Scientific was used to obtain cytoplasmic, membrane, nuclear soluble, chromatin bound and cytoskeletal protein extracts. The extracts were prepared according to the manufacturer's instructions. The subcellular extracts were used in SDS-PAGE (see section 2.2.3.5) and western blotting (see section 2.2.3.6).

2.2.3.3 Determination of protein concentration

The protein concentration of cell lysates was determined using the colorimetric Bradford assay, which is based on the binding of the dye Coomassie Blue G250 to proteins. 1 µl of sample lysate was mixed with 800 µl DPBS and 200 µl 5x concentrated Bio-Rad protein assay dye in a cuvette. After incubation for 5 minutes at RT, the absorption at 595 nm was measured using the Bio-Photometer Plus from Eppendorf AG. The protein concentration was determined by comparing the absorption with a predefined calibration curve (1–25 µg/ml) of bovine serum albumin (BSA).

2.2.3.4 Co-immunoprecipitation

Immunoprecipitation is a method to precipitate protein complexes out of whole-cell lysates with a specific antibody binding one target protein of said complexes. The specific antibody coupled to magnetic beads is used to separate the target protein from the lysate by applying a magnetic field. For this, 293T cells were seeded in 10 cm dishes and transfected one day later with plasmids coding for two differently tagged proteins. 24 hours after transfection, the cells were lysed as described in section 2.2.3.1 but with 1 ml interaction buffer instead of RIPA buffer. An input sample of the whole-cell extract was taken. The rest of the supernatant was incubated with 50 µl antibody-coupled magnetic beads from the µMACS isolation kit (Miltenyi Biotec) for 1 hour on ice. The suspension was transferred to a µ column, which was prior to this placed in a µMACS separator and equilibrated with 200 µl interaction buffer. The column was washed four times with 200 µl interaction buffer and once with 100 µl wash

buffer 2 from the kit. Elution was achieved by adding 20 µl of 95 °C hot elution buffer to the column and incubating for 5 minutes before adding another 50 µl of preheated elution buffer. The eluates were collected in 1.5 ml reaction tubes. Both, the input samples and the eluates were subjected to SDS-PAGE (see section 2.2.3.5) and western blotting (see section 2.2.3.6).

2.2.3.5 SDS-polyacrylamide gel electrophoresis

Sodium dodecyl sulphate-polyacrylamide gel electrophoresis (SDS-PAGE) was used to separate proteins according to their size within an electric field. The electrophoretic mobility depends on the amount of negatively charged SDS molecules bound to the proteins (Laemmli 1970). Polyacrylamide gels with a thickness of 1 or 1.5 mm and varying pore sizes were prepared as summarized in Table 2.17 and Table 2.18 using the Bio-Rad casting module. First, the separating gel was cast and layered with isopropanol to receive a smooth edge. After polymerization isopropanol was removed and the stacking gel was added on top and a comb was inserted to generate wells. Prior to electrophoresis, the protein samples were prepared as described in section 2.2.3.1 and then loaded onto the gel together with 5 µl of a protein ladder (Spectra Multicolor Broad Range; Thermo Scientific) used as a size standard. Electrophoresis was performed in 1x SDS running buffer for 60 minutes at 200 V. Afterwards, the gels were used for western blotting (see section 2.2.3.6).

Table 2.17: Composition of a SDS gel with a thickness of 1 mm.

component for 1 mm gel	separating gel		stacking gel
	12.5 %	15 %	4 %
ddH_2O [ml]	1.6	1.2	2.5
4x separating gel buffer [ml]	1.3	1.3	
4x stacking gel buffer [ml]	-	-	1.35
30 % polyacrylamide [ml]	2.1	2.5	0.65
10 % APS [µl]	50	50	50
TEMED [µl]	5	5	5

Table 2.18: Composition of a SDS gel with a thickness of 1.5 mm.

components for 1.5 mm gel	separating gel		stacking gel
	12.5 %	15 %	4 %
ddH_2O [ml]	2.9	2.0	2.5
4x separating gel buffer [ml]	2.4	2.4	-
4x stacking gel buffer [ml]	-	-	1.35
30 % polyacrylamide [ml]	2.1	2.5	0.65
10 % APS [µl]	96	96	50
TEMED [µl]	10	10	5

2.2.3.6 Western blotting

Western blotting is a method to transfer proteins from a SDS gel onto a nitrocellulose (NC) membrane on which they can be detected by antigen-antibody detection. For this, a blot sandwich was prepared containing two layers of blotting paper, the NC membrane, the SDS gel and two additional layers of blotting paper. All components were equilibrated in 1x transfer buffer prior to assembly. The sandwich was put into a transfer cassette together with fibre pads on each side. Next, the transfer cassette was placed in an electrophoresis chamber with the NC membrane facing the anode. The electrophoretic transfer was achieved with 120 mA for 16 hours at 4 °C or with 360 mA for 90 minutes at 4 °C, respectively. After transfer, the membrane was blocked with 5 % (w/v) nonfat dried milk powder in 1x TBS-T for 30 minutes at RT on an orbital shaker to block unspecific binding sites. Then, the membrane was incubated in primary antibody solution at 4 °C over night on an orbital shaker. Following three washing steps with TBS-T for 5 minutes each, the membrane was incubated with a HRP-conjugated secondary antibody for 1 hour at RT on an orbital shaker. The membrane was again washed three times with TBS-T for 5 minutes each and once with TBS. Detection of HRP activity was performed via chemiluminescence with Pierce™ ECL Plus Western Blotting Substrate, SuperSignal™ West Femto Maximum Sensitivity Substrate according to the manufacturer's instructions (both Thermo Scientific). Images were acquired with the ChemiDoc™ MP Imaging System (Bio-Rad).

3 Results

Survivin plays a major role in cancer due to its upregulation in most cancer entities and the association with chemo- and radioresistance. Its cancer specific characteristics make Survivin a promising target for cancer therapies. Most of Survivin's cellular roles are well documented such as its role as a member of the CPC. Here, Survivin takes part in the mitotic regulation by mediating chromosome condensation, proper kinetochore-microtubule attachments, the spindle assembly checkpoint and controlling the contractile apparatus. In addition, Survivin leads to the inhibition of cell death as a member of the IAP family. Nevertheless, the role of Survivin or the CPC during interphase, especially during DNA replication in S phase, still remains uncharacterized. As replication is an important factor for genomic integrity, it is of great importance to understand the fundamental mechanisms of Survivin and the CPC during interphase.

3.1 CPC co-localises with PCNA via INCENP's PIP-box motif

To begin with, the interaction between the CPC members and PCNA should be confirmed. Therefore, the PLA technology was applied (see section 2.2.2.8) to investigate protein interactions on an endogenous level. For PLA exponentially growing HeLa cells were seeded in 3 cm microscopic glass bottom dishes (MatTek Corporation) and 24 hours later the cells were fixed, permeabilised and unspecific binding sites were blocked. Incubation with the primary antibody was carried out over night at 4 °C. Afterwards, the cells were incubated with the PLA probes PLUS and MINUS followed by a ligation step and an amplification step to form a complex circular DNA structure. The fluorescent nucleotides, which were incorporated during the amplification step were detected via fluorescence microscopy (see Figure 3.1 A). The number of PLA signals per nucleus was determined using CellProfiler.

Samples only incubated with one primary antibody but both PLA probes served as negative controls. These samples should not show any PLA signal. The negative controls for Borealin, INCENP, Aurora B, PCNA (r) and PCNA (m) revealed low levels of PLA signals per cell (see Figure 3.1 B). The negative control for Survivin revealed on average 35 PLA signals per cell. However, each interaction sample of the respective

CPC member with PCNA resulted in significantly increased PLA signals indicating an interaction (see Figure 3.1 B).

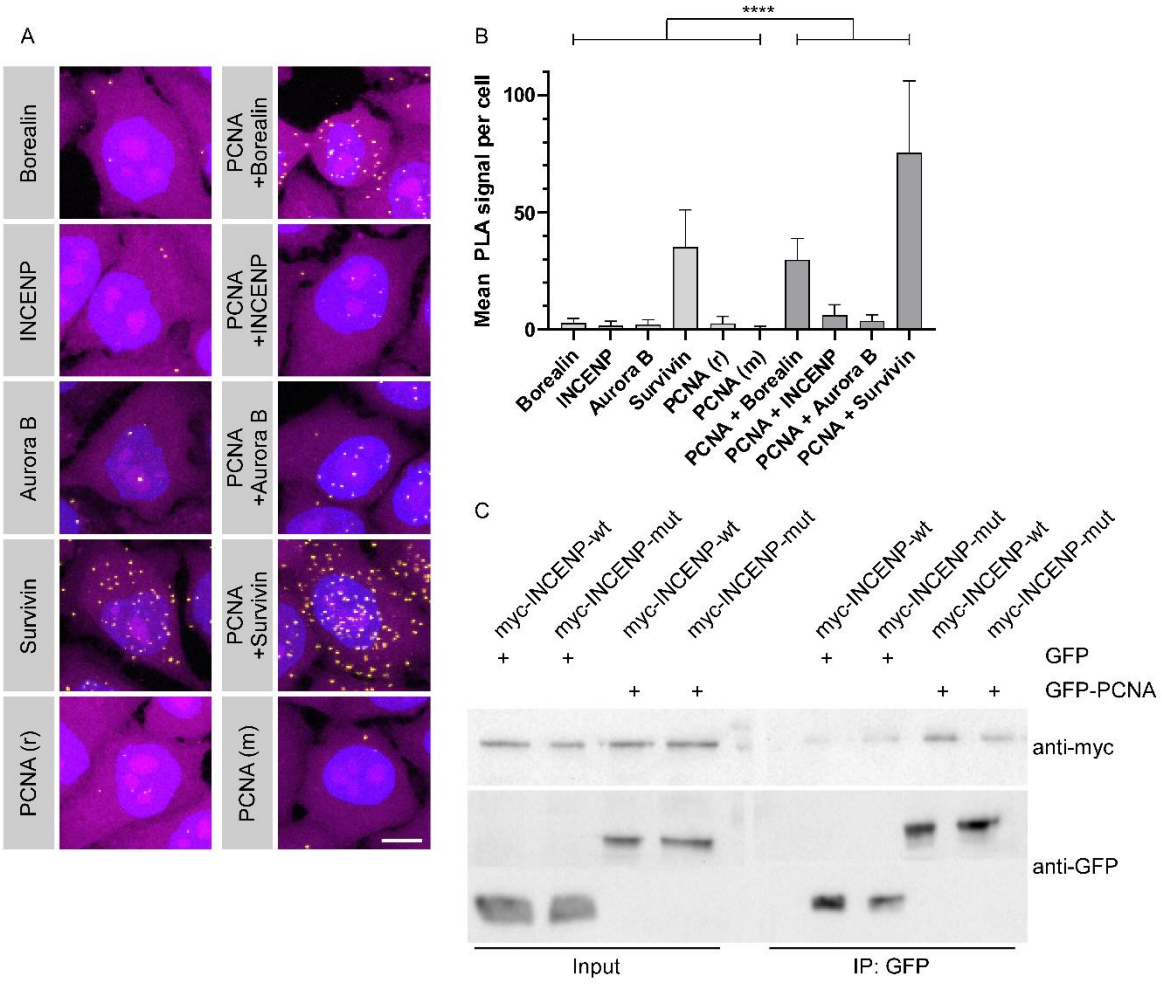

Figure 3.1: CPC members co-localise with PCNA mediated via INCENP's PIP-box motif

A) HeLa cells were used in a PLA to analyse the interaction between different CPC members and PCNA. Cells were stained with CellMask (magenta), DNA was stained with Hoechst (blue) and PLA signals are depicted in yellow. Representative images are shown. Scale bar: 10 µm. **B)** Quantitative analysis of the interaction between each CPC member and PCNA. The bar graph shows the mean number of PLA signals per cell with SD. Data was analysed by t-test. **** < 0.0001. n=3. More than 200 cells were counted. **C)** Western Blot analysis of IP samples. 293T cells were transfected with GFP or GFP-PCNA and myc-INCENPwt or myc-INCENPmut, respectively. GFP and GFP-PCNA were immunoprecipitated from whole-cell lysates using magnetic beads coupled to a GFP-specific antibody. The immunoprecipitates were subjected to immunoblot analysis. Membranes were incubated with antibodies specific for GFP and myc-tag. Co-transfection of GFP with INCENP variants served as controls.

Next, the interaction between the CPC members and PCNA should be confirmed by co-immunoprecipitation (see section 2.2.3.4) with preceding chromatin extraction. 293T cells were co-transfected with plasmids coding for GFP-PCNA together with Survivin-myc, Aurora B-myc, Borealin-myc or myc-INCENP, respectively. Prior to

immunoprecipitation, chromatin extraction was performed with the Chromatin Extraction kit from Abcam. One-third of the chromatin extraction was used as an input control. GFP-PCNA was immunoprecipitated from the chromatin extracts using magnetic beads coupled to a GFP-specific antibody (see section 2.2.3.4). The input lysates and immunoprecipitates were subjected to immunoblot analysis. Membranes were incubated with antibodies specific for GFP and myc-tag (see section 2.2.3.5 and 2.2.3.6). Co-transfection of GFP and one of the CPC members served as controls (see Appendix Figure 6.1 and Figure 6.2). To allow a better visualisation, the same samples were subjected to immunoblot analysis without using the GFP controls (see Figure 3.10 A). All GFP-PCNA immunoprecipitates (see Figure 3.10 A) showed a strong signal for myc, which indicates an interaction between all CPC members and PCNA.

To investigate which member of the CPC mediates the interaction with PCNA, co-immunoprecipitations were performed. Stefanie Mosel showed in her doctoral thesis (Mosel 2018) that INCENP contains a PIP (PCNA interacting protein) motif which is known to be responsible for most interactions of PCNA to other proteins. Therefore, a mutated form of INCENP was generated containing several mutations within the PIP-box-motif. For immunoprecipitation, 293T cells were co-transfected with plasmids coding for GFP-PCNA and myc-INCENP-wt or myc-INCENP-PIP-box-mutant, respectively. GFP-PCNA was immunoprecipitated from whole-cell lysates using magnetic beads coupled to a GFP-specific antibody (see section 2.2.3.4). The immunoprecipitates were subjected to immunoblot analysis. Membranes were incubated with antibodies specific for GFP and myc-tag (see section 2.2.3.5 and 2.2.3.6). Co-transfection of GFP with the INCENP variants served as controls. Both GFP immunoprecipitates showed a faint signal for myc. Myc-INCENP detected in the GFP-PCNA immunoprecipitate indicates an interaction between these two proteins. Furthermore, the reduced signal for myc-INCENP-PIP-box-mut indicates a loss of interaction due to the mutated PIP-box motif (see Figure 3.1 C).

3.2 Survivin depletion hinders the cells coping mechanisms regarding damaged-induced replication stress

Due to the observed interaction of the CPC members with PCNA, it is of great interest to unveil whether they have an impact on the replication process and a functional role during replication. If the replication cannot proceed as usual and is disturbed by various influences the cell experiences replication stress. Replication stress manifests in various forms such as under-replicated sites, metaphase breaks, anaphase bridges or 53BP1 nuclear bodies. Common fragile sites are mostly the affected regions where the effect of replication stress can be observed. In this context, we investigated the effect of Surivivn depletion on the cells coping mechanisms regarding damaged-induced replication stress.

3.2.1 Survivin depletion leads to metaphase gaps and breaks

To investigate whether Survivin has an impact on the replication process, chromosome spreading after depletion of Survivin was performed (see section 2.2.2.11). For this, HeLa cells were transfected with either a Survivin-specific or a non-targeting siRNA, which served as a control. After 48 hours of depletion, the cells were incubated for 2 hours with 0.08 µg/ml colcemid to arrest them in metaphase. Metaphase cells were detached from the bottom of a cell culture flask and collected. After incubation with sodium citrate and several fixation and washing steps, the spreads were performed manually by dropping the cell solution onto a microscopic slide. The slides were stained with Giemsa solution the next day. In Figure 3.2 metaphase spreads from cells after transfected with non-targeting siRNA (see Figure 3.2 A) or Survivin-specific siRNA (see Figure 3.2 B) with a full set of chromosomes are depicted. The white arrow shows a break in a metaphase chromosome. A fraction of the cell suspension was subjected to immunoblot analysis (see section 2.2.3.5 and 2.2.3.6) to assess the expression of Survivin after depletion (see Figure 3.2 E). Membranes were incubated with antibodies specific for Survivin and Tubulin, the latter serving as a loading control. Cells transfected with non-targeting siRNA showed low levels of breaks per metaphase, whereas cells treated with a Survivin-specific siRNA showed a significant increase of breaks per metaphase (see Figure 3.2 C). In addition, the number of metaphases with

breaks was increased after Survivin depletion in contrast to cells transfected with non-targeting siRNA (see Figure 3.2 D). Of note, both results allow inferences regarding a possible participation of Survivin during replication.

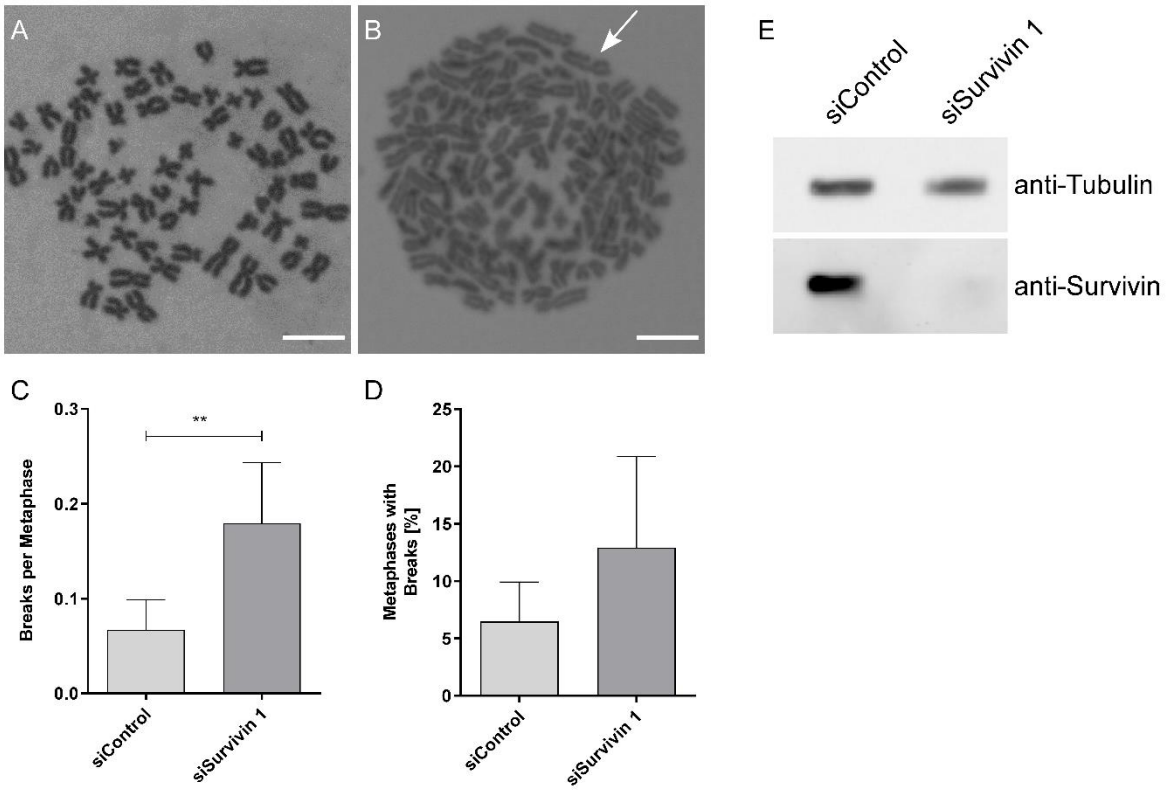

Figure 3.2: Survivin depletion leads to an increased number of breaks in metaphase chromosomes

A and B) Brightfield images of metaphase spreads with a full set of chromosomes. White arrow indicates a break or a gap on a chromosome. Scale bar: 10 µm. **C)** Quantitative analysis of breaks or gaps occurring per metaphase. The bar graph shows the mean number of breaks per metaphase with SD. Data was analysed by t-test. ** $p < 0.01$. n=3. More than 100 metaphases were analysed. **D)** Quantitative analysis of metaphases with breaks. The bar graph shows the mean number of metaphases with breaks with SD. Data was analysed by t-test. ** < 0.01. n=3. More than 100 metaphases were analysed. **E)** Immunoblotting was performed to assess the expression of Survivin after depletion. Membranes were incubated with antibodies specific for Survivin and Tubulin, which served as a loading control.

3.2.2 Survivin depletion leads to 53BP1 nuclear bodies

In general, gaps and breaks on metaphase chromosomes stem from that under-replicated sites or damaged DNA that was not properly processed. These damaged sites are known to be protected by an accumulation of 53BP1 in G1 phase

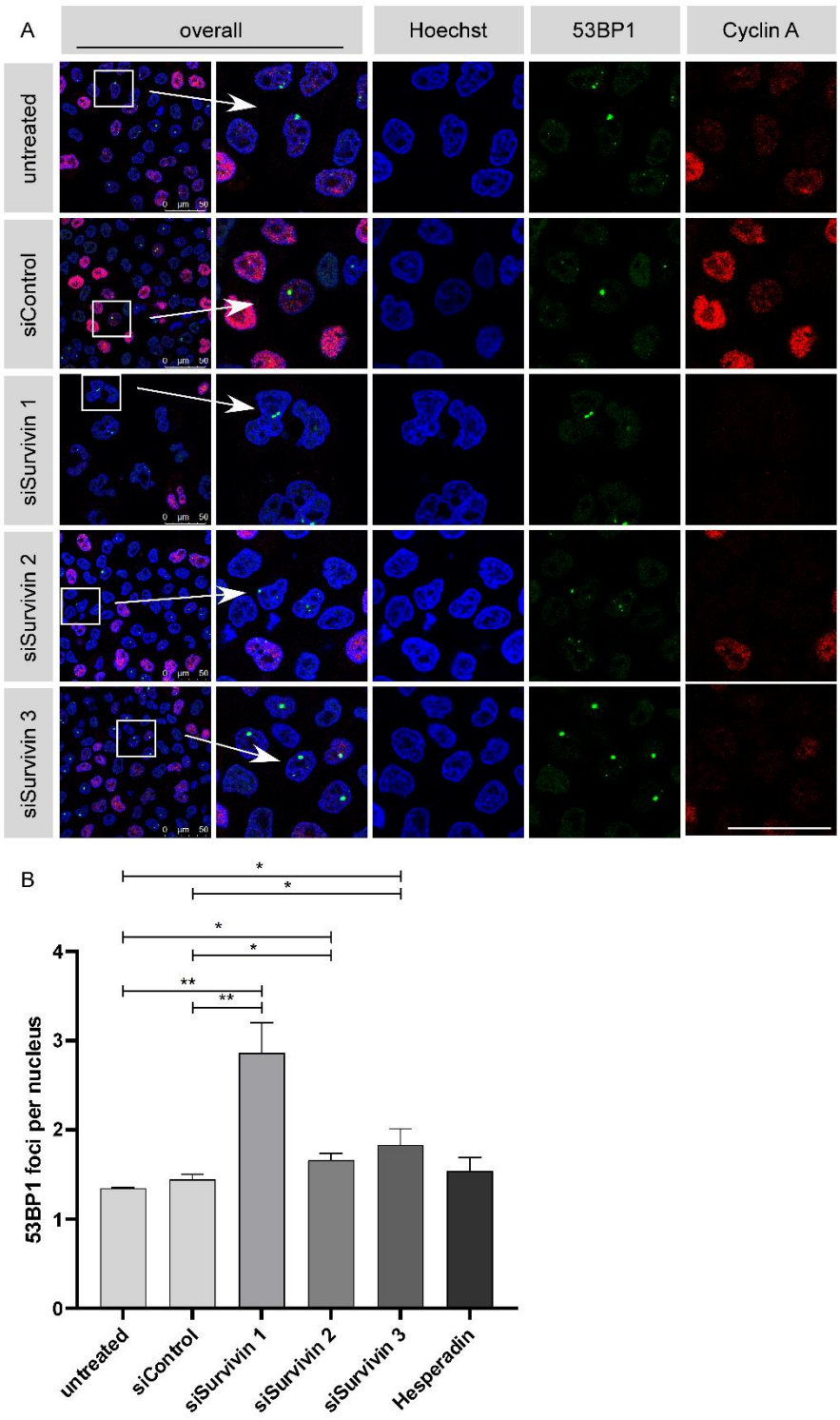

Figure 3.3: Survivin depletion leads to an increase of 53BP1 nuclear bodies in G1 phase cells

A) HeLa cells were transfected with Survivin-specific or non-targeting siRNA, fixed and permeabilised after 48 hours. Cells were immunostained with antibodies specific for 53BP1 (AF488, green) and cyclin A (AF568, red). DNA was stained with Hoechst (blue). **B)** Quantitative analysis of 53BP1 nuclear bodies in cells treated with Survivin-specific siRNAs, non-targeting siRNA and Hesperadin. The bar graph shows the mean number of 53BP1 nuclear bodies per nucleus with SD. Data was analysed by t-test. ** < 0.01. * < 0.05. n=3. More than 100 cells were counted.

(see Figure 3.3 A). To analyse whether Survivin or the CPC could be involved in processes during replication, cells were depleted of Survivin and analysed regarding persisting 53BP1 nuclear bodies in G1 phase. For this, HeLa cells were transfected with three different Survivin-specific siRNAs. After 48 hours of depletion, the cells were fixed and stained with an antibody specific for 53BP1 (see section 2.2.2.7). Staining with an antibody specific for cyclin A served as a marker for G2 phase cells, meaning that cyclin A negative cells were identified as G1 phase cells. Cells treated with Hesperadin served as a positive control. All cells transfected with Survivin-specific siRNA showed a significant increase in the number of 53BP1 nuclear bodies in G1 phase cells in contrast to untreated cells or cells transfected with non-targeting siRNA. Here, the use of the Survivin-specific siRNA labelled Survivin 1 resulted in the strongest increase of 53BP1 nuclear bodies among the tested siRNAs, indicating that Survivin depletion causes an increase of DNA damage. Cells treated with Hesperadin did not show higher numbers of 53BP1 nuclear bodies in contrast to untreated cells (see Figure 3.3 B).

3.2.3 Survivin depletion leads to mitotic DNA synthesis

Another sign indicating replication stress is a phenomenon called mitotic DNA synthesis (MiDAS). Here, the replication machinery is unable to complete replication in time so that the cells continue to replicate in mitosis (Minocherhomji et al. 2015). A possible disruptive factor is replication stress during S phase, which can slow down or even stall the replication fork. To investigate whether depletion of CPC members causes replication stress resulting in delayed genome replication during mitosis, EdU incorporation assays were performed (see section 2.2.2.9). For this, HeLa cells were transfected with Survivin-specific or Aurora B-specific siRNA. During the last 16 hours of depletion, the cells were incubated with the inhibitor RO-3306 to arrest them in G2 phase. Afterwards, the medium was replaced with fresh medium containing EdU and the cells were incubated for 30 minutes, before they were fixed and permeabilised. EdU foci were visualized by using the Click-iT™ EdU Alexa Fluor™ 488 Imaging kit. Cells treated with Aurora B-specific siRNA showed a slight increase of EdU foci whereas cells treated with Survivin-specific siRNA showed a significant increase of EdU foci in mitotic cells in contrast to untreated cells (see Figure 3.4 B). This hints towards the induction of replication stress by Survivin depletion.

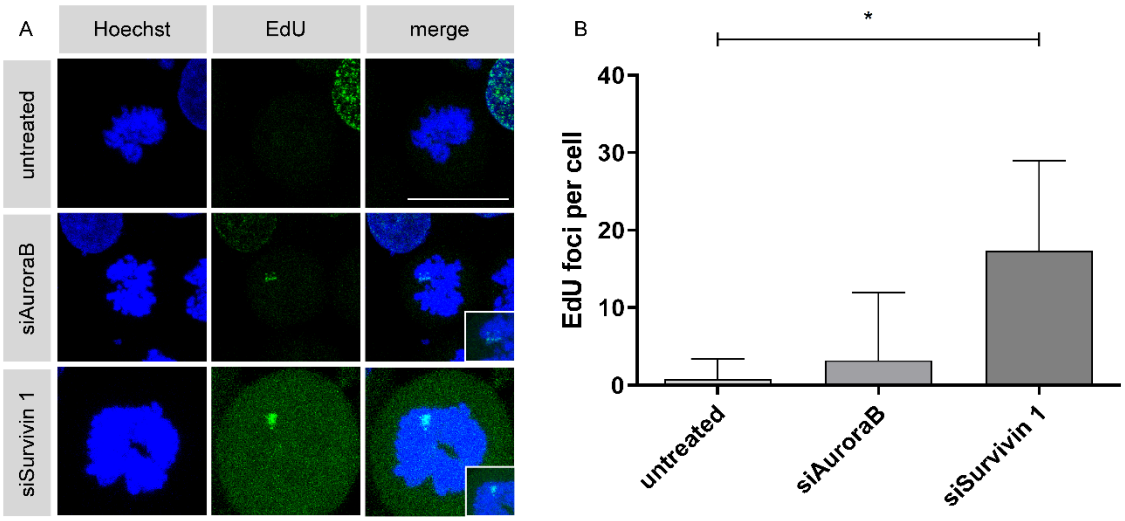

Figure 3.4: CPC depletion leads to mitotic DNA synthesis

A) HeLa cells were transfected with Survivin-specific or Aurora B-specific siRNA, fixed and permeabilised after 48 hours. During the last 16 hours of depletion the cells were incubated with RO-3306 to arrest them in G2 phase. Cells were stained with the Click-iT™ EdU Alexa Fluor™ 488 Imaging kit. DNA was stained with Hoechst (blue). **B)** Quantitative analysis of EdU foci in metaphase cells treated with Survivin-specific or Aurora B-specific siRNA. The bar graph shows the mean number of EdU foci per cell with SD. Data was analysed by t-test. * < 0.05. n=3. More than 50 cells were counted.

3.3 CPC localises to the chromatin after induction of replication stress

In initial experiments, we demonstrated that under normal conditions the CPC and PCNA are in close proximity and interact with each other (see section 3.1). Furthermore, we demonstrated that especially Survivin depletion leads to an increase of replication stress (see section 3.2.1). For this reason, we wanted to investigate the expression of each CPC member and their localisation to the different cell compartments after induction of replication stress. 293T cells were seeded in 10 cm dishes and treated 24 hours later either with 1 µM Camptothecin (CPT), 0.5 mM Hydroxyurea (HU) or irradiation (IR) with 10 Gy. Cells treated with CPT and HU were incubated for 80 minutes and irradiated cells for 2 hours. Afterwards, one quarter of the cells were used to prepare whole-cell lysates (see section 2.2.3.1) while the rest was subjected to subcellular fractionation (see section 2.2.3.2) using the Subcellular Protein Fractionation kit for cultured cells from Thermo Fisher Scientific. Cytoplasmic, soluble nuclear and chromatin-bound fractions were analysed via immunoblot

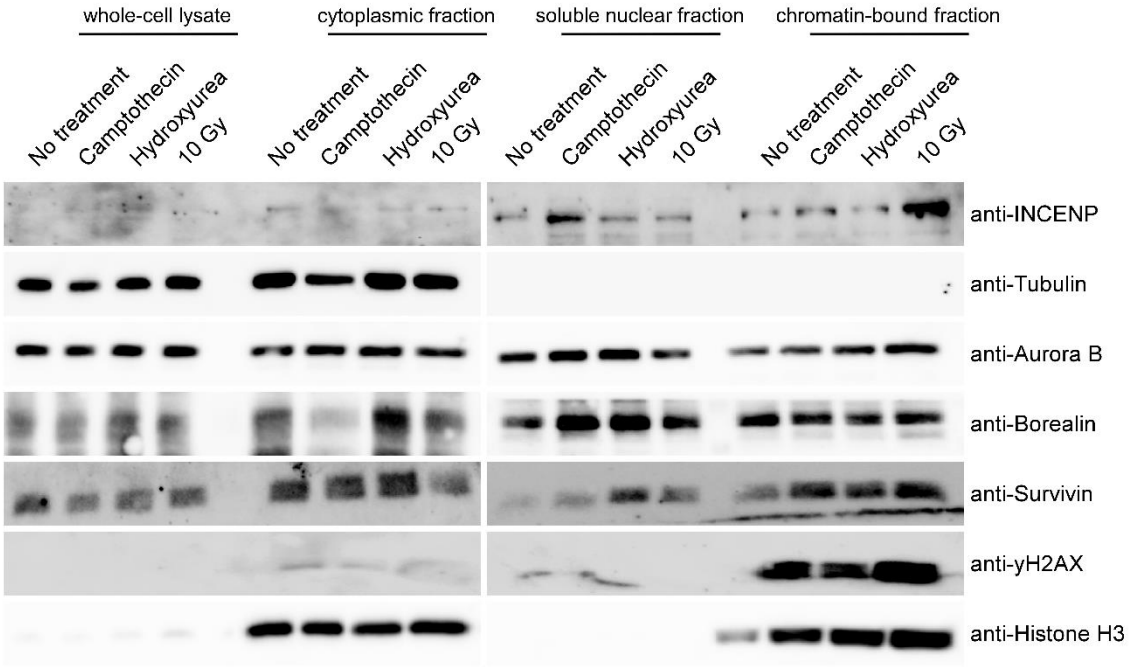

Figure 3.5: Localisation of the CPC after induction of replication stress

293T cells were treated with different reagents that induced replication stress, including 1 µM Camptothecin, 0.5 mM Hydroxyurea and irradiation with 10 Gy. Whole-cell extracts and subcellular fractions were generated and subjected to immunoblot analysis. Membranes were incubated with antibodies specific for INCENP, Tubulin, Aurora B, Borealin, Survivin, γH2AX (Ser139) and Histone H3. γH2AX served as a marker for DNA damage and repair, and Tubulin and Histone H3 served as loading controls for the cytoplasmic fraction and the chromatin fraction, respectively.

(see Figure 3.5). α-Tubulin as a protein of the cytoskeleton, was used as loading control and to confirm the purity of the cytoplasmic fraction. Histone H3 was used as loading control for the chromatin fraction. The nuclear and chromatin-bound fractions appeared to be completely free of cytoplasmic proteins. However, a strong signal of histone H3 was detected in the cytoplasmic fractions (see Figure 3.5), indicating that this sample was contaminated with nuclei. Treatments with CPT, HU and irradiation led to strong signals for the DNA damage and repair marker γH2AX, indicating that these treatments were effective. Faint signals of γH2AX could also be detected in the cytoplasmic fraction due to low purity of this fraction as histone H3 indicated. The majority of the CPC proteins, namely Aurora B, Borealin and Survivin, showed a similar protein levels in whole-cell lysates irrespective of the treatment. There was no detectable signal for INCENP in the whole-cell extractions. However, in the subcellular fraction's treated with CPT, HU and IR led to altered protein levels. The amount of INCENP was similar in nearly all samples, except for the soluble nuclear fraction after

treatment with CPT and the chromatin-bound fraction of the irradiation sample. Both samples showed increased levels of INCENP, indicating a shift of the protein to these subcellular compartments after treatment with either CPT or irradiation. The detected Aurora B levels were similar in all cytoplasmic fractions regardless of how they were treated. In the soluble nuclear fraction, the detected levels of Aurora B remained mostly constant, except after irradiation, where a decrease of Aurora B levels was detected. The chromatin-bound fraction showed an intriguing pattern, where the untreated sample had only a low level of Aurora B, but all treated samples showed highly increased protein levels. Here, the strongest increase of Aurora B was observed after irradiation. This indicates a shift of Aurora B to the chromatin after treatment with DNA-damaging agents especially after irradiation. For Borealin, protein levels detected in the cytoplasmic fraction showed a decrease after treatment with CPT and an increase after treatment with HU. Untreated and irradiated samples showed no alteration in the protein level. In contrast to the cytoplasmic fraction, the soluble nuclear fraction showed a strong increase of Borealin in all treated samples with the highest increase after treatment with CPT and HU. The chromatin-bound fraction showed no alterations of Borealin protein levels in any sample. Survivin showed similar protein levels in the cytoplasmic fractions after each treatment, except after irradiation, where less protein was detected. Only low levels of Survivin were detected in the soluble nuclear fraction in the untreated sample and after treatment with CPT, whereas after treatment with HU and irradiation the detected protein level was slightly increased. The chromatin-bound fraction showed a strong increase of the Survivin level after induction of treatment in contrast to the untreated cells. As seen for Aurora B, stronger Survivin bands were detected in the chromatin-bound fraction after treatment with DNA-damaging agents.

To confirm the data of the subcellular fractionation, the localisation pattern was also analysed by immunofluorescence. HeLa cells were either treated with 1 µM CPT, 0.5 mM HU or irradiation with 10 Gy. Cells treated with CPT and HU were incubated for 80 minutes and irradiated cells for 2 hours. Afterwards, the cells were pre-extracted with a cytoskeletal (CSK) buffer for 5 minutes at 4 °C. The advantage of the pre-extraction buffer is that all not chromatin-bound proteins are washed away and only chromatin-bound proteins remain for analysis. After incubation with the CSK

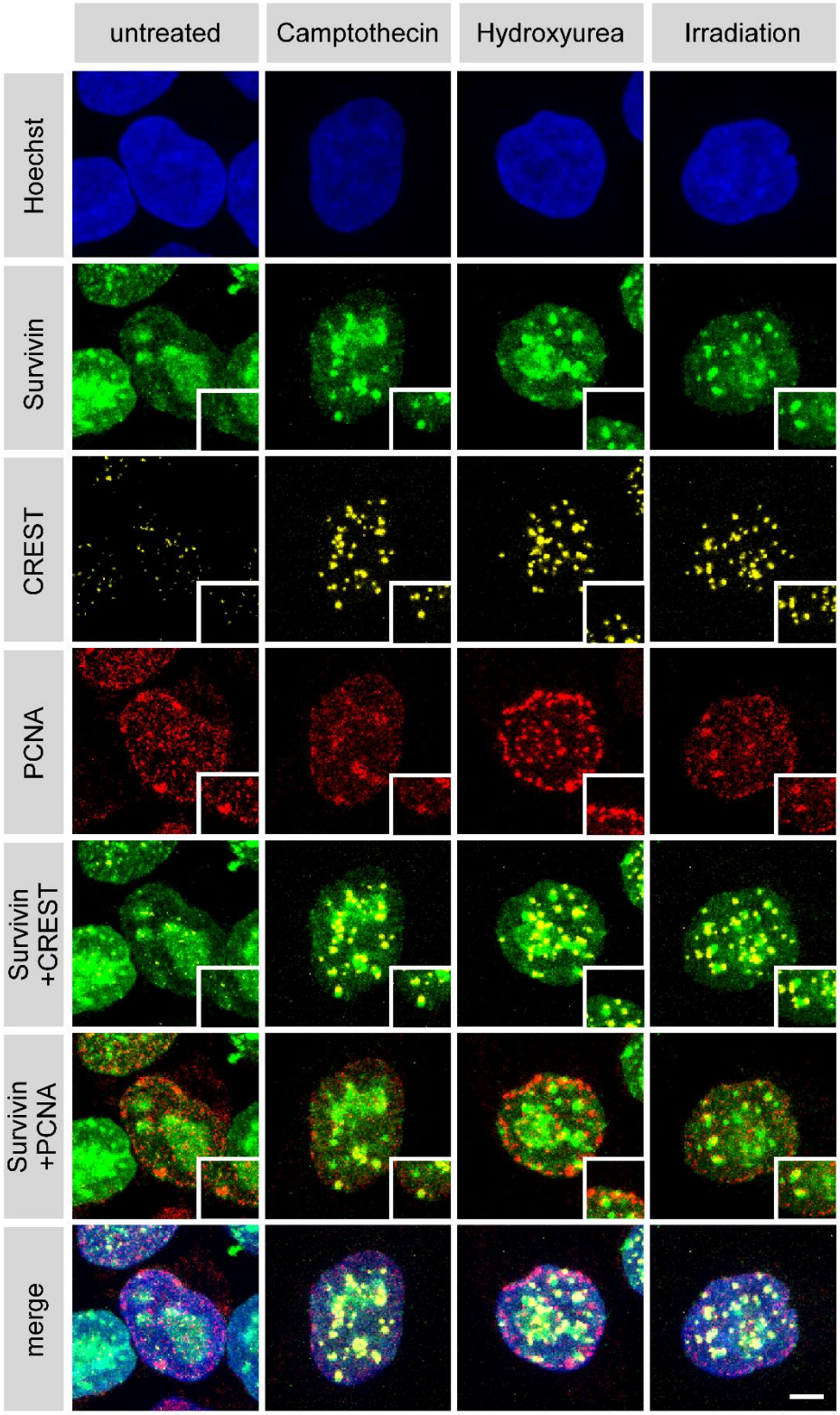

Figure 3.6: Localisation of Survivin after induction of replication stress

HeLa cells were treated with CPT, HU or irradiated with 10 Gy and were fixed 80 minutes after CPT and HU treatment and 2 hours after IR. Afterwards, they were permeabilised and immunostained with antibodies specific for Survivin (AF488, green), PCNA (AF633, red) and with a CREST anti-centromere autoimmune serum (AF568, yellow). DNA was stained with Hoechst (blue). Non-treated cells served as a control. Scale bar: 5 µm. The insets show higher magnifications.

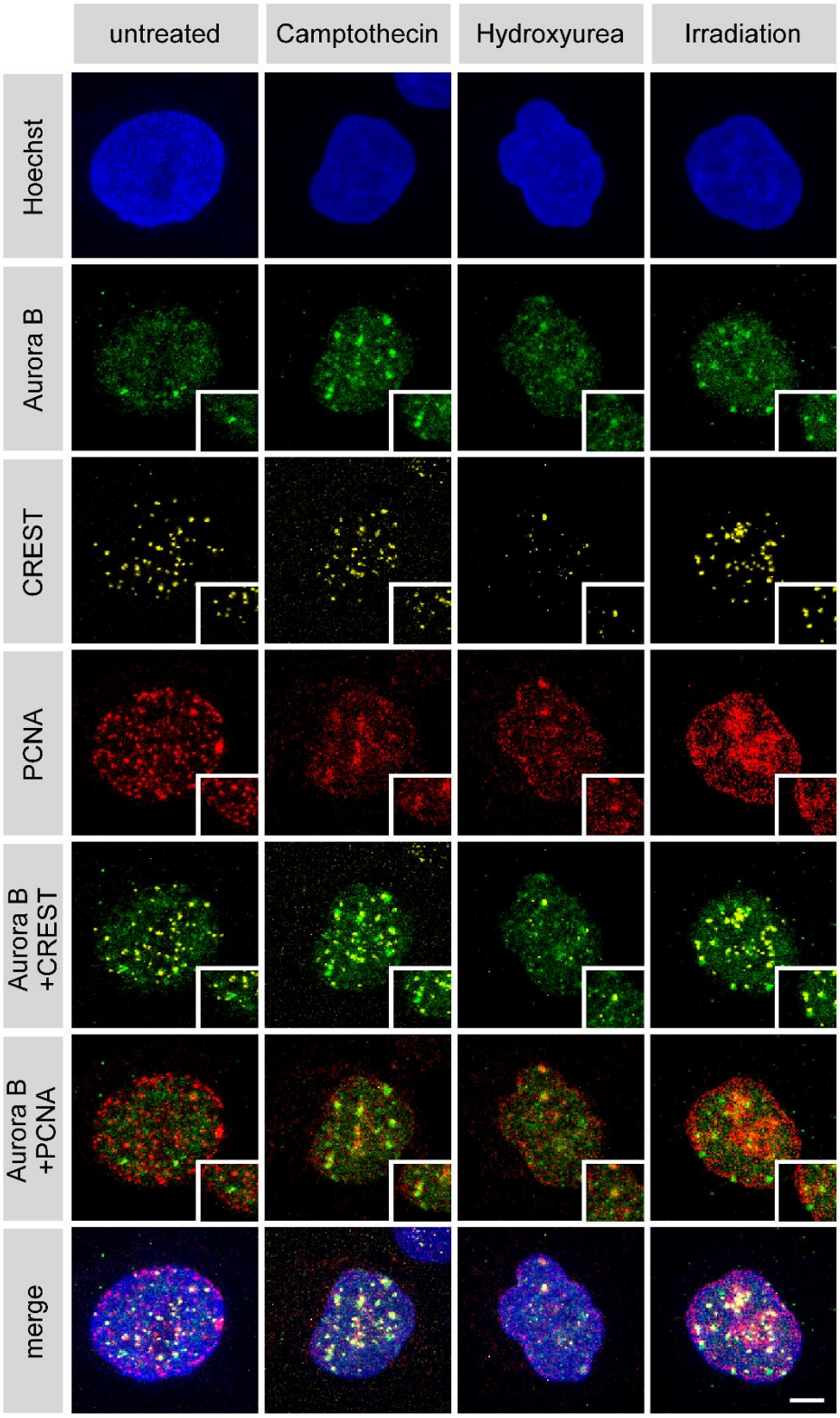

Figure 3.7: Localisation of Aurora B after induction of replication stress

HeLa cells were treated with CPT, HU or irradiated with 10 Gy and were fixed 80 minutes after CPT and HU treatment and 2 hours after IR. Afterwards, they were permeabilised and immunostained with antibodies specific for Aurora B (AF488, green), PCNA (AF633, red) and with a CREST anti-centromere autoimmune serum (AF568, yellow). DNA was stained with Hoechst (blue). Non-treated cells served as a control. Scale bar: 5 µm. The insets show higher magnifications.

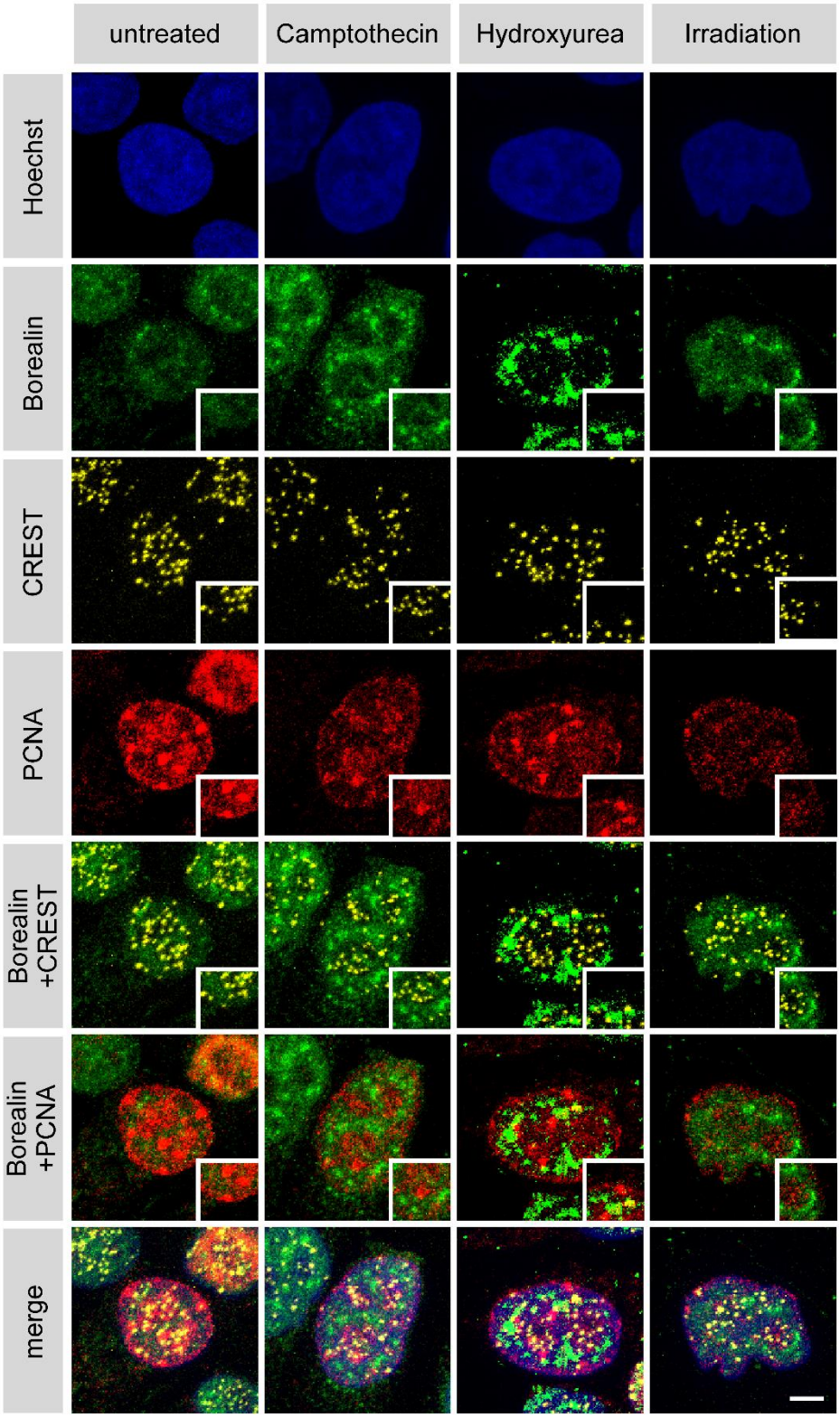

Figure 3.8: Localisation of Borealin after induction of replication stress

HeLa cells were treated with CPT, HU or irradiated with 10 Gy and were fixed 80 minutes after CPT and HU treatment and 2 hours after IR. Afterwards, they were permeabilised and immunostained with antibodies specific for Borealin (AF488, green), PCNA (AF633, red) and with a CREST anti-centromere autoimmune serum (AF568, yellow). DNA was stained with Hoechst (blue). Non-treated cells served as a control. Scale bar: 5 µm. The insets show higher magnifications.

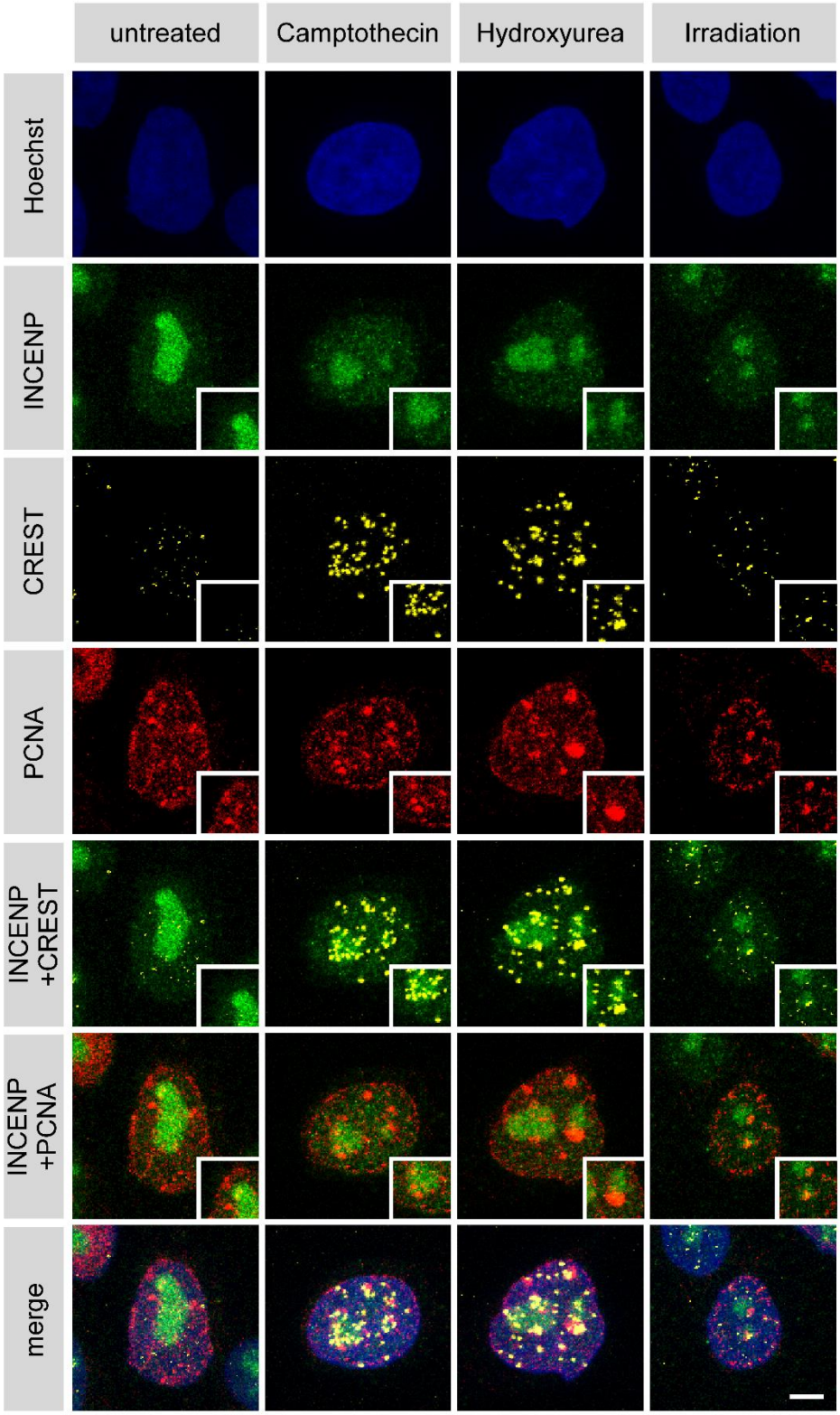

Figure 3.9: Localisation of INCENP after induction of replication stress

HeLa cells were treated with CPT, HU or irradiated with 10 Gy and were fixed 80 minutes after CPT and HU treatment and 2 hours after IR. Afterwards, they were permeabilised and immunostained with antibodies specific for INCENP (AF488, green), PCNA (AF633, red) and with a CREST anti-centromere autoimmune serum (AF568, yellow). DNA was stained with Hoechst (blue). Non-treated cells served as a control. Scale bar: 5 µm. The insets show higher magnifications.

buffer, the cells were fixed, permeabilised and immunostained with antibodies specific for Survivin (see Figure 3.6), Aurora B (see Figure 3.7), Borealin (see Figure 3.8), INCENP (see Figure 3.9), PCNA. To detect centromeres, the CREST anti-centromere autoimmune serum was used. PCNA is an important component of the replisome and is responsible to prevent the dissociation of DNA polymerases from the DNA strand. Here, immunodetection of PCNA was used to visualize replication sites. Furthermore, PCNA has a typical distribution pattern in S phase (Leonhardt et al. 2000; Nakamura et al. 1986; O'Keefe et al. 1992). It first forms distinct foci that are concentrated at the nucleoli as well as at peripheral sites of the nucleus. During ongoing replication, the foci increase in size while the number of foci decreases. Due to the specific PCNA pattern, cells could be assigned to S phase and, here, only those cells were depicted (see Figure 3.6Figure 3.9). In untreated cells, Survivin (see Figure 3.6) was evenly distributed throughout the nucleus, whereas in cells treated with CPT, HU or IR Survivin localised in distinct foci with the highest number of foci in the cells treated with irradiation. While the Survivin localisation did not coincide with replication sites or centromeric regions in untreated cells, the induction of replication stress led to the co-localisation of Survivin foci with PCNA and CREST, indicating that Survivin relocated towards the centromere and replication sites after induction of replication stress. In untreated cells, staining of Aurora B (see Figure 3.7) revealed an accumulation of the protein in some foci, but not as many as in treated cells. In untreated cells Aurora B foci did not localise to replication sites. However, in treated cells the increased number of foci co-localises with PCNA as well as centromeric regions, though the number of Aurora B foci did not increase as much after treatment with HU compared to the other treatments. Co-localisation of Aurora B with PCNA and centromeric regions after induction of replication stress might hint towards a participation of the CPC member in replication. Borealin (see Figure 3.8) showed no clear foci formation after induction of replication stress with a staining evenly distributed throughout the nucleus. However, some foci could be distinguished after treatment with CPT, but those foci co-localised with neither replication sites nor centromeric regions. In addition, Borealin’s even distribution did not allow any conclusions about the co-localisation with PCNA or centromeric regions after treatment with HU and irradiation. Immunostaining of INCENP (see Figure 3.9) appeared to be mainly restricted to the nucleoli in both, untreated and treated cells. INCENP foci seen after irradiation were smaller than those detected for Survivin and Aurora B, nevertheless, they co-localised with PCNA and the

centromere. Because of the differences observed between foci formed by INCENP compared to foci formed by other CPC members, inferences regarding a co-localisation of INCENP with replication sites and centromeric regions were not reliable.

3.4 CPC's interaction with PCNA is enhanced after irradiation

Previous immunoprecipitation and PLA experiments showed that the CPC interacts with PCNA in a cellular context (see section 3.1). Going further, we wanted to investigate whether this interaction becomes enhanced after induction of replication stress. This question was again addressed with PLA using HeLa cells expressing endogenous levels of CPC proteins and PCNA and immunoprecipitation in 293T cell lysates overexpressing CPC constructs tagged with myc and GFP-PCNA. For immunoprecipitation, 293T cells were co-transfected with plasmids coding for GFP-PCNA together with either Survivin-myc, Aurora B-myc, Borealin-myc or myc-INCENP. 24 hours after transfection, the cells were irradiated with 10 Gy and incubated for 2 hours. Prior to immunoprecipitation, chromatin extraction was performed with the Chromatin Extraction kit from Abcam. One-third of the chromatin extraction was used as an input control. GFP-PCNA was immunoprecipitated from the chromatin extracts using magnetic beads coupled to a GFP-specific antibody (see section 2.2.3.4). The input lysates and immunoprecipitates were subjected to immunoblot analysis. Membranes were incubated with antibodies specific for GFP and myc-tag (see section 2.2.3.5 and 2.2.3.6). Co-transfection with GFP and each CPC member served as controls (see Appendix Figure 6.1 and Figure 6.2). For better visualisation, the same samples were subjected to immunoblot analysis without using the GFP controls (see Figure 3.10 A). All GFP-PCNA immunoprecipitates showed a strong signal for myc in untreated samples (see section 3.1) as well as in irradiated samples, indicating an interaction of the CPC with PCNA even after irradiation. The relative signal intensities of the immunoprecipitated CPC members were quantified using ImageJ and normalised to those of immunoprecipitated GFP-PCNA (see Figure 3.10 B). Here, only minor alterations of the signal intensities of INCENP and Survivin could be measured, whereas Aurora B showed a faint decrease of signal intensity after irradiation. In contrast to these three CPC members, Borealin showed a significant increase of signal intensity after irradiation.

In order to investigate the interaction of the CPC members not only in lysates of cells overexpressing the protein of interest but also in cells expressing only endogenous levels of all components, PLA was performed. For this, exponentially growing HeLa cells were seeded in 3 cm microscopic glass bottom dishes (MatTek Corporation) and 24 hours after seeding the cells were irradiated with 10 Gy or treated with 0.5 mM HU

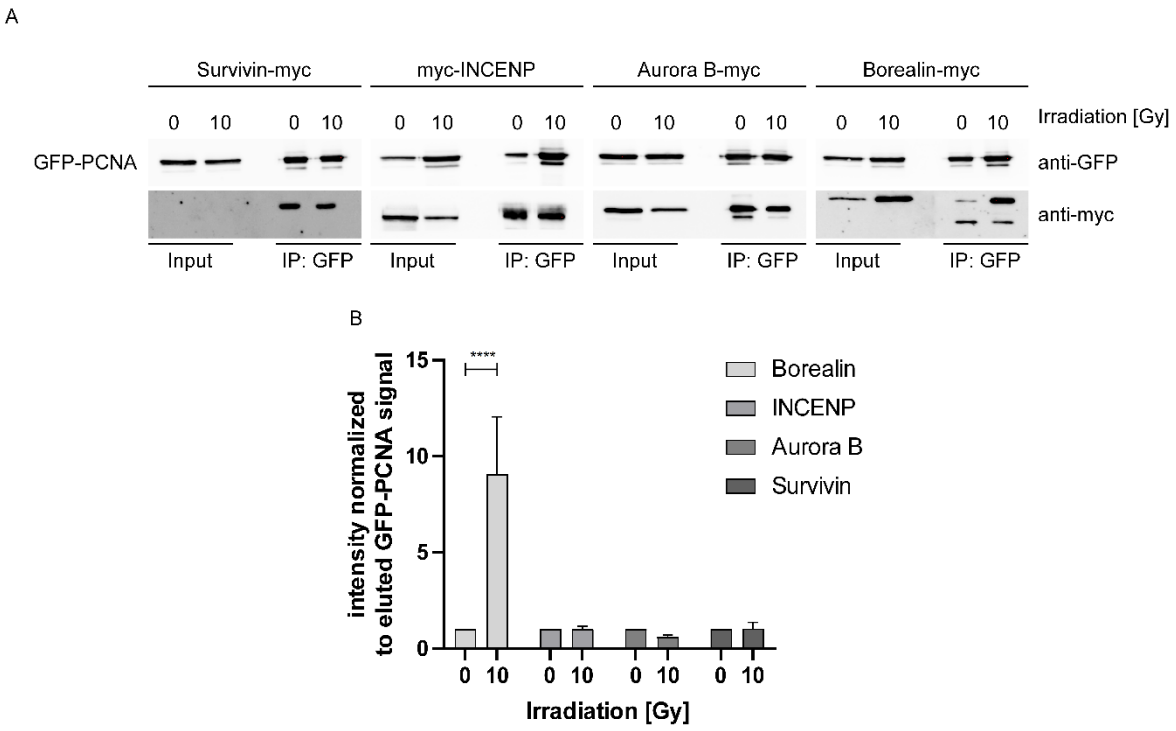

Figure 3.10: CPC members co-localise with PCNA after irradiation

A) Western Blot analysis of IP samples. 293T cells were co-transfected with plasmids coding for GFP-PCNA together with either Survivin-myc, myc-INCNEP, Aurora B-myc or Borealin-myc. HeLa cells were irradiated with 10 Gy and were fixed 2 hours after IR. Prior to immunoprecipitation, chromatin extraction was performed with the Chromatin Extraction kit from Abcam. One-third of the chromatin extraction was used as an input control. GFP-PCNA was immunoprecipitated from the chromatin extracts using magnetic beads coupled to a GFP-specific antibody. The input lysates and immunoprecipitates were subjected to immunoblot analysis. Membranes were incubated with antibodies specific for GFP and myc-tag. **B)** The bar graph shows the mean intensity of immunoprecipitated CPC members normalised to those of immunoprecipitated GFP-PCNA with SD. Data was analysed by t-test. **** < 0.0001. n=3.

for 80 minutes, fixed, permeabilised and unspecific binding sites were blocked. Incubation with the primary antibody was carried out over night at 4 °C. Afterwards, the cells were incubated with the PLA probes PLUS and MINUS followed by a ligation step and an amplification step to form a complex circular DNA structure. The fluorescent nucleotides, which were incorporated during the amplification step, can be detected

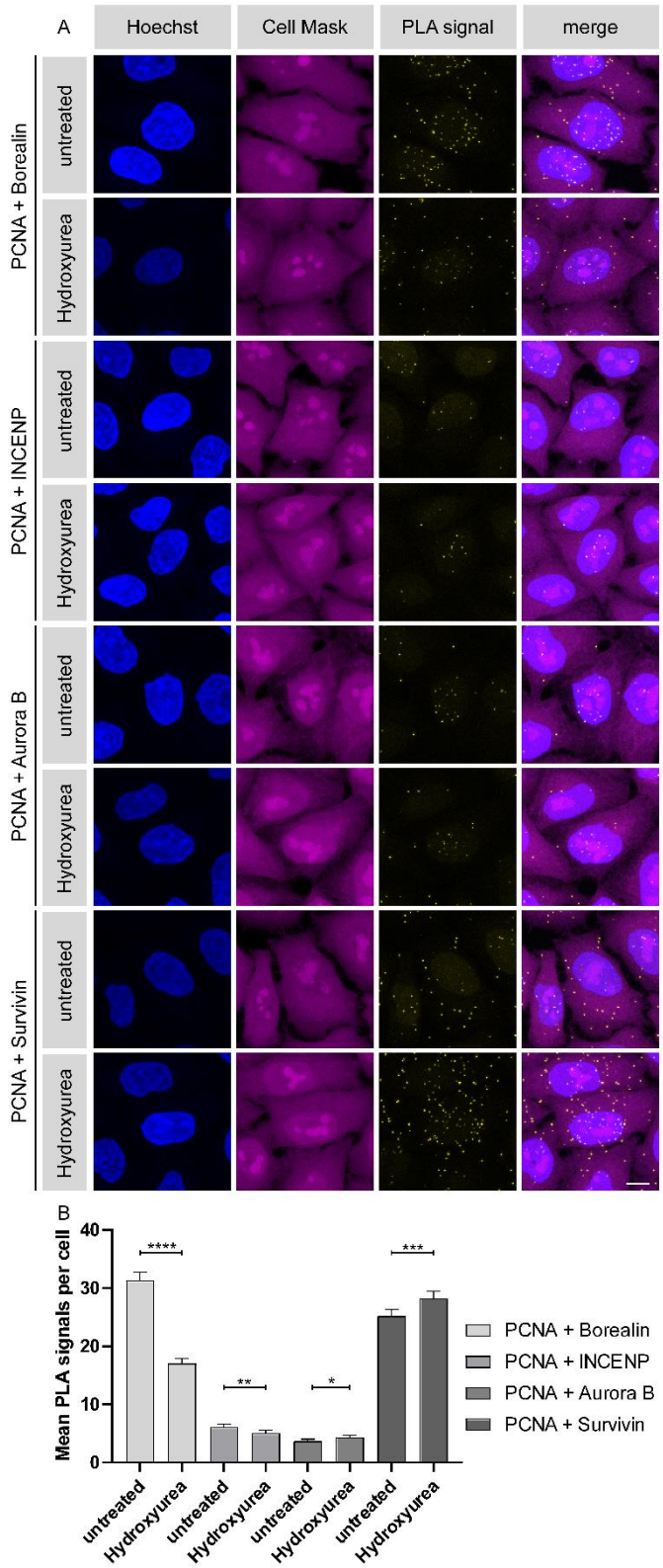

Figure 3.11: PLA reveals an interaction of the CPC with PCNA after treatment with HU

A) HeLa cells were used in a PLA to analyse the interaction between the different CPC members and PCNA after treatment with HU for 80 minutes. Representative images are shown. Scale bar: 10 µm. Cells were stained with CellMask (magenta), DNA was stained with Hoechst (blue) and PLA signals are depicted in yellow. **B)** Quantitative analysis of the interaction between each CPC member and PCNA without and with treatment with HU. The bar graph shows the mean number of PLA signals per cell with SD. Data was analysed by t-test. **** < 0.0001, *** < 0.001, ** < 0.01, * < 0.05. n=3. More than 200 cells were counted.

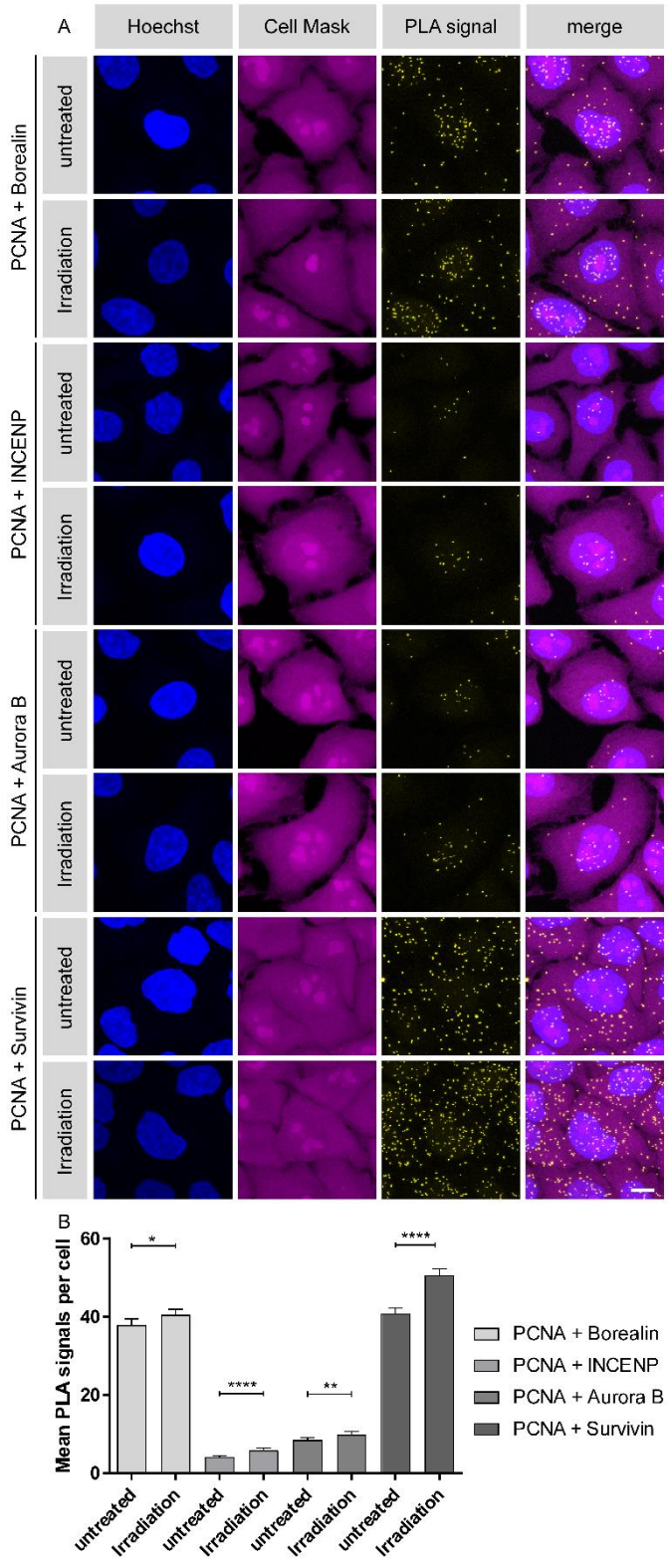

Figure 3.12: PLA reveals an interaction of the CPC with PCNA after irradiation

A) HeLa cells were used in PLA to analyse the interaction between the different CPC members and PCNA after irradiation. Cells were fixed 2 hours after IR. Representative images are shown. Scale bar: 10 µm. Cells were stained with CellMask (magenta), DNA was stained with Hoechst (blue) and PLA signals are depicted in yellow. **B)** Quantitative analysis of the interaction between each CPC member and PCNA without and with irradiation. The bar graph shows the mean number of PLA signals per cell with SD. Data was analysed by t-test. **** < 0.0001, ** < 0.01, * < 0.05. n=3. More than 200 cells were counted.

via fluorescence microscopy (see Figure 3.11 and Figure 3.12). The number of PLA signals per cell was determined using CellProfiler. The quantification revealed that treatment with HU significantly reduced the interaction of PCNA with Borealin and INCENP. In contrast, the same treatment led to a significant increase in interaction between Aurora B and Survivin with PCNA (see Figure 3.11 B). Quantitative analysis of the interaction of the CPC members with PCNA after irradiation revealed a significant increase in the numbers of signals for all CPC proteins, with INCENP and Survivin showing the most pronounced effects (see Figure 3.12 B).

3.5 CPC depletion affects replication machinery

Since we could show that the CPC members interact with PCNA and are located at replication sites, it was imperative to investigate whether the CPC could play a direct role during replication. In order to address this question, DNA combing assays were performed (see section 2.2.2.10) to visualize the progression of replication forks during replication and to give information about various aspects of DNA synthesis, such as replication fork speed, fork stalling or collapse, initiation and termination events and interorigin distances (IOD). For this, the DNA is sequentially labelled with halogenated thymidine analogues in two consecutive pulses. HeLa cells were transfected with either Survivin-specific, Aurora B-specific or non-targeting siRNA. Cells treated with Aphidicolin (Aph) served as a positive control. 48 hours after transfection, cells were sequentially pulse-labelled with CldU and IdU for 20 minutes each. The cells were harvested and DNA combing was performed as described in section 2.2.2.10. After fixation, denaturation and immunostaining, the image acquisition was performed with the EasyScan service by Genomic Vision. For analysis, the FiberStudio® Analysis Software was used.

Quantification of replication fork speed (see Figure 3.13 A) of cells transfected with non-targeting siRNA revealed an average speed of 0.886 kb/min. Treatment with Aph led to a decrease in replication fork speed with an average speed of 0.718 kb/min, which can be seen as a left-shift of the distribution. With average speeds of 0.872 kb/min for cells depleted of Aurora B and 0.997 kb/min for cells depleted of Survivin, reduced levels of CPC proteins did not result in an alteration of the replication

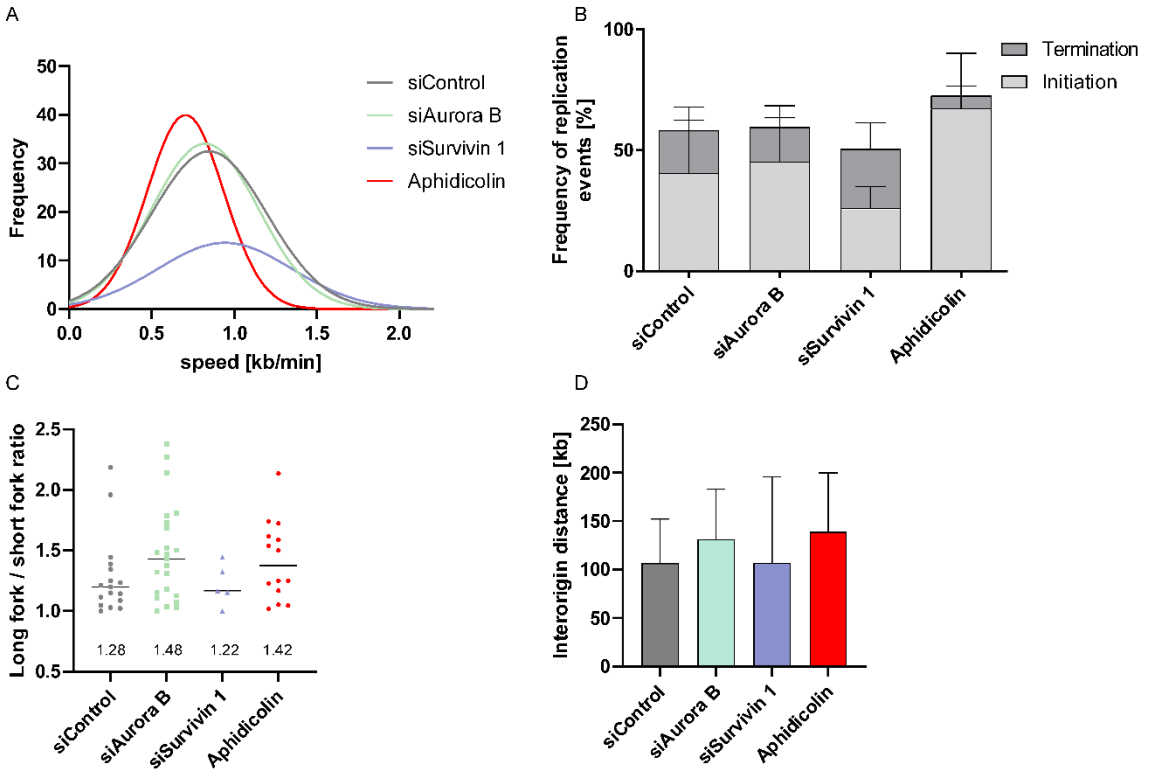

Figure 3.13: Effect of Survivin and Aurora B depletion on the replication machinery

HeLa cells were transfected either with Survivin-specific, Aurora B-specific or non-targeting siRNA. Cells treated with Aphidicolin (Aph) served as a positive control. DNA combing assay was performed as described (see section 2.2.2.10). **A)** The gaussian function shows the distribution and frequency of replication fork speeds in kb/min for control-depleted cells, cells depleted with Survivin- or Aurora B-specific siRNA and treated with Aph as a positive control. **B)** Bar graph shows the relative frequency of initiation and termination events with SD. **C)** The scatter plot shows the ratio of two diverging replication fork from one origin. A ratio of 1 indicates symmetry and a ratio above 1 indicates asymmetry. **D)** Bar graph shows the mean interorigin distances between two replication origins with SD. For all data: n=3.

fork speed (see Figure 3.13 A). Quantification of different replication events (see Figure 3.13 B) revealed in control-depleted cells a frequency of about 40 % for initiation and about 55 % for termination events. In contrast to that, depletion with an Aurora B-specific siRNA revealed an increase of initiation events, whereas the frequency of termination events remained similar. Initiation and termination frequencies were decreased for cells depleted with Survivin-specific siRNA. In the positive control, cells treated with Aph, a strong increase in initiation and termination events was observed. To quantify the symmetry of replication forks the ratio between the two diverging forks from the same origin was measured. A ratio of 1 indicates symmetry of the two forks, whereas a ratio higher than 1 indicates an asymmetric replication fork, which is an indicator for replication fork stalling (see Appendix Figure 6.3). Here, cells treated with non-targeting siRNA revealed a fork ratio of 1.28. Cells targeted with Aurora B-specific

siRNA and treated with Aph showed an increased ratio of 1.48 and 1.42, respectively. For cells treated with Survivin-specific siRNA a ratio of 1.22 was determined (see Figure 3.13 C). Furthermore, IOD's were determined by measuring the distance between two replication origins utilizing the DNA combing assay (see Appendix Figure 6.3). Quantification of IOD's for control-depleted cells revealed a distance of about 100 kb, whereas Aurora B depleted cells and cells treated with Aph showed with up to 120 kb an increase of distances. Survivin-depleted cells revealed no alteration of IOD's in comparison to control-depleted cells (see Figure 3.13 D).

3.6 CPC members interact with translesion polymerase η

We could show that CPC members exert influence on the replication machinery, since for example a depletion of Aurora B led to asymmetric replication forks. Therefore, we wanted to analyse in detail in which process the CPC is involved. Cells developed a mechanism to prevent collapse of forks that are stalling due to DNA damage causing replication stress. Here, a so-called translesion synthesis (TLS) can resume work as part of the replication machinery to bypass a DNA lesion. polymerases like Pol η, Pol ζ and REV1 are recruited to the stalled replication fork and replicate past the DNA lesion. Afterwards, the normal replicative DNA polymerase δ is restored and DNA synthesis can continue. In initial experiments to determine whether the CPC could be implicated in TLS, expression levels of Pol η after Survivin- and Aurora B-depletion and with or without irradiation should be analysed. For this, HeLa cells were seeded in 6-well plates and transfected 24 hours after seeding with non-targeting, Survivin-specific or Aurora B-specific siRNA. After 48 hours of depletion, the cells were irradiated with 10 Gy. After incubating the cells for 2 hours RIPA cell lysates were generated (see section 2.2.3.1). The lysates were subjected to immunoblot analysis and membranes were incubated with antibodies specific for Pol η, PCNA, Aurora B and Survivin (see section 2.2.3.5 and 2.2.3.6). Tubulin was used as a loading control. Immunoblot analysis (see Figure 3.14) revealed strongly decreased protein levels of Survivin and Aurora B, indicating a successful depletion of said proteins. However, consistent protein levels for PCNA, Aurora B and Survivin irrespective of depletion in non-irradiated cells was revealed. In addition, the protein level of Pol η was not affected by depletion of Survivin or Aurora B. In irradiated cells depleted for Survivin and Aurora B

the levels of said proteins were strongly decreased. In addition, protein levels of PCNA, Aurora B and Survivin in irradiated cells were consistent irrespective of depletion. However, the protein level of Pol η was slightly decreased after Survivin depletion and strongly decreased after Aurora B depletion, indicating that Survivin as well as Aurora B might play a role in TLS.

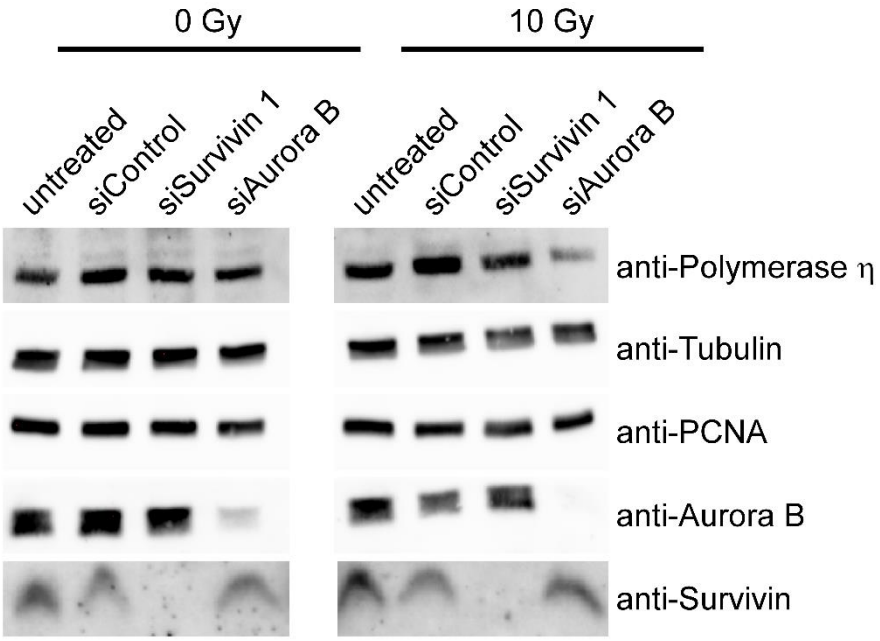

Figure 3.14: Expression levels of polymerase η after depletion of CPC members and concurrent irradiation

HeLa cells were transfected with non-targeting, Survivin-specific or Aurora B-specific siRNA. 48 hours after depletion, the cells were irradiated with 10 Gy. Whole-cell extracts were generated and subjected to immunoblot analysis. Membranes were incubated with antibodies specific for polymerase η, Tubulin, PCNA, Aurora B and Survivin. Tubulin served as a loading control.

To confirm whether the CPC interacts with polymerase η, co-immunoprecipitations were performed. For this, 293T cells were co-transfected with plasmids coding for FLAG-Pol η together with Survivin-myc, Aurora B-myc, Borealin-myc or myc-INCENP, respectively. 24 hours after transfection, the cells were irradiated with 10 Gy and incubated for 2 hours. Prior to immunoprecipitation, chromatin extraction was performed with the Chromatin Extraction kit from Abcam. One-third of the chromatin extraction was used as an input control. FLAG-Pol η was immunoprecipitated from the chromatin extracts using magnetic beads coupled to a FLAG-specific antibody (see

section 2.2.3.4). The input lysates and immunoprecipitates were subjected to immunoblot analysis. Membranes were incubated with antibodies specific for FLAG-tag or myc-tag (see section 2.2.3.5 and 2.2.3.6). All anti-FLAG immunoprecipitates showed a signal for myc-tag, indicating an interaction of the CPC with Pol η (see Figure 3.15 A). However, Pol η could not be detected in the immunoprecipitates, which hint towards a failed transfection. The signals for Borealin and Aurora B showed no differences between non-irradiated and irradiated cells, whereas Survivin revealed a slight decrease after irradiation. To verify these results on an endogenous level, membranes were also incubated with antibodies specific for Aurora B, Borealin and Survivin (see Figure 3.15 B). The endogenous levels were detected in samples, which did not overexpress the respective protein. Here, the FLAG immunoprecipitates showed a signal for Aurora B, which was not altered by irradiation, and a slight signal for Survivin. Borealin was not detected on an endogenous level.

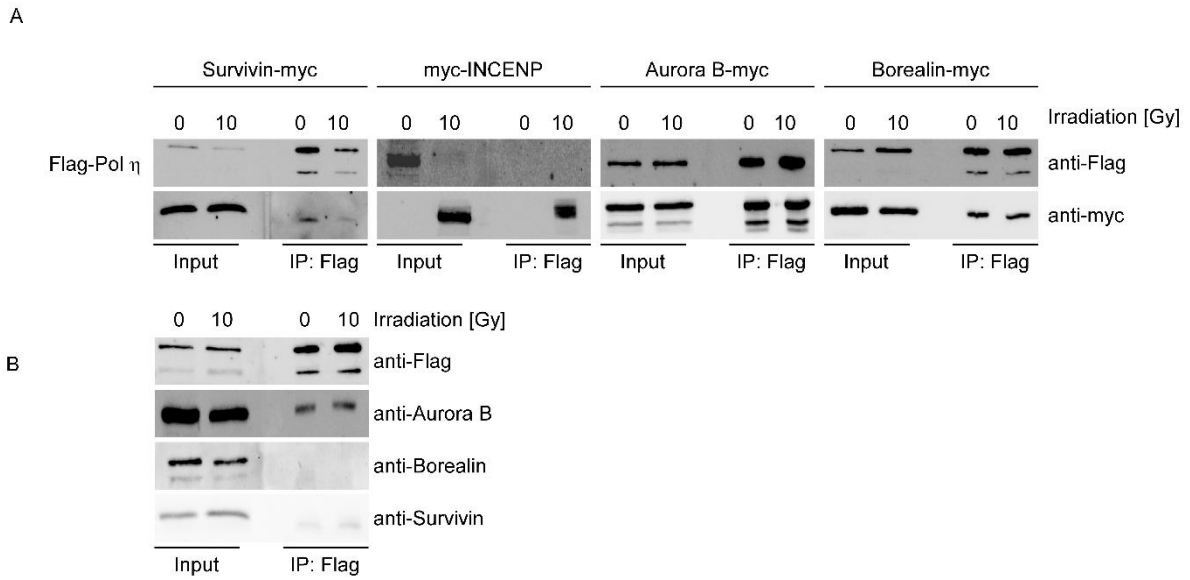

Figure 3.15: Co-immunoprecipitation reveals an interaction between CPC members and polymerase η

A) Western Blot analysis of IP samples. 293T cells were co-transfected with plasmids coding for FLAG-Pol η together with Survivin-myc, myc-INCENP, Aurora B-myc or Borealin-myc, respectively. 24 hours after transfection, the cells were irradiated with 10 Gy and incubated for 2 hours. Prior to immunoprecipitation, chromatin extraction was performed with the Chromatin Extraction kit from Abcam. One-third of the chromatin extraction was used as an input control. FLAG-Pol η was immunoprecipitated from the chromatin extracts using magnetic beads coupled to a FLAG-specific antibody. The input lysates and immunoprecipitates were subjected to immunoblot analysis. Membranes were incubated with antibodies specific for FLAG-tag and myc-tag. **B)** The same membranes were incubated with antibodies specific for Aurora B, Borealin and Survivin.

4 Discussion

Two processes are the major key players to maintain genome integrity, namely replication and mitosis. During replication, the genome is duplicated and then, during mitosis, divided equally and passed to the two daughter cells. A crucial role during mitosis devolves on the CPC. This complex is responsible for key steps during mitosis such as correct chromosome-microtubule attachments, activation of the spindle assembly checkpoint as well as construction and regulation of the contractile apparatus driving cytokinesis (Carmena et al. 2012b). One member of the CPC, Survivin, benefits from a dual role. Besides its participation in the CPC it belongs to the IAP family, and thus acts as an inhibitor of apoptosis (Ambrosini et al. 1997). Importantly, Survivin plays a major role in tumorigenesis: it is characterized by upregulation in most cancer entities and is associated with increased resistance against chemo- and radiotherapy. In addition, its cytoplasmic localisation was linked to a cytoprotective activity against treatment-induced apoptosis of tumour cells. However, the detailed role of the CPC and especially Survivin during interphase still remains elusive.

As part of her doctoral thesis, Elisabeth Schröder in our group could gain first evidence of such an additional, mitosis-independent function, since she detected the CPC proteins in interphase nuclei. Under physiological conditions Survivin is primarily localised to the cytoplasm due to its nuclear export signal (NES), but irradiation resulted in relocation of cytoplasmic Survivin to the nucleus where it accumulated at distinct nuclear foci. Interestingly, also the other CPC members could be detected at those irradiation-induced foci. More precisely, these CPC foci detected in interphase nuclei are located predominantly at centromeric regions. Furthermore, Survivin and Aurora B depletion resulted in an increase in persistent DNA double-strand breaks, indicative for a reduced cellular DNA repair capacity. These observations led to the assumption that the CPC might execute an additional role in interphase nuclei, especially after DNA damaged caused by irradiation or other DNA damaging agents. In general, an involvement of Survivin and the other CPC members in DNA damage response and repair was suggested (Capalbo et al. 2010; Reichert et al. 2011; Schröder 2014). Subsequently, it should be clarified if the CPC members are indeed directly involved in the irradiation-induced DNA damage response. Noteworthy, no distinct co-localisation with proteins of the DNA repair machinery could be detected,

however the bona fide DNA damage foci could be determined in close proximity to CPC and especially Survivin foci. As such, the data suggested no direct involvement of the CPC in DNA repair processes such as HDR or NHEJ, respectively, but rather a participation in processes attendant to DNA repair (Schröder 2014).
Moreover, a subsequent PhD project of Stefanie Mosel (née Schlesiger) revealed an interaction of the CPC member INCENP to PCNA (Mosel 2018). As PCNA is known as the DNA clamp essential for replication, these data for the first time established a direct connection between the CPC and DNA replication. In addition, recent studies demonstrated that the CPC, especially Aurora B resumes a role in response to replication stress (Smith 2002; Dheekollu et al. 2011; Zuazua-Villar et al. 2014; Mackay and Ullman 2015; Mosel 2018).
Despite these first hints towards an additional role of Survivin and the other CPC members in interphase, neither a distinct function resonating with the observed links to DNA replication nor the mechanistic details have so far been elucidated, which was therefore the major aim of this thesis.

4.1 Defining the localisation of the CPC in interphase nuclei and its influence on replication

So far, no comprehensive experimental studies have been conducted regarding the localisation of the CPC proteins during interphase. However, one may find a manageable repertory of assumptions and hypotheses, based on particular observations in differently targeted research endeavours. It was shown that INCENP and Aurora B already co-localise in interphase, and that death-receptor induced apoptosis results in a Caspase-7-mediated degradation of INCENP leading to a loss of the centromere-CPC interaction in mitosis (Faragher et al. 2007). Here, it was also demonstrated that Borealin co-localises with Aurora B in interphase and that CENP-C is the driving force mediating this co-localisation. Furthermore, Borealin is located in the nucleus during interphase where it interacts with the nucleoli-residing SUMO isopeptidase SENP3 (Gassmann et al. 2004; Andersen et al. 2005a; Rodriguez et al. 2006; Klein et al. 2009). Survivin's localisation during interphase is predominantly cytoplasmic and by inhibiting its interaction with CRM1 (see section 1.8.1) an accumulation inside the nucleus was revealed (Colnaghi et al. 2006). However, there are also contrary assumptions. It was shown that Aurora B, Borealin and Survivin are

degraded by the APC/CCdh1 from late mitosis to G1 phase (Connell et al. 2008; Tsunematsu et al. 2020). In addition, Cdh1 depletion leads to a constant expression of Aurora B and Borealin throughout the cell cycle, but causes reduced DNA replication efficiency (Tsunematsu et al. 2020). Up to know, no interaction of CPC members and replication proteins were described in literature. Initial experiments in our group revealed a possible interaction with the sliding clamp PCNA (Mosel 2018). Furthermore, our group showed that the CPC member INCENP contains a so-called PIP-box motif representing a typical PCNA binding domain (Mosel 2018).

In order to confirm these results, co-immunoprecipitations with exogenously expressed GFP-PCNA and CPC-myc constructs as well as PLA, allowing to analyse the interaction on an endogenous level, were performed. All CPC members could be detected in GFP-PCNA immunoprecipitates isolated from non-irradiated cells (see Figure 3.10). Further, the PLA revealed a co-localization in close proximity (less than 40 nm) to PCNA (see Figure 3.1), confirming the physical interaction of the CPC to PCNA in untreated, exponentially growing cells. As mentioned, co-immunoprecipitation revealed an interaction of the CPC members to PCNA, but to demonstrate a specific binding, cells were transfected with a plasmid coding for GFP. The fact that prior to immunoprecipitation all samples were subjected to chromatin extraction, control samples co-transfected with GFP and myc-CPC constructs could also show a signal for GFP, due to relocation to the nucleus. However, GFP is not chromatin-bound, and therefore the signal detected in these immunoprecipitates is a sign for unspecific binding. Nevertheless, bounded GFP to the GFP-coupled magnetic beads enhances the results which were obtained for co-transfection with GFP-PCNA and the CPC-myc constructs. While the GFP-PCNA immunoprecipitates revealed a myc detection and thus a binding to the CPC members, the GFP immunoprecipitates revealed no binding to the chromosomal passenger complex, which identifies the CPC as a specific binding partner of PCNA. However, a small amount of myc-INCENP was bound to GFP, but a significant higher part was bound to GFP-PCNA, also revealing a significant interaction between INCENP and PCNA (see Appendix Figure 6.1 and Figure 6.2). In contrast to the other CPC members, Borealin-myc was detected in only minor amounts in GFP-PCNA immunoprecipitates, which might be a result of degradation by APC/CCdh1 after G1 phase entry (Tsunematsu et al. 2020). The input samples of the Survivin-myc and GFP-PCNA co-transfection did not allow to detect any signal, but this might rely on the fact that those samples were present in a higher dilution as the immunoprecipitates.

In contrast to immunoprecipitation experiments, PLA allow to investigate protein-protein interactions at the endogenous level. Here, we could demonstrate that all CPC members are localized in close proximity of less than 40 nm to PCNA, thus confirming a direct binding in the physiological environment of the cell. Quantitative analysis of PLA foci was first performed within the whole cell (see Figure 3.1 B) and revealed significant fluorescent signals representing distinct sites of protein interaction. However, since a functionally relevant binding to PCNA is supposed to happen in the nucleus, we also included an analysis of PLA foci restricted to the cell nuclei by using an appropriate nuclear mask in the pipeline (see Appendix Figure 6.4). Anyway, the outcome of the analyses did not differ. Of note, to produce meaningful and reliable results, it is of utmost importance to also include proper negative controls. Here, the

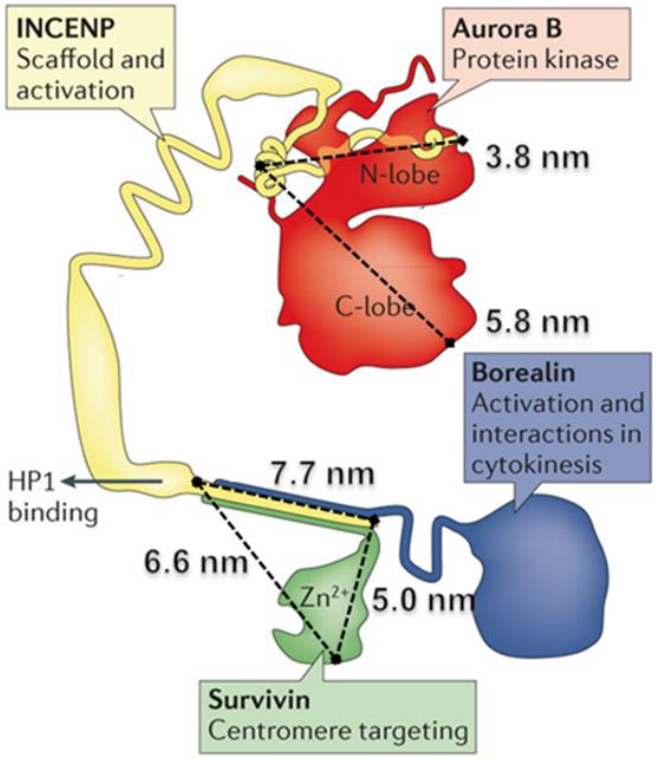

Figure 4.1: Distances between the CPC members

Schematic overview of the CPC and their measured distances to each other. Our working group could analyse distances not higher than 10 nm within the complex, which explain the fact that indeed all CPC member are in a close proximity of 40 nm to the replication factor PCNA as the results obtained by the PLA have shown. Modified by (Carmena and Wheelock et al. 2012; Mosel 2018).

only negative control producing a high level of background signal was the antibody directed against Survivin. In contrast, the other antibodies used in the PLA did not show

any relevant background signal, but resulted in significantly increased PLA signals when used in combination with the antibody directed against the possible interaction partner PCNA. In comparison, the relatively high concentration used in case of the Survivin antibody might result in a higher rate of unspecific binding. Despite this high background signal, analysis of PLA signals in the sample stained against Survivin and PCNA are significantly increased compared to the negative control. However, the PLA-detected interaction between PCNA and all four CPC members is quite conceivable, as the members of the chromosomal passenger complex are presumed to be arranged in close proximity to each other so that each binding site at any CPC member is not more than 40 nm away from the other complex components (see Figure 4.1).

As already mentioned, previous studies in our group already revealed a PIP-box motif in INCENP. For this, sequences of all CPC members were bioinformatically screened for typical PCNA binding motifs, such as APIM or a PIP-box (Warbrick 2000; Gilljam et al. 2009; Mosel 2018). Importantly, in these analyses, we could indeed only detect a possible PCNA binding motif in INCENP, but not in the other CPC members, indicating that the main interaction to PCNA is mediated by INCENP and that the other CPC members are in close proximity to PCNA due to their spatial vicinity to INCENP within the complex. To functionally validate the PIP-box motif, co-immunoprecipitations with ectopically expressed GFP-PCNA and either myc-INCENPwt or myc-INCENPmut, comprising a mutated PIP-box sequence, were performed. Here, in both GFP-PCNA immunoprecipitates the myc-tags of both INCENP variants could be detected, whereby the amount of PCNA-associated myc-INCENPmut was reduced in comparison to the detected wild-type form of INCENP, which implied an interaction of INCENP to PCNA via the PIP-box motif.

In all experiments performed so far, asynchronously growing cells were used. But it is well documented that PCNA is also involved in cellular processes like chromatin remodelling, DNA repair, sister-chromatid cohesion and cell cycle control and is therefore expressed throughout the cell cycle (Maga and Hubscher 2003; Strzalka and Ziemienowicz 2011). Thus, the observed interaction of CPC members with PCNA could also occur either in G1 or G2 phase. For this reason, immunofluorescence experiments (see Figure 3.6-Figure 3.9) were performed to curtail the co-localisation to S phase. Here, S phase cells were distinguished due to their specific PCNA distribution pattern in S phase (Schönenberger et al. 2015). Furthermore, the cells were incubated with CSK buffer to wash away all not-chromatin-bound components.

To note, Figure 3.6-Figure 3.9 show a representative selection of images that visualize the localisation of the CPC members. But, in general, the analysis of all acquired fluorescence reveals that not all CPC foci were co-localised to replication sites neither in untreated cells nor in cells treated with irradiation or DNA damage inducing agents. For Survivin (see Figure 3.6) it is obvious that increasing foci formation occurs after irradiation, but nevertheless not all foci were identical with PCNA or replication sites, respectively, but indeed some Survivin foci could show a co-localisation to PCNA, especially after induction of replication stress. Also, Aurora B (see Figure 3.7) foci formation is enhanced after induction of replication stress but only a small part of Aurora B foci co-localises with replication sites. Borealin (see Figure 3.8) was highly abundant, but some occurring foci could be correlated to PCNA localisation. For INCENP (see Figure 3.9) it was difficult to analyse the localisation pattern. Fluorescent signals all over nucleoplasm indicate a widespread distribution of INCENP, but also a significant accumulation in the nucleoli became obvious. However, a small amount of foci seemed to co-localise with PCNA foci. Nevertheless, as contrary assumptions claimed that Aurora B, Borealin and Survivin were degraded after G1 entry (Tsunematsu et al. 2020), it is obvious that all CPC members were expressed in S phase cells and at least a subpopulation of them co-localises with replication sites. To err on the side of caution, the experiments should be confirmed in synchronised S phase cells, to eliminate PCNA's distribution and participations throughout the cell cycle. However, replication foci are indicated by PCNA, as it is an essential component of the replisome. Indeed, the described results show a partial co-localisation between PCNA and the CPC-members but many sites of replication are not additionally occupied with the CPC. In this regard it can be concluded that the CPC is not a constant companion of the replisome but joins the replication fork only under certain conditions. As irradiation represents such a condition of an enhanced PCNA-CPC interaction, it is likely that the CPC associates with replication forks at irradiation-induced DNA damage.

It was therefore of interest to analyse the progression of replication forks in dependency of the CPC. For that purpose, DNA combing assays were performed. The DNA combing assay is used for a detailed profiling of DNA replication, thereby giving information about various aspects of DNA synthesis, such as replication fork speed, fork stalling or collapsing, initiation and termination events and interorigin distances (IOD). For this, the DNA is sequentially labelled by two consecutive pulses with

halogenated thymidine analogues. In contrast to the DNA fibre assay that was usually used in our working group the DNA combing assay allows accurate determination of the replication fork velocities. The force and speed are controlled by the combing machine that combed the DNA fibres by a constant factor of 2 kb/µm (Quinet et al. 2017a). Due to this fact, DNA combing is well suited to measure interorigin distances and new origin firing by preventing crossing of DNA fibres. The biggest disadvantages of DNA combing are the increased occurrence of DNA breakage during melting of the agarose plug and the fact that it is very time consuming in contrast to the DNA fibre assay. In the conducted analysis, DNA combing assay revealed a strong fork asymmetry, longer interorigin distances and a slight increase of initiation events in Aurora B-depleted cells. A reduced replication fork velocity could not be observed in cells depleted for Aurora B (see Figure 3.13). Furthermore, the data obtained for Survivin-depleted cells were not robust enough to provide adequate information. But it seems that in this case the replication fork speed, the fork asymmetry and the interorigin distances revealed no alteration. However, a decrease in initiation events could be observed, but as mentioned, the data for Survivin depletion were very inconsistent and thus only allow speculations. For future approaches, the cell number needed for this assay has to be exactly determined to prevent overlapping DNA on the slides. Nevertheless, in former approaches to determine the replication fork speed, our working group could show a significant slowdown in Survivin-depleted cells by performing DNA fibre assays (Schröder 2014; Mosel 2018). Slowdown of replication forks can occur by facing several obstacles such as DNA repeat sequences, DNA fragile sites, replication termination sites, replication slow zones transcription factors, absence of dNTPs and DNA lesions (Postow et al. 2001; Casper et al. 2002; Wyatt and Pittman 2006; Durkin and Glover 2007; Mirkin and Mirkin 2007; Barlow et al. 2013). The results obtained in this work, especially those which indicate a co-localisation with replication sites after irradiation or treatment with DNA damaging agents and replication fork stalling after Aurora B depletion give a hint that the CPC is directly involved in DNA-damage induced replication processes.

So far, it is clear that Survivin and the whole CPC are somehow involved in avoiding or repairing irradiation induced DNA damage. However, our investigations exclude that CPC members directly participate in DDS repair processes such as HDR or NHEJ. As increased replication fork stalling is observed upon CPC-member depletion, it can be concluded that the CPC rescues stalled replication forks at sites of DNA-damage,

thereby preventing collapsed forks and DNA double strand breaks. A mechanism which allows to copy damaged DNA is the PCNA-mediated translesion synthesis.

4.2 Survivin function in translesion synthesis

We could demonstrate a direct binding of the CPC to PCNA via INCENP's PIP-box motif, but a participation of Survivin in normal DNA synthesis seems unlikely as Survivin was localised predominantly to heterochromatin protein 1α (HP1α), especially to centromeric regions in interphase nuclei (Schröder 2014). If Survivin supports the process of DNA replication in general, one would expect a physical presence at all sites of replication. Though, our data demonstrated a co-localisation only to some replication sites especially after irradiation or treatment with other DNA damaging agents, which is another hint that CPC localisation to replication sites might be involved in PCNA-mediated translesion synthesis.

As mentioned, the sliding clamp PCNA is involved in many cellular processes throughout the cell cycle. But during DNA synthesis, PCNA resumes two important processes to maintain genome integrity. It is responsible for an enhanced DNA polymerase δ processivity and it is also involved in translesion synthesis. Here, polymerases like Pol η, Pol ζ and REV1 are recruited to the stalled replication fork, through a monoubiquitination of PCNA by Rad6 and Rad18 (Stelter and Ulrich 2003; Kannouche et al. 2004; Yeeles et al. 2013). Afterwards, TLS polymerases incorporate bases within the gap and are subsequently displaced by a replicative polymerase, which continues DNA synthesis (Johnson et al. 2000; Woodgate 2001; Moldovan et al. 2007; Shachar et al. 2009). Translesion synthesis is increasingly applied under circumstances that provoke DNA damage. Ionizing radiation and DNA damaging agents damage the DNA directly by inducing DSBs and SSBs or indirectly by inducing free radicals, which attack the DNA (Baskar et al. 2014). If these irradiation-induced lesions collide with replication forks, the replication machinery contributes to the formation of replication induced DSBs. These replication-induced DSBs are prevented by the translesion synthesis which allows bypassing or repairing of DNA lesions at locations of stalled DNA replication. During interphase, we could identify CPC co-localisation after irradiation at centromeric regions. These regions resume major roles during chromosome segregation including proper kinetochore assembly, mediating the

binding between spindle fibres and chromosomes and they are responsible for the recruiting of signalling components for proper kinetochore-microtubule attachments. However, centromeres consist of highly repetitive DNA sequences such as satellite DNAs and thus they are particularly prone and vulnerable for chromosome mis-segregation and aneuploidy. Chromosome alterations occur with a frequency of 40–60 % in centromeric regions (Barra and Fachinetti 2018). Since the process of translesion synthesis illustrates the interference of DNA damage repair and replication, we assumed that the CPC is directly involved in translesion synthesis as in this process the demonstrated PCNA-CPC interaction (this thesis and (Mosel 2018)) and the CPC connection to DNA damage (Schröder 2014) would converge.

Indeed, this work could clearly demonstrate that the CPC is associated with the translesion polymerase η. Expression studies (see Figure 3.14) substantiate this assumption. Here, expression levels of polymerase η are decreased after Aurora B depletion and irradiation. Since it is known that polymerase η expression is upregulated by the transcription factor p53 (Helton and Chen 2007), and p53 is a phosphorylation target of Aurora B (see section 1.7.3), an Aurora B regulated expression level of polymerase η is presumed and therefore a concentration-dependent association with the CPC could be assumed. Our data allow the suggestion that due to Aurora B depletion the transcription factor p53 is not activated by phosphorylation which in turn affects the expression of Pol η. Especially after irradiation this effect can be seen even more clearly due to Pol η participation in DNA-damage induced replication. In addition, co-immunoprecipitation experiments were performed and revealed a direct interaction of the CPC members to polymerase η. 293T cells were co-transfected with plasmids coding for FLAG-polymerase η together with Survivin-myc or Aurora B-myc or Borealin-myc or myc-INCENP, respectively. One-third of the chromatin extraction was used as an input control. FLAG-polymerase η was immunoprecipitated from the chromatin extracts using magnetic beads coupled to a FLAG-specific antibody (see section 2.2.3.4). In FLAG-immunoprecipitates a signal for myc was detected for Survivin, Aurora B and Borealin (see Figure 3.15 A). To ensure that the observed binding is not an artificial effect but is based on a physiological interaction, also the presence of endogenous CPC members in the precipitates was analysed and at least Aurora B and Survivin were identified (see Figure 3.15 B). Moreover, increasing metaphase gaps, subsequent 53BP1 nuclear bodies and mitotic synthesis (see Figure 3.2–Figure 3.4) after Survivin

depletion substantiate the fact that translesion synthesis could not proceed unobstructed. Thus, impaired translesion synthesis causes remaining of under-replicated sites after S phase exit. Also, to promote translesion synthesis and to prevent DSBs by collapsing replication forks, enhanced interaction of the CPC with PCNA and an increasing relocation to centromeric heterochromatin after irradiation were demonstrated. The enhanced interaction of the CPC to PCNA strengthen the suggestion that this interaction is translesion synthesis-dependent and that it is not relevant for “normal” replication. Furthermore, the findings that depletion of CPC members causes increased DNA DSBs (Schröder 2014) as well as increased replication fork stalling, especially after irradiation or treatment with DNA damaging agents (Schröder 2014; Mosel 2018), converge in the following hypothesis: The CPC initiates translesion synthesis by recruiting non-classical DNA polymerases such as DNA polymerase η to stalled replication forks at damaged DNA in centromeric regions. It is known that the translesion polymerases are frequently more error-prone (Hoeijmakers 2001) and therefore facilitate the generation of mutations due to their lack of exonucleolytic proofreading function. Thus, a strict regulation of translesion polymerases recruited to sites of DNA damage is required. Up to know, it is established that a monoubiquitination of PCNA by Rad6 and Rad18 is required for a polymerase switch between a high-fidelity polymerase and a translesion polymerase (Stelter and Ulrich 2003; Kannouche et al. 2004; Yeeles et al. 2013). However, the exact mechanisms for a controlled polymerase switching and the contribution of further proteins in this process are still elusive. Recent studies revealed an interesting scenario. In these studies, PDIP38 resumed a major role during translesion synthesis. PDIP38 sequesters polymerase η away from normal replication forks because of their low-fidelity, until polymerase η is activated by ATR and PKC phosphorylation (Peddu et al. 2018). Two studies demonstrated that phosphorylation of Pol η by ATR (Göhler et al. 2011) and PKC (Chen et al. 2008b) is critical for its function in intact cells. Indeed, the phosphorylation is necessary for recruitment to stalled replication forks with monoubiquitinated PCNA (Peddu et al. 2018). In this case, it is of no importance whether the replication machinery is released from high-fidelity polymerases such as polymerase δ due to the high affinity of polymerase η for Ub-PCNA (Peddu et al. 2018). Since the CPC members are increasingly located a heterochromatin following irradiation-induced DNA damage, the CPC-PCNA interaction contributes to the assumption that the CPC members are directly involved in a controlled exchange

between high-fidelity polymerases and translesion polymerases. However, in two different studies two kinases were identified to phosphorylate Pol η. It is conceivable that the kinase Aurora B directly phosphorylate Pol η for recruitment to sites of DNA damage.

The centromeric regions are especially prone to UV-photoproducts, as they contain a lot of AT-rich α satellites (Sullivan et al. 2017). Thus, such a CPC-facilitated polymerase switch may constitute an urgently required support mechanism in those DNA regions. Therefore, the CPC may function as an adaptor which recruits translesion polymerases to sites of stalled replication forks in centromeric regions and mediates the contact between PCNA in the stalled replisome and the recruited TLS-polymerases. Moreover, a direct CPC-involvement in the exchange step of the polymerases is conceivable (see Figure 4.2).

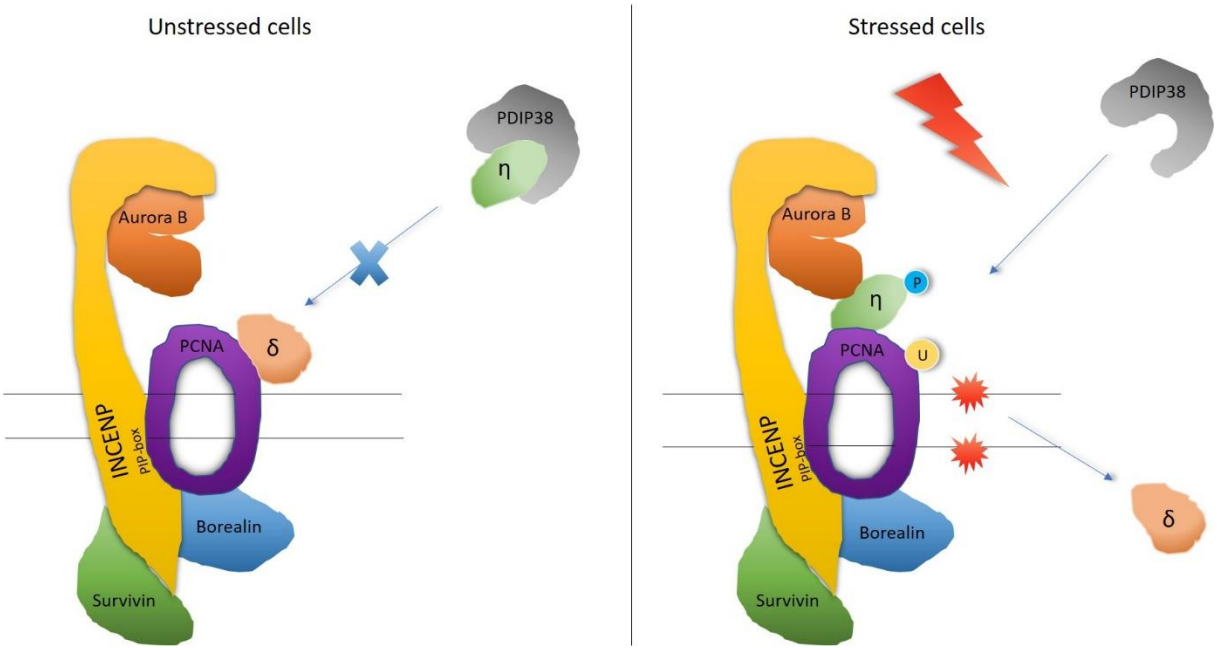

Figure 4.2: Modell of CPC's functional role during DNA replication of damaged DNA

The CPC is co-localised with the sliding clamp factor PCNA via INCENP's PIP-box motif. In unstressed cells the replicative polymerase δ is located at the replisome while synthesizing a new DNA strand. The polymerase η is sequestered by PDIP38 till the replisome converges an obstacle caused by irradiation or DNA-damaging agents (Tsunematsu et al. 2020). In this case, the Pol η is activated by phosphorylation and is recruited to the monoubiquitinated PCNA while the polymerase δ dissociates from the replisome (Peddu et al. 2018). Our data lead to the assumption that the CPC function as an adaptor for recruitment of the translesion polymerase η.

The systematic effects of an impaired translesion synthesis are phenotypically manifested in the disease Xeroderma pigmentosum variant (XPV) which is a milder subtype of xeroderma pigmentosum (XP). (Cordonnier et al. 1999). This disease is

caused by a mutation in the *POLH* gene, which encodes Pol η. Thus, TLS is not able to bypass UV-induced DNA damage or AFF adducts and consequently the replication fork stalls at these sites of DNA damage (Liu and Chen 2006). The majority of these stressed cells are eliminated by apoptosis due to a sustained activation of p53 but for a certain number of cells instead of polymerase η a more error-prone translesion polymerase incorporates nucleotides and causes mutations (Stary and Sarasin 2002) which leads to a phenotype of extreme sensitivity to sunlight, pigment disorders such as freckles and blisters and subsequently an increased appearance of skin cancer (Armenta et al. 2018). However, for cancer cells an enhanced TLS-ability is desirable as it offers the possibility to resist radiation therapy in cancer. This may deliver a further explanation for upregulated Survivin levels in many cancer cells, especially in tumours resistant to chemo- or radiotherapy. The cellular phenotype of XPV-cells after UV-irradiation is therefore comparable to the phenotype of Survivin-depleted cells which also show a delayed recovery from UV-induced DNA damage (Schröder 2014). The presented results show that Survivin and the other CPC-members counteract induced DNA-damage by enabling the replication of damaged DNA via their newly discovered function in TLS. In summary, the prominent role of Survivin as a radio-resistance factor is maybe not solely due to Survivin's antiapoptotic function but may also be due to the newly discovered function in translesion synthesis.

Further experiments are necessary to strengthen Survivin's and the CPC's role in translesion synthesis. Since, the ubiquitination status of PCNA is important for recruitment of translesion polymerases, co-localisation especially to monoubiquitinated PCNA should focused in further investigations by co-immunoprecipitations. If it emerges that especially the monoubiquitinated form co-precipitates with CPC-members and in relation to that, a suitable PCNA mutant could change these results, this would be another indication for an involvement of the CPC in TLS. Furthermore, it should be investigated if a depletion of the CPC members leads to a significant reduction of co-precipitated translesion polymerase η.

In conclusion, this project reveals a concrete function for the CPC in S phase (see Figure 4.3). Initial suspicions that the CPC is directly involved in the DNA repair process could not be substantiated, but expression, co-localisation of the CPC in interphase nuclei and further increased DSBs after depletion of CPC members, hinted to a functional role in response to DNA damage (Schröder 2014). Due to a relocation of the CPC proteins to centromeric heterochromatin especially in S phase and a

reduced replication fork speed after CPC depletion, a functional role in replication was suggested. Indeed, an interaction of the CPC with the sliding clamp protein PCNA was revealed, which is predominantly mediated by INCENP's PIP-motif. Interestingly, it was shown that all CPC members co-localised with PCNA, which hinted towards a replication participation as a complex (Mosel 2018). On this basis, a possible role of the CPC in replication shifted in the focus of further investigations. It was shown that the CPC-PCNA interaction was enhanced after irradiation and treatment with DNA-damaging agents, especially an enhanced relocation to centromeric heterochromatin was observed. Moreover, in the absence of CPC members, an increased replication fork stalling was revealed. These findings hinted to an involvement of the CPC only in replication processes linked to DNA damage. One prominent process is the translesion synthesis, where especially DNA lesions were repaired by translesion polymerases. Indeed, an interaction of the CPC with a translesion polymerase (Pol η) was demonstrated. A direct involvement of Survivin and the CPC in such a replication-correlated process explains the high incidence of Survivin upregulation in a plethora of different cancer entities leading to an increased resistance against radio- and presumably also chemotherapy.

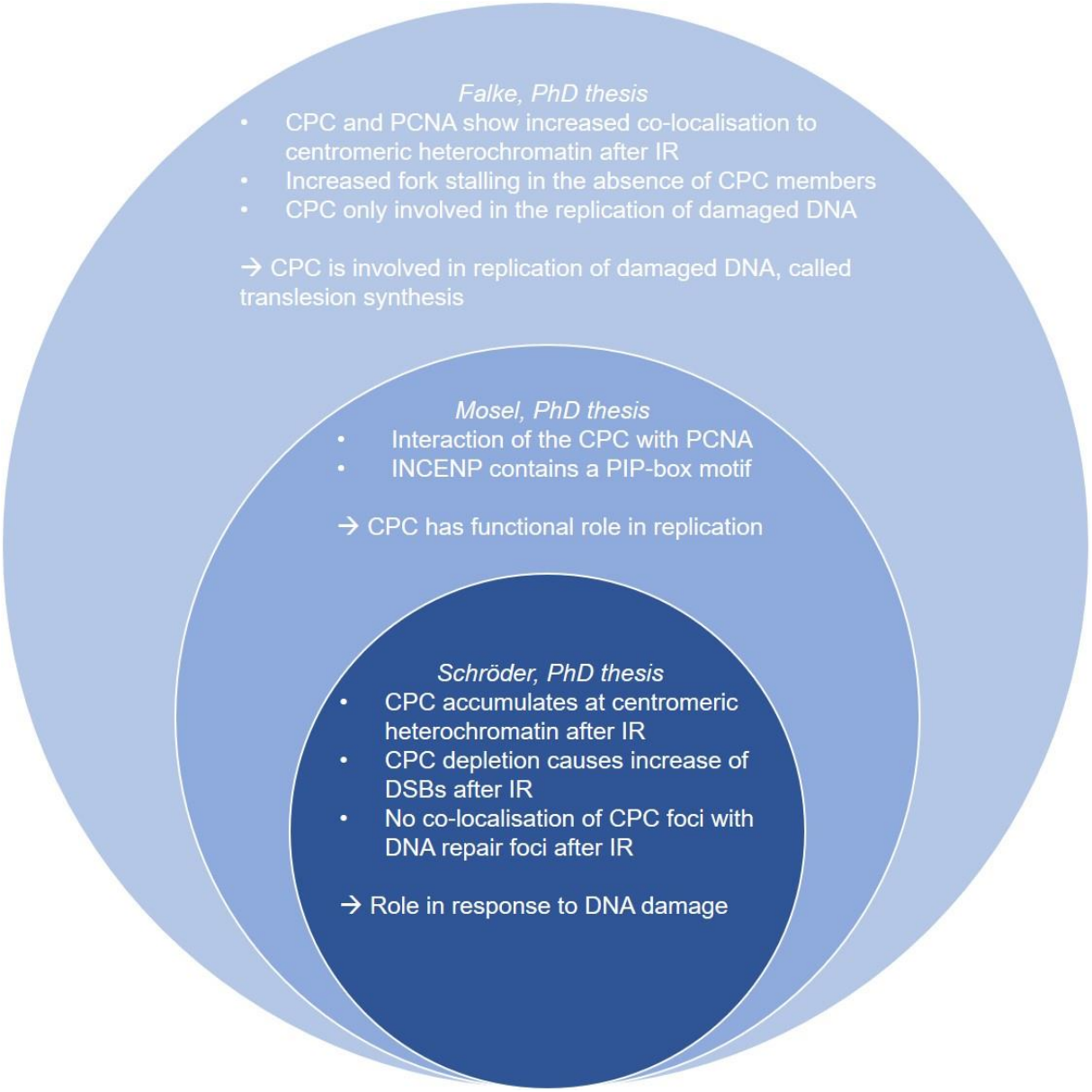

Figure 4.3: Schematic overview over the course of this research project

This overview represents the main findings assigned to the three subsequent subprojects regarding their research focus and the main messages deducted. Starting with the PhD thesis of Elisabeth Schröder (Schröder 2014), followed by the PhD project of Stefanie Mosel (Mosel 2018) and finally this thesis project.

5 References

Adams, R. R.; Eckley, D. M.; Vagnarelli, P.; Wheatley, S. P.; Gerloff, D. L.; Mackay, A. M. et al. (2001a): Human INCENP colocalizes with the Aurora-B/AIRK2 kinase on chromosomes and is overexpressed in tumour cells. In *Chromosoma* 110 (2), pp. 65–74. DOI: 10.1007/s004120100130.

Adams, R. R.; Maiato, H.; Earnshaw, W. C.; Carmena, M. (2001b): Essential roles of Drosophila inner centromere protein (INCENP) and aurora B in histone H3 phosphorylation, metaphase chromosome alignment, kinetochore disjunction, and chromosome segregation. In *J Cell Biol* 153 (4), pp. 865–880. DOI: 10.1083/jcb.153.4.865.

Adida, Colette; Berrebi, Dominique; Peuchmaur, Michael; Reyes-Mugica, Miguel; Altieri, Dario C. (1998): Anti-apoptosis gene, survivin, and prognosis of neuroblastoma. In *Lancet (London, England)* 351 (9106), pp. 882–883. DOI: 10.1016/S0140-6736(05)70294-4.

Agarwal, M. L.; Taylor, W. R.; Chernov, M. V.; Chernova, O. B.; Stark, G. R. (1998): The p53 network. In *The Journal of biological chemistry* 273 (1), pp. 1–4. DOI: 10.1074/jbc.273.1.1.

Aguilera, Andrés; García-Muse, Tatiana (2013): Causes of genome instability. In *Annual review of genetics* 47, pp. 1–32. DOI: 10.1146/annurev-genet-111212-133232.

Aguilera, Andrés; Gómez-González, Belén (2008): Genome instability: a mechanistic view of its causes and consequences. In *Nature reviews. Genetics* 9 (3), pp. 204–217. DOI: 10.1038/nrg2268.

Ahel, Ivan; Rass, Ulrich; El-Khamisy, Sherif F.; Katyal, Sachin; Clements, Paula M.; McKinnon, Peter J. et al. (2006): The neurodegenerative disease protein aprataxin resolves abortive DNA ligation intermediates. In *Nature* 443 (7112), pp. 713–716. DOI: 10.1038/nature05164.

Ainsztein, A. M.; Kandels-Lewis, S. E.; Mackay, A. M.; Earnshaw, W. C. (1998): INCENP centromere and spindle targeting: identification of essential conserved motifs and involvement of heterochromatin protein HP1. In *The Journal of cell biology* 143 (7), pp. 1763–1774. DOI: 10.1083/jcb.143.7.1763.

Alarcón, Claudio R.; Tavazoie, Sohail F. (2016): Cancer: Endothelial-cell killing promotes metastasis. In *Nature* 536 (7615), pp. 154–155. DOI: 10.1038/nature19465.

Almeida, Karen H.; Sobol, Robert W. (2007): A unified view of base excision repair: lesion-dependent protein complexes regulated by post-translational modification. In *DNA repair* 6 (6), pp. 695–711. DOI: 10.1016/j.dnarep.2007.01.009.

Altieri, Dario C. (2001): The molecular basis and potential role of survivin in cancer diagnosis and therapy. In *Trends in molecular medicine* 7 (12), pp. 542–547. DOI: 10.1016/s1471-4914(01)02243-2.

Altieri, Dario C. (2013): Targeting survivin in cancer. In *Cancer letters* 332 (2), pp. 225–228. DOI: 10.1016/j.canlet.2012.03.005.

Ambrosini, G.; Adida, C.; Altieri, D. C. (1997): A novel anti-apoptosis gene, survivin, expressed in cancer and lymphoma. In *Nature medicine* 3 (8), pp. 917–921. DOI: 10.1038/nm0897-917.

Amon, Angelika (1999): The spindle checkpoint. In *Current opinion in genetics & development* 9 (1), pp. 69–75. DOI: 10.1016/s0959-437x(99)80010-0.

Andersen, Jens S.; Lam, Yun W.; Leung, Anthony K. L.; Ong, Shao-En; Lyon, Carol E.; Lamond, Angus I.; Mann, Matthias (2005a): Nucleolar proteome dynamics. In *Nature* 433 (7021), pp. 77–83. DOI: 10.1038/nature03207.

Andersen, Sonja; Heine, Tina; Sneve, Ragnhild; König, Imbritt; Krokan, Hans E.; Epe, Bernd; Nilsen, Hilde (2005b): Incorporation of dUMP into DNA is a major source of spontaneous DNA damage, while excision of uracil is not required for cytotoxicity of fluoropyrimidines in mouse embryonic fibroblasts. In *Carcinogenesis* 26 (3), pp. 547–555. DOI: 10.1093/carcin/bgh347.

Anderson, M. W.; Reynolds, S. H.; You, M.; Maronpot, R. M. (1992): Role of proto-oncogene activation in carcinogenesis. In *Environmental health perspectives* 98, pp. 13–24. DOI: 10.1289/ehp.929813.

Andres, Sara N.; Vergnes, Alexandra; Ristic, Dejan; Wyman, Claire; Modesti, Mauro; Junop, Murray (2012): A human XRCC4-XLF complex bridges DNA. In *Nucleic acids research* 40 (4), pp. 1868–1878. DOI: 10.1093/nar/gks022.

Armelin, H. A.; Armelin, M. C.; Kelly, K.; Stewart, T.; Leder, P.; Cochran, B. H.; Stiles, C. D. (1984): Functional role for c-myc in mitogenic response to platelet-derived growth factor. In *Nature* 310 (5979), pp. 655–660. DOI: 10.1038/310655a0.

Armenta, Andrew M.; Massey, Paul R.; Khan, Sikandar G.; Tamura, Deborah; Levy, Moise L.; DiGiovanna, John J. et al. (2018): Variant subtype of xeroderma pigmentosum diagnosed in a 77-year-old woman. In *JAAD Case Reports* 4 (10), pp. 1074–1076. DOI: 10.1016/j.jdcr.2018.08.013.

Ayoub, Nabieh; Jeyasekharan, Anand D.; Venkitaraman, Ashok R. (2009): Mobilization and recruitment of HP1: a bimodal response to DNA breakage. In *Cell cycle (Georgetown, Tex.)* 8 (18), pp. 2945–2950.

Baldeyron, Céline; Soria, Gaston; Roche, Danièle; Cook, Adam J. L.; Almouzni, Geneviève (2011): HP1alpha recruitment to DNA damage by p150CAF-1 promotes homologous recombination repair. In *The Journal of cell biology* 193 (1), pp. 81–95. DOI: 10.1083/jcb.201101030.

Bannister, A. J.; Zegerman, P.; Partridge, J. F.; Miska, E. A.; Thomas, J. O.; Allshire, R. C.; Kouzarides, T. (2001a): Selective recognition of methylated lysine 9 on histone H3 by the HP1 chromo domain. In *Nature* 410 (6824), pp. 120–124. DOI: 10.1038/35065138.

Bannister, A. J.; Zegerman, P.; Partridge, J. F.; Miska, E. A.; Thomas, J. O.; Allshire, R. C.; Kouzarides, T. (2001b): Selective recognition of methylated lysine 9 on histone H3 by the HP1 chromo domain. In *Nature* 410 (6824), pp. 120–124. DOI: 10.1038/35065138.

Barber, Louise J.; Youds, Jillian L.; Ward, Jordan D.; McIlwraith, Michael J.; O'Neil, Nigel J.; Petalcorin, Mark I. R. et al. (2008): RTEL1 maintains genomic stability by suppressing homologous recombination. In *Cell* 135 (2), pp. 261–271. DOI: 10.1016/j.cell.2008.08.016.

Barlow, Jacqueline H.; Faryabi, Robert B.; Callén, Elsa; Wong, Nancy; Malhowski, Amy; Chen, Hua Tang et al. (2013): Identification of early replicating fragile sites that contribute to genome instability. In *Cell* 152 (3), pp. 620–632. DOI: 10.1016/j.cell.2013.01.006.

Barnum, Kevin J.; O'Connell, Matthew J. (2014): Cell cycle regulation by checkpoints. In *Methods in molecular biology (Clifton, N.J.)* 1170, pp. 29–40. DOI: 10.1007/978-1-4939-0888-2_2.

Barra, V.; Fachinetti, D. (2018): The dark side of centromeres: types, causes and consequences of structural abnormalities implicating centromeric DNA. In *Nat Commun* 9 (1), p. 4340. DOI: 10.1038/s41467-018-06545-y.

Barrett, Rachel M. A.; Colnaghi, Rita; Wheatley, Sally P. (2011): Threonine 48 in the BIR domain of survivin is critical to its mitotic and anti-apoptotic activities and can be phosphorylated by CK2 in vitro. In *Cell Cycle* 10 (3), pp. 538–548. DOI: 10.4161/cc.10.3.14758.

Bartek, Jiri; Lukas, Claudia; Lukas, Jiri (2004): Checking on DNA damage in S phase. In *Nature reviews. Molecular cell biology* 5 (10), pp. 792–804. DOI: 10.1038/nrm1493.

Bartek, Jiri; Lukas, Jiri (2001): Mammalian G1- and S-phase checkpoints in response to DNA damage. In *Current opinion in cell biology* 13 (6), pp. 738–747. DOI: 10.1016/s0955-0674(00)00280-5.

Baskar, Rajamanickam; Dai, Jiawen; Wenlong, Nei; Yeo, Richard; Yeoh, Kheng-Wei (2014): Biological response of cancer cells to radiation treatment. In *Frontiers in Molecular Biosciences* 1, p. 24. DOI: 10.3389/fmolb.2014.00024.

Baumann, Michael; Krause, Mechthild; Overgaard, Jens; Debus, Jürgen; Bentzen, Søren M.; Daartz, Juliane et al. (2016): Radiation oncology in the era of precision medicine. In *Nat Rev Cancer* 16 (4), pp. 234–249. DOI: 10.1038/nrc.2016.18.

Beardmore, Victoria A.; Ahonen, Leena J.; Gorbsky, Gary J.; Kallio, Marko J. (2004): Survivin dynamics increases at centromeres during G2/M phase transition and is regulated by microtubule-attachment and Aurora B kinase activity. In *Journal of cell science* 117 (Pt 18), pp. 4033–4042. DOI: 10.1242/jcs.01242.

Bell, Stephen P.; Dutta, Anindya (2002): DNA replication in eukaryotic cells. In *Annual review of biochemistry* 71, pp. 333–374. DOI: 10.1146/annurev.biochem.71.110601.135425.

Bell, Stephen P.; Kaguni, Jon M. (2013): Helicase loading at chromosomal origins of replication. In *Cold Spring Harbor Perspectives in Biology* 5 (6). DOI: 10.1101/cshperspect.a010124.

Bernstein, Nina K.; Williams, R. Scott; Rakovszky, Melissa L.; Cui, Diana; Green, Ruth; Karimi-Busheri, Feridoun et al. (2005): The molecular architecture of the mammalian DNA repair enzyme, polynucleotide kinase. In *Molecular cell* 17 (5), pp. 657–670. DOI: 10.1016/j.molcel.2005.02.012.

Bétous, Rémy; Mason, Aaron C.; Rambo, Robert P.; Bansbach, Carol E.; Badu-Nkansah, Akosua; Sirbu, Bianca M. et al. (2012): SMARCAL1 catalyzes fork regression and Holliday junction migration to maintain genome stability during DNA replication. In *Genes & development* 26 (2), pp. 151–162. DOI: 10.1101/gad.178459.111.

Bhatti, Shahzad; Kozlov, Sergei; Farooqi, Ammad Ahmad; Naqi, Ali; Lavin, Martin; Khanna, Kum Kum (2011): ATM protein kinase: the linchpin of cellular defenses to stress. In *Cellular and molecular life sciences : CMLS* 68 (18), pp. 2977–3006. DOI: 10.1007/s00018-011-0683-9.

Bickmore, Wendy A.; van Steensel, Bas (2013): Genome architecture: domain organization of interphase chromosomes. In *Cell* 152 (6), pp. 1270–1284. DOI: 10.1016/j.cell.2013.02.001.

Binz, Sara K.; Sheehan, Anne M.; Wold, Marc S. (2004): Replication protein A phosphorylation and the cellular response to DNA damage. In *DNA repair* 3 (8-9), pp. 1015–1024. DOI: 10.1016/j.dnarep.2004.03.028.

Birchler, James A.; Pal Bhadra, Manika; Bhadra, Utpal (2000): Making noise about silence: repression of repeated genes in animals. In *Current opinion in genetics & development* 10 (2), pp. 211–216. DOI: 10.1016/s0959-437x(00)00065-4.

Bonev, Boyan; Cavalli, Giacomo (2016): Organization and function of the 3D genome. In *Nat Rev Genet* 17 (11), pp. 661–678. DOI: 10.1038/nrg.2016.112.

Boos, Dominik; Sanchez-Pulido, Luis; Rappas, Mathieu; Pearl, Laurence H.; Oliver, Antony W.; Ponting, Chris P.; Diffley, John F. X. (2011): Regulation of DNA replication through Sld3-Dpb11 interaction is conserved from yeast to humans. In *Current biology : CB* 21 (13), pp. 1152–1157. DOI: 10.1016/j.cub.2011.05.057.

Bouwman, Peter; Jonkers, Jos (2012): The effects of deregulated DNA damage signalling on cancer chemotherapy response and resistance. In *Nat Rev Cancer* 12 (9), pp. 587–598. DOI: 10.1038/nrc3342.

Boveri, Theodor (1914): Zur Frage der Entstehung maligner Tumoren. Jena: Gustav Fischer. Available online at http://worldcatlibraries.org/wcpa/oclc/10215868.

Bradbury, E. M.; Inglis, R. J.; Matthews, H. R. (1974): Control of cell division by very lysine rich histone (F1) phosphorylation. In *Nature* 247 (5439), pp. 257–261. DOI: 10.1038/247257a0.

Branzei, Dana; Seki, Masayuki; Enomoto, Takemi (2004): Rad18/Rad5/Mms2-mediated polyubiquitination of PCNA is implicated in replication completion during replication stress. In *Genes to cells : devoted to molecular & cellular mechanisms* 9 (11), pp. 1031–1042. DOI: 10.1111/j.1365-2443.2004.00787.x.

Brasher, S. V.; Smith, B. O.; Fogh, R. H.; Nietlispach, D.; Thiru, A.; Nielsen, P. R. et al. (2000): The structure of mouse HP1 suggests a unique mode of single peptide recognition by the shadow chromo domain dimer. In *The EMBO journal* 19 (7), pp. 1587–1597. DOI: 10.1093/emboj/19.7.1587.

Bray, Freddie; Jemal, Ahmedin; Grey, Nathan; Ferlay, Jacques; Forman, David (2012): Global cancer transitions according to the Human Development Index (2008–2030): a population-based study. In *The Lancet. Oncology* 13 (8), pp. 790–801. DOI: 10.1016/S1470-2045(12)70211-5.

Brehm, A.; Miska, E. A.; McCance, D. J.; Reid, J. L.; Bannister, A. J.; Kouzarides, T. (1998): Retinoblastoma protein recruits histone deacetylase to repress transcription. In *Nature* 391 (6667), pp. 597–601. DOI: 10.1038/35404.

Brockdorff, Neil (2002): X-chromosome inactivation: closing in on proteins that bind Xist RNA. In *Trends in genetics : TIG* 18 (7), pp. 352–358. DOI: 10.1016/s0168-9525(02)02717-8.

Buchkovich, Karen; Duffy, Linda A.; Harlow, Ed (1989): The retinoblastoma protein is phosphorylated during specific phases of the cell cycle. In *Cell* 58 (6), pp. 1097–1105. DOI: 10.1016/0092-8674(89)90508-4.

Buckland, Robert J.; Watt, Danielle L.; Chittoor, Balasubramanyam; Nilsson, Anna Karin; Kunkel, Thomas A.; Chabes, Andrei (2014): Increased and imbalanced dNTP pools symmetrically promote both leading and lagging strand replication infidelity. In *PLoS genetics* 10 (12), e1004846. DOI: 10.1371/journal.pgen.1004846.

Byun, Tony S.; Pacek, Marcin; Yee, Muh-ching; Walter, Johannes C.; Cimprich, Karlene A. (2005): Functional uncoupling of MCM helicase and DNA polymerase

activities activates the ATR-dependent checkpoint. In *Genes & development* 19 (9), pp. 1040–1052. DOI: 10.1101/gad.1301205.

Caldecott, Keith W. (2008): Single-strand break repair and genetic disease. In *Nat Rev Genet* 9 (8), pp. 619–631. DOI: 10.1038/nrg2380.

Cancer today (2020). Available online at https://gco.iarc.fr/today/online-analysis-pie?v=2018&mode=cancer&mode_population=continents&population=900&populations=900&key=total&sex=0&cancer=39&type=0&statistic=5&prevalence=0&population_group=0&ages_group%5B%5D=0&ages_group%5B%5D=17&nb_items=7&group_cancer=1&include_nmsc=1&include_nmsc_other=1&half_pie=0&donut=0&population_group_globocan_id=, updated on 10/5/2020, checked on 10/5/2020.

Canzio, Daniele; Larson, Adam; Narlikar, Geeta J. (2014): Mechanisms of functional promiscuity by HP1 proteins. In *Trends in cell biology* 24 (6), pp. 377–386. DOI: 10.1016/j.tcb.2014.01.002.

Capalbo, Gianni; Dittmann, Klaus; Weiss, Christian; Reichert, Sebastian; Hausmann, Eva; Rödel, Claus; Rödel, Franz (2010): Radiation-induced survivin nuclear accumulation is linked to DNA damage repair. In *International journal of radiation oncology, biology, physics* 77 (1), pp. 226–234. DOI: 10.1016/j.ijrobp.2009.12.001.

Capalbo, Gianni; Rödel, Claus; Stauber, Roland H.; Knauer, Shirley K.; Bache, Matthias; Kappler, Matthias; Rödel, Franz (2007): The role of survivin for radiation therapy. Prognostic and predictive factor and therapeutic target. In *Strahlentherapie und Onkologie : Organ der Deutschen Rontgengesellschaft … [et al]* 183 (11), pp. 593–599. DOI: 10.1007/s00066-007-1800-4.

Carey, James F.; Schultz, Sharon J.; Sisson, Lisa; Fazzio, Thomas G.; Champoux, James J. (2003): DNA relaxation by human topoisomerase I occurs in the closed clamp conformation of the protein. In *Proceedings of the National Academy of Sciences of the United States of America* 100 (10), pp. 5640–5645. DOI: 10.1073/pnas.1031537100.

Carmena, Mar; Pinson, Xavier; Platani, Melpi; Salloum, Zeina; Xu, Zhenjie; Clark, Anthony et al. (2012a): The chromosomal passenger complex activates Polo kinase at centromeres. In *PLoS biology* 10 (1), e1001250. DOI: 10.1371/journal.pbio.1001250.

Carmena, Mar; Wheelock, Michael; Funabiki, Hironori; Earnshaw, William C. (2012b): The chromosomal passenger complex (CPC): from easy rider to the godfather of mitosis. In *Nat Rev Mol Cell Biol* 13 (12), pp. 789–803. DOI: 10.1038/nrm3474.

Carnero, A.; Hannon, G. J. (1998): The INK4 family of CDK inhibitors. In *Current topics in microbiology and immunology* 227, pp. 43–55. DOI: 10.1007/978-3-642-71941-7_3.

Carvalho, Ana; Carmena, Mar; Sambade, Clara; Earnshaw, William C.; Wheatley, Sally P. (2003): Survivin is required for stable checkpoint activation in taxol-treated HeLa cells. In *Journal of cell science* 116 (Pt 14), pp. 2987–2998. DOI: 10.1242/jcs.00612.

Casper, Anne M.; Nghiem, Paul; Arlt, Martin F.; Glover, Thomas W. (2002): ATR Regulates Fragile Site Stability. In *Cell* 111 (6), pp. 779–789. DOI: 10.1016/s0092-8674(02)01113-3.

Chaffer, Christine L.; Weinberg, Robert A. (2015): How does multistep tumorigenesis really proceed? In *Cancer discovery* 5 (1), pp. 22–24. DOI: 10.1158/2159-8290.CD-14-0788.

Chantalat, L.; Skoufias, D. A.; Kleman, J. P.; Jung, B.; Dideberg, O.; Margolis, R. L. (2000): Crystal structure of human survivin reveals a bow tie-shaped dimer with two unusual alpha-helical extensions. In *Molecular cell* 6 (1), pp. 183–189. Available online at https://pubmed.ncbi.nlm.nih.gov/10949039/.

Chapman, J. Ross; Taylor, Martin R. G.; Boulton, Simon J. (2012): Playing the end game: DNA double-strand break repair pathway choice. In *Molecular cell* 47 (4), pp. 497–510. DOI: 10.1016/j.molcel.2012.07.029.

Chatterjee, Nimrat; Walker, Graham C. (2017): Mechanisms of DNA damage, repair, and mutagenesis. In *Environmental and molecular mutagenesis* 58 (5), pp. 235–263. DOI: 10.1002/em.22087.

Chen, Helen H. W.; Kuo, Macus Tien (2017): Improving radiotherapy in cancer treatment: Promises and challenges. In *Oncotarget* 8 (37), pp. 62742–62758. DOI: 10.18632/oncotarget.18409.

Chen, Longchuan; Nievera, Christian J.; Lee, Alan Yueh-Luen; Wu, Xiaohua (2008a): Cell cycle-dependent complex formation of BRCA1.CtIP.MRN is important for DNA

double-strand break repair. In *The Journal of biological chemistry* 283 (12), pp. 7713–7720. DOI: 10.1074/jbc.M710245200.

Chen, Ping; Zhu, Jiang; Liu, Ding-Yi; Li, Hui-Yan; Xu, Nie; Hou, Mei (2014): Over-expression of survivin and VEGF in small-cell lung cancer may predict the poorer prognosis. In *Medical oncology (Northwood, London, England)* 31 (1), p. 775. DOI: 10.1007/s12032-013-0775-5.

Chen, Yih-wen; Cleaver, James E.; Hatahet, Zafer; Honkanen, Richard E.; Chang, Jang-Yang; Yen, Yun; Chou, Kai-ming (2008b): Human DNA polymerase eta activity and translocation is regulated by phosphorylation. In *Proceedings of the National Academy of Sciences of the United States of America* 105 (43), pp. 16578–16583. DOI: 10.1073/pnas.0808589105.

Cheng, Qiuying; Ling, Xiang; Haller, Andrew; Nakahara, Takahito; Yamanaka, Kentaro; Kita, Aya et al. (2012): Suppression of survivin promoter activity by YM155 involves disruption of Sp1-DNA interaction in the survivin core promoter. In *International journal of biochemistry and molecular biology* 3 (2), pp. 179–197. Available online at https://pubmed.ncbi.nlm.nih.gov/22773958/.

Chu, Youjun; Yao, Phil Y.; Wang, Wenwen; Wang, Dongmei; Wang, Zhikai; Zhang, Liangyu et al. (2011): Aurora B kinase activation requires survivin priming phosphorylation by PLK1. In *Journal of molecular cell biology* 3 (4), pp. 260–267. DOI: 10.1093/jmcb/mjq037.

Ciccia, Alberto; Bredemeyer, Andrea L.; Sowa, Mathew E.; Terret, Marie-Emilie; Jallepalli, Prasad V.; Harper, J. Wade; Elledge, Stephen J. (2009): The SIOD disorder protein SMARCAL1 is an RPA-interacting protein involved in replication fork restart. In *Genes & development* 23 (20), pp. 2415–2425. DOI: 10.1101/gad.1832309.

Ciccia, Alberto; Elledge, Stephen J. (2010): The DNA damage response: making it safe to play with knives. In *Molecular cell* 40 (2), pp. 179–204. DOI: 10.1016/j.molcel.2010.09.019.

Clausen, Anders R.; Zhang, Sufang; Burgers, Peter M.; Lee, Marietta Y.; Kunkel, Thomas A. (2013): Ribonucleotide incorporation, proofreading and bypass by human DNA polymerase δ. In *DNA repair* 12 (2), pp. 121–127. DOI: 10.1016/j.dnarep.2012.11.006.

Colnaghi, Rita; Connell, Claire M.; Barrett, Rachel M. A.; Wheatley, Sally P. (2006): Separating the anti-apoptotic and mitotic roles of survivin. In *The Journal of biological chemistry* 281 (44), pp. 33450–33456. DOI: 10.1074/jbc.C600164200.

Colnaghi, Rita; Wheatley, Sally P. (2010): Liaisons between survivin and Plk1 during cell division and cell death. In *J. Biol. Chem.* 285 (29), pp. 22592–22604. DOI: 10.1074/jbc.M109.065003.

Comings, D. E. (1973): A general theory of carcinogenesis. In *Proceedings of the National Academy of Sciences of the United States of America* 70 (12), pp. 3324–3328. DOI: 10.1073/pnas.70.12.3324.

Connell, Claire M.; Colnaghi, Rita; Wheatley, Sally P. (2008): Nuclear survivin has reduced stability and is not cytoprotective. In *The Journal of biological chemistry* 283 (6), pp. 3289–3296. DOI: 10.1074/jbc.M704461200.

Cordonnier, A. M.; Lehmann, A. R.; Fuchs, R. P. (1999): Impaired translesion synthesis in xeroderma pigmentosum variant extracts. In *Molecular and cellular biology* 19 (3), pp. 2206–2211. DOI: 10.1128/mcb.19.3.2206.

Costantini, Silvia; Woodbine, Lisa; Andreoli, Lucia; Jeggo, Penny A.; Vindigni, Alessandro (2007): Interaction of the Ku heterodimer with the DNA ligase IV/Xrcc4 complex and its regulation by DNA-PK. In *DNA repair* 6 (6), pp. 712–722. DOI: 10.1016/j.dnarep.2006.12.007.

Costanzo, Vincenzo; Robertson, Kirsten; Ying, Carol Y.; Kim, Edward; Avvedimento, Enrico; Gottesman, Max et al. (2000): Reconstitution of an ATM-Dependent Checkpoint that Inhibits Chromosomal DNA Replication following DNA Damage. In *Molecular cell* 6 (3), pp. 649–659. DOI: 10.1016/s1097-2765(00)00063-0.

Cottarel, Jessica; Frit, Philippe; Bombarde, Oriane; Salles, Bernard; Négrel, Aurélie; Bernard, Stéphanie et al. (2013): A noncatalytic function of the ligation complex during nonhomologous end joining. In *The Journal of cell biology* 200 (2), pp. 173–186. DOI: 10.1083/jcb.201203128.

Coumar, Mohane Selvaraj; Tsai, Fang-Ying; Kanwar, Jagat Rakesh; Sarvagalla, Sailu; Cheung, Chun Hei Antonio (2013): Treat cancers by targeting survivin: just a dream or future reality? In *Cancer Treatment Reviews* 39 (7), pp. 802–811. DOI: 10.1016/j.ctrv.2013.02.002.

Cowieson, Nathan P.; Partridge, Janet F.; Allshire, Robin C.; McLaughlin, Paul J. (2000): Dimerisation of a chromo shadow domain and distinctions from the chromodomain as revealed by structural analysis. In *Current biology : CB* 10 (9), pp. 517–525. DOI: 10.1016/s0960-9822(00)00467-x.

Craig, Jeffrey M. (2005): Heterochromatin--many flavours, common themes. In *BioEssays* 27 (1), pp. 17–28. DOI: 10.1002/bies.20145.

Cremer, Thomas; Cremer, Marion; Dietzel, Steffen; Müller, Stefan; Solovei, Irina; Fakan, Stanislav (2006): Chromosome territories--a functional nuclear landscape. In *Current opinion in cell biology* 18 (3), pp. 307–316. DOI: 10.1016/j.ceb.2006.04.007.

Croce, Carlo M. (2008): Oncogenes and cancer. In *The New England journal of medicine* 358 (5), pp. 502–511. DOI: 10.1056/NEJMra072367.

Danaei, Goodarz; Vander Hoorn, Stephen; Lopez, Alan D.; Murray, Christopher J. L.; Ezzati, Majid (2005): Causes of cancer in the world: comparative risk assessment of nine behavioural and environmental risk factors. In *Lancet (London, England)* 366 (9499), pp. 1784–1793. DOI: 10.1016/S0140-6736(05)67725-2.

Dang, Chi V. (2012): MYC on the path to cancer. In *Cell* 149 (1), pp. 22–35. DOI: 10.1016/j.cell.2012.03.003.

Deegan, Tom D.; Yeeles, Joseph Tp; Diffley, John Fx (2016): Phosphopeptide binding by Sld3 links Dbf4-dependent kinase to MCM replicative helicase activation. In *The EMBO journal* 35 (9), pp. 961–973. DOI: 10.15252/embj.201593552.

Delacour-Larose, Marlène; Thi, My-Nhung Hoang; Dimitrov, Stefan; Molla, Annie (2007): Role of survivin phosphorylation by aurora B in mitosis. In *Cell cycle (Georgetown, Tex.)* 6 (15), pp. 1878–1885. DOI: 10.4161/cc.6.15.4482.

DeLuca, Jennifer G.; Musacchio, Andrea (2012): Structural organization of the kinetochore-microtubule interface. In *Current opinion in cell biology* 24 (1), pp. 48–56. DOI: 10.1016/j.ceb.2011.11.003.

Deveraux, Q. L.; Reed, J. C. (1999): IAP family proteins--suppressors of apoptosis. In *Genes & development* 13 (3), pp. 239–252. DOI: 10.1101/gad.13.3.239.

Dewar, James M.; Low, Emily; Mann, Matthias; Räschle, Markus; Walter, Johannes C. (2017): CRL2Lrr1 promotes unloading of the vertebrate replisome from chromatin during replication termination. In *Genes & development* 31 (3), pp. 275–290. DOI: 10.1101/gad.291799.116.

Dewar, James M.; Walter, Johannes C. (2017): Mechanisms of DNA replication termination. In *Nat Rev Mol Cell Biol* 18 (8), pp. 507–516. DOI: 10.1038/nrm.2017.42.

Dheekollu, Jayaraju; Wiedmer, Andreas; Hayden, James; Speicher, David; Gotter, Anthony L.; Yen, Tim; Lieberman, Paul M. (2011): Timeless links replication termination to mitotic kinase activation. In *PloS one* 6 (5), e19596. DOI: 10.1371/journal.pone.0019596.

Dillon, Niall (2004): Heterochromatin structure and function. In *Biology of the Cell* 96 (8), pp. 631–637. DOI: 10.1016/j.biolcel.2004.06.003.

Dimitrova, D. S.; Gilbert, D. M. (2000): Temporally coordinated assembly and disassembly of replication factories in the absence of DNA synthesis. In *Nature cell biology* 2 (10), pp. 686–694. DOI: 10.1038/35036309.

Dobrynin, Grzegorz; Popp, Oliver; Romer, Tina; Bremer, Sebastian; Schmitz, Michael H. A.; Gerlich, Daniel W.; Meyer, Hemmo (2011): Cdc48/p97-Ufd1-Npl4 antagonizes Aurora B during chromosome segregation in HeLa cells. In *J Cell Sci* 124 (Pt 9), pp. 1571–1580. DOI: 10.1242/jcs.069500.

Douglas, Max E.; Ali, Ferdos Abid; Costa, Alessandro; Diffley, John F. X. (2018): The mechanism of eukaryotic CMG helicase activation. In *Nature* 555 (7695), pp. 265–268. DOI: 10.1038/nature25787.

Durkin, Sandra G.; Glover, Thomas W. (2007): Chromosome fragile sites. In *Annual review of genetics* 41, pp. 169–192. DOI: 10.1146/annurev.genet.41.042007.165900.

Earnshaw, W. C.; Allshire, R. C.; Black, B. E.; Bloom, K.; Brinkley, B. R.; Brown, W. et al. (2013): Esperanto for histones: CENP-A, not CenH3, is the centromeric histone H3 variant. In *Chromosome research : an international journal on the molecular, supramolecular and evolutionary aspects of chromosome biology* 21 (2), pp. 101–106. DOI: 10.1007/s10577-013-9347-y.

Earnshaw, W. C.; Rothfield, N. (1985): Identification of a family of human centromere proteins using autoimmune sera from patients with scleroderma. In *Chromosoma* 91 (3-4), pp. 313–321. DOI: 10.1007/bf00328227.

Engels, K.; Knauer, S. K.; Metzler, D.; Simf, C.; Struschka, O.; Bier, C. et al. (2007): Dynamic intracellular survivin in oral squamous cell carcinoma: underlying molecular mechanism and potential as an early prognostic marker. In *The Journal of pathology* 211 (5), pp. 532–540. DOI: 10.1002/path.2134.

Evrin, Cecile; Clarke, Pippa; Zech, Juergen; Lurz, Rudi; Sun, Jingchuan; Uhle, Stefan et al. (2009): A double-hexameric MCM2-7 complex is loaded onto origin DNA during licensing of eukaryotic DNA replication. In *Proceedings of the National Academy of Sciences of the United States of America* 106 (48), pp. 20240–20245. DOI: 10.1073/pnas.0911500106.

Fan, Jie; Pavletich, Nikola P. (2012): Structure and conformational change of a replication protein A heterotrimer bound to ssDNA. In *Genes & development* 26 (20), pp. 2337–2347. DOI: 10.1101/gad.194787.112.

Fang, G.; Yu, H.; Kirschner, M. W. (1998): The checkpoint protein MAD2 and the mitotic regulator CDC20 form a ternary complex with the anaphase-promoting complex to control anaphase initiation. In *Genes & development* 12 (12), pp. 1871–1883. DOI: 10.1101/gad.12.12.1871.

Fanning, Ellen; Klimovich, Vitaly; Nager, Andrew R. (2006): A dynamic model for replication protein A (RPA) function in DNA processing pathways. In *Nucleic acids research* 34 (15), pp. 4126–4137. DOI: 10.1093/nar/gkl550.

Faragher, Alison J.; Sun, Xiao-Ming; Butterworth, Michael; Harper, Nick; Mulheran, Mike; Ruchaud, Sandrine et al. (2007): Death receptor-induced apoptosis reveals a novel interplay between the chromosomal passenger complex and CENP-C during interphase. In *Molecular biology of the cell* 18 (4), pp. 1337–1347. DOI: 10.1091/mbc.e06-05-0409.

Fetz, Verena; Knauer, Shirley K.; Bier, Carolin; Kries, Jens Peter von; Stauber, Roland H. (2009): Translocation Biosensors - Cellular System Integrators to Dissect CRM1-Dependent Nuclear Export by Chemicogenomics. In *Sensors (Basel, Switzerland)* 9 (7), pp. 5423–5445. DOI: 10.3390/s90705423.

Fidler, Miranda M.; Soerjomataram, Isabelle; Bray, Freddie (2016): A global view on cancer incidence and national levels of the human development index. In *International journal of cancer* 139 (11), pp. 2436–2446. DOI: 10.1002/ijc.30382.

Fragkos, Michalis; Ganier, Olivier; Coulombe, Philippe; Méchali, Marcel (2015): DNA replication origin activation in space and time. In *Nat Rev Mol Cell Biol* 16 (6), pp. 360–374. DOI: 10.1038/nrm4002.

Franz, André; Orth, Michael; Pirson, Paul A.; Sonneville, Remi; Blow, J. Julian; Gartner, Anton et al. (2011): CDC-48/p97 coordinates CDT-1 degradation with GINS

chromatin dissociation to ensure faithful DNA replication. In *Molecular cell* 44 (1), pp. 85–96. DOI: 10.1016/j.molcel.2011.08.028.

Friedberg, Errol C. (2003): DNA damage and repair. In *Nature* 421 (6921), pp. 436–440. DOI: 10.1038/nature01408.

Fu, Dragony; Calvo, Jennifer A.; Samson, Leona D. (2012): Balancing repair and tolerance of DNA damage caused by alkylating agents. In *Nat Rev Cancer* 12 (2), pp. 104–120. DOI: 10.1038/nrc3185.

Fukuda, S.; Hoggatt, J.; Singh, P.; Abe, M.; Speth, J. M.; Hu, P. et al. (2015): Survivin modulates genes with divergent molecular functions and regulates proliferation of hematopoietic stem cells through Evi-1. In *Leukemia* 29 (2), pp. 433–440. DOI: 10.1038/leu.2014.183.

Fyodorov, Dmitry V.; Zhou, Bing-Rui; Skoultchi, Arthur I.; Bai, Yawen (2018): Emerging roles of linker histones in regulating chromatin structure and function. In *Nature reviews. Molecular cell biology* 19 (3), pp. 192–206. DOI: 10.1038/nrm.2017.94.

Gaillard, Pierre-Henri L.; Martini, Emmanuelle M.-D; Kaufman, Paul D.; Stillman, Bruce; Moustacchi, Ethel; Almouzni, Geneviève (1996): Chromatin Assembly Coupled to DNA Repair: A New Role for Chromatin Assembly Factor I. In *Cell* 86 (6), pp. 887–896. DOI: 10.1016/s0092-8674(00)80164-6.

Garg, Himani; Suri, Prerna; Gupta, Jagdish C.; Talwar, G. P.; Dubey, Shweta (2016): Survivin: a unique target for tumor therapy. In *Cancer cell international* 16, p. 49. DOI: 10.1186/s12935-016-0326-1.

Gassmann, Reto; Carvalho, Ana; Henzing, Alexander J.; Ruchaud, Sandrine; Hudson, Damien F.; Honda, Reiko et al. (2004): Borealin: a novel chromosomal passenger required for stability of the bipolar mitotic spindle. In *J Cell Biol* 166 (2), pp. 179–191. DOI: 10.1083/jcb.200404001.

Ge, Xin Quan; Blow, J. Julian (2010): Chk1 inhibits replication factory activation but allows dormant origin firing in existing factories. In *The Journal of cell biology* 191 (7), pp. 1285–1297. DOI: 10.1083/jcb.201007074.

Ghosal, Gargi; Chen, Junjie (2013): DNA damage tolerance: a double-edged sword guarding the genome. In *Translational cancer research* 2 (3), pp. 107–129. DOI: 10.3978/j.issn.2218-676X.2013.04.01.

Gilljam, Karin M.; Feyzi, Emadoldin; Aas, Per A.; Sousa, Mirta M. L.; Müller, Rebekka; Vågbø, Cathrine B. et al. (2009): Identification of a novel, widespread, and functionally important PCNA-binding motif. In *The Journal of cell biology* 186 (5), pp. 645–654. DOI: 10.1083/jcb.200903138.

Göhler, Thomas; Sabbioneda, Simone; Green, Catherine M.; Lehmann, Alan R. (2011): ATR-mediated phosphorylation of DNA polymerase η is needed for efficient recovery from UV damage. In *The Journal of cell biology* 192 (2), pp. 219–227. DOI: 10.1083/jcb.201008076.

Goto, Hidemasa; Yasui, Yoshihiro; Kawajiri, Aie; Nigg, Erich A.; Terada, Yasuhiko; Tatsuka, Masaaki et al. (2003): Aurora-B regulates the cleavage furrow-specific vimentin phosphorylation in the cytokinetic process. In *The Journal of biological chemistry* 278 (10), pp. 8526–8530. DOI: 10.1074/jbc.M210892200.

Gottlieb, Tanya M.; Jackson, Stephen P. (1993): The DNA-dependent protein kinase: Requirement for DNA ends and association with Ku antigen. In *Cell* 72 (1), pp. 131–142. DOI: 10.1016/0092-8674(93)90057-w.

Grallert, Beáta; Boye, Erik (2008): The multiple facets of the intra-S checkpoint. In *Cell cycle (Georgetown, Tex.)* 7 (15), pp. 2315–2320. DOI: 10.4161/cc.6389.

Green, Brian M.; Finn, Kenneth J.; Li, Joachim J. (2010): Loss of DNA replication control is a potent inducer of gene amplification. In *Science* 329 (5994), pp. 943–946. DOI: 10.1126/science.1190966.

Grewal, Shiv I. S.; Jia, Songtao (2007): Heterochromatin revisited. In *Nature reviews. Genetics* 8 (1), pp. 35–46. DOI: 10.1038/nrg2008.

Grundy, Gabrielle J.; Rulten, Stuart L.; Zeng, Zhihong; Arribas-Bosacoma, Raquel; Iles, Natasha; Manley, Katie et al. (2013): APLF promotes the assembly and activity of non-homologous end joining protein complexes. In *The EMBO journal* 32 (1), pp. 112–125. DOI: 10.1038/emboj.2012.304.

Gu, Jiafeng; Lu, Haihui; Tippin, Brigette; Shimazaki, Noriko; Goodman, Myron F.; Lieber, Michael R. (2007): XRCC4:DNA ligase IV can ligate incompatible DNA ends and can ligate across gaps. In *The EMBO journal* 26 (4), pp. 1010–1023. DOI: 10.1038/sj.emboj.7601559.

Gully, Chris P.; Velazquez-Torres, Guermarie; Shin, Ji-Hyun; Fuentes-Mattei, Enrique; Wang, Edward; Carlock, Colin et al. (2012): Aurora B kinase phosphorylates

and instigates degradation of p53. In *Proceedings of the National Academy of Sciences of the United States of America* 109 (24), E1513-22. DOI: 10.1073/pnas.1110287109.

Hahn, William C.; Weinberg, Robert A. (2002): Rules for making human tumor cells. In *The New England journal of medicine* 347 (20), pp. 1593–1603. DOI: 10.1056/NEJMra021902.

Hammel, Michal; Rey, Martial; Yu, Yaping; Mani, Rajam S.; Classen, Scott; Liu, Mona et al. (2011): XRCC4 protein interactions with XRCC4-like factor (XLF) create an extended grooved scaffold for DNA ligation and double strand break repair. In *The Journal of biological chemistry* 286 (37), pp. 32638–32650. DOI: 10.1074/jbc.M111.272641.

Hanahan, Douglas; Weinberg, Robert A. (2000): The Hallmarks of Cancer. In *Cell* 100 (1), pp. 57–70. DOI: 10.1016/s0092-8674(00)81683-9.

Hanahan, Douglas; Weinberg, Robert A. (2011): Hallmarks of cancer: the next generation. In *Cell* 144 (5), pp. 646–674. DOI: 10.1016/j.cell.2011.02.013.

Hansemann, David (1890): Ueber asymmetrische Zelltheilung in Epithelkrebsen und deren biologische Bedeutung. In *Archiv f. pathol. Anat.* 119 (2), pp. 299–326. DOI: 10.1007/BF01882039.

Haracska, Lajos; Torres-Ramos, Carlos A.; Johnson, Robert E.; Prakash, Satya; Prakash, Louise (2004): Opposing effects of ubiquitin conjugation and SUMO modification of PCNA on replicational bypass of DNA lesions in Saccharomyces cerevisiae. In *Molecular and cellular biology* 24 (10), pp. 4267–4274. DOI: 10.1128/mcb.24.10.4267-4274.2004.

Harper, J. Wade; Elledge, Stephen J. (2007): The DNA damage response: ten years after. In *Molecular cell* 28 (5), pp. 739–745. DOI: 10.1016/j.molcel.2007.11.015.

Hauf, Silke; Cole, Richard W.; LaTerra, Sabrina; Zimmer, Christine; Schnapp, Gisela; Walter, Rainer et al. (2003): The small molecule Hesperadin reveals a role for Aurora B in correcting kinetochore-microtubule attachment and in maintaining the spindle assembly checkpoint. In *J Cell Biol* 161 (2), pp. 281–294. DOI: 10.1083/jcb.200208092.

Hayashi-Takanaka, Yoko; Yamagata, Kazuo; Nozaki, Naohito; Kimura, Hiroshi (2009): Visualizing histone modifications in living cells: spatiotemporal dynamics of

H3 phosphorylation during interphase. In *The Journal of cell biology* 187 (6), pp. 781–790. DOI: 10.1083/jcb.200904137.

Heller, Ryan C.; Kang, Sukhyun; Lam, Wendy M.; Chen, Shuyan; Chan, Clara S.; Bell, Stephen P. (2011): Eukaryotic origin-dependent DNA replication in vitro reveals sequential action of DDK and S-CDK kinases. In *Cell* 146 (1), pp. 80–91. DOI: 10.1016/j.cell.2011.06.012.

Helton, E. Scott; Chen, Xinbin (2007): p53 modulation of the DNA damage response. In *Journal of Cellular Biochemistry* 100 (4), pp. 883–896. DOI: 10.1002/jcb.21091.

Hengst, L.; Reed, S. I. (1998): Inhibitors of the Cip/Kip family. In *Current topics in microbiology and immunology* 227, pp. 25–41. DOI: 10.1007/978-3-642-71941-7_2.

Herrup, Karl; Yang, Yan (2007): Cell cycle regulation in the postmitotic neuron: oxymoron or new biology? In *Nature reviews. Neuroscience* 8 (5), pp. 368–378. DOI: 10.1038/nrn2124.

Hirota, Toru; Lipp, Jesse J.; Toh, Ban-Hock; Peters, Jan-Michael (2005): Histone H3 serine 10 phosphorylation by Aurora B causes HP1 dissociation from heterochromatin. In *Nature* 438 (7071), pp. 1176–1180. DOI: 10.1038/nature04254.

Hoeijmakers, J. H. (2001): Genome maintenance mechanisms for preventing cancer. In *Nature* 411 (6835), pp. 366–374. DOI: 10.1038/35077232.

Hoffman, William H.; Biade, Siham; Zilfou, Jack T.; Chen, Jiandong; Murphy, Maureen (2002): Transcriptional repression of the anti-apoptotic survivin gene by wild type p53. In *The Journal of biological chemistry* 277 (5), pp. 3247–3257. DOI: 10.1074/jbc.M106643200.

Holloman, William K. (2011): Unraveling the mechanism of BRCA2 in homologous recombination. In *Nature structural & molecular biology* 18 (7), pp. 748–754. DOI: 10.1038/nsmb.2096.

Honda, Reiko; Körner, Roman; Nigg, Erich A. (2003): Exploring the functional interactions between Aurora B, INCENP, and survivin in mitosis. In *Molecular biology of the cell* 14 (8), pp. 3325–3341. DOI: 10.1091/mbc.e02-11-0769.

Huang, Chih-Yang; Ju, Da-Tong; Chang, Chih-Fen; Muralidhar Reddy, P.; Velmurugan, Bharath Kumar (2017): A review on the effects of current chemotherapy drugs and natural agents in treating non-small cell lung cancer. In *BioMedicine* 7 (4), p. 23. DOI: 10.1051/bmdcn/2017070423.

Huang, L. C.; Clarkin, K. C.; Wahl, G. M. (1996): Sensitivity and selectivity of the DNA damage sensor responsible for activating p53-dependent G1 arrest. In *Proceedings of the National Academy of Sciences of the United States of America* 93 (10), pp. 4827–4832. DOI: 10.1073/pnas.93.10.4827.

Huebner, R. J.; Todaro, G. J. (1969): Oncogenes of RNA tumor viruses as determinants of cancer. In *Proceedings of the National Academy of Sciences of the United States of America* 64 (3), pp. 1087–1094. DOI: 10.1073/pnas.64.3.1087.

Huisinga, Kathryn L.; Brower-Toland, Brent; Elgin, Sarah C. R. (2006): The contradictory definitions of heterochromatin: transcription and silencing. In *Chromosoma* 115 (2), pp. 110–122. DOI: 10.1007/s00412-006-0052-x.

Hümmer, Stefan; Mayer, Thomas U. (2009): Cdk1 negatively regulates midzone localization of the mitotic kinesin Mklp2 and the chromosomal passenger complex. In *Current biology : CB* 19 (7), pp. 607–612. DOI: 10.1016/j.cub.2009.02.046.

Iliakis, George; Wang, Ya; Guan, Jun; Wang, Huichen (2003): DNA damage checkpoint control in cells exposed to ionizing radiation. In *Oncogene* 22 (37), pp. 5834–5847. DOI: 10.1038/sj.onc.1206682.

Ilves, Ivar; Petojevic, Tatjana; Pesavento, James J.; Botchan, Michael R. (2010): Activation of the MCM2-7 helicase by association with Cdc45 and GINS proteins. In *Molecular cell* 37 (2), pp. 247–258. DOI: 10.1016/j.molcel.2009.12.030.

Im, Jun-Sub; Ki, Sang-Hee; Farina, Andrea; Jung, Dong-Soo; Hurwitz, Jerard; Lee, Joon-Kyu (2009): Assembly of the Cdc45-Mcm2-7-GINS complex in human cells requires the Ctf4/And-1, RecQL4, and Mcm10 proteins. In *Proceedings of the National Academy of Sciences of the United States of America* 106 (37), pp. 15628–15632. DOI: 10.1073/pnas.0908039106.

Jackson, Stephen P.; Bartek, Jiri (2009): The DNA-damage response in human biology and disease. In *Nature* 461 (7267), pp. 1071–1078. DOI: 10.1038/nature08467.

Jacobs, Steven A.; Khorasanizadeh, Sepideh (2002): Structure of HP1 chromodomain bound to a lysine 9-methylated histone H3 tail. In *Science* 295 (5562), pp. 2080–2083. DOI: 10.1126/science.1069473.

Jenuwein, T.; Allis, C. D. (2001): Translating the histone code. In *Science (New York, N.Y.)* 293 (5532), pp. 1074–1080. DOI: 10.1126/science.1063127.

Jeyaprakash, A. Arockia; Basquin, Claire; Jayachandran, Uma; Conti, Elena (2011): Structural basis for the recognition of phosphorylated histone h3 by the survivin subunit of the chromosomal passenger complex. In *Structure (London, England : 1993)* 19 (11), pp. 1625–1634. DOI: 10.1016/j.str.2011.09.002.

Jeyaprakash, A. Arockia; Klein, Ulf R.; Lindner, Doris; Ebert, Judith; Nigg, Erich A.; Conti, Elena (2007): Structure of a Survivin-Borealin-INCENP core complex reveals how chromosomal passengers travel together. In *Cell* 131 (2), pp. 271–285. DOI: 10.1016/j.cell.2007.07.045.

Jiang, Yuying; Saavedra, Harold I.; Holloway, Michael P.; Leone, Gustavo; Altura, Rachel A. (2004): Aberrant regulation of survivin by the RB/E2F family of proteins. In *The Journal of biological chemistry* 279 (39), pp. 40511–40520. DOI: 10.1074/jbc.M404496200.

Johnson, R. D.; Jasin, M. (2000): Sister chromatid gene conversion is a prominent double-strand break repair pathway in mammalian cells. In *The EMBO journal* 19 (13), pp. 3398–3407. DOI: 10.1093/emboj/19.13.3398.

Johnson, R. E.; Washington, M. T.; Haracska, L.; Prakash, S.; Prakash, L. (2000): Eukaryotic polymerases iota and zeta act sequentially to bypass DNA lesions. In *Nature* 406 (6799), pp. 1015–1019. DOI: 10.1038/35023030.

Jones, Rebecca M.; Petermann, Eva (2012): Replication fork dynamics and the DNA damage response. In *Biochem J* 443 (1), pp. 13–26. DOI: 10.1042/BJ20112100.

Jossen, Rachel; Bermejo, Rodrigo (2013): The DNA damage checkpoint response to replication stress: A Game of Forks. In *Frontiers in genetics* 4, p. 26. DOI: 10.3389/fgene.2013.00026.

Kang, Jungseog; Chaudhary, Jaideep; Dong, Hui; Kim, Soonjoung; Brautigam, Chad A.; Yu, Hongtao (2011): Mitotic centromeric targeting of HP1 and its binding to Sgo1 are dispensable for sister-chromatid cohesion in human cells. In *Molecular biology of the cell* 22 (8), pp. 1181–1190. DOI: 10.1091/mbc.E11-01-0009.

Kannouche, Patricia L.; Wing, Jonathan; Lehmann, Alan R. (2004): Interaction of Human DNA Polymerase η with Monoubiquitinated PCNA. In *Molecular cell* 14 (4), pp. 491–500. DOI: 10.1016/s1097-2765(04)00259-x.

Kastan, Michael B.; Zhan, Qimin; El-Deiry, Wafik S.; Carrier, France; Jacks, Tyler; Walsh, William V. et al. (1992): A mammalian cell cycle checkpoint pathway utilizing

p53 and GADD45 is defective in ataxia-telangiectasia. In *Cell* 71 (4), pp. 587–597. DOI: 10.1016/0092-8674(92)90593-2.

Kato, J.; Matsushime, H.; Hiebert, S. W.; Ewen, M. E.; Sherr, C. J. (1993): Direct binding of cyclin D to the retinoblastoma gene product (pRb) and pRb phosphorylation by the cyclin D-dependent kinase CDK4. In *Genes & development* 7 (3), pp. 331–342. DOI: 10.1101/gad.7.3.331.

Kaufman, Paul D.; Kobayashi, Ryuji; Kessler, Naama; Stillman, Bruce (1995): The p150 and p60 subunits of chromatin assemblyfactor I: A molecular link between newly synthesized histories and DNA replication. In *Cell* 81 (7), pp. 1105–1114. DOI: 10.1016/s0092-8674(05)80015-7.

Kelly, Alexander E.; Ghenoiu, Cristina; Xue, John Z.; Zierhut, Christian; Kimura, Hiroshi; Funabiki, Hironori (2010): Survivin reads phosphorylated histone H3 threonine 3 to activate the mitotic kinase Aurora B. In *Science* 330 (6001), pp. 235–239. DOI: 10.1126/science.1189505.

Kelly, Kathleen; Cochran, Brent H.; Stiles, Charles D.; Leder, Philip (1983): Cell-specific regulation of the c-myc gene by lymphocyte mitogens and platelet-derived growth factor. In *Cell* 35 (3), pp. 603–610. DOI: 10.1016/0092-8674(83)90092-2.

Khanna, K. K.; Jackson, S. P. (2001): DNA double-strand breaks: signaling, repair and the cancer connection. In *Nature genetics* 27 (3), pp. 247–254. DOI: 10.1038/85798.

Kim, Seong-Tae; Xu, Bo; Kastan, Michael B. (2002): Involvement of the cohesin protein, Smc1, in Atm-dependent and independent responses to DNA damage. In *Genes & development* 16 (5), pp. 560–570. DOI: 10.1101/gad.970602.

Kitagawa, Risa; Bakkenist, Christopher J.; McKinnon, Peter J.; Kastan, Michael B. (2004): Phosphorylation of SMC1 is a critical downstream event in the ATM-NBS1-BRCA1 pathway. In *Genes & development* 18 (12), pp. 1423–1438. DOI: 10.1101/gad.1200304.

Klein, Ulf R.; Haindl, Markus; Nigg, Erich A.; Muller, Stefan (2009): RanBP2 and SENP3 function in a mitotic SUMO2/3 conjugation-deconjugation cycle on Borealin. In *Molecular biology of the cell* 20 (1), pp. 410–418. DOI: 10.1091/mbc.e08-05-0511.

Klein, Ulf R.; Nigg, Erich A.; Gruneberg, Ulrike (2006): Centromere targeting of the chromosomal passenger complex requires a ternary subcomplex of Borealin,

Survivin, and the N-terminal domain of INCENP. In *Molecular biology of the cell* 17 (6), pp. 2547–2558. DOI: 10.1091/mbc.E05-12-1133.

Knauer, Shirley K.; Bier, Carolin; Habtemichael, Negusse; Stauber, Roland H. (2006): The Survivin-Crm1 interaction is essential for chromosomal passenger complex localization and function. In *EMBO Reports* 7 (12), pp. 1259–1265. DOI: 10.1038/sj.embor.7400824.

Knauer, Shirley K.; Krämer, Oliver H.; Knösel, Thomas; Engels, Knut; Rödel, Franz; Kovács, Adorján F. et al. (2007a): Nuclear export is essential for the tumor-promoting activity of survivin. In *FASEB journal : official publication of the Federation of American Societies for Experimental Biology* 21 (1), pp. 207–216. DOI: 10.1096/fj.06-5741com.

Knauer, Shirley K.; Mann, Wolf; Stauber, Roland H. (2007b): Survivin's dual role: an export's view. In *Cell cycle (Georgetown, Tex.)* 6 (5), pp. 518–521. DOI: 10.4161/cc.6.5.3902.

Knudson, A. G. (1971): Mutation and cancer: statistical study of retinoblastoma. In *Proceedings of the National Academy of Sciences of the United States of America* 68 (4), pp. 820–823. DOI: 10.1073/pnas.68.4.820.

Koch, André; Krug, Karsten; Pengelley, Stuart; Macek, Boris; Hauf, Silke (2011): Mitotic substrates of the kinase aurora with roles in chromatin regulation identified through quantitative phosphoproteomics of fission yeast. In *Science signaling* 4 (179), rs6. DOI: 10.1126/scisignal.2001588.

Kornberg, R. D. (1977): Structure of chromatin. In *Annual review of biochemistry* 46, pp. 931–954. DOI: 10.1146/annurev.bi.46.070177.004435.

Kouzarides, Tony (2007): Chromatin modifications and their function. In *Cell* 128 (4), pp. 693–705. DOI: 10.1016/j.cell.2007.02.005.

Kumagai, Akiko; Shevchenko, Anna; Shevchenko, Andrej; Dunphy, William G. (2010): Treslin collaborates with TopBP1 in triggering the initiation of DNA replication. In *Cell* 140 (3), pp. 349–359. DOI: 10.1016/j.cell.2009.12.049.

Kumagai, Akiko; Shevchenko, Anna; Shevchenko, Andrej; Dunphy, William G. (2011): Direct regulation of Treslin by cyclin-dependent kinase is essential for the onset of DNA replication. In *The Journal of cell biology* 193 (6), pp. 995–1007. DOI: 10.1083/jcb.201102003.

Kumar, Dinesh; Abdulovic, Amy L.; Viberg, Jörgen; Nilsson, Anna Karin; Kunkel, Thomas A.; Chabes, Andrei (2011): Mechanisms of mutagenesis in vivo due to imbalanced dNTP pools. In *Nucleic acids research* 39 (4), pp. 1360–1371. DOI: 10.1093/nar/gkq829.

Kunkel, T. A. (2009): Evolving views of DNA replication (in)fidelity. In *Cold Spring Harbor symposia on quantitative biology* 74, pp. 91–101. DOI: 10.1101/sqb.2009.74.027.

Kunkel, Thomas A. (2004): DNA replication fidelity. In *The Journal of biological chemistry* 279 (17), pp. 16895–16898. DOI: 10.1074/jbc.R400006200.

Kunkel, Thomas A.; Burgers, Peter M. (2008): Dividing the workload at a eukaryotic replication fork. In *Trends in cell biology* 18 (11), pp. 521–527. DOI: 10.1016/j.tcb.2008.08.005.

Kwon, So Hee; Workman, Jerry L. (2011): The changing faces of HP1: From heterochromatin formation and gene silencing to euchromatic gene expression: HP1 acts as a positive regulator of transcription. In *BioEssays* 33 (4), pp. 280–289. DOI: 10.1002/bies.201000138.

Lachner, M.; O'Carroll, D.; Rea, S.; Mechtler, K.; Jenuwein, T. (2001): Methylation of histone H3 lysine 9 creates a binding site for HP1 proteins. In *Nature* 410 (6824), pp. 116–120. DOI: 10.1038/35065132.

Laemmli, U. K. (1970): Cleavage of structural proteins during the assembly of the head of bacteriophage T4. In *Nature* 227 (5259), pp. 680–685. DOI: 10.1038/227680a0.

Lampson, Michael A.; Cheeseman, Iain M. (2011): Sensing centromere tension: Aurora B and the regulation of kinetochore function. In *Trends in cell biology* 21 (3), pp. 133–140. DOI: 10.1016/j.tcb.2010.10.007.

Lavine, S. D.; Petrovich, Z.; Cohen-Gadol, A. A.; Masri, L. S.; Morton, D. L.; O'Day, S. J. et al. (1999): Gamma knife radiosurgery for metastatic melanoma: an analysis of survival, outcome, and complications. In *Neurosurgery* 44 (1), 59-64; discussion 64-6. DOI: 10.1097/00006123-199901000-00031.

Lee, M. H.; Reynisdóttir, I.; Massagué, J. (1995): Cloning of p57KIP2, a cyclin-dependent kinase inhibitor with unique domain structure and tissue distribution. In *Genes & development* 9 (6), pp. 639–649. DOI: 10.1101/gad.9.6.639.

Lengauer, C.; Kinzler, K. W.; Vogelstein, B. (1998): Genetic instabilities in human cancers. In *Nature* 396 (6712), pp. 643–649. DOI: 10.1038/25292.

Lens, Susanne M. A.; Wolthuis, Rob M. F.; Klompmaker, Rob; Kauw, Jos; Agami, Reuven; Brummelkamp, Thijn et al. (2003): Survivin is required for a sustained spindle checkpoint arrest in response to lack of tension. In *The EMBO journal* 22 (12), pp. 2934–2947. DOI: 10.1093/emboj/cdg307.

Leonhardt, H.; Rahn, H. P.; Weinzierl, P.; Sporbert, A.; Cremer, T.; Zink, D.; Cardoso, M. C. (2000): Dynamics of DNA replication factories in living cells. In *J Cell Biol* 149 (2), pp. 271–280. DOI: 10.1083/jcb.149.2.271.

Levine, Arnold J. (1997): p53, the Cellular Gatekeeper for Growth and Division. In *Cell* 88 (3), pp. 323–331. DOI: 10.1016/s0092-8674(00)81871-1.

Li, F. (2005): Role of survivin and its splice variants in tumorigenesis. In *British journal of cancer* 92 (2), pp. 212–216. DOI: 10.1038/sj.bjc.6602340.

Li, F.; Ackermann, E. J.; Bennett, C. F.; Rothermel, A. L.; Plescia, J.; Tognin, S. et al. (1999): Pleiotropic cell-division defects and apoptosis induced by interference with survivin function. In *Nature cell biology* 1 (8), pp. 461–466. DOI: 10.1038/70242.

Li, F.; Ambrosini, G.; Chu, E. Y.; Plescia, J.; Tognin, S.; Marchisio, P. C.; Altieri, D. C. (1998): Control of apoptosis and mitotic spindle checkpoint by survivin. In *Nature* 396 (6711), pp. 580–584. DOI: 10.1038/25141.

Li, Fengzhi (2014): Anticancer drug FL118 is more than a survivin inhibitor: where is the Achilles' heel of cancer? In *American journal of cancer research* 4 (3), pp. 304–311. Available online at https://pubmed.ncbi.nlm.nih.gov/24959385/.

Li, Sicong; Kanno, Shin-ichiro; Watanabe, Reiko; Ogiwara, Hideaki; Kohno, Takashi; Watanabe, Go et al. (2011): Polynucleotide kinase and aprataxin-like forkhead-associated protein (PALF) acts as both a single-stranded DNA endonuclease and a single-stranded DNA 3' exonuclease and can participate in DNA end joining in a biochemical system. In *The Journal of biological chemistry* 286 (42), pp. 36368–36377. DOI: 10.1074/jbc.M111.287797.

Li, Xuan; Heyer, Wolf-Dietrich (2008): Homologous recombination in DNA repair and DNA damage tolerance. In *Cell research* 18 (1), pp. 99–113. DOI: 10.1038/cr.2008.1.

Li, Zhongdao; Pearlman, Alexander H.; Hsieh, Peggy (2016a): DNA mismatch repair and the DNA damage response. In *DNA repair* 38, pp. 94–101. DOI: 10.1016/j.dnarep.2015.11.019.

Li, Zhui; Ren, Wei; Zeng, Qiu; Chen, Siyu; Zhang, Mao; Zhao, Yu et al. (2016b): Effects of survivin on angiogenesis in vivo and in vitro. In *American Journal of Translational Research* 8 (2), pp. 270–283.

Liao, Hongwei; Ji, Fang; Helleday, Thomas; Ying, Songmin (2018): Mechanisms for stalled replication fork stabilization: new targets for synthetic lethality strategies in cancer treatments. In *EMBO Reports* 19 (9). DOI: 10.15252/embr.201846263.

Lim, Shuhui; Kaldis, Philipp (2013): Cdks, cyclins and CKIs: roles beyond cell cycle regulation. In *Development (Cambridge, England)* 140 (15), pp. 3079–3093. DOI: 10.1242/dev.091744.

Ling, Xiang; Cao, Shousong; Cheng, Qiuying; Keefe, James T.; Rustum, Youcef M.; Li, Fengzhi (2012): A novel small molecule FL118 that selectively inhibits survivin, Mcl-1, XIAP and cIAP2 in a p53-independent manner, shows superior antitumor activity. In *PloS one* 7 (9), e45571. DOI: 10.1371/journal.pone.0045571.

Liu, Dan; Lampson, Michael A. (2009): Regulation of kinetochore-microtubule attachments by Aurora B kinase. In *Biochemical Society transactions* 37 (Pt 5), pp. 976–980. DOI: 10.1042/BST0370976.

Liu, Dan; Vader, Gerben; Vromans, Martijn J. M.; Lampson, Michael A.; Lens, Susanne M. A. (2009): Sensing chromosome bi-orientation by spatial separation of aurora B kinase from kinetochore substrates. In *Science* 323 (5919), pp. 1350–1353. DOI: 10.1126/science.1167000.

Liu, Gang; Chen, Xinbin (2006): DNA polymerase eta, the product of the xeroderma pigmentosum variant gene and a target of p53, modulates the DNA damage checkpoint and p53 activation. In *Molecular and cellular biology* 26 (4), pp. 1398–1413. DOI: 10.1128/MCB.26.4.1398-1413.2006.

Löbrich, Markus; Jeggo, Penny A. (2007 Nov): The impact of a negligent G2/M checkpoint on genomic instability and cancer induction. England (11).

Lombard, David B.; Chua, Katrin F.; Mostoslavsky, Raul; Franco, Sonia; Gostissa, Monica; Alt, Frederick W. (2005): DNA repair, genome stability, and aging. In *Cell* 120 (4), pp. 497–512. DOI: 10.1016/j.cell.2005.01.028.

Lopes, M.; Cotta-Ramusino, C.; Pellicioli, A.; Liberi, G.; Plevani, P.; Muzi-Falconi, M. et al. (2001): The DNA replication checkpoint response stabilizes stalled replication forks. In *Nature* 412 (6846), pp. 557–561. DOI: 10.1038/35087613.

Lord, Christopher J.; Ashworth, Alan (2012): The DNA damage response and cancer therapy. In *Nature* 481 (7381), pp. 287–294. DOI: 10.1038/nature10760.

Luger, K.; Mäder, A. W.; Richmond, R. K.; Sargent, D. F.; Richmond, T. J. (1997): Crystal structure of the nucleosome core particle at 2.8 A resolution. In *Nature* 389 (6648), pp. 251–260. DOI: 10.1038/38444.

Luijsterburg, Martijn S.; Dinant, Christoffel; Lans, Hannes; Stap, Jan; Wiernasz, Elzbieta; Lagerwerf, Saskia et al. (2009): Heterochromatin protein 1 is recruited to various types of DNA damage. In *The Journal of cell biology* 185 (4), pp. 577–586. DOI: 10.1083/jcb.200810035.

Ma, Yunmei; Pannicke, Ulrich; Schwarz, Klaus; Lieber, Michael R. (2002): Hairpin Opening and Overhang Processing by an Artemis/DNA-Dependent Protein Kinase Complex in Nonhomologous End Joining and V(D)J Recombination. In *Cell* 108 (6), pp. 781–794. DOI: 10.1016/s0092-8674(02)00671-2.

Machida, Shinichi; Takizawa, Yoshimasa; Ishimaru, Masakazu; Sugita, Yukihiko; Sekine, Satoshi; Nakayama, Jun-Ichi et al. (2018): Structural Basis of Heterochromatin Formation by Human HP1. In *Molecular cell* 69 (3), 385-397.e8. DOI: 10.1016/j.molcel.2017.12.011.

Machida, Yuichi J.; Hamlin, Joyce L.; Dutta, Anindya (2005): Right place, right time, and only once: replication initiation in metazoans. In *Cell* 123 (1), pp. 13–24. DOI: 10.1016/j.cell.2005.09.019.

Mackay, Douglas R.; Ullman, Katharine S. (2015): ATR and a Chk1-Aurora B pathway coordinate postmitotic genome surveillance with cytokinetic abscission. In *Molecular biology of the cell* 26 (12), pp. 2217–2226. DOI: 10.1091/mbc.E14-11-1563.

Maga, Giovanni; Hubscher, Ulrich (2003): Proliferating cell nuclear antigen (PCNA): a dancer with many partners. In *Journal of cell science* 116 (Pt 15), pp. 3051–3060. DOI: 10.1242/jcs.00653.

Mailand, N.; Falck, J.; Lukas, C.; Syljuâsen, R. G.; Welcker, M.; Bartek, J.; Lukas, J. (2000): Rapid destruction of human Cdc25A in response to DNA damage. In *Science (New York, N.Y.)* 288 (5470), pp. 1425–1429. DOI: 10.1126/science.288.5470.1425.

Maison, Christèle; Almouzni, Geneviève (2004): HP1 and the dynamics of heterochromatin maintenance. In *Nature reviews. Molecular cell biology* 5 (4), pp. 296–304. DOI: 10.1038/nrm1355.

Malivert, Laurent; Ropars, Virginie; Nunez, Marcela; Drevet, Pascal; Miron, Simona; Faure, Guilhem et al. (2010): Delineation of the Xrcc4-interacting region in the globular head domain of cernunnos/XLF. In *The Journal of biological chemistry* 285 (34), pp. 26475–26483. DOI: 10.1074/jbc.M110.138156.

Mari, Pierre-Olivier; Florea, Bogdan I.; Persengiev, Stephan P.; Verkaik, Nicole S.; Brüggenwirth, Hennie T.; Modesti, Mauro et al. (2006): Dynamic assembly of end-joining complexes requires interaction between Ku70/80 and XRCC4. In *Proceedings of the National Academy of Sciences of the United States of America* 103 (49), pp. 18597–18602. DOI: 10.1073/pnas.0609061103.

Marians, Kenneth J. (2018): Lesion Bypass and the Reactivation of Stalled Replication Forks. In *Annual review of biochemistry* 87, pp. 217–238. DOI: 10.1146/annurev-biochem-062917-011921.

Maric, Marija; Maculins, Timurs; Piccoli, Giacomo de; Labib, Karim (2014): Cdc48 and a ubiquitin ligase drive disassembly of the CMG helicase at the end of DNA replication. In *Science* 346 (6208), p. 1253596. DOI: 10.1126/science.1253596.

Martincorena, Iñigo; Campbell, Peter J. (2015): Somatic mutation in cancer and normal cells. In *Science (New York, N.Y.)* 349 (6255), pp. 1483–1489. DOI: 10.1126/science.aab4082.

Martincorena, Iñigo; Raine, Keiran M.; Gerstung, Moritz; Dawson, Kevin J.; Haase, Kerstin; van Loo, Peter et al. (2017): Universal Patterns of Selection in Cancer and Somatic Tissues. In *Cell* 171 (5), 1029-1041.e21. DOI: 10.1016/j.cell.2017.09.042.

Marusawa, Hiroyuki; Matsuzawa, Shu-ichi; Welsh, Kate; Zou, Hua; Armstrong, Robert; Tamm, Ingo; Reed, John C. (2003): HBXIP functions as a cofactor of survivin in apoptosis suppression. In *The EMBO journal* 22 (11), pp. 2729–2740. DOI: 10.1093/emboj/cdg263.

Masutani, C.; Sugasawa, K.; Yanagisawa, J.; Sonoyama, T.; Ui, M.; Enomoto, T. et al. (1994): Purification and cloning of a nucleotide excision repair complex involving the xeroderma pigmentosum group C protein and a human homologue of yeast RAD23. In *The EMBO journal* 13 (8), pp. 1831–1843.

McGhee, J. D.; Felsenfeld, G. (1980): Nucleosome structure. In *Annual review of biochemistry* 49, pp. 1115–1156. DOI: 10.1146/annurev.bi.49.070180.005343.

Merrick, Catherine J.; Jackson, Dean; Diffley, John F. X. (2004): Visualization of altered replication dynamics after DNA damage in human cells. In *The Journal of biological chemistry* 279 (19), pp. 20067–20075. DOI: 10.1074/jbc.M400022200.

Minc, E.; Allory, Y.; Worman, H. J.; Courvalin, J. C.; Buendia, B. (1999): Localization and phosphorylation of HP1 proteins during the cell cycle in mammalian cells. In *Chromosoma* 108 (4), pp. 220–234. DOI: 10.1007/s004120050372.

Minocherhomji, Sheroy; Ying, Songmin; Bjerregaard, Victoria A.; Bursomanno, Sara; Aleliunaite, Aiste; Wu, Wei et al. (2015): Replication stress activates DNA repair synthesis in mitosis. In *Nature* 528 (7581), pp. 286–290. DOI: 10.1038/nature16139.

Mirkin, Ekaterina V.; Mirkin, Sergei M. (2007): Replication fork stalling at natural impediments. In *Microbiology and molecular biology reviews : MMBR* 71 (1), pp. 13–35. DOI: 10.1128/MMBR.00030-06.

Misteli, Tom (2007): Beyond the sequence: cellular organization of genome function. In *Cell* 128 (4), pp. 787–800. DOI: 10.1016/j.cell.2007.01.028.

Mitchell, James R.; Hoeijmakers, Jan H. J.; Niedernhofer, Laura J. (2003): Divide and conquer: nucleotide excision repair battles cancer and ageing. In *Current opinion in cell biology* 15 (2), pp. 232–240. DOI: 10.1016/s0955-0674(03)00018-8.

Miyazawa-Onami, Mayumi; Araki, Hiroyuki; Tanaka, Seiji (2017): Pre-initiation complex assembly functions as a molecular switch that splits the Mcm2-7 double hexamer. In *EMBO Reports* 18 (10), pp. 1752–1761. DOI: 10.15252/embr.201744206.

Moggs, J. G.; Grandi, P.; Quivy, J. P.; Jónsson, Z. O.; Hübscher, U.; Becker, P. B.; Almouzni, G. (2000): A CAF-1-PCNA-mediated chromatin assembly pathway triggered by sensing DNA damage. In *Molecular and cellular biology* 20 (4), pp. 1206–1218. DOI: 10.1128/mcb.20.4.1206-1218.2000.

Moldovan, George-Lucian; Pfander, Boris; Jentsch, Stefan (2007): PCNA, the maestro of the replication fork. In *Cell* 129 (4), pp. 665–679. DOI: 10.1016/j.cell.2007.05.003.

Moreno, Sara Priego; Bailey, Rachael; Campion, Nicholas; Herron, Suzanne; Gambus, Agnieszka (2014): Polyubiquitylation drives replisome disassembly at the termination of DNA replication. In *Science* 346 (6208), pp. 477–481. DOI: 10.1126/science.1253585.

Morgan, D. O. (1995): Principles of CDK regulation. In *Nature* 374 (6518), pp. 131–134. DOI: 10.1038/374131a0.

Mosel (2018): A novel role for the chromosomal passenger complex in DNA replication and damage response. dissertation. University of Duisburg-Essen, Essen.

Muchmore, S. W.; Chen, J.; Jakob, C.; Zakula, D.; Matayoshi, E. D.; Wu, W. et al. (2000): Crystal structure and mutagenic analysis of the inhibitor-of-apoptosis protein survivin. In *Molecular cell* 6 (1), pp. 173–182. Available online at https://pubmed.ncbi.nlm.nih.gov/10949038/.

Mullis, Kary B.; Faloona, Fred A. (1987): [21] Specific synthesis of DNA in vitro via a polymerase-catalyzed chain reaction. In *Methods in enzymology* 155, pp. 335–350. DOI: 10.1016/0076-6879(87)55023-6.

Musacchio, Andrea (2011): Spindle assembly checkpoint: the third decade. In *Philosophical transactions of the Royal Society of London. Series B, Biological sciences* 366 (1584), pp. 3595–3604. DOI: 10.1098/rstb.2011.0072.

Musacchio, Andrea; Salmon, Edward D. (2007): The spindle-assembly checkpoint in space and time. In *Nature reviews. Molecular cell biology* 8 (5), pp. 379–393. DOI: 10.1038/nrm2163.

Na, Young-Soon; Yang, Soo-Jin; Kim, Seung-Mi; Jung, Kyung-Ah; Moon, Jai-Hee; Shin, Jae-Sik et al. (2012): YM155 induces EGFR suppression in pancreatic cancer cells. In *PloS one* 7 (6), e38625. DOI: 10.1371/journal.pone.0038625.

Nakahara, Takahito; Kita, Aya; Yamanaka, Kentaro; Mori, Masamichi; Amino, Nobuaki; Takeuchi, Masahiro et al. (2011): Broad spectrum and potent antitumor activities of YM155, a novel small-molecule survivin suppressant, in a wide variety of human cancer cell lines and xenograft models. In *Cancer science* 102 (3), pp. 614–621. DOI: 10.1111/j.1349-7006.2010.01834.x.

Nakamura, Hiromu; Morita, Toshiteru; Sato, Chikako (1986): Structural organizations of replicon domains during DNA synthetic phase in the mammalian nucleus. In *Experimental cell research* 165 (2), pp. 291–297. DOI: 10.1016/0014-4827(86)90583-5.

Nakayama, J.; Rice, J. C.; Strahl, B. D.; Allis, C. D.; Grewal, S. I. (2001): Role of histone H3 lysine 9 methylation in epigenetic control of heterochromatin assembly. In *Science (New York, N.Y.)* 292 (5514), pp. 110–113. DOI: 10.1126/science.1060118.

Neelsen, Kai J.; Lopes, Massimo (2015): Replication fork reversal in eukaryotes: from dead end to dynamic response. In *Nat Rev Mol Cell Biol* 16 (4), pp. 207–220. DOI: 10.1038/nrm3935.

Nick McElhinny, S. A.; Snowden, C. M.; McCarville, J.; Ramsden, D. A. (2000): Ku recruits the XRCC4-ligase IV complex to DNA ends. In *Molecular and cellular biology* 20 (9), pp. 2996–3003. DOI: 10.1128/mcb.20.9.2996-3003.2000.

Nielsen, Anders Lade; Oulad-Abdelghani, Mustapha; Ortiz, José A.; Remboutsika, Eumorphia; Chambon, Pierre; Losson, Régine (2001): Heterochromatin Formation in Mammalian Cells. In *Molecular cell* 7 (4), pp. 729–739. DOI: 10.1016/s1097-2765(01)00218-0.

Nielsen, Peter R.; Nietlispach, Daniel; Mott, Helen R.; Callaghan, Juliana; Bannister, Andrew; Kouzarides, Tony et al. (2002): Structure of the HP1 chromodomain bound to histone H3 methylated at lysine 9. In *Nature* 416 (6876), pp. 103–107. DOI: 10.1038/nature722.

Nimonkar, Amitabh V.; Genschel, Jochen; Kinoshita, Eri; Polaczek, Piotr; Campbell, Judith L.; Wyman, Claire et al. (2011): BLM-DNA2-RPA-MRN and EXO1-BLM-RPA-MRN constitute two DNA end resection machineries for human DNA break repair. In *Genes & development* 25 (4), pp. 350–362. DOI: 10.1101/gad.2003811.

Nimrat Chatterjee; Beatriz A. Santillan; John H. Wilson (2013): Microsatellite Repeats: Canaries in the Coalmine. In : Stress-Induced Mutagenesis: Springer, New York, NY, pp. 119–150. Available online at https://link.springer.com/chapter/10.1007/978-1-4614-6280-4_7.

Nishi, Ryotaro; Okuda, Yuki; Watanabe, Eriko; Mori, Toshio; Iwai, Shigenori; Masutani, Chikahide et al. (2005): Centrin 2 stimulates nucleotide excision repair by

interacting with xeroderma pigmentosum group C protein. In *Molecular and cellular biology* 25 (13), pp. 5664–5674. DOI: 10.1128/MCB.25.13.5664-5674.2005.

Nishibuchi, Gohei; Machida, Shinichi; Osakabe, Akihisa; Murakoshi, Hiromu; Hiragami-Hamada, Kyoko; Nakagawa, Reiko et al. (2014): N-terminal phosphorylation of HP1α increases its nucleosome-binding specificity. In *Nucleic acids research* 42 (20), pp. 12498–12511. DOI: 10.1093/nar/gku995.

Norbury, C.; Nurse, P. (1992): Animal cell cycles and their control. In *Annual review of biochemistry* 61, pp. 441–470. DOI: 10.1146/annurev.bi.61.070192.002301.

Nouspikel, T. (2009): DNA repair in mammalian cells : Nucleotide excision repair: variations on versatility. In *Cellular and molecular life sciences : CMLS* 66 (6), pp. 994–1009. DOI: 10.1007/s00018-009-8737-y.

Nowell, P. C. (1976): The clonal evolution of tumor cell populations. In *Science (New York, N.Y.)* 194 (4260), pp. 23–28. DOI: 10.1126/science.959840.

Nozawa, Ryu-Suke; Nagao, Koji; Masuda, Hiro-Taka; Iwasaki, Osamu; Hirota, Toru; Nozaki, Naohito et al. (2010): Human POGZ modulates dissociation of HP1alpha from mitotic chromosome arms through Aurora B activation. In *Nature cell biology* 12 (7), pp. 719–727. DOI: 10.1038/ncb2075.

Nyberg, Kara A.; Michelson, Rhett J.; Putnam, Charles W.; Weinert, Ted A. (2002): Toward maintaining the genome: DNA damage and replication checkpoints. In *Annual review of genetics* 36, pp. 617–656. DOI: 10.1146/annurev.genet.36.060402.113540.

O'Connor, D. S.; Grossman, D.; Plescia, J.; Li, F.; Zhang, H.; Villa, A. et al. (2000): Regulation of apoptosis at cell division by p34cdc2 phosphorylation of survivin. In *Proceedings of the National Academy of Sciences of the United States of America* 97 (24), pp. 13103–13107. DOI: 10.1073/pnas.240390697.

Odell, Ian D.; Wallace, Susan S.; Pederson, David S. (2013): Rules of engagement for base excision repair in chromatin. In *Journal of cellular physiology* 228 (2), pp. 258–266. DOI: 10.1002/jcp.24134.

Ogawa, T.; Okazaki, T. (1980): Discontinuous DNA replication. In *Annual review of biochemistry* 49, pp. 421–457. DOI: 10.1146/annurev.bi.49.070180.002225.

Ohtsubo, M.; Theodoras, A. M.; Schumacher, J.; Roberts, J. M.; Pagano, M. (1995): Human cyclin E, a nuclear protein essential for the G1-to-S phase transition. In *Molecular and cellular biology* 15 (5), pp. 2612–2624. DOI: 10.1128/mcb.15.5.2612.

O'Keefe, R. T.; Henderson, S. C.; Spector, D. L. (1992): Dynamic organization of DNA replication in mammalian cell nuclei: spatially and temporally defined replication of chromosome-specific alpha-satellite DNA sequences. In *J Cell Biol* 116 (5), pp. 1095–1110. DOI: 10.1083/jcb.116.5.1095.

Orlando, Valerio (2003): Polycomb, Epigenomes, and Control of Cell Identity. In *Cell* 112 (5), pp. 599–606. DOI: 10.1016/s0092-8674(03)00157-0.

Pacek, Marcin; Tutter, Antonin V.; Kubota, Yumiko; Takisawa, Haruhiko; Walter, Johannes C. (2006): Localization of MCM2-7, Cdc45, and GINS to the site of DNA unwinding during eukaryotic DNA replication. In *Molecular cell* 21 (4), pp. 581–587. DOI: 10.1016/j.molcel.2006.01.030.

Painter, R. B.; Young, B. R. (1980): Radiosensitivity in ataxia-telangiectasia: a new explanation. In *Proceedings of the National Academy of Sciences of the United States of America* 77 (12), pp. 7315–7317. DOI: 10.1073/pnas.77.12.7315.

Palmer, D. K.; O'Day, K.; Wener, M. H.; Andrews, B. S.; Margolis, R. L. (1987): A 17-kD centromere protein (CENP-A) copurifies with nucleosome core particles and with histones. In *The Journal of cell biology* 104 (4), pp. 805–815. DOI: 10.1083/jcb.104.4.805.

Pang, D.; Yoo, S.; Dynan, W. S.; Jung, M.; Dritschilo, A. (1997): Ku proteins join DNA fragments as shown by atomic force microscopy. In *Cancer research* 57 (8), pp. 1412–1415.

Papouli, Efterpi; Chen, Shuhua; Davies, Adelina A.; Huttner, Diana; Krejci, Lumir; Sung, Patrick; Ulrich, Helle D. (2005): Crosstalk between SUMO and ubiquitin on PCNA is mediated by recruitment of the helicase Srs2p. In *Molecular cell* 19 (1), pp. 123–133. DOI: 10.1016/j.molcel.2005.06.001.

Paull, Tanya T.; Rogakou, Emmy P.; Yamazaki, Vikky; Kirchgessner, Cordula U.; Gellert, Martin; Bonner, William M. (2000): A critical role for histone H2AX in recruitment of repair factors to nuclear foci after DNA damage. In *Current biology : CB* 10 (15), pp. 886–895. DOI: 10.1016/s0960-9822(00)00610-2.

Peddu, Chandana; Zhang, Sufang; Zhao, Hong; Wong, Agnes; Lee, Ernest Y. C.; Lee, Marietta Y. W. T.; Zhang, Zhongtao (2018): Phosphorylation Alters the Properties of Pol η: Implications for Translesion Synthesis. In *iScience* 6, pp. 52–67. DOI: 10.1016/j.isci.2018.07.009.

Perrone, Serafina; Lotti, Federica; Geronzi, Ursula; Guidoni, Elisa; Longini, Mariangela; Buonocore, Giuseppe (2016): Oxidative Stress in Cancer-Prone Genetic Diseases in Pediatric Age: The Role of Mitochondrial Dysfunction. In *Oxidative medicine and cellular longevity* 2016, p. 4782426. DOI: 10.1155/2016/4782426.

Perry, J. Jefferson P.; Yannone, Steven M.; Holden, Lauren G.; Hitomi, Chiharu; Asaithamby, Aroumougame; Han, Seungil et al. (2006): WRN exonuclease structure and molecular mechanism imply an editing role in DNA end processing. In *Nature structural & molecular biology* 13 (5), pp. 414–422. DOI: 10.1038/nsmb1088.

Petermann, Eva; Caldecott, Keith W. (2006): Evidence that the ATR/Chk1 pathway maintains normal replication fork progression during unperturbed S phase. In *Cell cycle (Georgetown, Tex.)* 5 (19), pp. 2203–2209. DOI: 10.4161/cc.5.19.3256.

Petermann, Eva; Helleday, Thomas (2010): Pathways of mammalian replication fork restart. In *Nat Rev Mol Cell Biol* 11 (10), pp. 683–687. DOI: 10.1038/nrm2974.

Pfander, Boris; Moldovan, George-Lucian; Sacher, Meik; Hoege, Carsten; Jentsch, Stefan (2005): SUMO-modified PCNA recruits Srs2 to prevent recombination during S phase. In *Nature* 436 (7049), pp. 428–433. DOI: 10.1038/nature03665.

Polyak, Kornelia; Lee, Mong-Hong; Erdjument-Bromage, Hediye; Koff, Andrew; Roberts, James M.; Tempst, Paul; Massagué, Joan (1994): Cloning of p27Kip1, a cyclin-dependent kinase inhibitor and a potential mediator of extracellular antimitogenic signals. In *Cell* 78 (1), pp. 59–66. DOI: 10.1016/0092-8674(94)90572-x.

Pommier, Yves (2006): Topoisomerase I inhibitors: camptothecins and beyond. In *Nature reviews. Cancer* 6 (10), pp. 789–802. DOI: 10.1038/nrc1977.

Pommier, Yves; Cherfils, Jacqueline (2005): Interfacial inhibition of macromolecular interactions: nature's paradigm for drug discovery. In *Trends in pharmacological sciences* 26 (3), pp. 138–145. DOI: 10.1016/j.tips.2005.01.008.

Pommier, Yves; Marchand, Christophe (2005): Interfacial inhibitors of protein-nucleic acid interactions. In *Current medicinal chemistry. Anti-cancer agents* 5 (4), pp. 421–429. DOI: 10.2174/1568011054222337.

Postow, L.; Crisona, N. J.; Peter, B. J.; Hardy, C. D.; Cozzarelli, N. R. (2001): Topological challenges to DNA replication: conformations at the fork. In *Proceedings of the National Academy of Sciences of the United States of America* 98 (15), pp. 8219–8226. DOI: 10.1073/pnas.111006998.

Potenski, Catherine J.; Klein, Hannah L. (2014): How the misincorporation of ribonucleotides into genomic DNA can be both harmful and helpful to cells. In *Nucleic acids research* 42 (16), pp. 10226–10234. DOI: 10.1093/nar/gku773.

Prioleau, Marie-Noëlle; MacAlpine, David M. (2016): DNA replication origins-where do we begin? In *Genes & development* 30 (15), pp. 1683–1697. DOI: 10.1101/gad.285114.116.

Pylayeva-Gupta, Yuliya; Grabocka, Elda; Bar-Sagi, Dafna (2011): RAS oncogenes: weaving a tumorigenic web. In *Nat Rev Cancer* 11 (11), pp. 761–774. DOI: 10.1038/nrc3106.

Quinet, Annabel; Carvajal-Maldonado, Denisse; Lemacon, Delphine; Vindigni, Alessandro (2017a): Chapter Three - DNA Fiber Analysis: Mind the Gap! In Brandt F. Eichman (Ed.): Methods in Enzymology : DNA Repair Enzymes: Cell, Molecular, and Chemical Biology, vol. 591: Academic Press, pp. 55–82. Available online at http://www.sciencedirect.com/science/article/pii/S0076687917301143.

Quinet, Annabel; Lemaçon, Delphine; Vindigni, Alessandro (2017b): Replication Fork Reversal: Players and Guardians. In *Molecular cell* 68 (5), pp. 830–833. DOI: 10.1016/j.molcel.2017.11.022.

Rand, Eyal; Cedar, Howard (2003): Regulation of imprinting: A multi-tiered process. In *Journal of Cellular Biochemistry* 88 (2), pp. 400–407. DOI: 10.1002/jcb.10352.

Rea, S.; Eisenhaber, F.; O'Carroll, D.; Strahl, B. D.; Sun, Z. W.; Schmid, M. et al. (2000): Regulation of chromatin structure by site-specific histone H3 methyltransferases. In *Nature* 406 (6796), pp. 593–599. DOI: 10.1038/35020506.

Reichert, Sebastian; Rödel, Claus; Mirsch, Johanna; Harter, Patrick N.; Tomicic, Maja T.; Mittelbronn, Michel et al. (2011): Survivin inhibition and DNA double-strand break repair: a molecular mechanism to overcome radioresistance in glioblastoma. In

Radiotherapy and oncology : journal of the European Society for Therapeutic Radiology and Oncology 101 (1), pp. 51–58. DOI: 10.1016/j.radonc.2011.06.037.

Remus, Dirk; Beuron, Fabienne; Tolun, Gökhan; Griffith, Jack D.; Morris, Edward P.; Diffley, John F. X. (2009): Concerted loading of Mcm2-7 double hexamers around DNA during DNA replication origin licensing. In *Cell* 139 (4), pp. 719–730. DOI: 10.1016/j.cell.2009.10.015.

Reuter, Simone; Gupta, Subash C.; Chaturvedi, Madan M.; Aggarwal, Bharat B. (2010): Oxidative stress, inflammation, and cancer: how are they linked? In *Free radical biology & medicine* 49 (11), pp. 1603–1616. DOI: 10.1016/j.freeradbiomed.2010.09.006.

Richmond, Timothy J.; Davey, Curt A. (2003): The structure of DNA in the nucleosome core. In *Nature* 423 (6936), pp. 145–150. DOI: 10.1038/nature01595.

Roberts, Steven A.; Strande, Natasha; Burkhalter, Martin D.; Strom, Christina; Havener, Jody M.; Hasty, Paul; Ramsden, Dale A. (2010): Ku is a 5'-dRP/AP lyase that excises nucleotide damage near broken ends. In *Nature* 464 (7292), pp. 1214–1217. DOI: 10.1038/nature08926.

Rödel, F.; Sprenger, T.; Kaina, B.; Liersch, T.; Rödel, C.; Fulda, S.; Hehlgans, S. (2012): Survivin as a prognostic/predictive marker and molecular target in cancer therapy. In *Current medicinal chemistry* 19 (22), pp. 3679–3688. DOI: 10.2174/092986712801661040.

Rodriguez, J. A.; Lens, S. M. A.; Span, S. W.; Vader, G.; Medema, R. H.; Kruyt, F. A. E.; Giaccone, G. (2006): Subcellular localization and nucleocytoplasmic transport of the chromosomal passenger proteins before nuclear envelope breakdown. In *Oncogene* 25 (35), pp. 4867–4879. DOI: 10.1038/sj.onc.1209499.

Rogakou, E. P.; Pilch, D. R.; Orr, A. H.; Ivanova, V. S.; Bonner, W. M. (1998): DNA double-stranded breaks induce histone H2AX phosphorylation on serine 139. In *The Journal of biological chemistry* 273 (10), pp. 5858–5868. DOI: 10.1074/jbc.273.10.5858.

Rothbart, Scott B.; Strahl, Brian D. (2014): Interpreting the language of histone and DNA modifications. In *Biochimica et biophysica acta* 1839 (8), pp. 627–643. DOI: 10.1016/j.bbagrm.2014.03.001.

Ruchaud, Sandrine; Carmena, Mar; Earnshaw, William C. (2007): Chromosomal passengers: conducting cell division. In *Nat Rev Mol Cell Biol* 8 (10), pp. 798–812. DOI: 10.1038/nrm2257.

Sah, Nand K.; Seniya, Chandrabhan (2015): Survivin splice variants and their diagnostic significance. In *Tumour biology : the journal of the International Society for Oncodevelopmental Biology and Medicine* 36 (9), pp. 6623–6631. DOI: 10.1007/s13277-015-3865-5.

Saha, Anjanabha; Wittmeyer, Jacqueline; Cairns, Bradley R. (2006): Chromatin remodelling: the industrial revolution of DNA around histones. In *Nature reviews. Molecular cell biology* 7 (6), pp. 437–447. DOI: 10.1038/nrm1945.

Sanchez, Y.; Wong, C.; Thoma, R. S.; Richman, R.; Wu, Z.; Piwnica-Worms, H.; Elledge, S. J. (1997): Conservation of the Chk1 checkpoint pathway in mammals: linkage of DNA damage to Cdk regulation through Cdc25. In *Science (New York, N.Y.)* 277 (5331), pp. 1497–1501. DOI: 10.1126/science.277.5331.1497.

Sánchez, Irma; Dynlacht, Brian David (2005): New insights into cyclins, CDKs, and cell cycle control. In *Seminars in cell & developmental biology* 16 (3), pp. 311–321. DOI: 10.1016/j.semcdb.2005.02.007.

Sanger, F.; Nicklen, S.; Coulson, A. R. (1977): DNA sequencing with chain-terminating inhibitors. In *Proceedings of the National Academy of Sciences of the United States of America* 74 (12), pp. 5463–5467. DOI: 10.1073/pnas.74.12.5463.

Sartori, Alessandro A.; Lukas, Claudia; Coates, Julia; Mistrik, Martin; Fu, Shuang; Bartek, Jiri et al. (2007): Human CtIP promotes DNA end resection. In *Nature* 450 (7169), pp. 509–514. DOI: 10.1038/nature06337.

Saunders, W. S.; Chue, C.; Goebl, M.; Craig, C.; Clark, R. F.; Powers, J. A. et al. (1993): Molecular cloning of a human homologue of Drosophila heterochromatin protein HP1 using anti-centromere autoantibodies with anti-chromo specificity. In *Journal of cell science* 104 (Pt 2), pp. 573–582.

Schafer, K. A. (1998): The cell cycle: a review. In *Veterinary pathology* 35 (6), pp. 461–478. DOI: 10.1177/030098589803500601.

Schalch, Thomas; Steiner, Florian A. (2017): Structure of centromere chromatin: from nucleosome to chromosomal architecture. In *Chromosoma* 126 (4), pp. 443–455. DOI: 10.1007/s00412-016-0620-7.

Schönenberger, Felix; Deutzmann, Anja; Ferrando-May, Elisa; Merhof, Dorit (2015): Discrimination of cell cycle phases in PCNA-immunolabeled cells. In *BMC Bioinformatics* 16, p. 180. DOI: 10.1186/s12859-015-0618-9.

Schröder (2014): Dissecting the role of the radiation resistance factor survivin in DNA damage response. dissertation. University of Duisburg-Essen, Essen.

Schubbert, Suzanne; Shannon, Kevin; Bollag, Gideon (2007): Hyperactive Ras in developmental disorders and cancer. In *Nature reviews. Cancer* 7 (4), pp. 295–308. DOI: 10.1038/nrc2109.

Scully, Ralph; Xie, Anyong; Nagaraju, Ganesh (2004): Molecular functions of BRCA1 in the DNA damage response. In *Cancer biology & therapy* 3 (6), pp. 521–527. DOI: 10.4161/cbt.3.6.842.

Sessa, Fabio; Mapelli, Marina; Ciferri, Claudio; Tarricone, Cataldo; Areces, Liliana B.; Schneider, Thomas R. et al. (2005): Mechanism of Aurora B activation by INCENP and inhibition by hesperadin. In *Molecular cell* 18 (3), pp. 379–391. DOI: 10.1016/j.molcel.2005.03.031.

Shachar, Sigal; Ziv, Omer; Avkin, Sharon; Adar, Sheera; Wittschieben, John; Reissner, Thomas et al. (2009): Two-polymerase mechanisms dictate error-free and error-prone translesion DNA synthesis in mammals. In *The EMBO journal* 28 (4), pp. 383–393. DOI: 10.1038/emboj.2008.281.

Shaltiel, Indra A.; Krenning, Lenno; Bruinsma, Wytse; Medema, René H. (2015): The same, only different - DNA damage checkpoints and their reversal throughout the cell cycle. In *J Cell Sci* 128 (4), pp. 607–620. DOI: 10.1242/jcs.163766.

Sheaff, R.; Ilsley, D.; Kuchta, R. (1991): Mechanism of DNA polymerase alpha inhibition by aphidicolin. In *Biochemistry* 30 (35), pp. 8590–8597. DOI: 10.1021/bi00099a014.

Sherr, C. J.; Roberts, J. M. (1995): Inhibitors of mammalian G1 cyclin-dependent kinases. In *Genes & development* 9 (10), pp. 1149–1163. DOI: 10.1101/gad.9.10.1149.

Shibahara, Kei-ichi; Stillman, Bruce (1999): Replication-Dependent Marking of DNA by PCNA Facilitates CAF-1-Coupled Inheritance of Chromatin. In *Cell* 96 (4), pp. 575–585. DOI: 10.1016/s0092-8674(00)80661-3.

Shimada, Kenji; Pasero, Philippe; Gasser, Susan M. (2002): ORC and the intra-S-phase checkpoint: a threshold regulates Rad53p activation in S phase. In *Genes & development* 16 (24), pp. 3236–3252. DOI: 10.1101/gad.239802.

Shimizu, Ippei; Yoshida, Yohko; Suda, Masayoshi; Minamino, Tohru (2014): DNA damage response and metabolic disease. In *Cell Metabolism* 20 (6), pp. 967–977. DOI: 10.1016/j.cmet.2014.10.008.

Shinoura, Nobusada; Yamada, Ryoji; Okamoto, Koichiro; Nakamura, Osamu; Shitara, Nobuyuki (2002): Local recurrence of metastatic brain tumor after stereotactic radiosurgery or surgery plus radiation. In *Journal of neuro-oncology* 60 (1), pp. 71–77. DOI: 10.1023/a:1020256721761.

Siddiqui, Khalid; On, Kin Fan; Diffley, John F. X. (2013): Regulating DNA replication in eukarya. In *Cold Spring Harbor Perspectives in Biology* 5 (9). DOI: 10.1101/cshperspect.a012930.

Sinha, Rajeshwar P.; Häder, Donat P. (2002): UV-induced DNA damage and repair: a review. In *Photochemical & photobiological sciences : Official journal of the European Photochemistry Association and the European Society for Photobiology* 1 (4), pp. 225–236. DOI: 10.1039/b201230h.

Smith, M.Mitchell (2002): Centromeres and variant histones: what, where, when and why? In *Current opinion in cell biology* 14 (3), pp. 279–285. DOI: 10.1016/s0955-0674(02)00331-9.

Smothers, James F.; Henikoff, Steven (2000): The HP1 chromo shadow domain binds a consensus peptide pentamer. In *Current biology : CB* 10 (1), pp. 27–30. DOI: 10.1016/s0960-9822(99)00260-2.

Sonneville, Remi; Moreno, Sara Priego; Knebel, Axel; Johnson, Clare; Hastie, C. James; Gartner, Anton et al. (2017): CUL-2LRR-1 and UBXN-3 drive replisome disassembly during DNA replication termination and mitosis. In *Nature cell biology* 19 (5), pp. 468–479. DOI: 10.1038/ncb3500.

Soutoglou, Evi; Dorn, Jonas F.; Sengupta, Kundan; Jasin, Maria; Nussenzweig, Andre; Ried, Thomas et al. (2007): Positional stability of single double-strand breaks in mammalian cells. In *Nature cell biology* 9 (6), pp. 675–682. DOI: 10.1038/ncb1591.

Stary, Anne; Sarasin, Alain (2002): Molecular mechanisms of UV-induced mutations as revealed by the study of DNA polymerase η in human cells. In *Research in microbiology* 153 (7), pp. 441–445. DOI: 10.1016/s0923-2508(02)01343-8.

Stauber, Roland H.; Wünsch, Desiree; Knauer, Shirley K.; Fetz, Verena (2010): An update on the pathobiological relevance of nuclear receptors for cancers of the head and neck. In *Histology and histopathology* 25 (8), pp. 1093–1104. DOI: 10.14670/HH-25.1093.

Steitz, J. A. (2004): RNAi: A Guide to Gene Silencing, edited by Gregory J. Hannon. 2003. Cold Spring Harbor Laboratory Press, Cold Spring Harbor, NY. ISBN: 0-87969-641-9. In *RNA* 10 (3), p. 350. DOI: 10.1261/rna.5244104.

Stelter, Philipp; Ulrich, Helle D. (2003): Control of spontaneous and damage-induced mutagenesis by SUMO and ubiquitin conjugation. In *Nature* 425 (6954), pp. 188–191. DOI: 10.1038/nature01965.

Stewart, Grant S.; Wang, Bin; Bignell, Colin R.; Taylor, A. Malcolm R.; Elledge, Stephen J. (2003): MDC1 is a mediator of the mammalian DNA damage checkpoint. In *Nature* 421 (6926), pp. 961–966. DOI: 10.1038/nature01446.

Stewart, L.; Redinbo, M. R.; Qiu, X.; Hol, W. G.; Champoux, J. J. (1998): A model for the mechanism of human topoisomerase I. In *Science (New York, N.Y.)* 279 (5356), pp. 1534–1541. DOI: 10.1126/science.279.5356.1534.

Stracker, Travis H.; Petrini, John H. J. (2011): The MRE11 complex: starting from the ends. In *Nature reviews. Molecular cell biology* 12 (2), pp. 90–103. DOI: 10.1038/nrm3047.

Stratton, Michael R.; Campbell, Peter J.; Futreal, P. Andrew (2009): The cancer genome. In *Nature* 458 (7239), pp. 719–724. DOI: 10.1038/nature07943.

Strzalka, Wojciech; Ziemienowicz, Alicja (2011): Proliferating cell nuclear antigen (PCNA): a key factor in DNA replication and cell cycle regulation. In *Annals of Botany* 107 (7), pp. 1127–1140. DOI: 10.1093/aob/mcq243.

Stucki, Manuel; Jackson, Stephen P. (2006): gammaH2AX and MDC1: anchoring the DNA-damage-response machinery to broken chromosomes. In *DNA repair* 5 (5), pp. 534–543. DOI: 10.1016/j.dnarep.2006.01.012.

Sudakin, V.; Chan, G. K.; Yen, T. J. (2001): Checkpoint inhibition of the APC/C in HeLa cells is mediated by a complex of BUBR1, BUB3, CDC20, and MAD2. In *J Cell Biol* 154 (5), pp. 925–936. DOI: 10.1083/jcb.200102093.

Sugiyama, Tomohiko; Kowalczykowski, Stephen C. (2002): Rad52 protein associates with replication protein A (RPA)-single-stranded DNA to accelerate Rad51-mediated displacement of RPA and presynaptic complex formation. In *The Journal of biological chemistry* 277 (35), pp. 31663–31672. DOI: 10.1074/jbc.M203494200.

Sullivan, Lori L.; Chew, Kimberline; Sullivan, Beth A. (2017): α satellite DNA variation and function of the human centromere. In *Nucleus* 8 (4), pp. 331–339. DOI: 10.1080/19491034.2017.1308989.

Sullivan, Richard; Alatise, Olusegun Isaac; Anderson, Benjamin O.; Audisio, Riccardo; Autier, Philippe; Aggarwal, Ajay et al. (2015): Global cancer surgery: delivering safe, affordable, and timely cancer surgery. In *The Lancet. Oncology* 16 (11), pp. 1193–1224. DOI: 10.1016/S1470-2045(15)00223-5.

Talbert, Paul B.; Ahmad, Kami; Almouzni, Geneviève; Ausió, Juan; Berger, Frederic; Bhalla, Prem L. et al. (2012): A unified phylogeny-based nomenclature for histone variants. In *Epigenetics & chromatin* 5, p. 7. DOI: 10.1186/1756-8935-5-7.

Talbert, Paul B.; Henikoff, Steven (2013): Phylogeny as the basis for naming histones. In *Trends in genetics : TIG* 29 (9), pp. 499–500. DOI: 10.1016/j.tig.2013.06.009.

Tanaka, Seiji; Nakato, Ryuichiro; Katou, Yuki; Shirahige, Katsuhiko; Araki, Hiroyuki (2011): Origin association of Sld3, Sld7, and Cdc45 proteins is a key step for determination of origin-firing timing. In *Current biology : CB* 21 (24), pp. 2055–2063. DOI: 10.1016/j.cub.2011.11.038.

Tercero, J. A.; Diffley, J. F. (2001): Regulation of DNA replication fork progression through damaged DNA by the Mec1/Rad53 checkpoint. In *Nature* 412 (6846), pp. 553–557. DOI: 10.1038/35087607.

Thompson, Larry H. (2012): Recognition, signaling, and repair of DNA double-strand breaks produced by ionizing radiation in mammalian cells: the molecular choreography. In *Mutation research* 751 (2), pp. 158–246. DOI: 10.1016/j.mrrev.2012.06.002.

Thu, Yee Mon; Bielinsky, Anja-Katrin (2013): Enigmatic roles of Mcm10 in DNA replication. In *Trends in biochemical sciences* 38 (4), pp. 184–194. DOI: 10.1016/j.tibs.2012.12.003.

Tonna, Stephen; El-Osta, Assam; Cooper, Mark E.; Tikellis, Chris (2010): Metabolic memory and diabetic nephropathy: potential role for epigenetic mechanisms. In *Nat Rev Nephrol* 6 (6), pp. 332–341. DOI: 10.1038/nrneph.2010.55.

Tracey, Lorraine; Pérez-Rosado, Alberto; Artiga, Maria Jesús; Camacho, Francisca I.; Rodríguez, Antonia; Martínez, Nerea et al. (2005): Expression of the NF-kappaB targets BCL2 and BIRC5/Survivin characterizes small B-cell and aggressive B-cell lymphomas, respectively. In *The Journal of pathology* 206 (2), pp. 123–134. DOI: 10.1002/path.1768.

Trakala, Marianna; Fernández-Miranda, Gonzalo; Pérez de Castro, Ignacio; Heeschen, Christopher; Malumbres, Marcos (2013): Aurora B prevents delayed DNA replication and premature mitotic exit by repressing p21(Cip1). In *Cell cycle (Georgetown, Tex.)* 12 (7), pp. 1030–1041. DOI: 10.4161/cc.24004.

Trivedi, Prasad; Palomba, Francesco; Niedzialkowska, Ewa; Digman, Michelle A.; Gratton, Enrico; Stukenberg, P. Todd (2019): The inner centromere is a biomolecular condensate scaffolded by the chromosomal passenger complex. In *Nature cell biology* 21 (9), pp. 1127–1137. DOI: 10.1038/s41556-019-0376-4.

Tsai, Chun J.; Kim, Sunny A.; Chu, Gilbert (2007): Cernunnos/XLF promotes the ligation of mismatched and noncohesive DNA ends. In *Proceedings of the National Academy of Sciences of the United States of America* 104 (19), pp. 7851–7856. DOI: 10.1073/pnas.0702620104.

Tsukahara, Tatsuya; Tanno, Yuji; Watanabe, Yoshinori (2010): Phosphorylation of the CPC by Cdk1 promotes chromosome bi-orientation. In *Nature* 467 (7316), pp. 719–723. DOI: 10.1038/nature09390.

Tsunematsu, Takaaki; Arakaki, Rieko; Kawai, Hidehiko; Ruppert, Jan; Tsuneyama, Koichi; Ishimaru, Naozumi et al. (2020): APC/CCdh1 is required for the termination of chromosomal passenger complex activity upon mitotic exit. In *J Cell Sci* 133 (18). DOI: 10.1242/jcs.251314.

Types of Cancer Treatment - National Cancer Institute. Types of Cancer Treatment (2020). Available online at https://www.cancer.gov/about-cancer/treatment/types, updated on 4/6/2020, checked on 4/8/2020.

Uren, Anthony G.; Wong, Lee; Pakusch, Miha; Fowler, Kerry J.; Burrows, Francis J.; Vaux, David L.; Choo, K.H.Andy (2000): Survivin and the inner centromere protein INCENP show similar cell-cycle localization and gene knockout phenotype. In *Current biology : CB* 10 (21), pp. 1319–1328. DOI: 10.1016/s0960-9822(00)00769-7.

Vader, Gerben; Kauw, Jos J. W.; Medema, René H.; Lens, Susanne M. A. (2006): Survivin mediates targeting of the chromosomal passenger complex to the centromere and midbody. In *EMBO Reports* 7 (1), pp. 85–92. DOI: 10.1038/sj.embor.7400562.

Vaira, V.; Lee, C. W.; Goel, H. L.; Bosari, S.; Languino, L. R.; Altieri, D. C. (2007): Regulation of survivin expression by IGF-1/mTOR signaling. In *Oncogene* 26 (19), pp. 2678–2684. DOI: 10.1038/sj.onc.1210094.

Valerie, Kristoffer; Povirk, Lawrence F. (2003): Regulation and mechanisms of mammalian double-strand break repair. In *Oncogene* 22 (37), pp. 5792–5812. DOI: 10.1038/sj.onc.1206679.

Vassilev, Lyubomir T.; Tovar, Christian; Chen, Shaoqing; Knezevic, Dejan; Zhao, Xiaolan; Sun, Hongmao et al. (2006): Selective small-molecule inhibitor reveals critical mitotic functions of human CDK1. In *Proceedings of the National Academy of Sciences of the United States of America* 103 (28), pp. 10660–10665. DOI: 10.1073/pnas.0600447103.

Vermeulen, Katrien; van Bockstaele, Dirk R.; Berneman, Zwi N. (2003): The cell cycle: a review of regulation, deregulation and therapeutic targets in cancer. In *Cell proliferation* 36 (3), pp. 131–149. DOI: 10.1046/j.1365-2184.2003.00266.x.

Vértessy, Béata G.; Tóth, Judit (2009): Keeping uracil out of DNA: physiological role, structure and catalytic mechanism of dUTPases. In *Accounts of chemical research* 42 (1), pp. 97–106. DOI: 10.1021/ar800114w.

Vignard, Julien; Mirey, Gladys; Salles, Bernard (2013): Ionizing-radiation induced DNA double-strand breaks: a direct and indirect lighting up. In *Radiotherapy and oncology : journal of the European Society for Therapeutic Radiology and Oncology* 108 (3), pp. 362–369. DOI: 10.1016/j.radonc.2013.06.013.

Viguera, E.; Canceill, D.; Ehrlich, S. D. (2001): Replication slippage involves DNA polymerase pausing and dissociation. In *The EMBO journal* 20 (10), pp. 2587–2595. DOI: 10.1093/emboj/20.10.2587.

Visconti, Roberta; Grieco, Domenico (2009): New insights on oxidative stress in cancer. In *Current opinion in drug discovery & development* 12 (2), pp. 240–245.

Vogelstein, Bert; Kinzler, Kenneth W. (2004): Cancer genes and the pathways they control. In *Nature medicine* 10 (8), pp. 789–799. DOI: 10.1038/nm1087.

Voitenleitner, C.; Fanning, E.; Nasheuer, H. P. (1997): Phosphorylation of DNA polymerase alpha-primase by cyclin A-dependent kinases regulates initiation of DNA replication in vitro. In *Oncogene* 14 (13), pp. 1611–1615. DOI: 10.1038/sj.onc.1200975.

Volle, Catherine; Dalal, Yamini (2014): Histone variants: the tricksters of the chromatin world. In *Current opinion in genetics & development* 25, 8-14,138. DOI: 10.1016/j.gde.2013.11.006.

Vong, Queenie P.; Cao, Kan; Li, Hoi Y.; Iglesias, Pablo A.; Zheng, Yixian (2005): Chromosome alignment and segregation regulated by ubiquitination of survivin. In *Science* 310 (5753), pp. 1499–1504. DOI: 10.1126/science.1120160.

Walker, D. H.; Maller, J. L. (1991): Role for cyclin A in the dependence of mitosis on completion of DNA replication. In *Nature* 354 (6351), pp. 314–317. DOI: 10.1038/354314a0.

Wang, Fangwei; Dai, Jun; Daum, John R.; Niedzialkowska, Ewa; Banerjee, Budhaditya; Stukenberg, P. Todd et al. (2010): Histone H3 Thr-3 phosphorylation by Haspin positions Aurora B at centromeres in mitosis. In *Science* 330 (6001), pp. 231–235. DOI: 10.1126/science.1189435.

Warbrick, E. (2000): The puzzle of PCNA's many partners. In *BioEssays : news and reviews in molecular, cellular and developmental biology* 22 (11), pp. 997–1006. DOI: 10.1002/1521-1878(200011)22:11<997::AID-BIES6>3.0.CO;2-#.

Weber, Christopher M.; Henikoff, Steven (2014): Histone variants: dynamic punctuation in transcription. In *Genes & development* 28 (7), pp. 672–682. DOI: 10.1101/gad.238873.114.

Weiler, K. S.; Wakimoto, B. T. (1995): Heterochromatin and gene expression in Drosophila. In *Annual review of genetics* 29, pp. 577–605. DOI: 10.1146/annurev.ge.29.120195.003045.

Weinberg, R. A. (1991): Tumor suppressor genes. In *Science (New York, N.Y.)* 254 (5035), pp. 1138–1146. DOI: 10.1126/science.1659741.

Wenzel; Singh (2018): Cell-cycle Checkpoints and Aneuploidy on the Path to Cancer. In *In Vivo* 32 (1), pp. 1–5.

Weterings, Eric; Chen, David J. (2008): The endless tale of non-homologous end-joining. In *Cell Res* 18 (1), pp. 114–124. DOI: 10.1038/cr.2008.3.

Wheatley, Sally P. (2011): Chromosome 'by-Aurora-ientation' during mitosis. In *Cell biology international* 35 (6), pp. 575–578. DOI: 10.1042/CBI20100911.

Wheatley, Sally P.; Barrett, Rachel M.; Andrews, Paul D.; Medema, Rene H.; Morley, Simon J.; Swedlow, Jason R.; Lens, Susanne M. A. (2007): Phosphorylation by aurora-B negatively regulates survivin function during mitosis. In *Cell cycle (Georgetown, Tex.)* 6 (10), pp. 1220–1230. DOI: 10.4161/cc.6.10.4179.

Wheatley, Sally P.; Henzing, Alexander J.; Dodson, Helen; Khaled, Walid; Earnshaw, William C. (2004): Aurora-B phosphorylation in vitro identifies a residue of survivin that is essential for its localization and binding to inner centromere protein (INCENP) in vivo. In *The Journal of biological chemistry* 279 (7), pp. 5655–5660. DOI: 10.1074/jbc.M311299200.

Wold, M. S. (1997): Replication protein A: a heterotrimeric, single-stranded DNA-binding protein required for eukaryotic DNA metabolism. In *Annual review of biochemistry* 66, pp. 61–92. DOI: 10.1146/annurev.biochem.66.1.61.

Woodgate, Roger (2001): Evolution of the two-step model for UV-mutagenesis. In *Mutation Research/DNA Repair* 485 (1), pp. 83–92. DOI: 10.1016/s0921-8777(00)00076-8.

World Cancer Report 2014 (2014). Lyon: IARC Press. Available online at http://publications.iarc.fr/Non-Series-Publications/World-Cancer-Reports/World-Cancer-Report-2014.

Wu, Liming; Ma, Chi A.; Zhao, Yongge; Jain, Ashish (2011): Aurora B interacts with NIR-p53, leading to p53 phosphorylation in its DNA-binding domain and subsequent

functional suppression. In *J. Biol. Chem.* 286 (3), pp. 2236–2244. DOI: 10.1074/jbc.M110.174755.

Wu, Peï-Yu; Frit, Philippe; Meesala, SriLakshmi; Dauvillier, Stéphanie; Modesti, Mauro; Andres, Sara N. et al. (2009): Structural and functional interaction between the human DNA repair proteins DNA ligase IV and XRCC4. In *Molecular and cellular biology* 29 (11), pp. 3163–3172. DOI: 10.1128/MCB.01895-08.

Wyatt, Michael D.; Pittman, Douglas L. (2006): Methylating agents and DNA repair responses: Methylated bases and sources of strand breaks. In *Chemical research in toxicology* 19 (12), pp. 1580–1594. DOI: 10.1021/tx060164e.

Xu, Chunsen; Yamamoto-Ibusuki, Mutsuko; Yamamoto, Yutaka; Yamamoto, Satoko; Fujiwara, Saori; Murakami, Keiichi et al. (2014): High survivin mRNA expression is a predictor of poor prognosis in breast cancer: a comparative study at the mRNA and protein level. In *Breast cancer (Tokyo, Japan)* 21 (4), pp. 482–490. DOI: 10.1007/s12282-012-0403-9.

Xu, Yong; Fang, Fang; Ludewig, Gabriele; Jones, Grace; Jones, Davy (2004): A mutation found in the promoter region of the human survivin gene is correlated to overexpression of survivin in cancer cells. In *DNA and cell biology* 23 (7), pp. 419–429. DOI: 10.1089/1044549041474788.

Yang, Wei (2011): Surviving the sun: repair and bypass of DNA UV lesions. In *Protein science : a publication of the Protein Society* 20 (11), pp. 1781–1789. DOI: 10.1002/pro.723.

Yano, Ken-ichi; Morotomi-Yano, Keiko; Wang, Shih-Ya; Uematsu, Naoya; Lee, Kyung-Jong; Asaithamby, Aroumougame et al. (2008): Ku recruits XLF to DNA double-strand breaks. In *EMBO Reports* 9 (1), pp. 91–96. DOI: 10.1038/sj.embor.7401137.

Yao, Nina Y.; O'Donnell, Mike (2009): Replisome structure and conformational dynamics underlie fork progression past obstacles. In *Current opinion in cell biology* 21 (3), pp. 336–343. DOI: 10.1016/j.ceb.2009.02.008.

Yates, Maïlyn; Maréchal, Alexandre (2018): Ubiquitylation at the Fork: Making and Breaking Chains to Complete DNA Replication. In *International journal of molecular sciences* 19 (10). DOI: 10.3390/ijms19102909.

Yazdi, Parvin T.; Wang, Yi; Zhao, Song; Patel, Nimitt; Lee, Eva Y-H P.; Qin, Jun (2002): SMC1 is a downstream effector in the ATM/NBS1 branch of the human S-phase checkpoint. In *Genes & development* 16 (5), pp. 571–582. DOI: 10.1101/gad.970702.

Yeeles, Joseph T. P.; Deegan, Tom D.; Janska, Agnieszka; Early, Anne; Diffley, John F. X. (2015): Regulated eukaryotic DNA replication origin firing with purified proteins. In *Nature* 519 (7544), pp. 431–435. DOI: 10.1038/nature14285.

Yeeles, Joseph T. P.; Poli, Jérôme; Marians, Kenneth J.; Pasero, Philippe (2013): Rescuing stalled or damaged replication forks. In *Cold Spring Harbor Perspectives in Biology* 5 (5), a012815. DOI: 10.1101/cshperspect.a012815.

Yekezare, Mona; Gómez-González, Belén; Diffley, John F. X. (2013): Controlling DNA replication origins in response to DNA damage - inhibit globally, activate locally. In *J Cell Sci* 126 (Pt 6), pp. 1297–1306. DOI: 10.1242/jcs.096701.

Yi, Qi; Chen, Qinfu; Liang, Cai; Yan, Haiyan; Zhang, Zhenlei; Xiang, Xingfeng et al. (2018): HP1 links centromeric heterochromatin to centromere cohesion in mammals. In *EMBO Reports* 19 (4). DOI: 10.15252/embr.201745484.

Yoo, S.; Dynan, W. S. (1999): Geometry of a complex formed by double strand break repair proteins at a single DNA end: recruitment of DNA-PKcs induces inward translocation of Ku protein. In *Nucleic acids research* 27 (24), pp. 4679–4686. DOI: 10.1093/nar/27.24.4679.

Yu, Xiaochun; Fu, Shuang; Lai, Maoyi; Baer, Richard; Chen, Junjie (2006): BRCA1 ubiquitinates its phosphorylation-dependent binding partner CtIP. In *Genes & development* 20 (13), pp. 1721–1726. DOI: 10.1101/gad.1431006.

Zachos, George; Rainey, Michael D.; Gillespie, David A. F. (2005): Chk1-dependent S-M checkpoint delay in vertebrate cells is linked to maintenance of viable replication structures. In *Molecular and cellular biology* 25 (2), pp. 563–574. DOI: 10.1128/MCB.25.2.563-574.2005.

Zarebski, Miroslaw; Wiernasz, Elzbieta; Dobrucki, Jurek W. (2009): Recruitment of heterochromatin protein 1 to DNA repair sites. In *Cytometry. Part A : the journal of the International Society for Analytical Cytology* 75 (7), pp. 619–625. DOI: 10.1002/cyto.a.20734.

Zeng, Y.; Forbes, K. C.; Wu, Z.; Moreno, S.; Piwnica-Worms, H.; Enoch, T. (1998): Replication checkpoint requires phosphorylation of the phosphatase Cdc25 by Cds1 or Chk1. In *Nature* 395 (6701), pp. 507–510. DOI: 10.1038/26766.

Zhang, Fan; Fan, Qiang; Ren, Keqin; Andreassen, Paul R. (2009): PALB2 functionally connects the breast cancer susceptibility proteins BRCA1 and BRCA2. In *Molecular cancer research : MCR* 7 (7), pp. 1110–1118. DOI: 10.1158/1541-7786.MCR-09-0123.

Zhang, Hengshan; Lawrence, Christopher W. (2005): The error-free component of the RAD6/RAD18 DNA damage tolerance pathway of budding yeast employs sister-strand recombination. In *Proceedings of the National Academy of Sciences of the United States of America* 102 (44), pp. 15954–15959. DOI: 10.1073/pnas.0504586102.

Zhang, Hong (2007): Molecular signaling and genetic pathways of senescence: Its role in tumorigenesis and aging. In *Journal of cellular physiology* 210 (3), pp. 567–574. DOI: 10.1002/jcp.20919.

Zheng, Li; Jia, Jia; Finger, L. David; Guo, Zhigang; Zer, Cindy; Shen, Binghui (2011): Functional regulation of FEN1 nuclease and its link to cancer. In *Nucleic acids research* 39 (3), pp. 781–794. DOI: 10.1093/nar/gkq884.

Zou, L.; Stillman, B. (2000): Assembly of a complex containing Cdc45p, replication protein A, and Mcm2p at replication origins controlled by S-phase cyclin-dependent kinases and Cdc7p-Dbf4p kinase. In *Molecular and cellular biology* 20 (9), pp. 3086–3096. DOI: 10.1128/mcb.20.9.3086-3096.2000.

Zou, Lee; Elledge, Stephen J. (2003): Sensing DNA damage through ATRIP recognition of RPA-ssDNA complexes. In *Science* 300 (5625), pp. 1542–1548. DOI: 10.1126/science.1083430.

Zuazua-Villar, P.; Rodriguez, R.; Gagou, M. E.; Eyers, P. A.; Meuth, M. (2014): DNA replication stress in CHK1-depleted tumour cells triggers premature (S-phase) mitosis through inappropriate activation of Aurora kinase B. In *Cell Death Dis* 5 (5), e1253. DOI: 10.1038/cddis.2014.231.

6 Appendix

6.1 Supplemented figures

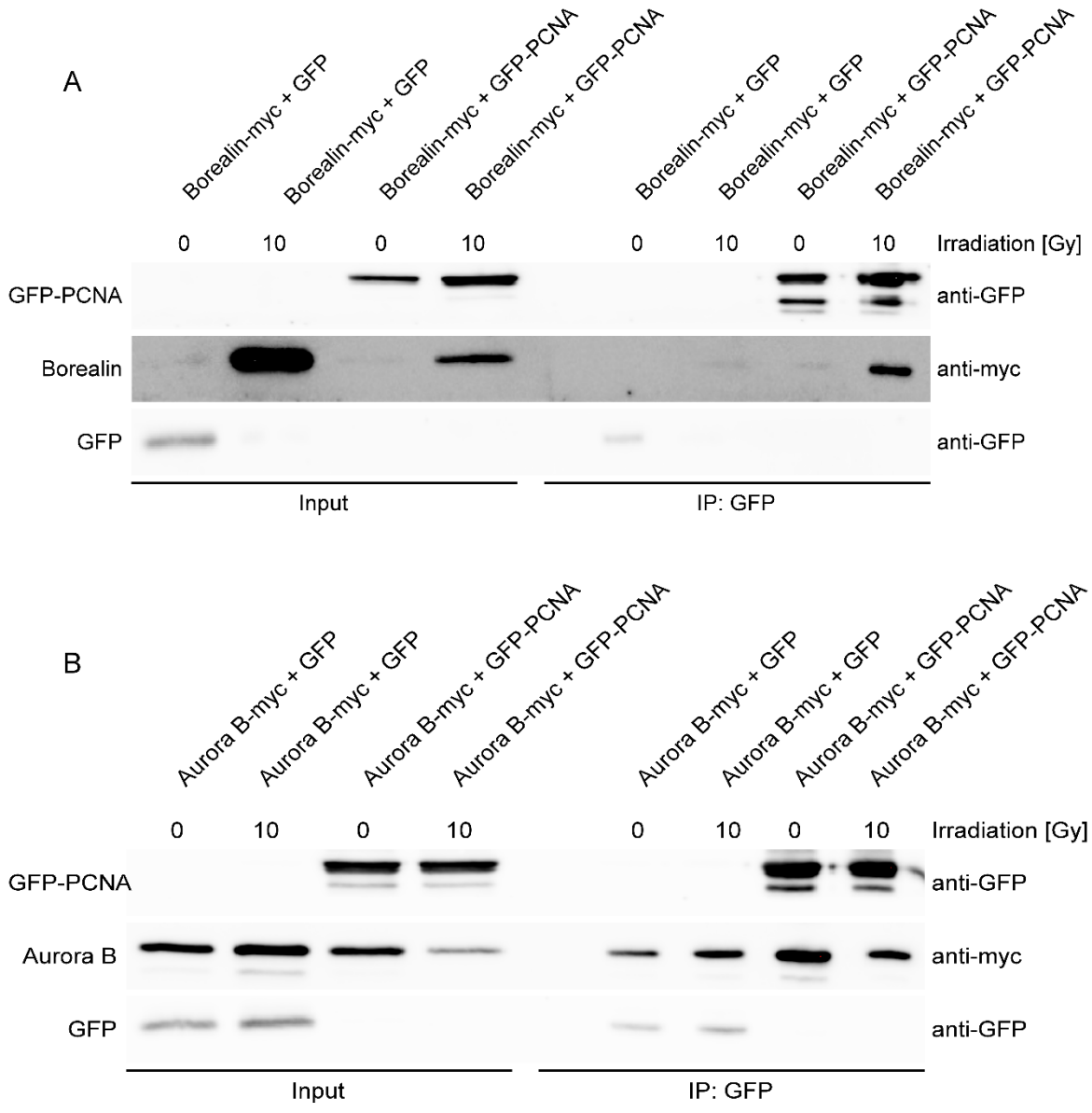

Figure 6.1: Immunoprecipitation of Borealin-myc and Aurora B-myc with GFP-PCNA

Western Blot analysis of IP samples. 293T cells were co-transfected with plasmids coding for GFP-PCNA together with Borealin-myc **(A)** or Aurora B-myc **(B)**, respectively. Co-transfection of GFP with each CPC member served as controls. 24 hours after transfection, the cells were irradiated with 10 Gy and incubated for 2 hours. Prior to immunoprecipitation, chromatin extraction was performed with the Chromatin Extraction kit from Abcam. One-third of the chromatin extraction was used as an input control. GFP-PCNA was immunoprecipitated from the chromatin extracts using magnetic beads coupled to a GFP-specific antibody. The input lysates and immunoprecipitates were subjected to immunoblot analysis. Membranes were incubated with antibodies specific for GFP or myc-tag.

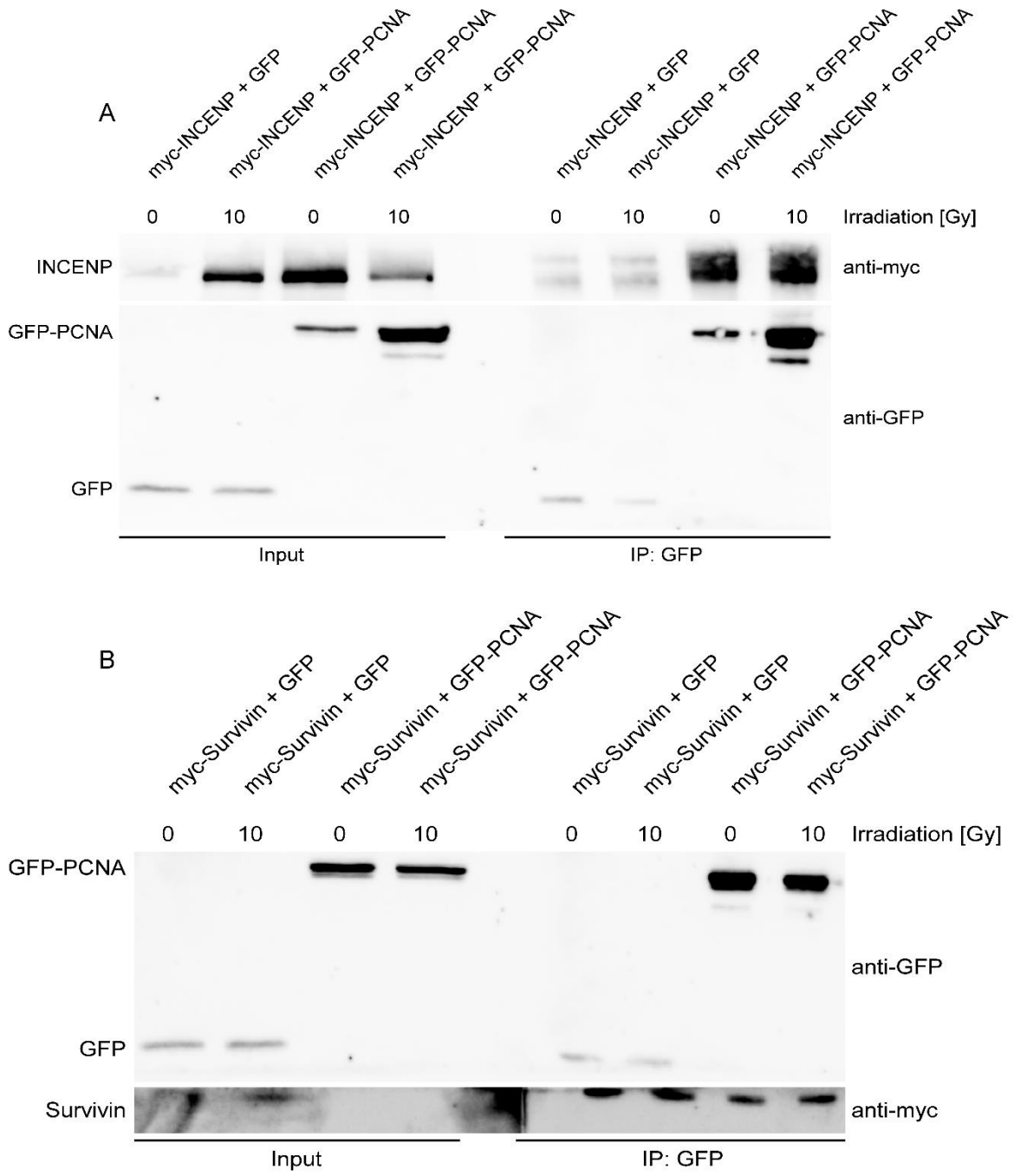

Figure 6.2: Immunoprecipitation of myc-INCENP and Survivin-myc with GFP-PCNA

Western Blot analysis of IP samples. 293T cells were co-transfected with plasmids coding for GFP-PCNA together with myc-INCENP **(A)** or Survivin-myc **(B)**, respectively. Co-transfection of GFP with each CPC member served as controls. 24 hours after transfection, the cells were irradiated with 10 Gy and incubated for 2 hours. Prior to immunoprecipitation, chromatin extraction was performed with the Chromatin Extraction kit from Abcam. One-third of the chromatin extraction was used as an input control. GFP-PCNA was immunoprecipitated from the chromatin extracts using magnetic beads coupled to a GFP-specific antibody. The input lysates and immunoprecipitates were subjected to immunoblot analysis. Membranes were incubated with antibodies specific for GFP or myc-tag.

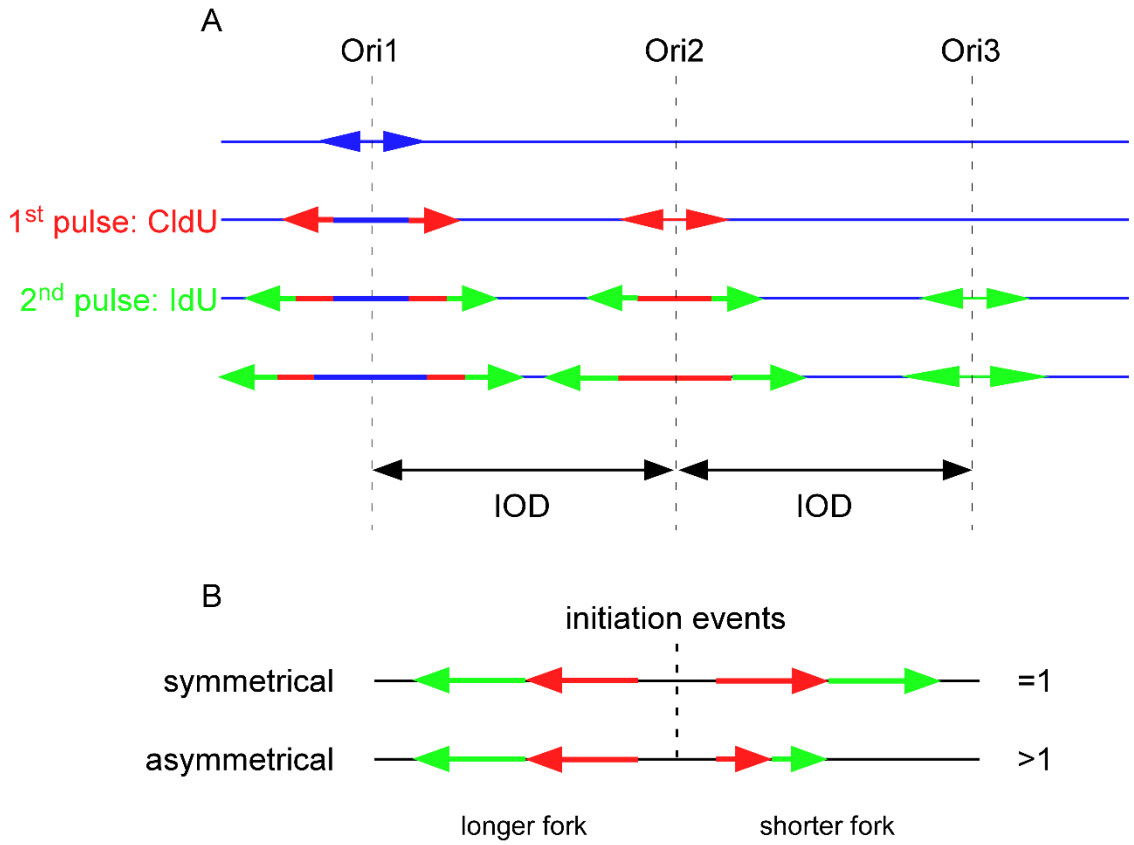

Figure 6.3: Schematic overview of the DNA combing assay

A) Exponentially growing HeLa cells were sequentially pulse-labelled with CldU (red) and IdU (green) for 20 minutes each. The cells were harvested and DNA combing was performed as described in section 2.2.2.10. After fixation, denaturation and immunostaining, the image acquisition was performed with the EasyScan service by Genomic Vision. For analysis, the FiberStudio® Analysis Software was used. Three major events can be discerned. DNA replication initiates before the first pulse (Ori1), during the first pulse (Ori2) or during the second pulse (Ori3). DNA is depicted in blue. Direction of the bidirectional replication forks are depicted with arrows. DNA replication origins were depicted as Ori. IOD was determined by measuring origin distances. **B)** Schematic overview of how long fork/short fork ratios are determined. A ratio equalling 1 indicates fork symmetry and a ratio >1 indicates an asymmetric fork. Modified after (Stanojcic et al. 2016).

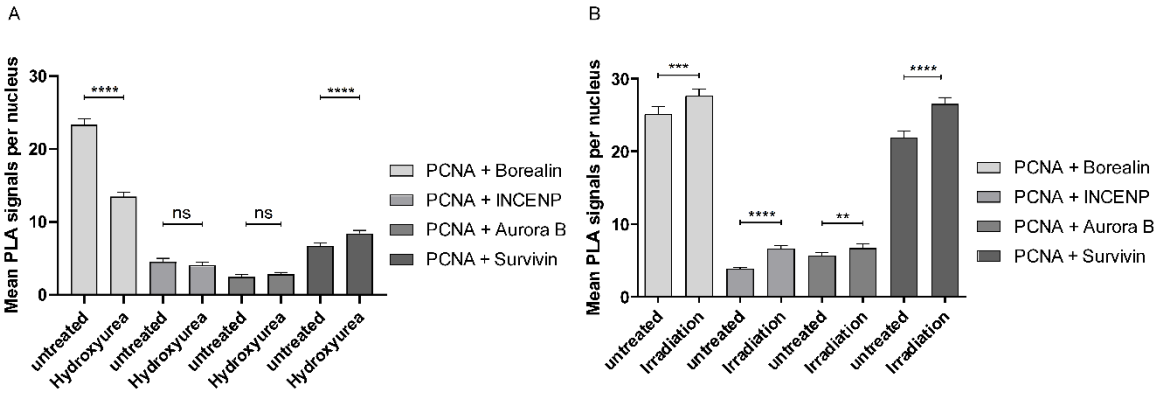

Figure 6.4: Interaction between CPC members and PCNA within the nucleus

A) Quantitative analysis of the interaction between each CPC member and PCNA within the nucleus after treatment with HU. The bar graph shows the mean number of PLA signals per nucleus with SD. Data was analysed by t-test. **** < 0.0001. n=3. More than 200 cells were counted. **B)** Quantitative analysis of the interaction between each CPC member and PCNA within the nucleus after irradiation. The bar graph shows the mean number of PLA signals per nucleus with SD. Data was analysed by t-test. **** < 0.0001, *** < 0.001, ** < 0.01. n=3. More than 200 cells were counted.

6.2 Amino acids

Table 6.1: Amino acids.

one letter code	three letter code	amino acid
A	Ala	alanine
C	Cys	cysteine
D	Asp	aspartic acid
E	Glu	glutamic acid
F	Phe	phenylalanine
G	Gly	glycine
H	His	histidine
I	Ile	isoleucine
K	Lys	lysine
L	Leu	leucine
M	Met	methionine
N	Asn	asparagine
P	Pro	proline
Q	Gln	glutamine
R	Arg	arginine
S	Ser	serine
T	Thr	threonine
V	Val	valine
W	Trp	tryptophan
Y	Tyr	tyrosine

6.3 Danksagung

An dieser Stelle möchte ich mich bei allen Menschen bedanken, die mir in den letzten Jahren stets zur Seite standen.
Zuallererst möchte ich bei Prof. Dr. Shirley Knauer bedanken, die mir die Chance gegeben hat, meine Doktorarbeit in ihrer Arbeitsgruppe anzufertigen. Shirley, ich danke dir für deine Unterstützung während der drei Jahre – das Projekt war weiß Gott nicht immer einfach.
Mein Dank geht auch an Herrn Prof. Dr. Christian Johannes, für die Übernahme des Zweitgutachtens für diese Arbeit.
Ich danke auch Herrn Prof. Dr. Dominik Boos für die wissenschaftliche Unterstützung als Mentor im GRK 1739. Außerdem geht mein Dank an Herrn Prof. Dr. Alexander Schramm, an den ich mich stets mit Fragen wenden konnte.
Ein besonders herzlicher Dank geht an die „Knauer Power“, vor allem an Dr. Astrid Hensel und Dr. Elisabeth Schröder, ohne euch hätte ich es nicht geschafft. Liebe Astrid, deine Unterstützung, wenn es mal nicht so lief, war Gold wert und dafür danke ich dir ganz besonders. Liebe Elli, dir konnte ich selbst dumme Fragen stellen. Dein Engagement für die Arbeitsgruppe und für jeden Einzelnen von uns war außergewöhnlich. Danke für die Quizabende, die mir sehr fehlen werden.
Außerdem bedanke ich mich bei meinen Büropartnern, Alex Höing und Paul Stahl. Ihr seid die besten Kollegen, die man sich wünschen kann. Wenn das Horn von Gondor ruft, schlägt unsere Stunde. Bierspezialitäten, Kickerturniere und Fantasy Football (bei denen Alex nicht mitreden kann) sind Tagesordnungspunkte auf unserer Agenda. Hoffentlich kann sich Alex in Zukunft den Kickerpokal erschummeln. Danke Jungs!
Ein großes Dankeschön geht an meine Familie. Mama und Papa, ohne euch wäre ich nie so weit gekommen. Es gibt keine besseren Eltern als euch. Charlotte, du bist zwar unglaublich nervig als kleine Schwester, aber ich konnte immer auf deine Unterstützung zählen. Danke für die vielen Mittagessen, selbstgemachten Marmeladen und Eierliköre, die mir den Schreibprozess erleichtert haben.
Zuletzt geht mein Dank Julie. Danke für deine unglaubliche Unterstützung, dass du mich immer wieder motiviert hast und dass du durchweg an mich geglaubt hast. Ohne dich säße ich wahrscheinlich immer noch am ersten Satz dieser Arbeit.

6.4 Publications, oral presentations and poster presentations

Publications

Menke K, Schwermer M, **Falke K**, Felenda J, Beckmann C, Stintzig F, Voigt A, Schramm A, Zuzak TJ. Taraxacum officinale extract induces antitumorigenic effects in ovarian carcinoma cell lines. EJGO, no. 1, 2019. DOI: 10.12892/ejgo4460.2019

Korff JM, Menke K, Schwermer M, **Falke K**, Schramm A, Längler A, Zuzak TJ. Antitumoral effects of Curcumin (Curcuma longa L.) and Thymoquinone (Nigella sativa L.) on neuroblastoma cell lines. Brief report. Complementary medicine research, 2019. DOI: 10.1159/000509765

Menke K, Schwermer M, **Falke K**, Eisenbraun J, Schramm A, Zuzak TJ. Preclinical investigation of interaction of mistletoe extract (Viscum album L.) with radio- and chemotherapy in pediatric tumor cell lines. Phymed, 2019. DOI: 10.1016/j.phymed.2019.09.123

Falke K ‡, Schröder E ‡, Mosel S, Boos D, Knauer SK. An old passenger as a new driver: Survivin's role in replication fork dynamics causes DNA instability and tumor radioresistance. ‡equal author contribution. *In preparation*.

Oral presentations

06/2018	GRK 1739, Annual Meeting 2018, Düsseldorf
05/2019	GRK 1739, Annual Meeting 2019, Möhnesee
06/2020	GRK 1739, Annual Meeting 2020, Via Zoom

Poster presentations

01/2019	Network Meeting GRK 1739 and GRK 1657, Höchst/Odenwald
10/2019	GRK 1739 International Conference: DNA damage and beyond, Essen

6.5 Curriculum vitae

The curriculum vitae is not included for reasons of data protection.

6.6 Eidesstattliche Erklärungen

Erklärung:

Hiermit erkläre ich, gem. § 6 Abs. (2) e) der Promotionsordnung der Fakultät für Biologie zur Erlangung des Dr. rer. nat., dass ich keine anderen Promotionen bzw. Promotionsversuche in der Vergangenheit durchgeführt habe.

Essen, den _____ _____

Katharina Falke

Erklärung:

Hiermit erkläre ich, gemäß § 6 Abs. (2) f) der Promotionsordnung der Fakultät für Biologie, dass mir die Gelegenheit zum vorliegenden Promotionsverfahren nicht kommerziell vermittelt worden ist. Insbesondere habe ich keine Organisation eingeschaltet, die gegen Entgelt Betreuerinnen und Betreuer für die Anfertigung von Dissertationen sucht oder die mir obliegenden Pflichten hinsichtlich der Prüfungsleistungen für mich ganz oder teilweise erledigt. Hilfe Dritter wurde bis jetzt und wird auch künftig nur in wissenschaftlich vertretbarem und prüfungsrechtlich zulässigem Ausmaß in Anspruch genommen. Mir ist bekannt, dass Unwahrheiten hinsichtlich der vorstehenden Erklärung die Zulassung zur Promotion ausschließen bzw. später zum Verfahrensabbruch oder zur Rücknahme des Titels führen können.

Essen, den _____ _____

Katharina Falke

Erklärung:

Hiermit erkläre ich, gem. § 6 Abs. (2) g) der Promotionsordnung der Fakultät für Biologie zur Erlangung der Dr. rer. nat., dass ich das Arbeitsgebiet, dem das Thema „Functional characterisation of Survivin and the CPC in replication stress“ zuzuordnen ist, in Forschung und Lehre vertrete und den Antrag von Katharina Falke befürworte und die Betreuung auch im Falle eines Weggangs, wenn nicht wichtige Gründe dem entgegenstehen, weiterführen werde.

Essen, den _____ _____

Prof. Dr. Shirley Knauer